Phosphorus-containing ligands in transition metal chemistry

Andrews, Christopher David

Award date:
2001

Awarding institution:
University of Bath

Phosphorus-containing Ligands in Transition Metal Chemistry

Submitted by Christopher David Andrews
for the degree of Ph.D.
of the University of Bath
2001

CAndrews

ProQuest LLC
789 East Eisenhower Parkway
P.O. Box 1346
Ann Arbor, MI 48106-1346

Memorandum

The work described in this thesis was carried out by the author between October 1997 and December 2000 within the Department of Chemistry at the University of Bath, under the supervision of Professor Michael Green and Dr. Andrew Burrows. Unless otherwise indicated the work is original and has not been submitted for any other degree.

Summary

The complexes $[MoCl(CO)(\eta^4\text{-}1,3\text{-}P_2C_2Bu^t_2)(\eta^5\text{-}C_5R_5)]$ (R = H **1**, Me **2**) were prepared by the reaction of *tert*-butylphosphaalkyne with $[MoCl(CO)_3(\eta^5\text{-}C_5R_5)]$. Complex **1** may be oxidised in solution by water or methanol to give the phosphaphosphonietinyl complexes $[MoCl(CO)\{\eta^3,\lambda^3,\lambda^5\text{-}PC_2Bu^t_2PH(OR')\}(\eta^5\text{-}C_5H_5)]$ (R' = H **3**, Me **4**).

The reactions of $[MoCl(CO)\{\eta^2(4e)\text{-}PhC{\equiv}CR\}(\eta^5\text{-}L)][BF_4]$ (L = C_5H_5, $C_5H_4Bu^t$, R = Ph or Me) with $AgBF_4$, ethene and *tert*-butylphosphaalkyne give the complexes $[Mo(CO)(=C\{Bu^t\}\overline{P\{\eta^2\text{-}C(Bu^t)=P\}C\{R\}=C\{R'\}})(\eta^5\text{-}L)][BF_4]$ (**6** L = C_5H_5, R = R' = Ph; **8** L = C_5H_5, R ≠ R' = Ph or Me; **12** L = $C_5H_4Bu^t$, R = R' = Ph). Only one of the two possible isomers of **8** is observed. The reaction of **6** with DIBAL-H results in the addition of 'H⁻' to the carbene carbon, resulting in the formation of the complex $[Mo(CO)(\text{-}CH\{Bu^t\}\overline{P\{\eta^2\text{-}C(Bu^t)=P\}\{\eta^2\text{-}C(Ph)=C(Ph)\}})(\eta^5\text{-}C_5H_5)]$, **13**.

The reactions between the functionalised phosphines $Ph_2PNC_4H_3C(O)Me$ (**L**^{1}), $Ph_2PCH_2C(O)Ph$ (**L**^{2}) and $Ph_2PCH_2C(O)NPh_2$ (**L**^{3}) and $[MoCl(CO)_3(\eta^5\text{-}C_5R_5)]$ produce the complexes *lat*-$[MoCl(CO)_2(L\text{-}P)(\eta^5\text{-}C_5R_5)]$, **14 – 19** (L = **L**^{1}, **L**^{2} or **L**^{3}, R = H or Me). Reacting these complexes with $AgBF_4$ gives the complexes $[Mo(CO)_2(L\text{-}P,O)(\eta^5\text{-}C_5R_5)]$, **20 – 25**, where the phosphine acts as a bidentate ligand. Subsequent addition of $[PhCH_2NEt_3][Cl]$ regenerates complexes **14 – 19**. The complexes $[Mo(CO)_2(L\text{-}P,O)(\eta^5\text{-}C_5H_5)]$ (L = **L**^{1}, **20** or **L**^{2}, **22**) may also be made by direct addition of HBF_4 and the phosphine to $[Mo(CH_3)(CO)_3(\eta^5\text{-}C_5H_5)]$.

The phosphino-enolate complex $[Mo(CO)_2\{Ph_2PCH{=}C(O)Ph\text{-}P,O\}(\eta^5\text{-}C_5H_5)]$, **26**, may be produced by reacting $[MoCl(CO)_2(\mathbf{L}^2\text{-}P)(\eta^5\text{-}C_5H_5)]$, **16**, with BuLi, or **22** with NEt_3. Reacting the phosphino-enolate complex with HBF_4 regenerates **22**.

Displacement of the oxygen atom is seen in a number of cases in the reactions between phosphines and **20**, **22** and $[Mo(CO)_2(\mathbf{L}^3\text{-}P,O)(\eta^5\text{-}C_5H_5)]$, **24**. The products

of these reactions exist in the *diag* conformation. It is believed that these reactions are sterically controlled.

The complex $[Pd_3(P{\equiv}CBu^t)_2(\mu\text{-dppm})_3][PF_6]_2$, **39** was prepared from the reaction of *tert*-butylphosphaalkyne with $[Pd_3(\mu_3\text{-CO})(\mu\text{-dppm})_3][PF_6]_2$. Multinuclear NMR studies indicate that the phosphaalkyne ligands coordinate in an η^1 fashion. Crystals of the phosphinidene complex $[Pd_3\{(CH_3)CO\}(\mu_3\text{-}PCH_2Bu^t)(\mu\text{-dppm})_3][PF_6]_2$, **40**, were obtained whilst attempting to obtain X-ray quality crystals of **39**.

Acknowledgements

I would first like to thank my supervisors, Professor Michael Green and Dr. Andrew Burrows for supervising my research for the duration of my PhD studies at the University of Bath.

Many of the results in this thesis would not have been possible without the assistance of others, so thanks must go to Dr. Mary Mahon and Ross Harrington at the University of Bath and to Dr John Jeffery at Bristol University for X-ray crystal structure determinations, to NMR spectroscopists Harry and Dave, and to CHN analyst Alan Carver. Special thanks must go to Dr. Cameron Jones of Cardiff University, for the kind gifts of *tert*-butylphosphaalkyne.

Thanks must also go to Dr Andrew Weller, Dr Jason Lynam, Dr Claire Beddows, Dr Mark Palmer, Ross Harrington, Maurizio Varrone and everyone else who has worked alongside me in the laboratory for putting up with my bad habits and strange taste in music.

I thank the University of Bath for financial support over the three years.

Finally I would like to thank my parents for all their support and encouragement over the years.

ABBREVIATIONS USED

$\eta^2(xe)$	η^2 bonded *via x* electrons
Bu^t	*tert*-Butyl group
cod	Cyclooctadiene
Cp	Cyclopentadienyl
Cp*	Pentamethylcyclopentadienyl
Cy	Cyclohexyl
DIBAL-H	Diisobutylaluminiumhydride
dmba	*N,N*-dimethylbenzamine
dpph	Bis(diphenylphosphino)hexane
dppm	Bis(diphenylphosphino)methane
Et	Ethyl
Ind	Indenyl
IR	Infra-red spectroscopy
L	Ligand
L-*P*	Phosphorus coordinated ligand
L-*P,O*	Phosphorus and oxygen coordinated ligand
M	Metal atom
Me	Methyl group
MeCN	Acetonitrile
Mes*	2,4,6-tris(*tert*-butyl)phenyl group
NMR	Nuclear Magnetic Resonance
Ph	Phenyl group
Pr^i	Isopropyl group
R	Alkyl group
THF	Tetrahydrofuran
X	Halide

Relating to NMR

at	Apparent triplet

br	Broad
d	Doublet
J	Coupling constant (in Hertz)
m	Multiplet
ppm	Parts per million
sept	Septet
s	Singlet
t	Triplet

Relating to IR

ν	Frequency

Relating to X-ray Diffraction

a,b,c	Unit cell length in Å
α,β,γ	Angles between pairs of sides
Z	Number of molecules in unit cell
U	Volume of unit cell in $Å^3$

CONTENTS

1 Phosphaalkynes in Transition Metal Chemistry

1.1 Introduction to Phosphaalkynes

1.1.1 Scope of Review

Phosphaalkynes have been known since 1961 when Gier[1] first prepared phosphaacetylene, HC≡P. However this compound, in common with the other phosphaalkynes first synthesised, is not stable at room temperature. Although this lack of stability discouraged the study of such species, the synthesis of the *tert*-butyl derivatised version by Becker[2] in 1981 allowed the chemistry of phosphaalkynes to be more readily investigated. Since this synthesis, and that of similarly stabilised phosphaalkynes such as 1-adamantylphosphaalkyne, there has been a growing interest in phosphaalkynes and especially their organometallic chemistry.[3] In the interests of brevity, this chapter will cover transition metal complexes of phosphaalkynes, the cyclooligomerisation reactions of phosphaalkynes, and the co-oligomerisation reactions of phosphaalkynes with alkynes. Other aspects of the chemistry of phosphaalkynes at transition metal centres, such as insertion into M-H bonds and co-oligomerisation reactions with species other than alkynes, will not be covered.

1.1.2 Synthesis

The most common preparation of thermally stable phosphaalkynes takes place in two steps,[4] as shown in Scheme 1.1. First, the appropriate carboxylic acid chloride is combined with tris(trimethylsilyl)phosphine in a non-polar solvent such as cyclohexane and heated under reflux. The acyl phosphine **1.1** which is the initial product of this reaction undergoes spontaneous 1,3-trimethylsilyl migration to give a phosphaalkene, **1.2**, (predominately in the *Z* isomeric form) as the product. This is then passed over solid NaOH at 120-200°C to induce elimination of hexamethyldisiloxane. As most phosphaalkynes undergo thermal oligomerisation if subjected to prolonged heating at such temperatures to give the tetraphosphacubane

derivatives,[5] the usual procedure is to drip the phosphaalkene onto a bed of heated NaOH under vacuum. When the reaction occurs, the generated volatile phosphaalkyne/siloxane mixture can be trapped in a liquid N_2 bath. This mixture can then be fractionally distilled to give the pure phosphaalkyne, **1.3**, in reasonable yield (60% for final step, ~45% overall).

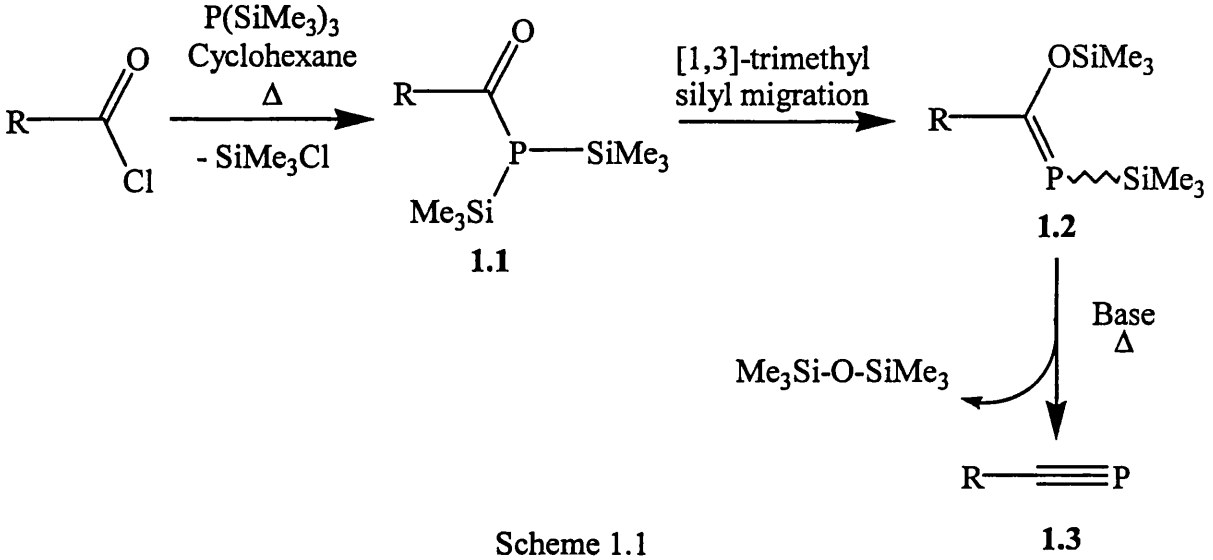

Scheme 1.1

A recent adaptation of this procedure[6] replaces the need for the complicated apparatus required for the last step. If the phosphaalkene **1.2** is dissolved in tetraglyme with a catalytic amount of the lithium salt $LiN(SiMe_3)_2$, the elimination reaction can be carried out at the lower temperature of 50°C. The phosphaalkyne produced may then be distilled from the product mixture.

1.2 Organometallic Complexes of Phosphaalkynes

1.2.1 Coordination Modes of Phosphaalkynes

Phosphaalkynes can coordinate to metals in either an η^1 or an η^2 manner. In η^1-coordination, the lone pair of electrons on the phosphorus donates electron density to an empty d-type orbital on the metal. With the η^2-coordination mode, electron density from the filled π orbitals is donated to empty orbitals on the metal, whilst

back-bonding occurs between filled d orbitals on the metal and the π* orbitals of the phosphaalkyne. This is similar to the bonding in the analogous alkyne complexes, and is shown in Figure 1.1.

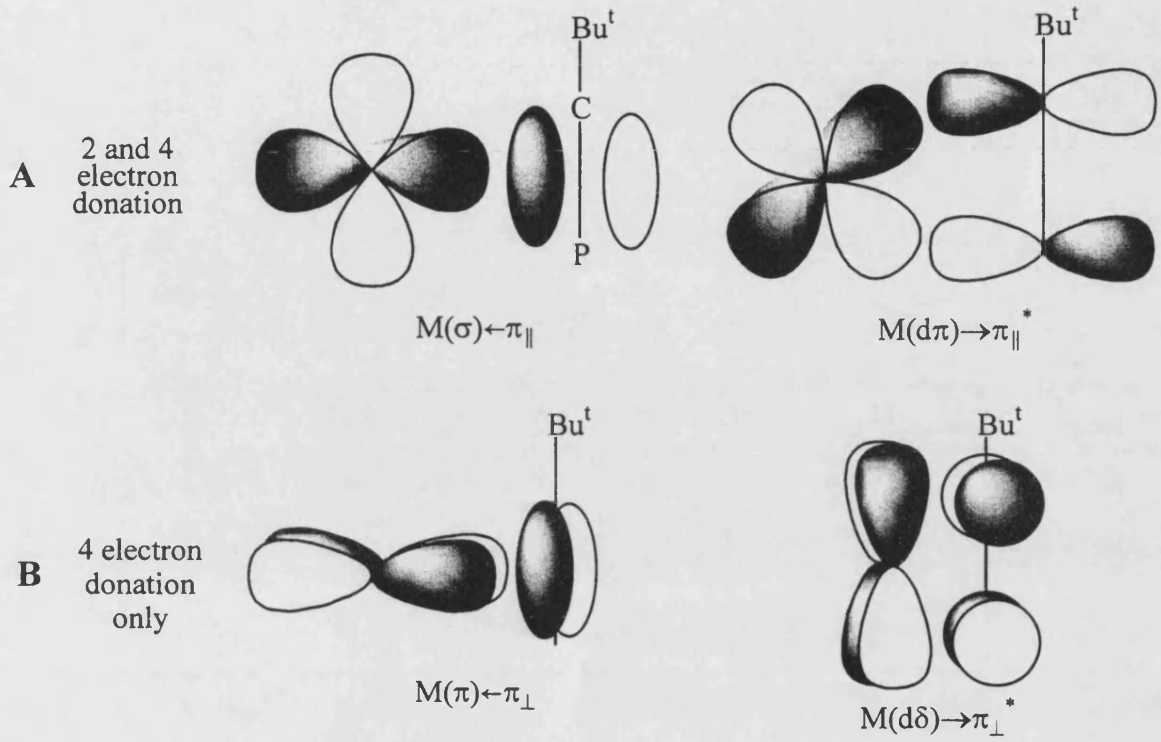

Figure 1.1: Orbital interactions in η^2-phosphaalkyne coordination

The number of mononuclear phosphaalkyne coordination complexes is still relatively small, partly because of the ability of phosphaalkynes to undergo metal-mediated oligomerisations or coupling reactions with other ligands on the metal centre. The majority of phosphaalkyne complexes contain the ligand in the η^2-coordination mode. This is thought to be due to the energy mismatch between the d orbitals on the metal, and the lone-pair of electrons on the phosphorus. The η^1-coordination mode is usually only observed when either the π system of the phosphaalkyne is already engaged in bonding to another metal, or the metal centre is very sterically hindered.

Like alkynes, η^2-coordinated phosphaalkynes can use either 2 or 4 electrons from their π orbitals to coordinate to a metal centre. When 2 electrons are donated, the interactions used are a donation from a set of π bonding orbitals (those parallel to the

plane of the coordination) to the metal centre. Back donation occurs between the metal and the π antibonding orbitals (Figure 1.1, **A**). When 4 electrons are donated, there is an additional set of interactions with the π bonding and antibonding orbitals perpendicular to the plane of the coordination (Figure 1.1, **B**). However, compared to alkynes, the incidence of η^2(4e)-bonding in mononuclear phosphaalkyne complexes is rare.

1.2.2 ^{31}P NMR Spectroscopy as a Tool in Determining Coordination Mode

Work by Templeton[7] has indicated that the coordination mode of alkynes to transition metal centres may be determined by examining the chemical shifts of the acetylenic carbon atoms in the ^{13}C NMR spectra. For example, in Mo(II) and W(II) complexes, the chemical shifts are in the ranges shown in Figure 1.2.

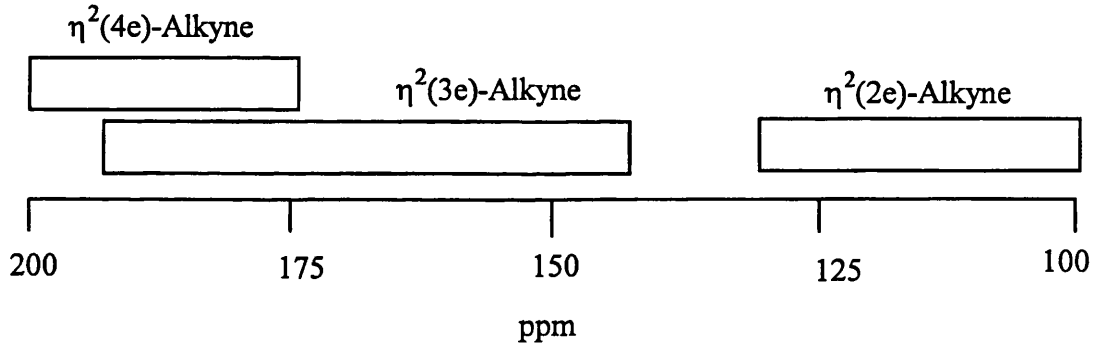

Figure 1.2: ^{13}C NMR chemical shift ranges for acetylenic carbons in alkyne complexes

Unfortunately, for phosphaalkynes the difference in the chemical shifts of the acetylenic carbons for the different coordination modes is too small to be diagnostic. Although the chemical shifts for η^1-coordinated phosphaalkynes are in a distinct region (155 - 185 ppm), those for the η^2(2e)- and η^2(4e)-coordinated ligands are less clearly defined. A comparison of the chemical shift values in the η^2(2e)-phosphaalkyne complex **1.4b** (310.6 ppm), with those for the η^2(4e)-phosphaalkyne complex **1.9** (315.2 ppm) indicates that the differences may be small (see Section 1.2.3.1). In contrast, the ^{31}P NMR spectra of coordinated phosphaalkynes show distinct variations between coordination modes. When the phosphaalkyne coordinates to the metal, the phosphorus atom is deshielded. The degree of

deshielding depends upon the coordination mode, and in turn affects the chemical shift of the phosphorus. For instance, free *tert*-butylphosphaalkyne has a chemical shift of –69 ppm, while η^2(2e)-coordinated phosphaalkynes have chemical shifts of approximately +80-250 ppm. Since η^2(4e)-coordinated phosphaalkynes use more electron density in coordinating to metal centres, they are deshielded more, and thus their signals in the ^{31}P NMR spectra are moved in the low field direction, and observed at approximately +400-550 ppm. The signals for η^1 phosphaalkynes are at higher field, since the coordination of the lone pair has a lesser effect on the shielding of the phosphorus nucleus. Their signals can be found in a large range of –150 - +50ppm. The range of signals for phosphaalkynes in ^{31}P NMR spectra is shown in Figure 1.3. As there is no overlap between the regions, the ^{31}P NMR chemical shift provides good evidence for the coordination mode.

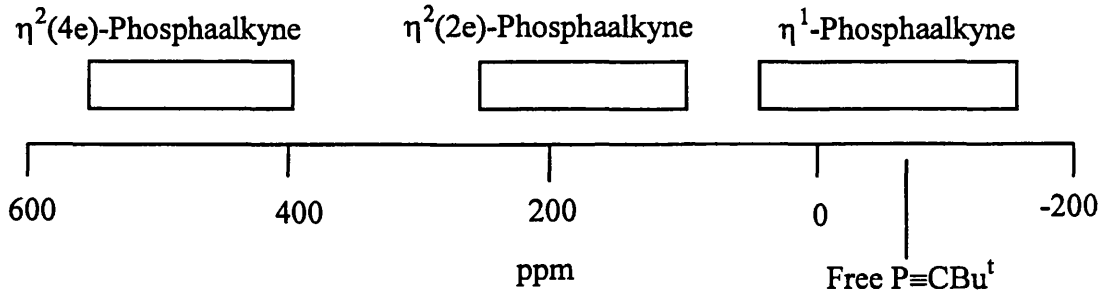

Figure 1.3: ^{31}P NMR chemical shift ranges in phosphaalkyne complexes

Although ^{31}P NMR spectroscopy is a useful diagnostic tool for phosphaalkyne complexes, the products made by the coupling reactions of one or more phosphaalkyne molecules on a metal centre, with each other and/or other ligands, are more difficult to identify by this means. For these compounds, X-ray crystallographic studies are the only certain way to identify them. To illustrate the points made in this section, where available values for δ(P) and δ(C) have been given throughout the chapter.

1.2.3 η^2-Coordinated Phosphaalkynes

1.2.3.1 η^2-Coordinated Phosphaalkynes on a Single Metal Centre

To date, mononuclear complexes with η^2-coordinated phosphaalkynes have been prepared with platinum, titanium, zirconium, tantalum and molybdenum as the central metal.

Binger and co-workers synthesised the titanium and zirconocene η^2(2e)-phosphaalkyne complexes **1.4** by various routes (Scheme 1.2).[8] An X-ray crystal structure has confirmed the η^2-bonding mode, and reveals that the P-C bond length is considerably lengthened upon coordination [1.636(2) Å, compared to 1.536(2) Å in the uncoordinated phosphaalkyne]. This is consistent with the back donation of electron density into the π^* orbitals (see Figure 1.1).

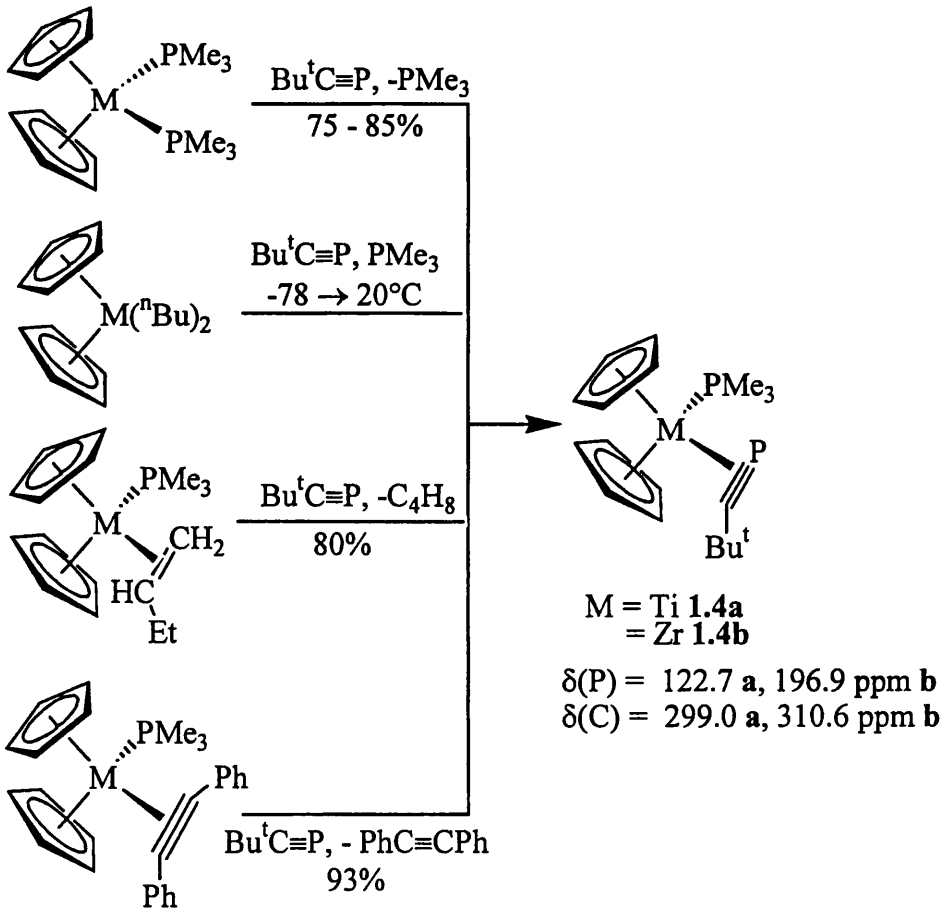

Scheme 1.2

The platinum phosphaalkyne complexes $[Pt\{\eta^2(2e)\text{-}P{\equiv}CBu^t\}(PR_3)_2]$ can be made by a variety of routes,[9] as shown in Scheme 1.3. A single crystal X-ray analysis of $[Pt\{\eta^2(2e)\text{-}P{\equiv}CBu^t\}(PPh_3)_2]$ reveals that the P-C bond length is 1.672(13) Å. The increased length of the P-C bond compared to that seen in the titanium complex is presumably a consequence of the more electron rich metal increasing the back donation to the π^* orbitals of the phosphaalkyne.

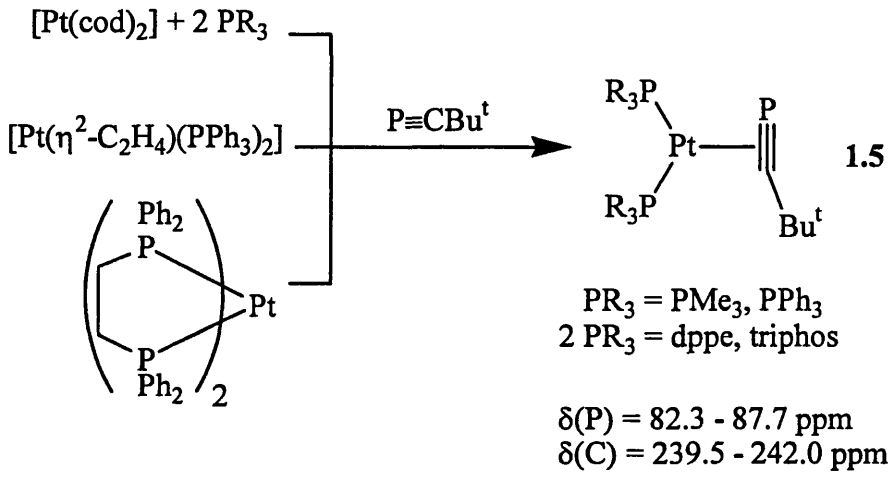

Scheme 1.3

Stilbene can be displaced by *tert*-butylphosphaalkyne from the zwitterionic 16 electron complex $[Mo(\eta^2\text{-}PhCH{=}CHPh)\{\eta^2\text{-}(MeO)_2POBF_2OP(OMe)_2\}(\eta^5\text{-}C_5H_5)]$, to give the $\eta^2(4e)$-phosphaalkyne complex shown in Scheme 1.4.[10] A similar reaction[11] can be carried out using the molybdenum complex $[Mo(\eta^2\text{-}PhCH{=}CHPh)\{P(OMe)_3\}_2(\eta^5\text{-}C_5H_5)][BF_4]$, the product of which is shown in Scheme 1.5.

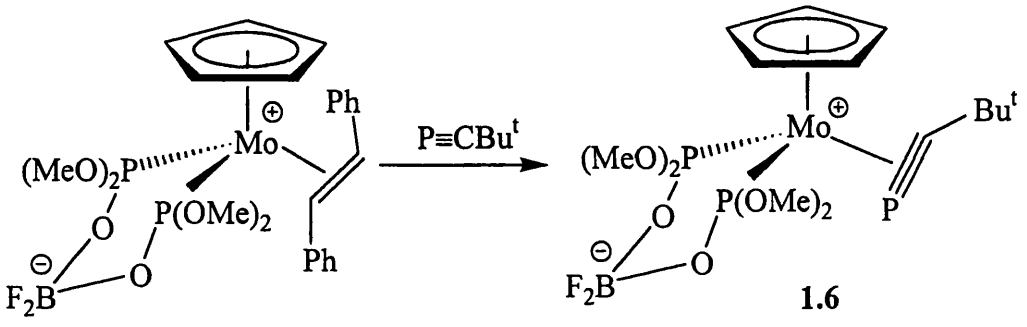

Scheme 1.4

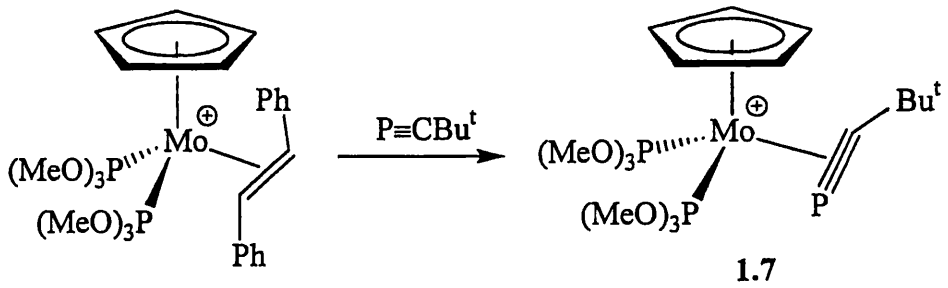

1.7

$\delta(P) = 492.3$ ppm
$\delta(C) = 334.6$ ppm

Scheme 1.5

The tantalum complex $[TaCl_2(CO)_2(\eta^5\text{-}C_5Me_5)].THF$ reacts with *tert*-butylphosphaalkyne with loss of carbon monoxide to give the complex $[TaCl_2\{\eta^2(4e)\text{-}P{\equiv}CBu^t\}(\eta^5\text{-}C_5Me_5)]$.[12] This is shown in Scheme 1.6.

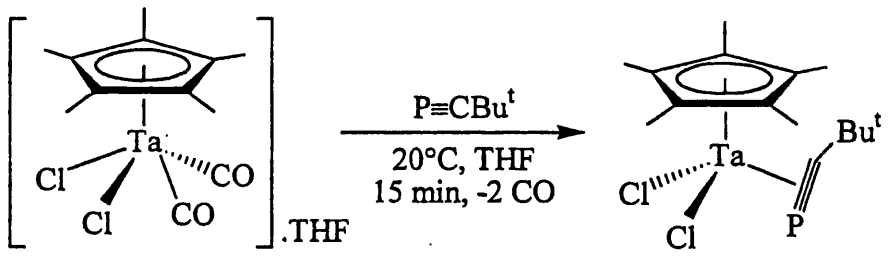

1.8

$\delta(P) = 509.9$ ppm
$\delta(C) = 337.2$ ppm

Scheme 1.6

The $\eta^2(4e)$-phosphaalkyne complex **1.9** was prepared by Nixon and co-workers by reacting $[WF(CO)_3(C_6H_4CH_2NMeCH_2CH_2NMe_2)]$ with *tert*-butylphosphaalkyne.[13] The complex exists only as an intermediate in a phosphaalkyne – carbon monoxide coupling reaction, but is identified by its $^{31}P\{^1H\}$ NMR spectrum. The reaction is shown in Scheme 1.7.

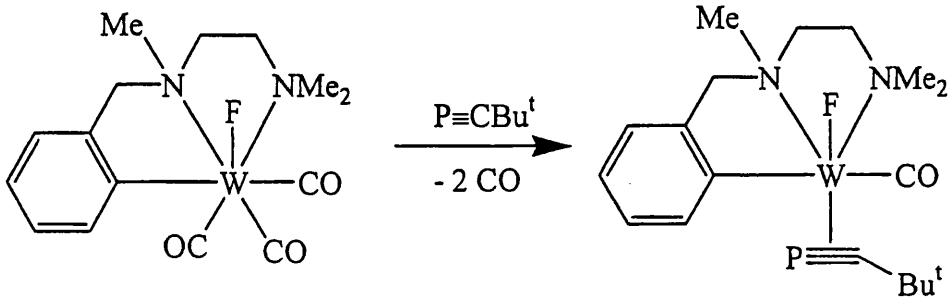

1.9

$\delta(P) = 452.4$ ppm
$\delta(C) = 315.2$ ppm

Scheme 1.7

1.2.3.2 η^2-Coordinated Phosphaalkynes on Multiple Metal Centres

It has been shown[14] that several dinuclear metal complexes react with alkynes to form tetrahedral bimetallic complexes where the alkynes are coordinated in an η^2,η^2 manner, using all four π electrons. These dinuclear complexes can also react with *tert*-butylphosphaalkyne to form the analogous phosphaalkyne complexes.[15] For example, the molybdenum dimer $[Mo_2(CO)_4(\eta^5\text{-}C_5H_5)_2]$ reacts with *tert*-butylphosphaalkyne to form the complex **1.10**, as shown in Scheme 1.8.

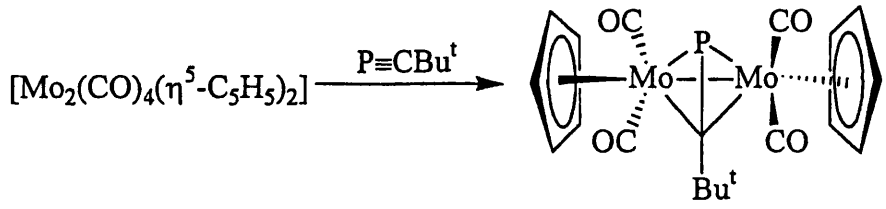

Scheme 1.8 **1.10**

A single crystal X-ray crystallographic study on **1.10** indicated that the P-C bond length is 1.719(3) Å. This is longer than in the platinum η^2(2e) complexes, but not as long a P-C single bond (1.82 – 1.87 Å). This is consistent with the population of the second set of π^* orbitals.

Mixed bimetallic complexes of this type may also be made,[15b] as shown in Scheme 1.9.

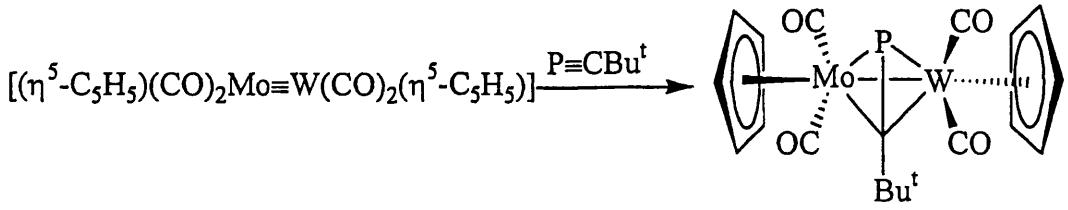

1.11

Scheme 1.9

A third type of η^2-coordinated phosphaalkyne complex is known.[16] This contains a trimetallic core, and the phosphaalkyne in a μ_3,η^2-bonding mode. An example shown in Scheme 1.9.

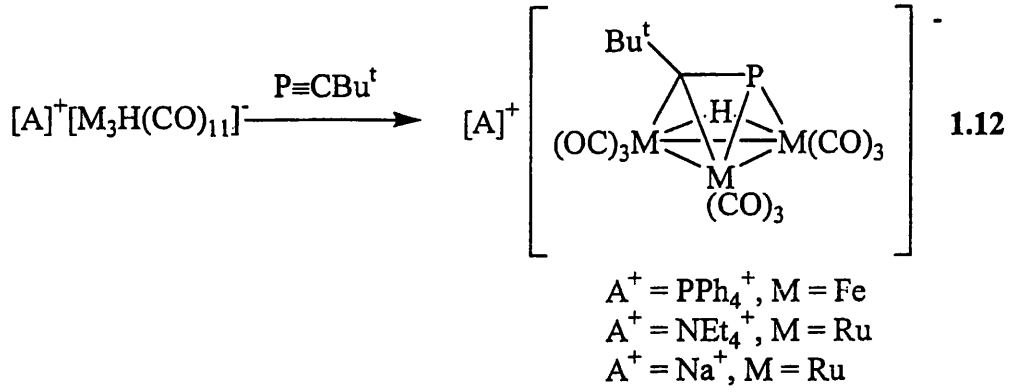

$A^+ = PPh_4^+$, M = Fe
$A^+ = NEt_4^+$, M = Ru
$A^+ = Na^+$, M = Ru

Scheme 1.10 δ(P) = 274.2 - 295.6 ppm

1.2.4 η^1-Coordinated Phosphaalkynes

The reaction of either *tert*-butyl or 1-adamantylphosphaalkyne with the complexes *trans*-$[M(N_2)_2(R_2PCH_2CH_2PR_2)_2]$, results in the displacement of either one or both dinitrogen ligands by the phosphaalkyne to give the complexes **1.13a-c** and **1.14a-c** (Scheme 1.11).[17] The steric bulk of the two chelating phosphines is such that η^2 coordination is unfavourable, so the phosphaalkynes adopt η^1-coordination.

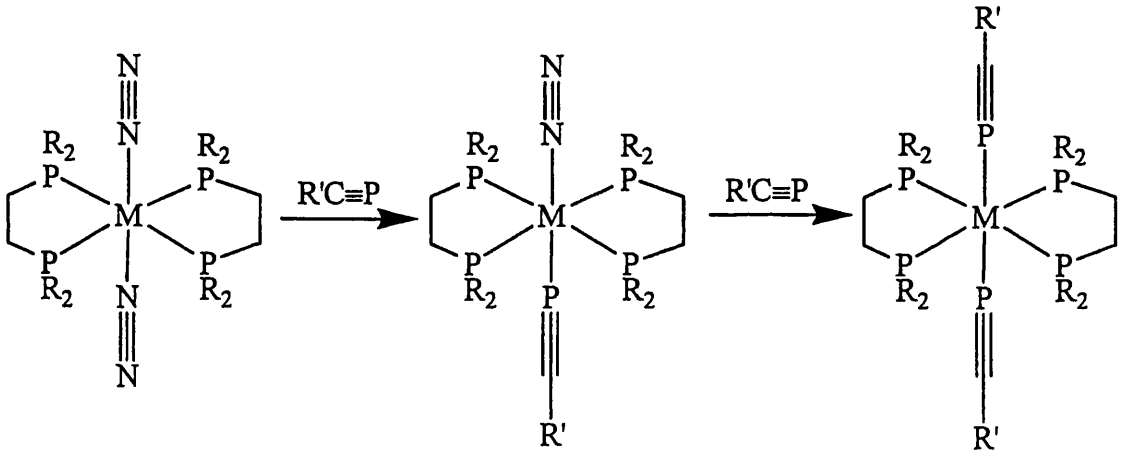

1.13a-c

a - M = Mo, R = Et, R' = Bu^t δ(P) = 7.2 ppm **a**
b - M = Mo, R = Et, R' = 1-Ad 10.0 ppm **b**
c - M = W, R = Ph, R' = Bu^t 0.1 ppm **c**

1.14a-c

δ(P) = 0.3 ppm **a**
7.7 ppm **b**
-16.9 ppm **c**

Scheme 1.11

The related complexes $[M(CO)_3(PCy_3)_2(\eta^1\text{-}P{\equiv}CMes^*)]$ (M = Mo, **1.15a** or W, **1.15b**)[18], $[Ru(CO)_2(PPh_3)_2(\eta^1\text{-}P{\equiv}CMes^*)]$ **1.16**[19], *trans*-$[ReCl(\eta^1\text{-}P{\equiv}CBu^t)(dppe)_2]$ **1.17**[20], and *trans*-$[FeH(\eta^1\text{-}P{\equiv}CBu^t)(dppe)_2][A]$ (A = BPh_4^-, **1.18a** or BF_4^-, **1.18b**)[20b,21] have also been prepared. Their syntheses are shown in Schemes 1.12 – 1.15. Crystallographic studies have shown that upon coordination the P≡C bond length is comparable with that in the free phosphaalkyne [1.520(12) Å for **14a**, 1.54(2) Å for **15b**, 1.512(5) Å for **18b**].

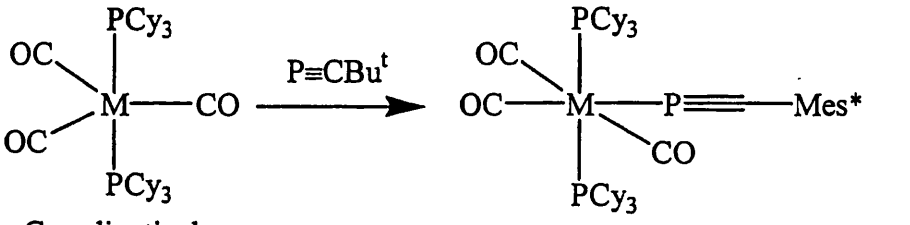

Coordinatively unsaturated

1.15a+b

M = Mo, **a**
M = W, **b**

δ(P) = 54.1 ppm, **a**
24.4 ppm, **b**

Scheme 1.12

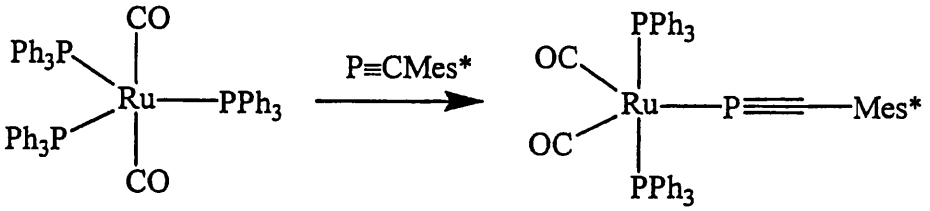

1.16

δ(P) = 45.3 ppm
δ(C) = 158.7 ppm

Scheme 1.13

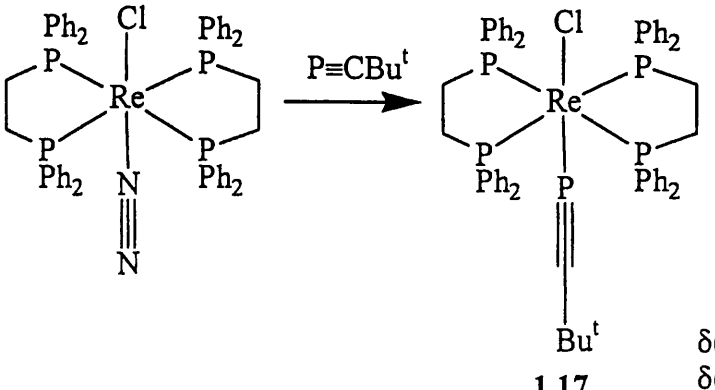

1.17

δ(P) = -154.0ppm
δ(C) = 183.4 ppm

Scheme 1.14

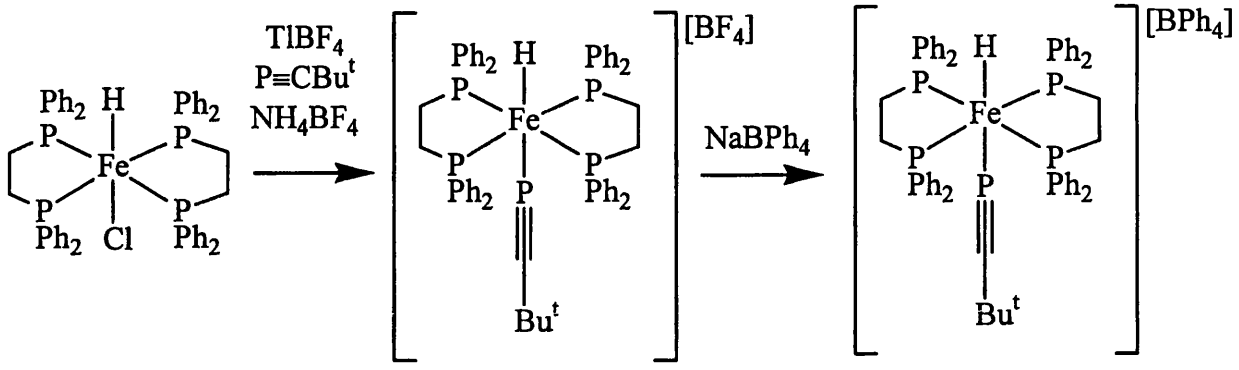

1.18a **1.18b**

δ(P) = -154.0ppm
δ(C) = 183.4 ppm

Scheme 1.15

The P≡C bond in η^1-coordinated phosphaalkynes is activated to nucleophiles. The rhenium complex *trans*-[ReCl(η^1-P≡CBu^t)(dppe)$_2$], **1.17**, reacts with water[20] to form the novel η^1-phosphinidine oxide complex *trans*-[ReCl{η^1-P(O)CH$_2$Bu^t}(dppe)$_2$], **1.19**, as shown in Scheme 1.16.

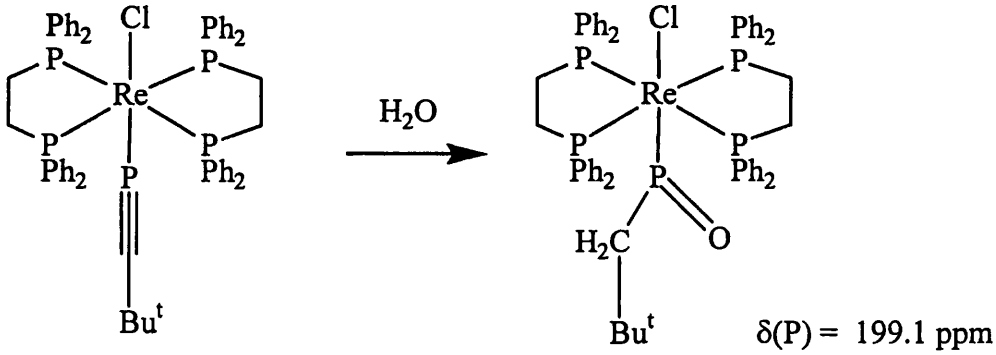

1.17 **1.19**

δ(P) = 199.1 ppm

Scheme 1.16

The iron complex *trans*-[Fe(dppe)$_2$(η^1-P≡CBu^t)H][BF$_4$], **1.18a**, undergoes spontaneous decomposition[20b] to give the η^1-fluorophosphaalkene complex *trans*-[Fe(dppe)$_2$(η^1-PF=CHBu^t)H][FeCl$_2$F], **1.20**. The reaction involves formal addition of HF across the triple bond. The HF is assumed to have originated from the BF_4^- counterion, whilst the unusual anion indicates that the solvent must be involved. Reacting **1.18a** with HBF$_4$ gives the tetrafluoroborate derivative of **1.20**.[21]

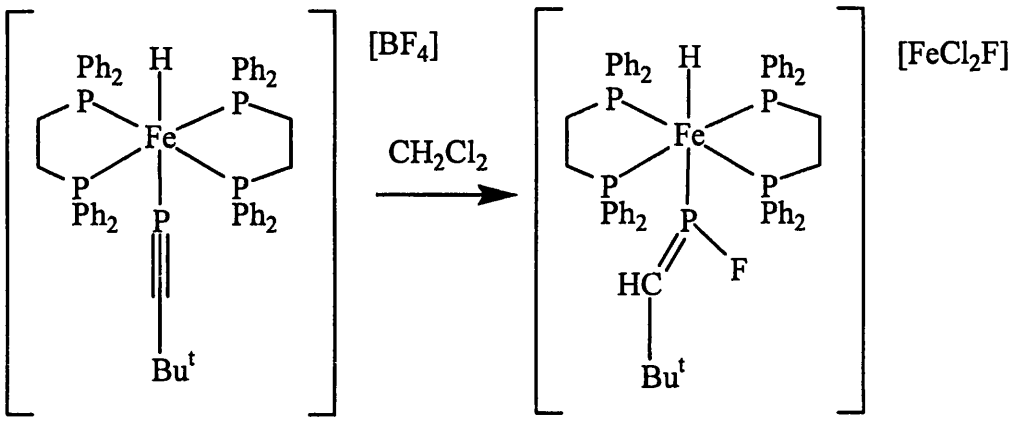

1.18a **1.20**

$\delta(P) = 177.6$ ppm

Scheme 1.17

1.2.5 Mixed η^1- and η^2-Coordinated Phosphaalkynes

Unlike the analogous alkyne complexes, an η^2-coordinated phosphaalkyne may coordinate to another metal centre *via* the lone pair of electrons on phosphorus. In this situation, the phosphaalkyne is undergoing both η^2- and η^1-coordination at the same time.

The platinum η^2(2e)-phosphaalkyne complexes shown in Scheme 1.3 can coordinate to a $M(CO)_5$ metal fragment,[3b] an example of which is shown in Scheme 1.18.

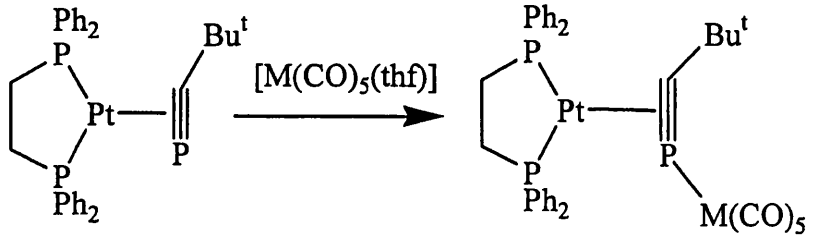

M = Cr, Mo, W

1.21

Scheme 1.18

If the titanocene phosphaalkyne complex $[Ti(PMe_3)\{\eta^2(2e)\text{-}P{\equiv}CBu^t\}(\eta^5\text{-}C_5H_5)_2]$ is reacted with BEt_3, the Lewis acid abstracts the phosphine[8]. The product, is the

dimeric species **1.22** shown in Scheme 1.19. One of the phosphaalkynes is coordinating in an η^2(4e) manner to one titanium centre, and in an η^1 fashion to the other. NMR evidence suggests that **1.22** exists in equilibrium with a mononuclear η^2(4e)-phosphaalkyne complex, but structural confirmation is not available.

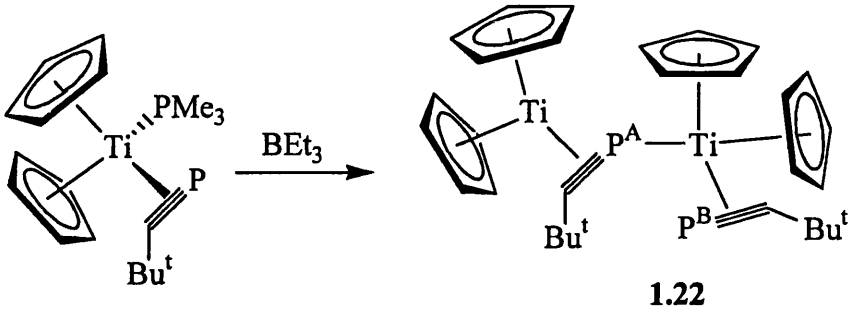

1.22

δ(P) = 438.4 ppm, P^A
73.5 ppm, P^B

Scheme 1.19

In contrast, the zirconocene analogue forms the trimeric system **1.23**, which is shown in Scheme 1.20. Each phosphaalkyne is coordinating as an η^2(2e)-donor to one zirconium centre, and in an η^1 manner to another. The P-C bond lengths in this complex [1.646(4) – 1.649(4) Å] are similar to that observed for complex **1.4b**.

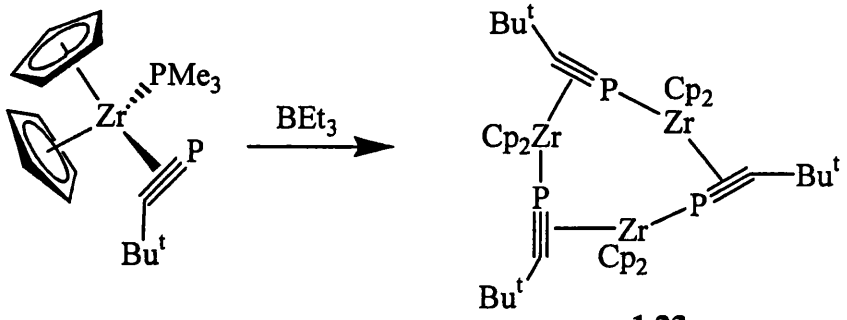

1.23

δ(P) = 198.7 ppm
δ(C) = 301.2 ppm

Scheme 1.20

The μ_2,η^2,η^2-phosphaalkyne complexes have been shown to coordinate to a variety of metal fragments.[22] For example, $[Mo_2(CO)_4(\mu_2,\eta^2,\eta^2\text{-P}{\equiv}CBu^t)(\eta^5\text{-}C_5H_5)_2]$ will react with $[W(CO)_5(THF)]$ to produce the trimetallic complex **1.24** shown in Scheme

1.21, in which the phosphaalkyne is formally acting as a six electron donor. The C-P bond length of 1.732(4) Å is similar to that for **1.10** [1.719(3) Å].

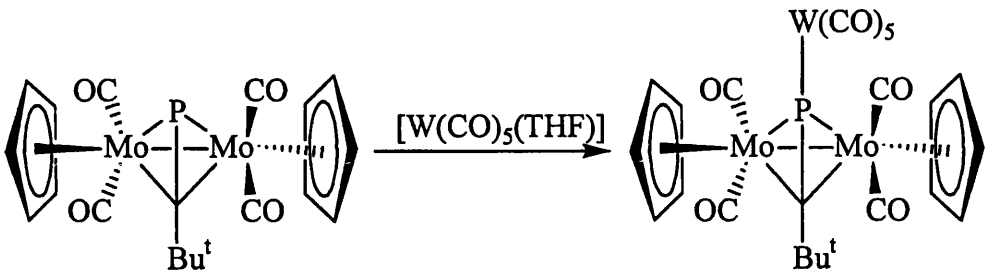

1.10 **1.24**

Scheme 1.21

Another type of trimetallic complex in which the phosphaalkyne coordinates in both an η^2,η^2 and an η^1 manner is known.[9b] By reacting the mononuclear platinum complex [Pt{η^2(2e)-P≡CBu^t}(dppe)] with either of the iron carbonyl clusters [$Fe_2(CO)_9$] or [$Fe_3(CO)_{12}$], a trimetallic three membered Fe_2Pt ring is formed. The phosphaalkyne transversely bridges the Fe-Fe bond, so that the phosphorus atom is coordinated to all three metal centres. This is shown in Scheme 1.22.

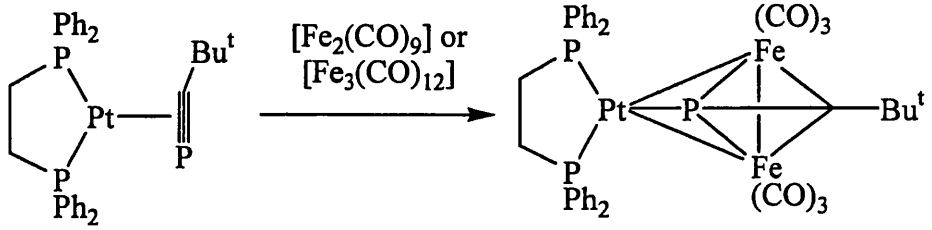

1.25

δ(P) = 87.9 ppm

P-C = 1.703(6) Å

Scheme 1.22

If the platinum phosphaalkyne complex [Pt{η^2(2e)-P≡CBu^t}(PPh_3)$_2$] is reacted with [$Pd(PPh_3)_4$], then the pentametallic cluster **1.26** shown in Scheme 1.23 is formed.[23] Each phosphaalkyne is coordinating using both P≡C π-bonds and its lone pair. If [$Pd(PPh_3)_4$] is reacted with free *tert*-butylphosphaalkyne, then the pentapalladium analogue is formed.[3b]

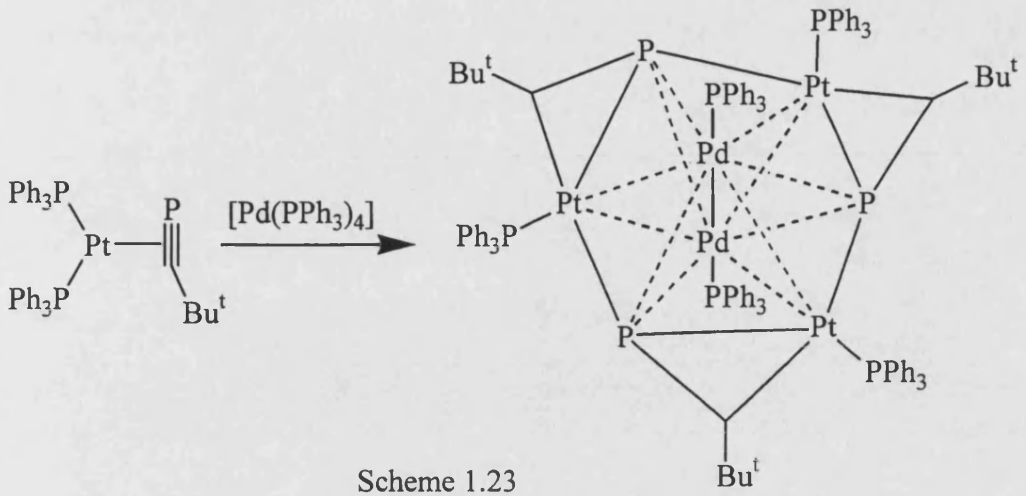

Scheme 1.23 **1.26**

1.3 Metal-mediated Coupling Reactions of Phosphaalkynes

1.3.1 Phosphaalkyne Cyclooligomerisations

The thermal oligomerisation of neat phosphaalkyne is believed to proceed initially *via* a dimerisation.[5] It is thought that two molecules of the phosphaalkyne undergo a classically symmetry forbidden [2+2] cycloaddition to produce free 1,3-diphosphacyclobutadiene, **1.27**. This unstable species is then believed to undergo another two cyclisation reactions to give the stable tetraphosphacubane **1.28** as the end product (Scheme 1.24).

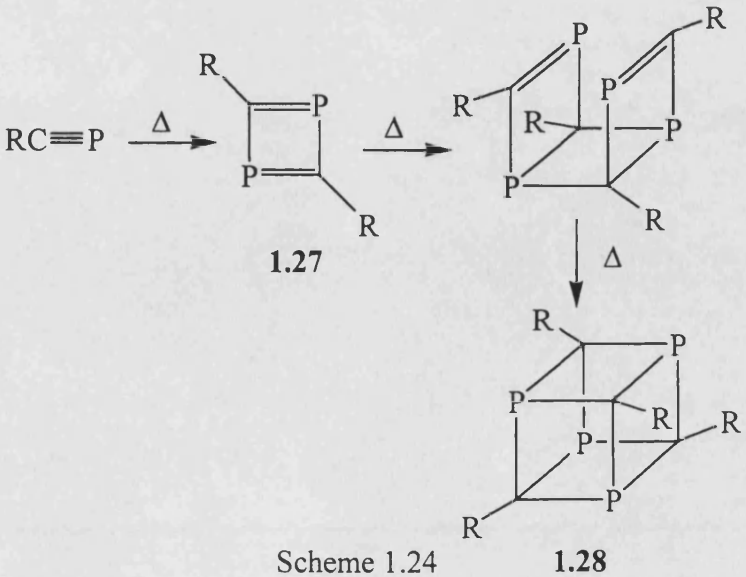

Scheme 1.24 **1.28**

Addition of a Lewis acid such as EX_3 (E = Al or Ga, X = halide) or AlR_3 initiates the cyclooligomerisation at lower temperatures (0 - 20°C), leading to the formation of a variety of cage compounds, with incorporation of the Lewis acid moiety.[24] The precise nature of the product depends upon the identity and ratio of the reactants used.

The reactions of phosphaalkynes on unsaturated transition metal centres are characterised by such cyclooligomerisations. However, the presence of the metal centre allows the stabilisation of otherwise reactive products.

The transition metal mediated cyclooligomerisation of alkynes often occurs as a trimerisation to give the benzene derivatives.[25] For example, the nickel complex $[Ni(CO)_2(PPh_3)_2]$ is used commercially as a catalyst in the synthesis of trisubstituted benzene derivatives from the terminal alkyne $HC{\equiv}CCO_2Me$. In contrast, the analogous reactions with phosphaalkynes often result in a dimerisation to produce 1,3-diphosphacyclobutadiene rings, η^4-coordinated to the metal centre.

1.3.1.1 Dimerisation of Phosphaalkynes

When nickel bis(acetylacetonate) is reduced with *n*-butyl lithium, with the subsequent addition of *tert*-butylphosphaalkyne, the product is a Ni^0 sandwich compound with two η^4-1,3-diphosphacyclobutadiene ligands (Scheme 1.25).[26]

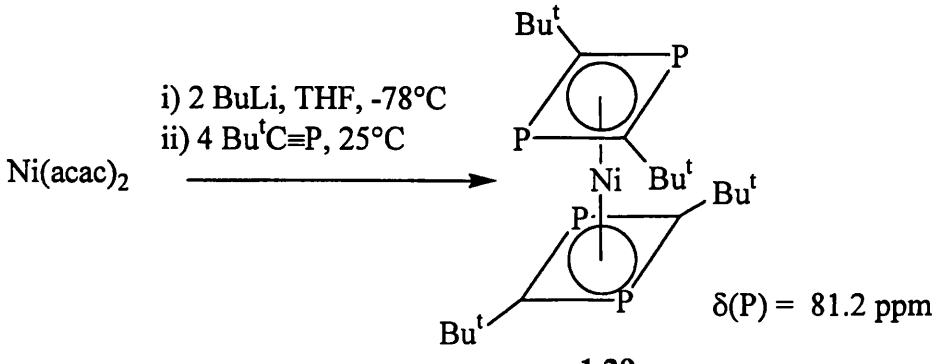

1.29

Scheme 1.25

If the complexes $[M(\eta^2\text{-}C_2H_4)_2(\eta^5\text{-}L)]$ (where M = Co or Rh, and L = C_5H_5, C_5Me_5 or C_9H_7) are reacted with two equivalents of phosphaalkyne, then the ethene is displaced to form the η^4-1,3-diphosphacyclobutadiene complexes as is shown in Scheme 1.26.[27]

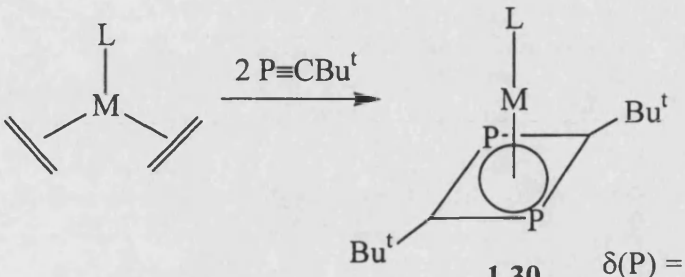

1.30 δ(P) = 18 - 50 ppm

M = Co or Rh
L = η^5-C_5H_5, C_5Me_5 or C_9H_7

Scheme 1.26

When the metal is cobalt, these complexes are formed in good yield (~85%). With rhodium however, the yields are much lower (30 - 50%) due to competing side reactions. One of these reactions, which occurs when L = indenyl, leads to the formation of the trinuclear rhodium complex **1.31**, shown in Figure 1.4 in 13% yield.[27d]

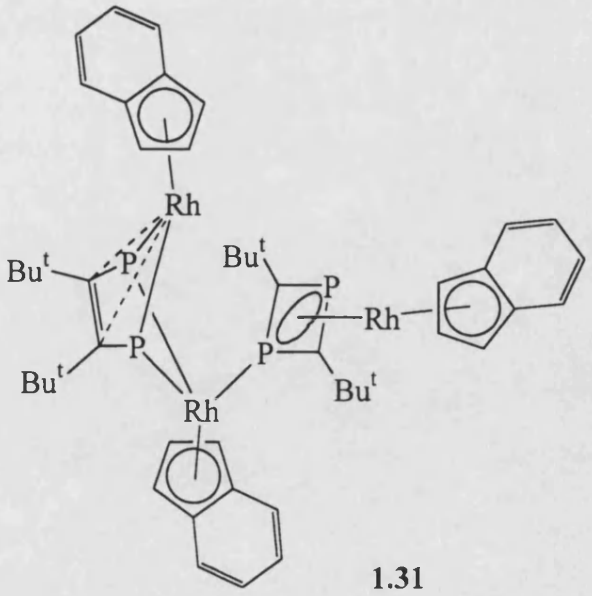

1.31

Figure 1.4: Structure of complex **1.31**

The mechanism for the formation of these η^4-1,3-diphosphacyclobutadiene complexes has been suggested to proceed *via* the formation of diphospha-metallacyclopentadiene complexes. This suggestion is supported by the reaction of $[RhCl(\eta^2\text{-}C_2H_4)_2]_2$ with *tert*-butylphosphaalkyne in the presence of PMe_3, shown in Scheme 1.27.[28]

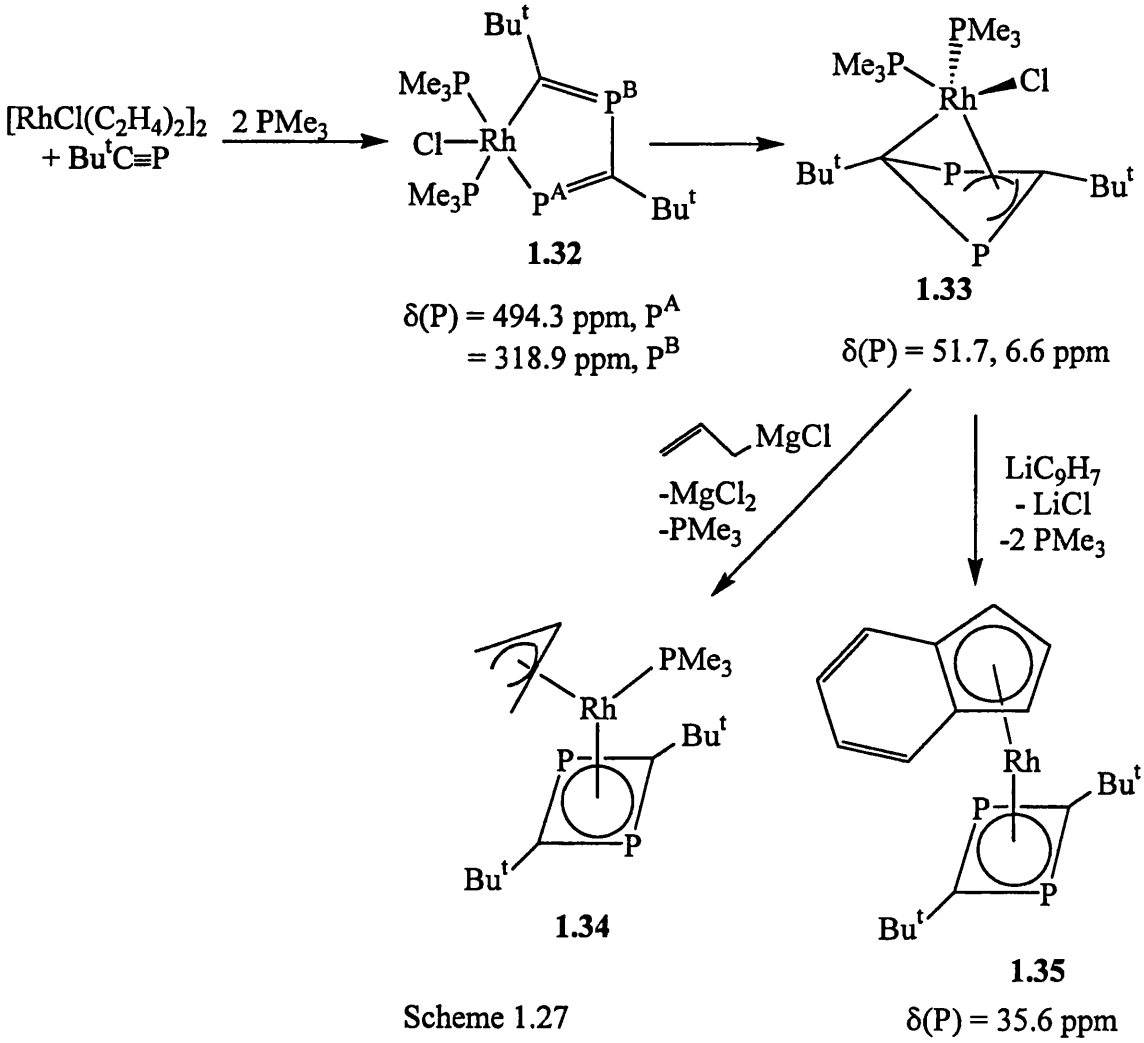

Scheme 1.27

In solution **1.32** slowly rearranges to form **1.33**. In this complex, the four-membered ring is not considered to bind in an η^4 fashion, but instead has η^1,η^3 character. This can be converted to the more usual η^4 1,3-diphosphacyclobutadiene complex by reacting **1.33** with either an allyl Grignard reagent, or with lithium indenyl.

The first step in the dimerisation of phosphaalkynes at transition metal centres is believed to be the formation of an η^2-bonded phosphaalkyne complex. Such a

reaction is seen when a second equivalent of *tert*-butylphosphaalkyne is added to the η^2(4e)-phosphaalkyne complex **1.6**.[10b] The product is the η^4 1,3-diphosphacyclobutadiene complex **1.37**, as shown in Scheme 1.28.

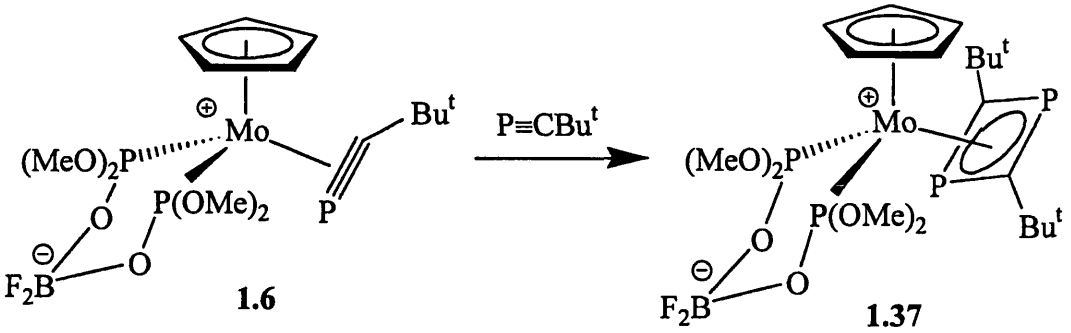

1.6 **1.37**

Scheme 1.28 δ(P) = 56.5, 51.1 ppm

Not all phosphaalkyne cyclodimerisations give 1,3-diphosphacyclobutadiene complexes. Whilst this four membered ring is formed by a 'head-to-tail' dimerisation, a 'head-to-head' mechanism is also possible to give as the product an η^4 1,2-diphosphacyclobutadiene complex. In the reaction between the titanium complex [Ti(η^4-C_8H_8)(η^8-C_8H_8)] and two equivalents of phosphaalkyne, two products, **1.38** and **1.39**, are formed (Scheme 1.29).[29] Increasing the steric bulk of the substituent on the phosphaalkyne increases the relative proportion of **1.38** in the product mixture, presumably as in this complex steric interactions are minimised. So when R = Bu^t, the product ratio between **1.38** and **1.39** is 11:9, whilst if R = 1-adamantyl, the ratio is 3:2. If R = N(Pr^i)(SiMe$_3$), **1.38** is selectively formed.

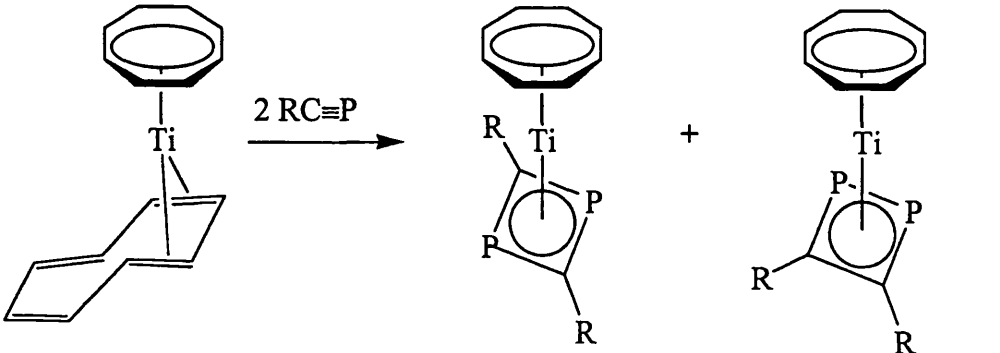

R = Bu^t, **a**
= 1-Ad, **b**
= N(Pr^i)(SiMe$_3$), **c**

1.38a-c
δ(P) = 214.5, **a**
= 213.4, **b**
= 117.0, **c**

1.39a+b
δ(P) = 133.6, **a**
= 139.7, **b**

Scheme 1.29

The reaction of the tantalum complex $[TaCl_2\{\eta^2(4e)\text{-}P{\equiv}CBu^t\}(\eta^5\text{-}C_5Me_5)]$ with *tert*-butylphosphaalkyne is more selective. The 1,2-diphosphacyclobutadiene complex **1.40**, as shown in Scheme 1.30, is quantitatively formed.[12]

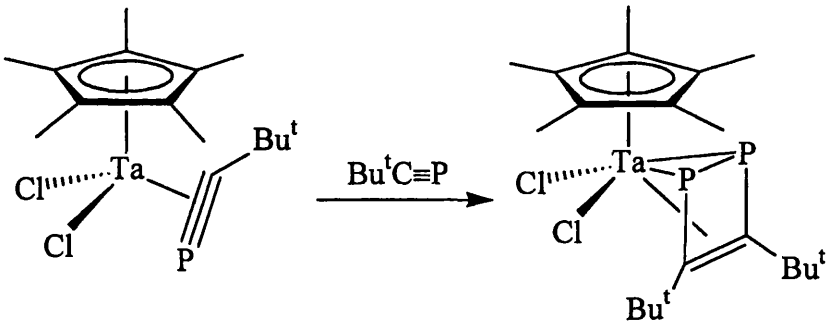

1.8 **1.40**

Scheme 1.30 $\delta(P) = 31.8$ ppm

Computational work carried out by Nguyen and co-workers[30] indicates that in the free state, the formation of the 1,2-diphosphacyclobutadiene ring is both kinetically and thermodynamically favoured. This is also true for both the systems $[Co(\eta^4\text{-}1,3\text{-}P_2C_2Bu^t_2)(\eta^5\text{-}L)]$ and $[Ti(\eta^4\text{-}1,3\text{-}P_2C_2Bu^t_2)(\eta^4\text{-}cot)]$. The reaction mechanism *via* the diphospha-metallacyclopentadiene complexes as proposed by Binger and Regitz[28] was possible for the titanium complex, but energetically disfavoured for the cobalt system. However, another possible intermediate was found, a tilted 1,3-diphosphabicyclo[1.1.0]butadienyl complex, as shown in Figure 1.5.

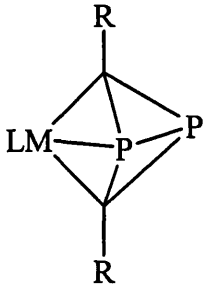

1.41

M = Co or Ti
L = η^5-C_5H_5 or η^4-C_8H_8
R = H or Me

Figure 1.5: Putative reaction intermediate in phosphaalkyne dimerisation

This proposed intermediate is itself related to a known product of metal-mediated phosphaalkyne dimerisation.[3b,31] A zirconium analogue has been prepared through

many routes, which are believed to proceed *via* the η^2(4e) phosphaalkyne complex **1.42** (Scheme 1.31).

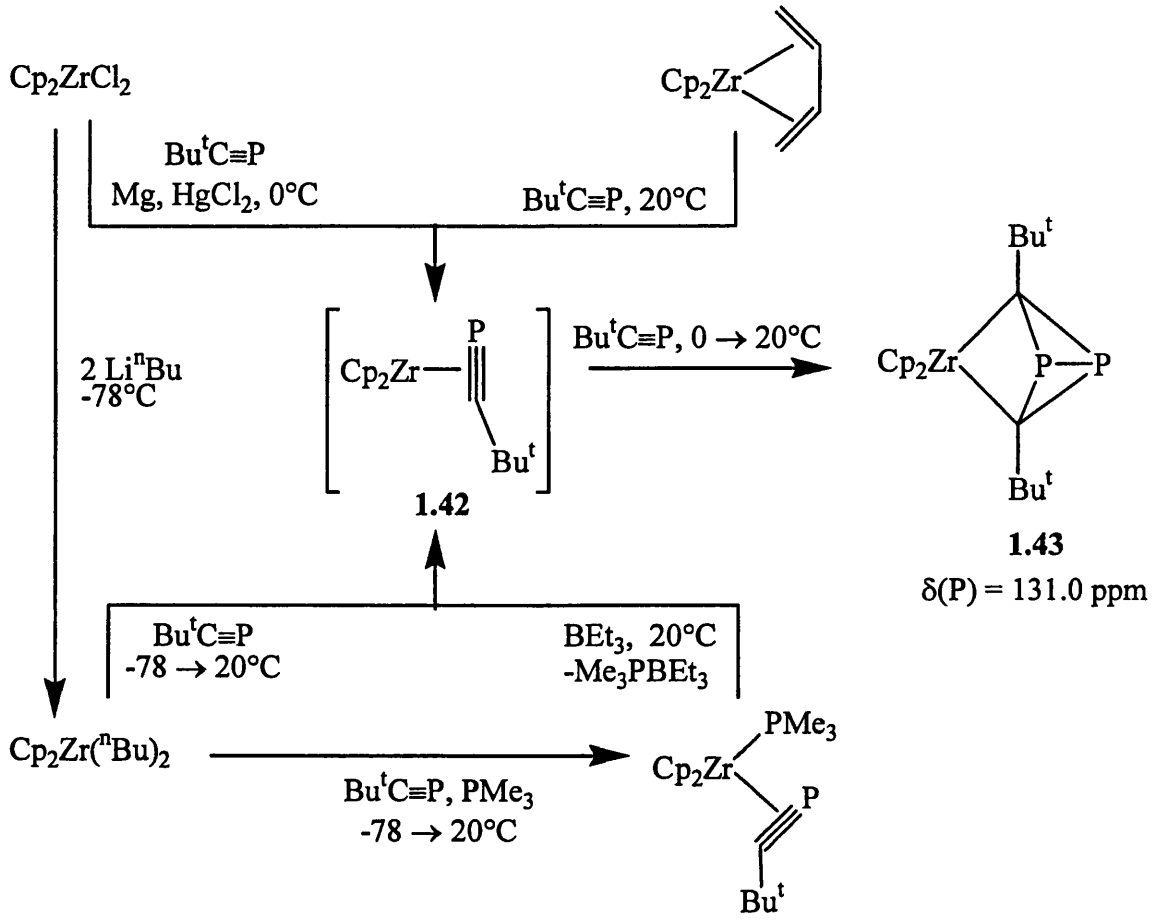

Scheme 1.31 **1.5b**

If the zirconium complex **1.43** is reacted with the nickel complex $[NiCl_2(PPh_3)_2]$, the nickel is believed to be exchanged with the zirconium to give the analogous nickel complex **1.44**.[32] This is not itself observed, as it is thought to be highly unstable and to decompose *via* the 1,2-diphospha-4-nickella-cyclopentadiene complex **1.45** to give another unstable proposed intermediate, free 1,2-diphosphaacyclobutadiene, **1.46**. This is then believed to dimerise by a [2+2] cycloaddition to give the tetrameric species **1.47**, shown in Scheme 1.32, which has been isolated.

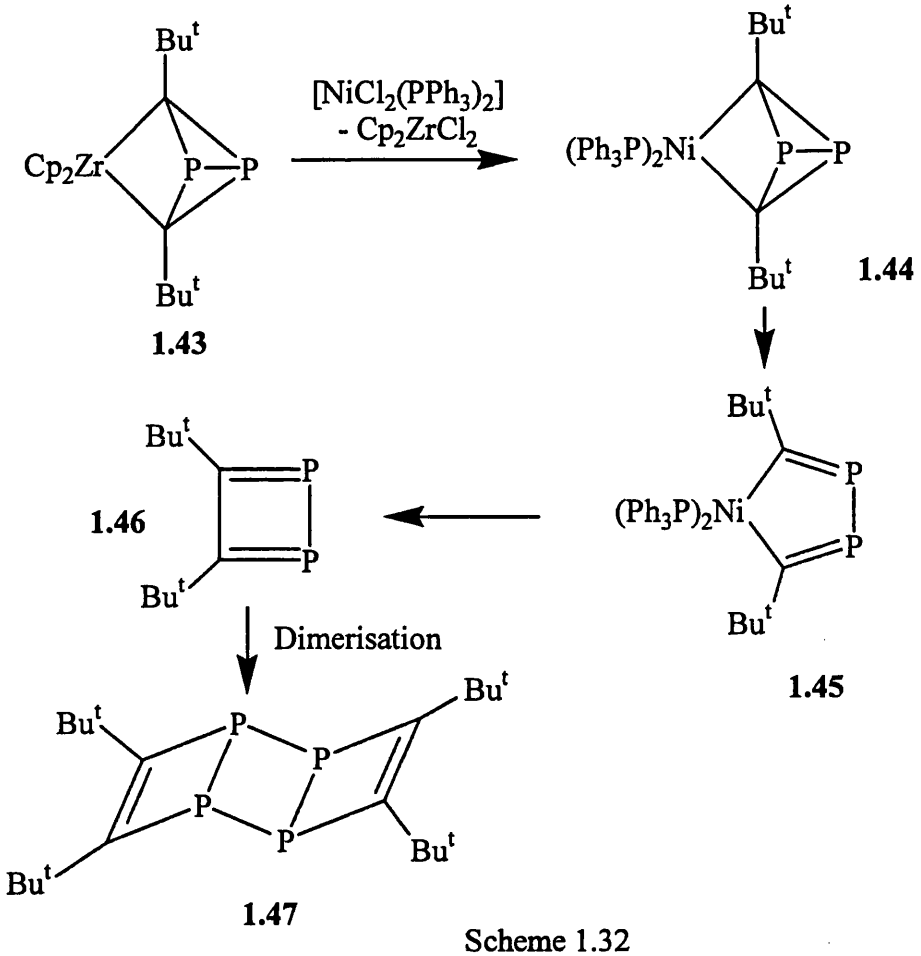

Scheme 1.32

Although most 1,3-diphosphacyclobutadiene complexes are stable, they do undergo some reactions. The lone pairs of electrons on the phosphorus atoms can be used to coordinate to other metal centres. For example, if in the preparation of $[Co(\eta^4\text{-}1,3\text{-}P_2C_2Bu^t_2)(\eta^5\text{-}C_5H_5)]$ an excess of $[Co(\eta^2\text{-}C_2H_4)_2(\eta^5\text{-}C_5H_5)]$ is used, the dinuclear and trinuclear complexes **1.48** and **1.49** shown in Scheme 1.33 are formed.[27b,c] With the addition of more phosphaalkyne, the Co-P σ-bond to phosphorus can be broken and more of the simple 1,3-diphosphacyclobutadiene complex produced.

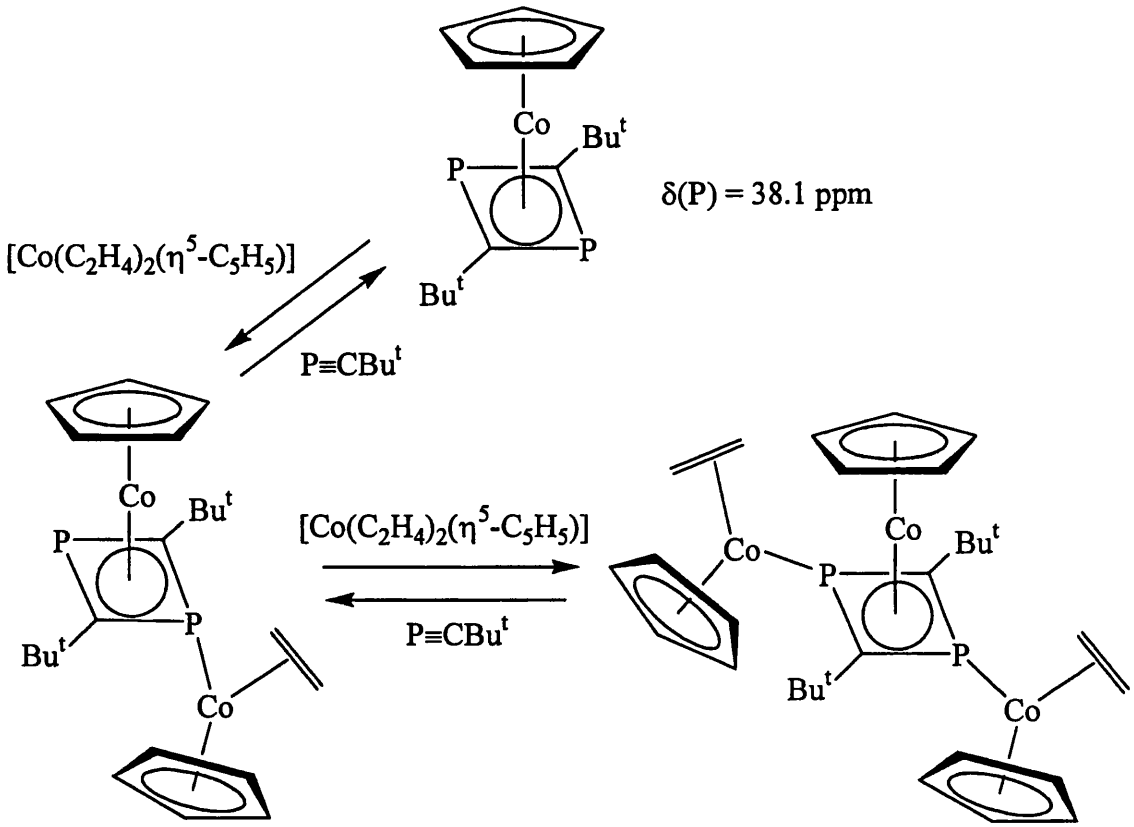

1.48

δ(P) = 134.9, -32.0 ppm

1.49

δ(P) = 85.9 ppm

Scheme 1.33

Similar reactions of this type have been shown to occur with the rhodium analogues.[33] By reacting $[Rh(\eta^4\text{-}1,3\text{-}P_2C_2Bu^t_2)(\eta^5\text{-}C_5H_5)]$ with $[Rh(\mu\text{-}Cl)(\eta^2\text{-}C_2H_4)_2]_2$, the hexametallic complex **1.50** shown in Figure 1.6 is formed.

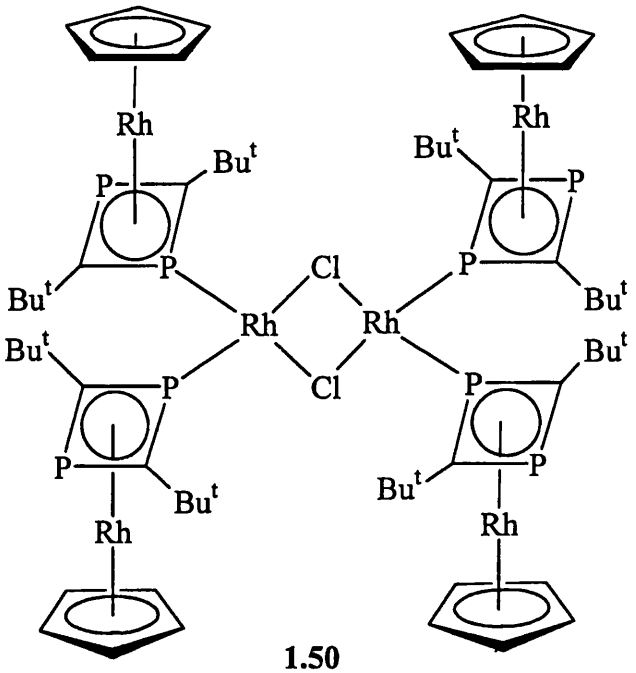

1.50

Figure 1.6: Structure of hexametallic complex **1.50**

An unusual phenomenon is seen in the crystal structure of $[Mo(CO)_2(\eta^4\text{-}1,3\text{-}P_2C_2Bu^t_2)(\eta^5\text{-}C_9H_7)][BF_4]$, **1.51**, which is made by reacting $[Mo(CO)_2(MeCN)_2(\eta^5\text{-}C_9H_7)][BF_4]$ with *tert*-butylphosphaalkyne.[34] Although in solution it is a normal η^4-1,3-diphosphacyclobutadiene complex on the NMR timescale, in the solid state it no longer acts as such. Instead the heterocyclic ring is coordinated in an η^3 fashion, with one of the fluorine atoms from the BF_4^- counter ion interacting with the non-coordinated phosphorus atom [P-F distance = 1.536(5) Å] (Figure 1.7).

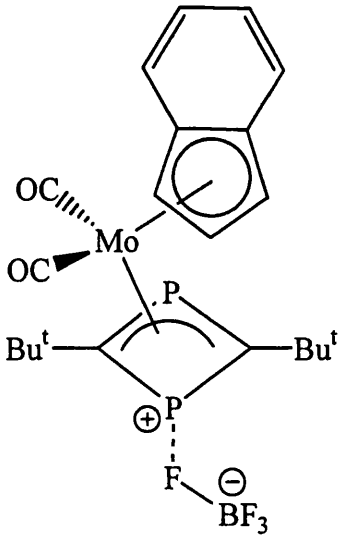

Figure 1.7: Structure of **1.51** in the solid state

1.3.1.2 Other Oligomerisation Reactions of Phosphaalkynes

Although the cyclisation reactions of phosphaalkynes at metal centres are most commonly dimerisations, there are some examples of cyclooligomerisations known.

In the reaction between tantalum pentachloride and *tert*-butylphosphaalkyne, two molecules of phosphaalkyne initially insert into two Ta-Cl bonds.[35] A [2+2] cyclisation reaction then produces the 1,3-diphospha-5-tantalabicyclo[1.1.0]pentane system **1.52**. This is assumed to react with a third molecule of phosphaalkyne and rearrange to give the unstable phosphenium cation **1.53**. Ring closure with the formation of a P-P bond gives the final product **1.54**. The proposed reaction scheme is shown in Scheme 1.34. The origin of the oxygen atom in the final product is not known at this time.

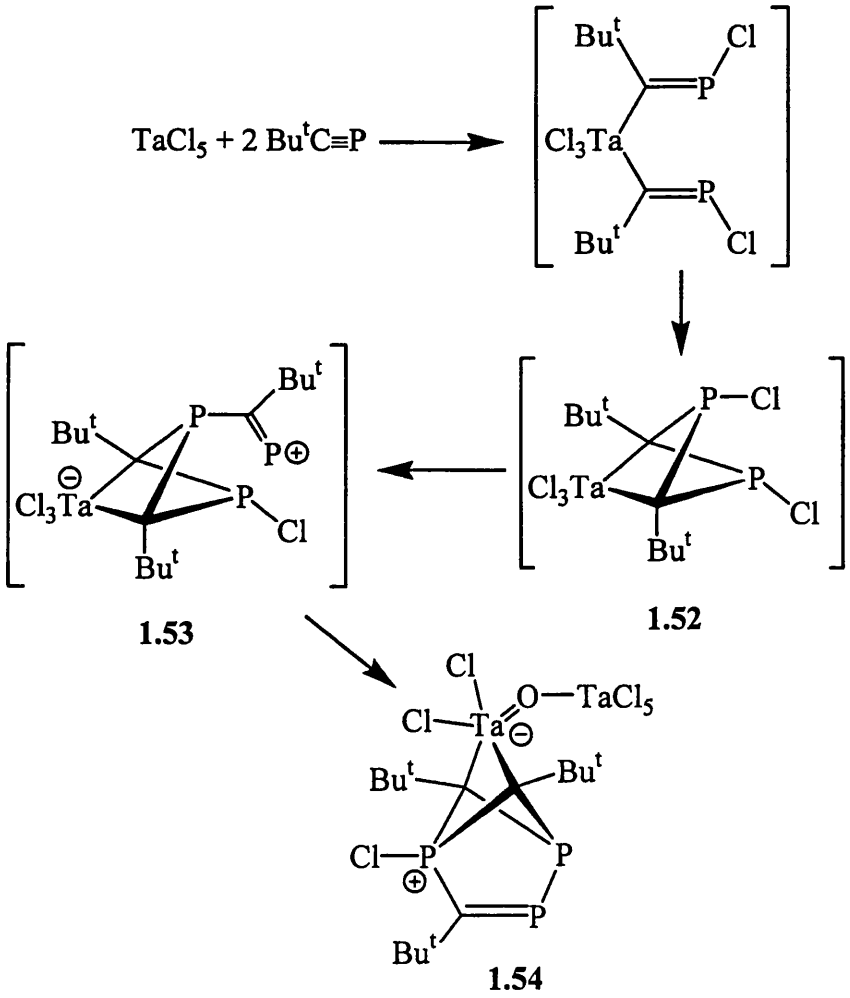

1.52 **1.53** **1.54**

Scheme 1.34

When *tert*-butylphosphaalkyne is reacted with $[V(\eta^5\text{-}C_5Me_5)(\eta^6\text{-}C_{10}H_8)]$, the naphthalene is displaced to give the 14 electron vanadium complex **1.55** shown in Scheme 1.35.[36] The unusual trimeric ligand is a derivative of 1,3,5-diphosphaprismane, and exists in equilibrium between the two isomers shown, as denoted by the temperature dependance of two of the peaks in the ^{31}P NMR spectrum. At room temperature only one broad signal is seen, but at temperatures below -100°C, this splits into two signals. If **1.55** is reacted with carbon monoxide, there is a rearrangement of the ligand into a Dewar 1,3,5-triphosphabenzene π-bonded to the metal by the two C=P bonds.

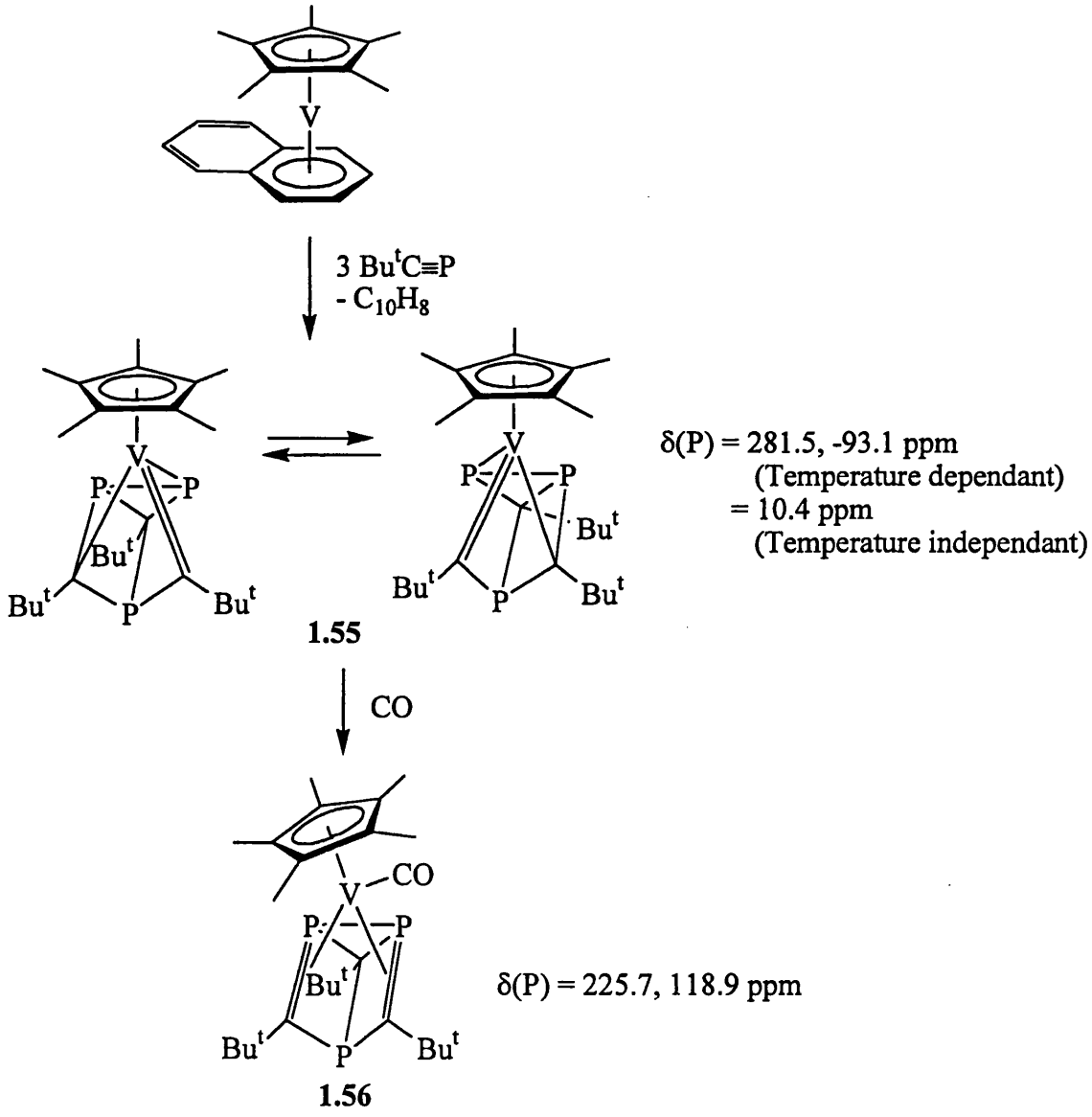

Scheme 1.35

Trimerisation of *tert*-butylphosphaalkyne is also observed when it is reacted with $[RhCl(PPr^i_3)_3]$.[37] The product is the dinuclear complex **1.57**, shown in Scheme 1.36, which is formed in good yield.

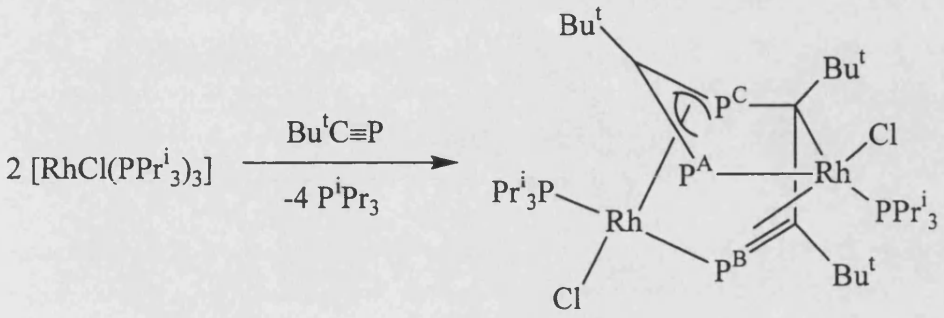

1.57

δ(P) = 206.7 ppm, P^A
201.6 ppm, P^B
24.7 ppm, P^C

Scheme 1.36

The trimerisation of a phosphaalkyne at a molybdenum centre has been reported.[38] However, the product of this reaction between *tert*-butylphosphaalkyne and $[Mo(\eta^6\text{-}C_7H_8)(CO)_3]$ (as shown in Scheme 1.37) is now not believed to have the initially suggested structure, containing a 1,3,5-triphosphabenzene, though its true identity is still unknown.

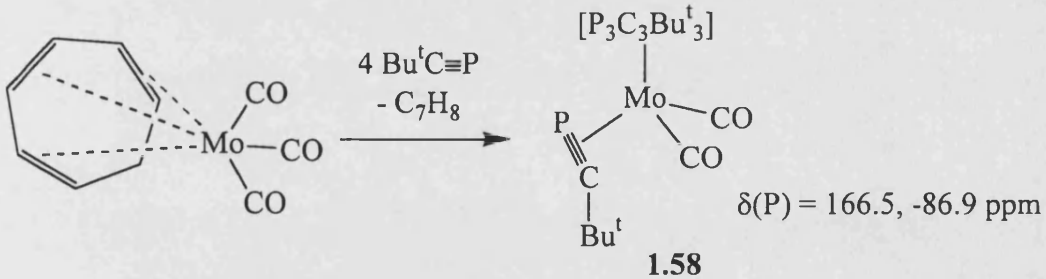

δ(P) = 166.5, -86.9 ppm

1.58

But not

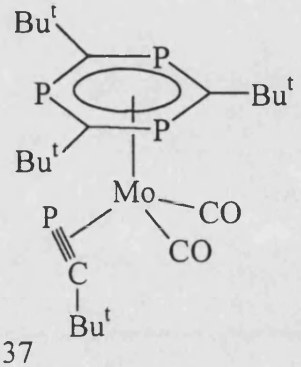

Scheme 1.37

A zwitterionic ruthenium phosphaalkyne trimer complex **1.59** has been synthesised by Nixon and co-workers.[39] It is believed to be formed after an attack by the PF_6^- anion of the initial product, a 1,3-diphosphacyclobutadiene complex, on the 4-membered ring, with subsequent addition of a third molecule of phosphaalkyne. The overall reaction is shown in Scheme 1.38.

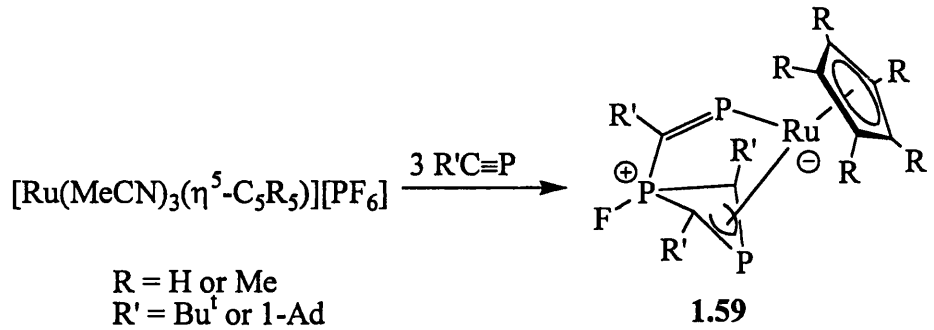

Scheme 1.38

If the hafnium cyclooctatetraene complexes $[Hf(\eta^4\text{-}C_4H_6)(\eta^8\text{-}1,4\text{-}C_8H_6R_2)]$ (R = H or $SiMe_3$) are reacted with three equivalents of *tert*-butylphosphaalkyne, the products formed depend upon the nature of the substituents on the cyclooctatetraene ring.[40] When R = $SiMe_3$, the product **1.60** contains a 7-hafna-1,3,5-triphosphanorbornadiene moiety, which can be viewed as being a Dewar 1,3,5-triphosphabenzene ring with the hafnium inserted into the central C-P bond. By reacting this with C_2Cl_6 the Dewar 1,3,5-triphosphabenzene **1.61** can be eliminated. If however, R = H, a different phosphaalkyne trimer, **1.62**, is formed (though its identity is still unclear). Reacting **1.62** with C_2Cl_6 in toluene displaces 1,3,5-triphosphabenzene **1.63**, whilst doing so in pentane creates the 1,3,5-triphosphabicyclo[3.1.0]hexene,-η^3,η^1-diyl hafnium complex **1.64**. These reactions are summarised in Scheme 1.39.

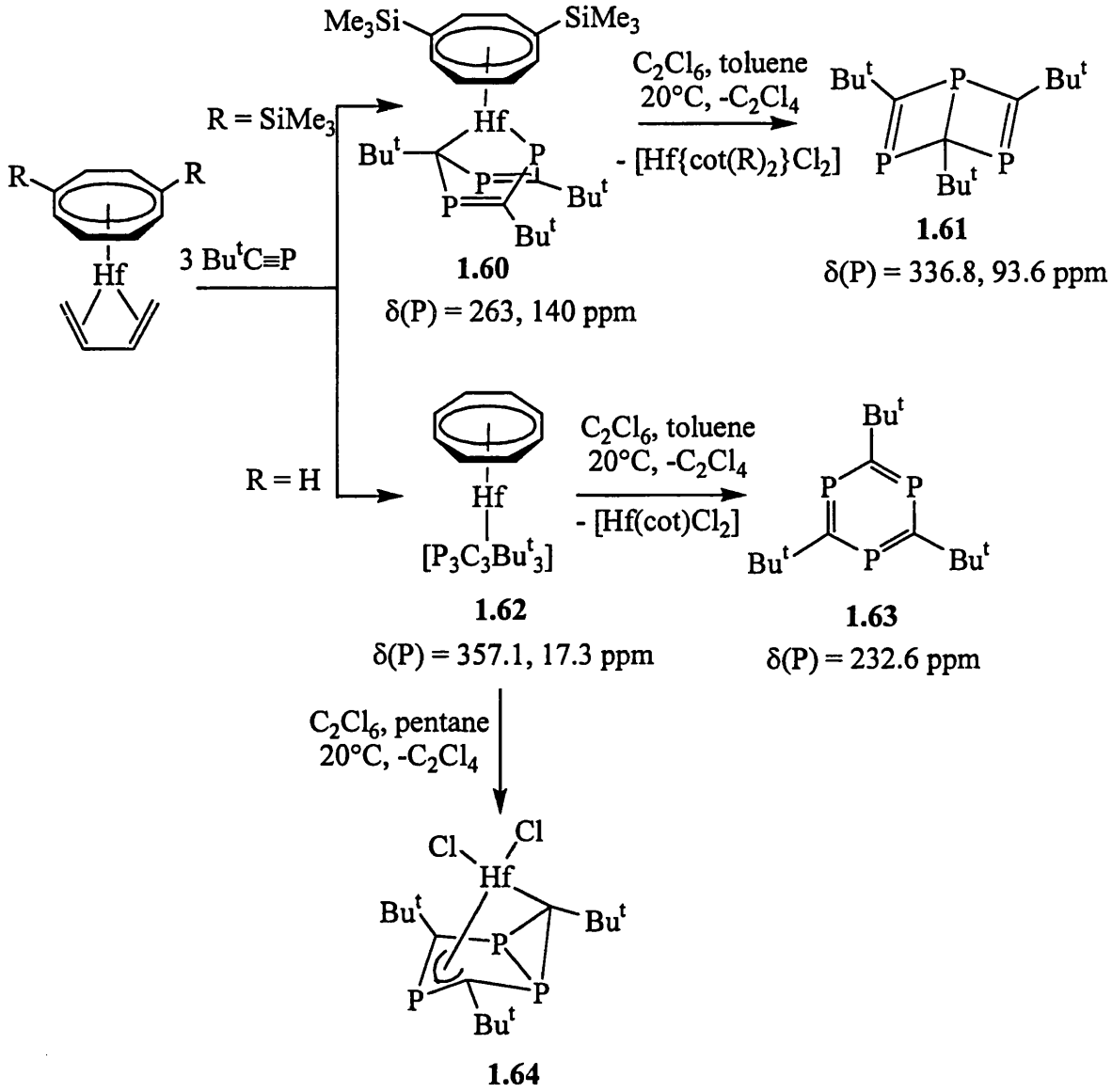

Scheme 1.39

Reacting the hafnium complex **1.62** with another equivalent of phosphaalkyne leads to the formation of the η^4-1,3,5,7-tetraphosphabarrelene complex **1.65** shown in Scheme 1.40. This complex may also be made by reacting [Hf(η^4-C_4H_6)(η^8-1,4-C_8H_8)] directly with 4 equivalents of phosphaalkyne.

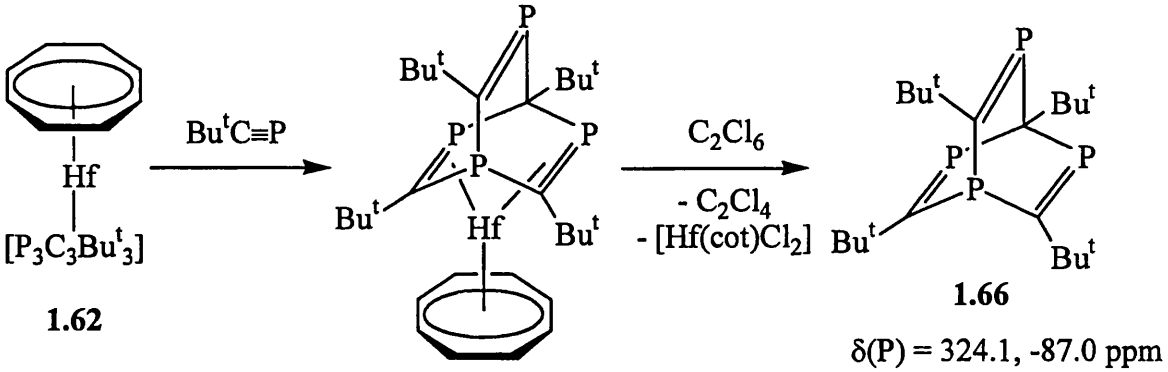

Scheme 1.40

The analogous zirconium complex **1.67** can be prepared directly by the reaction between four equivalents of *tert*-butylphosphaalkyne and $[Zr(\eta^4\text{-}C_8H_8)(\eta^8\text{-}C_8H_8)]$, as shown in Scheme 1.41.[41]

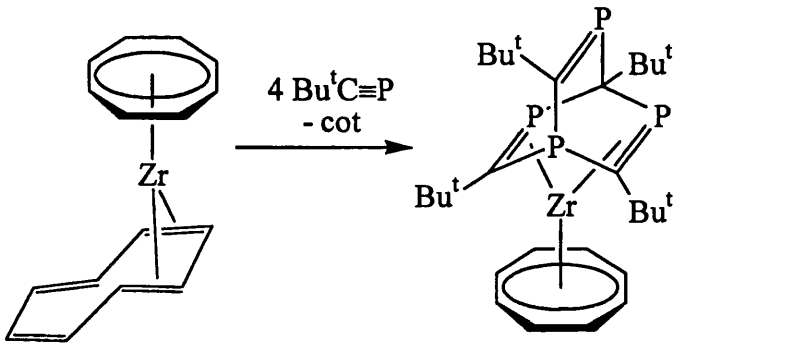

Scheme 1.41

The first example of the pentamerisation of a phosphaalkyne has recently been published.[42] By reacting mesitylphosphaalkyne with $[W(CO)_5(THF)]$ at low temperature, complex **1.68** was formed in low yield (Scheme 1.42). The basic structure resembles that of the thermally derived hafnium metalla-norbornadiene complex **1.60**, but with two extra phosphaalkyne molecules inserted into the M-P bonds.

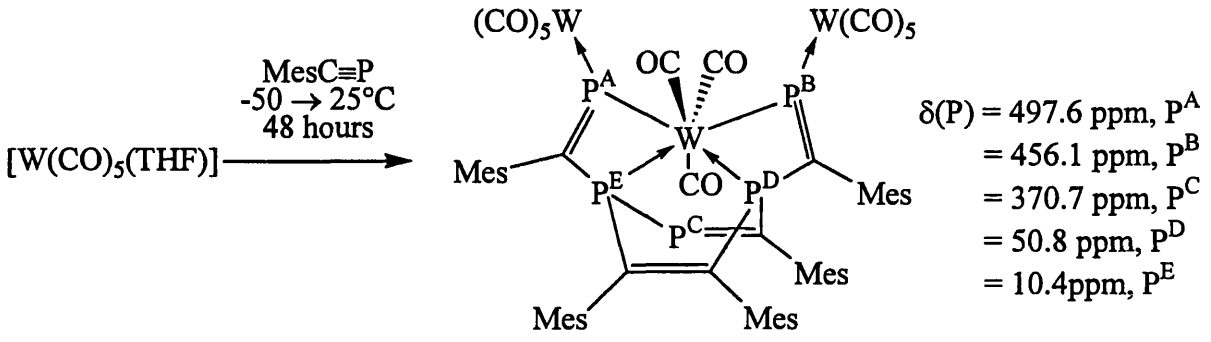

1.68

Scheme 1.42

1.3.1.3 Reorganisation Reactions of Phosphaalkynes at Transition Metal Centres

All the complexes in Sections 3.3.1.1 and 3.3.1.2 have been made by simple coupling reactions between molecules of phosphaalkyne at a metal centre, and hence have the general formula $L_nM(P_xC_xR_x)$ where $x \geq 2$. There is another range of cyclisation products formed from phosphaalkynes where the ligands do not obey this general formula.

When *tert*-butylphosphaalkyne is reacted with either $[Fe(\eta^2\text{-}C_2H_4)_2(\eta^6\text{-}C_6H_5Me)]$ or $[Fe(\eta^4\text{-}C_{11}H_{10})(\eta^6\text{-}C_6H_5Me)]$, the major product is the 1,3-diphosphacyclobutadiene complex **1.69**. However, two other sandwich products, **1.70** and **1.71**, are formed which contain di- and triphosphacyclopentadienyl ligands (Scheme 1.43).[43]

One of the low yield side products of the reaction between *tert*-butylphosphaalkyne and $[Rh(\eta^2\text{-}C_2H_4)_2(\eta^5\text{-}C_9H_7)]$ (Scheme 1.25) has the structure shown in Figure 1.8. This complex, **1.72**, is effectively the result of a cotrimerisation between two equivalents of phosphaalkyne, and one equivalent of P_2. The P_2 is believed to originate from the metathesis of another two molecules of phosphaalkyne as di(*tert*-butyl)acetylene, the other product of the metathesis reaction, has been detected in the reaction mixture.[27d]

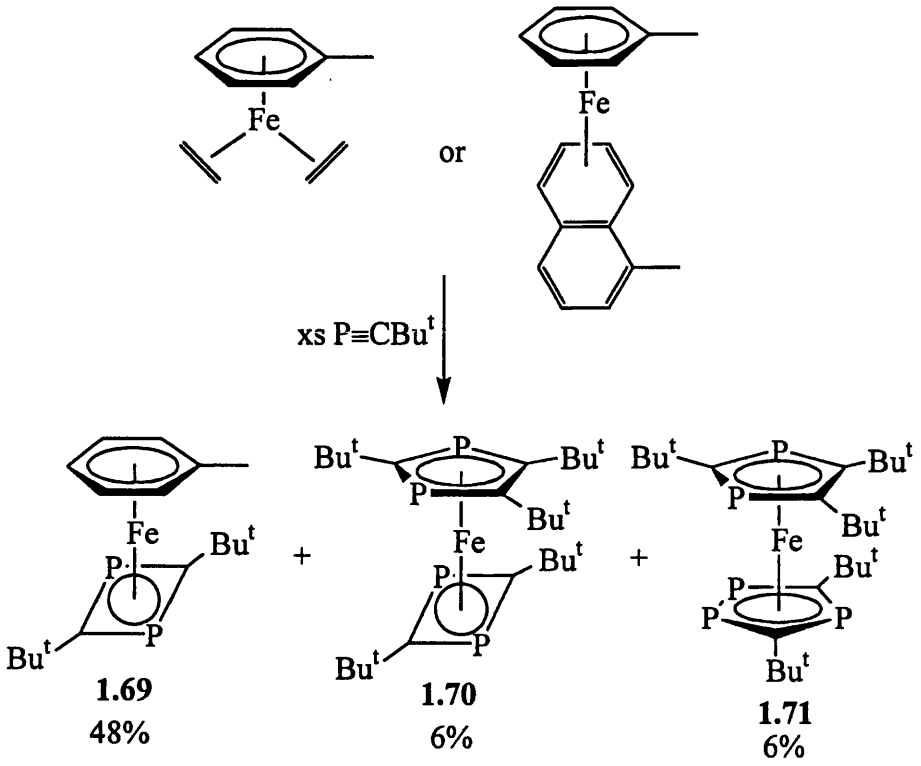

Scheme 1.43

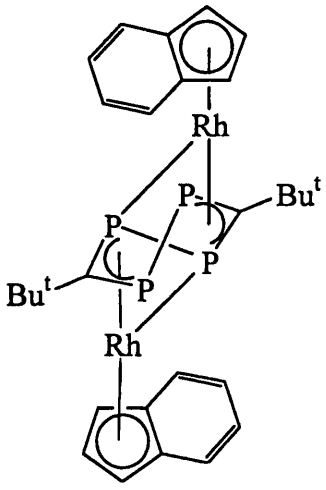

Figure 1.8: Structure of complex **1.72**

Cloke, Nixon and their co-workers have studied co-condensation reactions using metal vapour synthesis. The co-condensation of *tert*-butylphosphaalkyne with metal vapour has produced several reorganisation products, although reorganisation does not occur in all cases (see Section 2.1.1). If the metal is vanadium, the sandwich complex **1.73** is the product in 20% yield, with the metal coordinated to both di- and triphosphacyclopentadienyl ligands (Scheme 1.44).[44] Although overall there are the

same number of phosphorus atoms as *tert*-butyl groups, neither of the two rings has an equal number. The chromium analogue may also be prepared by this route.[3c]

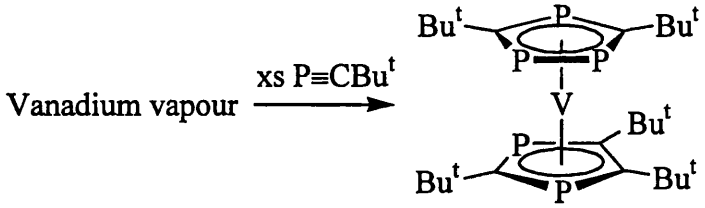

Scheme 1.44 **1.73**

When nickel vapour is used, the complex produced is that shown in Scheme 1.45, though only in 3% yield. It incorporates a triphosphacyclopentadienyl ring together with a phosphirenyl cationic ligand.[45]

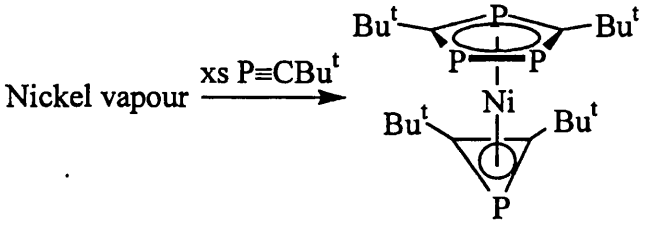

Scheme 1.45 **1.74**

When the metal is scandium, the product (in 5 – 10% yield) is the triple decker complex **1.75**, incorporating a 1,3,5-triphosphabenzene ring, plus two triphosphacyclopentadienyl ligands (Scheme 1.46).[46] In this example, although the central ring has equal numbers of phosphorus atoms to *tert*-butyl groups, neither of the outer rings do. Overall, there are nine phosphorus atoms to seven *tert*-butyl groups.

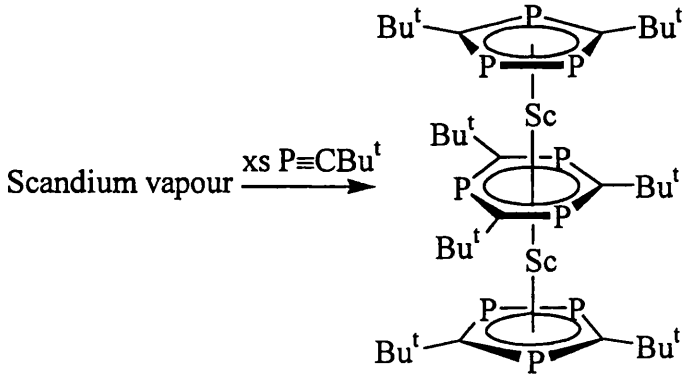

Scheme 1.46 **1.75**

1.3.2 Alkyne – Phosphaalkyne Coupling Reactions

In general, when a mixture of an alkyne and a phosphaalkyne are reacted in the presence of a metal centre, the alkyne molecules will couple with each other, whilst the same occurs with the phosphaalkyne molecules.[27c] However, some examples of alkyne-phosphaalkyne coupling reactions have been discovered.

When the half-sandwich cobalt complex $[Co(\eta^2\text{-}C_2H_4)_2(\eta^5\text{-}C_5H_5)]$ is reacted with the sterically demanding alkyne $Me_3SiC{\equiv}CSiMe_3$, the dimeric species $[Co_2(Me_3SiC_2SiMe_3)(\eta^5\text{-}C_5H_5)_2]$ is formed. This, when reacted with another equivalent of alkyne plus two equivalents of *tert*-butylphosphaalkyne, gives three different products (Scheme 1.47).

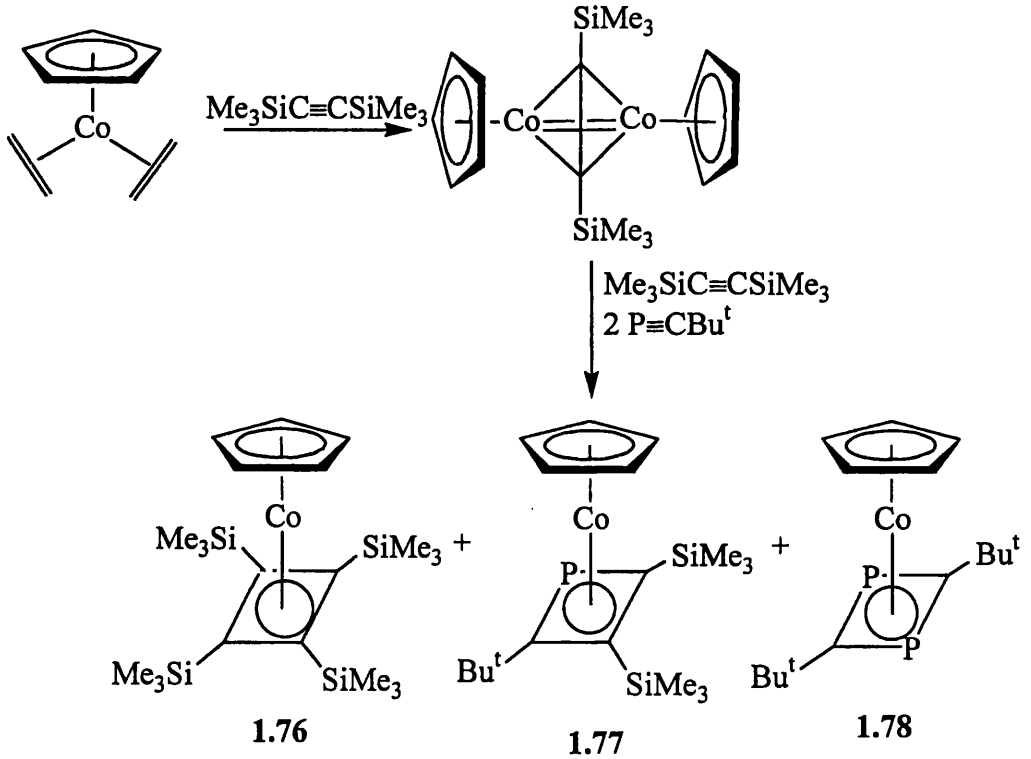

1.76 **1.77** **1.78**

Scheme 1.47

The 1,3-diphosphacyclobutadiene complex **1.78** formed by the [2+2] cycloaddition of two phosphaalkyne molecules is one product, as is the analogous cyclobutadiene complex **1.76** formed by the dimerisation of the coordinated and uncoordinated alkyne molecules. The third product, **1.77**, is the product of a [2+2] cycloaddition between the alkyne and phosphaalkyne and is formed in 31% yield. The bulky

groups on the alkyne are needed to prevent the trimerisation of the alkyne into the hexa-substituted benzene.[47]

When the diphenylmetallocenes $[MPh_2(\eta^5\text{-}C_5H_5)_2]$ (M = Ti or Zr) are heated to 80°C, benzyne complexes can be formed. These complexes react instantaneously with one equivalent of *tert*-butylphosphaalkyne to give 1-phospha-3-metallaindene derivatives, **1.79**, as shown in Scheme 1.48.[48]

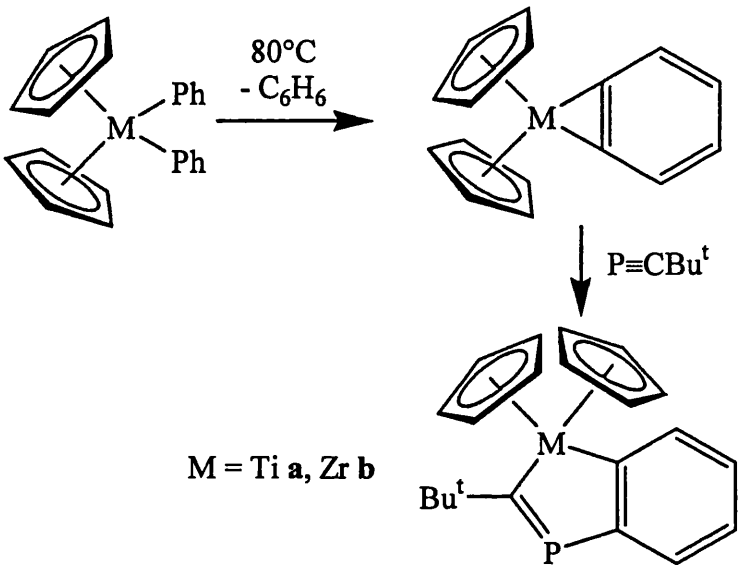

Scheme 1.48 **1.79a+b**

Another alkyne-phosphaalkyne codimerisation in the coordination sphere of a zirconocene occurs when the complex $[Zr(PMe_3)\{\eta^2(2e)\text{-}P{\equiv}CBu^t\}(\eta^5\text{-}C_5H_5)_2]$ is reacted with an alkyne.[8] The product is the 1-phospha-3-zirconacyclopentadiene complex **1.80**, as shown in Scheme 1.49. The new P-C and Zr-C bonds are labile, and so in solution the product only exists in equilibrium with the starting materials. By adding BEt_3 to remove PMe_3 the product can be obtained in almost quantitative yield. This reaction can also be carried out with alkenes to give the 1-phospha-3-zirconacyclopentene complexes.

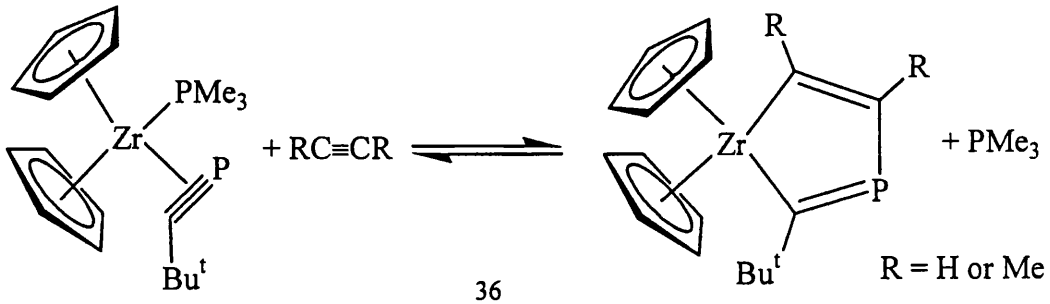

1.4b

Green and co-workers found that the η^2(4e)-phosphaalkyne complex **1.7** reacted with but-2-yne over 2 weeks to produce the 1-metalla-3-phosphacyclopentatriene complex **1.81**, as shown in Scheme 1.50.[11b]

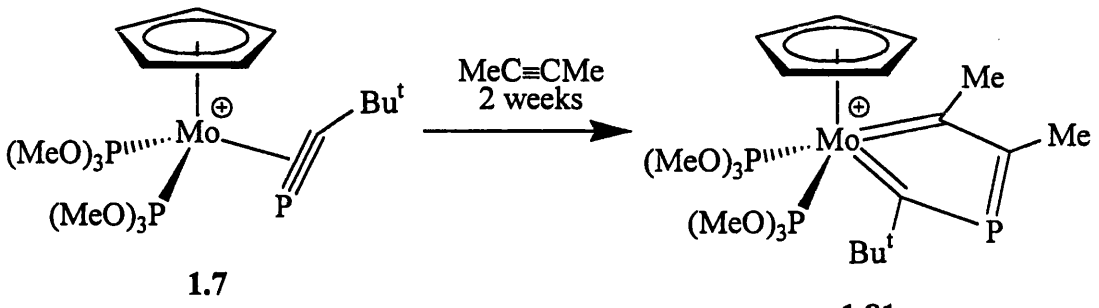

1.7 Scheme 1.50 **1.81**

Binger and co-workers have published an account of a cotrimerisation reaction between an alkyne and two phosphaalkyne molecules on a rhodium centre.[49] The product, **1.82**, has a structure resembling that of the ruthenium complex **1.59**, which is the product of a phosphaalkyne trimerisation.

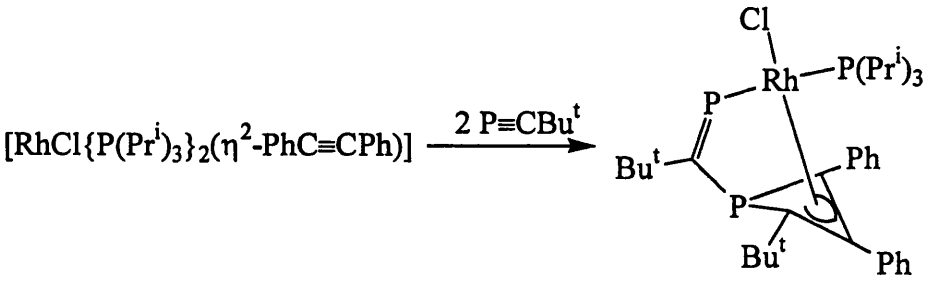

Scheme 1.51 **1.82**

If *tert*-butylphosphaalkyne is added to the tetrahedral iridium cluster [Ir_4(μ-PPh_2)(μ-H)(CO)$_9$($Ph_2PC{\equiv}CPh$)], an alkyne-phosphaalkyne coupling reaction occurs to form the complex **1.83** which contains a 2-phosphabutadienylphosphine chain.[50] The same product can also be made by reacting [Ir_4(CO)$_{10}$($Ph_2PC{\equiv}CPh$)(PPh_2H)] with *tert*-butylphosphaalkyne. In the product, the four iridium atoms take up a "butterfly" or "spiked triangle" arrangement, consistent with Wade's Rules. These reactions are shown in Scheme 1.52.

The iron complex $[Fe(\eta^2\text{-}C_2H_4)_2(\eta^6\text{-}C_6H_5Me)]$ has been shown to react with *tert*-butylphosphaalkyne to produce a 1,3-diphosphacyclobutadiene complex, plus reorganisation products (Scheme 1.43). However, if the iron-ethene complex is reacted at low temperature first with a terminal alkyne, and then with 4 equivalents of *tert*-butylphosphaalkyne, a cotrimerisation can occur with the yield in the region of 35 – 50%.[51] The product, **1.84**, is shown in Scheme 1.53. The mechanism of the reaction is believed to be a [2+2+2] cyclisation, and it may be significant that the substituted alkynic carbon is always adjacent to a phosphorus. Reacting the complex with $FeCl_3$ or halogenated hydrocarbons can remove the 1,3-diphosphabenzene from the metal.

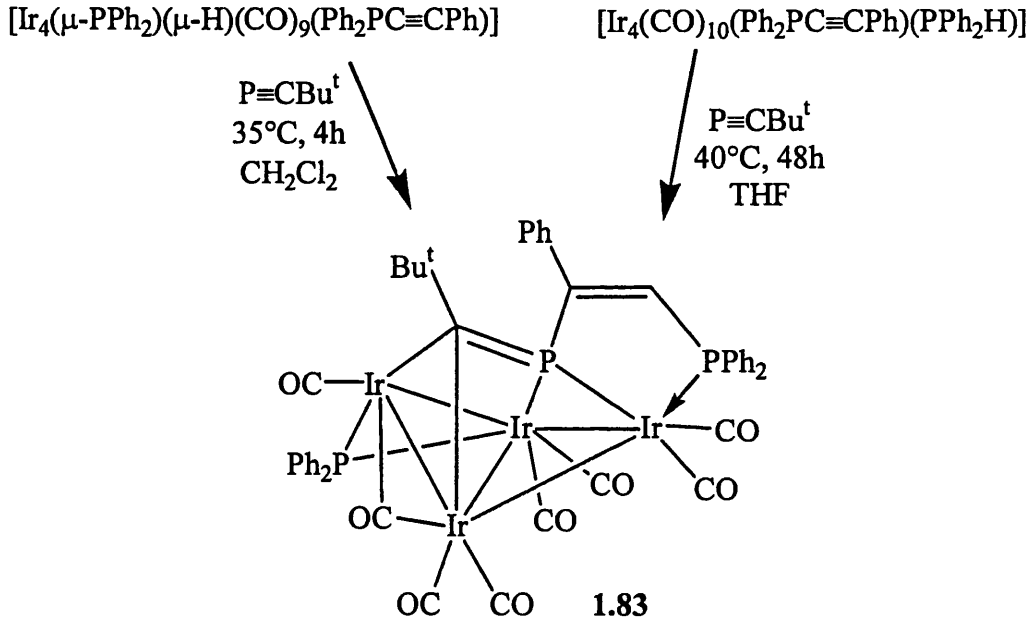

Scheme 1.52

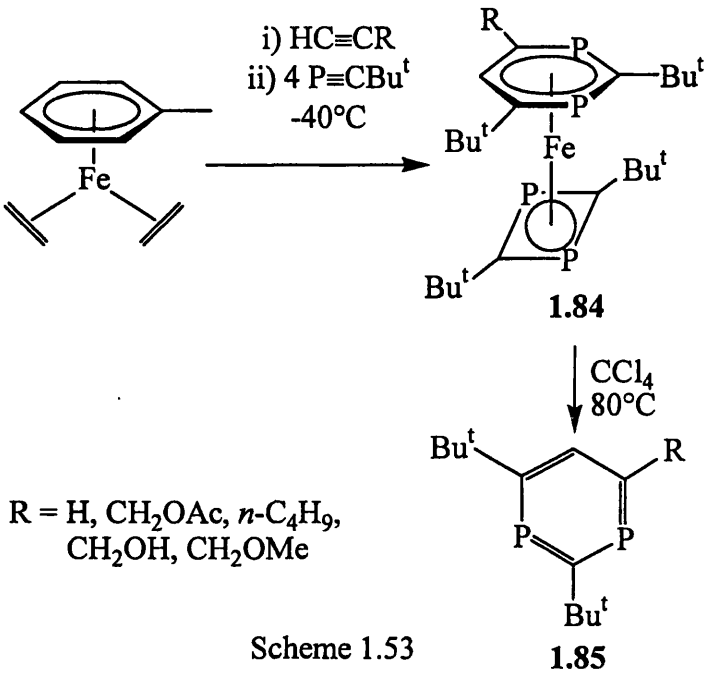

R = H, CH_2OAc, n-C_4H_9, CH_2OH, CH_2OMe

Scheme 1.53

1.4 Summary

The chemistry of phosphaalkynes on transition metal centres is varied and offers much scope for investigation. Although parallels have been drawn between phosphaalkyne complexes and their alkyne analogues, the cyclooligomerisation reactions of these two related species at transition metal centres show distinct differences. Such cyclooligomerisation reactions, and the related co-cyclooligomerisation reactions of phosphaalkynes with other unsaturated species such as alkynes are currently attracting much interest.

The coordination of a phosphaalkyne to a metal centre may occur either in an η^2 manner, by utilising the π-bonding and antibonding orbitals (either as a 2 electron donor by using 1 set of orbitals, or as a 4 electron donor by using both), or in an η^1 manner *via* the lone pair of electrons on the phosphorus. Complexation to two metal centres is possible by a combination of η^2 and η^1 coordination.

The cyclooligomerisation of phosphaalkynes on transition metal centres has been shown to give a range of products, from dimerisations to give 1,3-diphosphacyclobutadiene complexes, to more complex tetramerisation and

pentamerisation products. Co-cyclooligomerisation with alkynes has been shown to be uncommon, though examples have been observed.

1.5 References

1 T.E. Gier, *J. Am. Chem. Soc.*,1961, **83**, 1769.

2 G. Becker, G. Gresser and W. Uhl, *Z. Naturforsch*, 1981, **36b**, 16.

3 a) M. Regitz and P. Binger, *Angew. Chem., Int. Ed. Engl.*, 1988, **27**, 1465.
b) Reviews by M. Regitz and P. Binger, *Multiple Bonds and Low Coordination in Phosphorus Chemistry*, Thieme, 1990 (and references therein).
c) J.F. Nixon, *Chem. Soc. Rev.*, 1995, **24**, 319.
d) J.F. Nixon, *Chem. Rev.*,1988, **88**, 1327.

4 W. Rösch, U Hees and M Regitz, *Chem Ber.*, 1987, **120**, 1645.

5 W. Rösch, U. Vogelbacher, T. Allspach and M. Regitz, *J. Organomet. Chem.*, 1986, **306**, 39.

6 C. Jones, *Personal communication.*

7 J.L. Templeton and B.C. Ward, *J. Am. Chem. Soc.*, 1980, **102**, 3288.

8 P. Binger. B. Biedenbach, A.T. Herrmann, F. Langhauser, P Betz, R. Goddard and C. Krüger, *Chem. Ber.*, 1990, **123**, 1607.

9 a) J.C.T.R. Burkett-St Laurent, P.B. Hitchcock, H.W. Kroto and J.F. Nixon, *J. Chem. Soc., Chem. Commun.*, 1981, 1141.
b) S.I. Alresayes, P.B. Hitchcock, M.F. Meidine and J.F. Nixon, *J. Chem. Soc., Chem. Commun.*, 1984, 1080.
c) S.I. Alresayes, S.I. Klein, H.W. Kroto, M.F. Meidine and J.F. Nixon, *J. Chem. Soc., Chem. Commun.*, 1983, 930.

10 a) G. Brauers, M. Green, C. Jones and J.F. Nixon, *J. Chem. Soc., Chem. Commun.*, 1995, 1125.
b) G Brauers, PhD Thesis, University of Bath, 1993.

11 a) C.J. Beddows and M. Green. *Abstr. Pap. Am. Chem. Soc.*, 1998, **216**, INOR-Part 2.
b) C.J. Beddows, PhD Thesis, University of Bath 1999.

12 A.D. Burrows, A. Dransfeld, M. Green, J.C. Jeffery, C. Jones, J.M. Lynam and M.T. Nguyen, *Angew. Chem., Int. Ed.,* accepted for publication.

13 M.H.A. Benvenutti, P.B. Hitchcock, J.L. Kiplinger, J.F. Nixon and T.G. Richmond, *Chem. Commun.*, 1997, 1539.

14 G.A. Wilkinson, F.G.A. Stone, E.W. Abel (Eds), *Comprehensive Organometallic Chemistry*, Pergamon, Oxford, 1982.

a) R.D.W. Kemmitt and D.R. Russell, Vol. 5, p.239.

b) W.P. Jolly, Vol. 6, p.135.

c) R. Davies and L.A.P Kane-Maguise, Vol. 3, p. 1176.

15 a) J.C.T.R. Burket-St. Laurent, P.B. Hitchcock, H.W. Kroto, M.F. Meidine and J.F. Nixon, *J. Organomet. Chem.*, 1982, **238**, C82.

b) R. Bartsch, J.F. Nixon and N. Sarjudeen, *J. Organomet. Chem.*, 1985, **294**, 267.

c) G. Becker, W.A. Herrmann, W. Kalcher, G.W. Kriechbaum, C. Pahl, C.T. Wagner and M.L. Ziegler, *Angew. Chem., Int. Ed. Engl.*, 1983, **22**, 413.

16 M.F. Meidine, J.F. Nixon and R. Mathieu, *J. Organomet. Chem.*, 1986, **314**, 307.

17 P.B. Hitchcock, M.J. Maah, J.F.Nixon, J.A. Zora, G.J. Leigh and M.A. Baker, *Angew. Chem., Int. Ed. Engl.*, 1987, **26**, 474.

18 T. Gröer, G. Baum and M. Scheer, *Organometallics*, 1998, **17**, 5916.

19 R.B. Bedford, A.F. Hill, J.D.E.T. Wilton-Ely, M.D. Francis and C. Jones, *Inorg. Chem.*, 1997, **36**, 5142.

20 P.B. Hitchcock, J.A. Johnson, M.A.N.D.A. Lemos, M.F. Meidine, J.F. Nixon and A.J.L.Pombeiro, *J. Chem. Soc., Chem. Commun.*, 1992, 645.

21 M.F. Meidine, M.A.N.D.A. Lemos, A.J.L. Pombeiro, J.F. Nixon and P.B. Hitchcock, *J. Chem. Soc., Dalton Trans.*, 1998, 3319.

b) P.B. Hitchcock, M.A.N.D.A. Lemos, M.F. Meidine, J.F. Nixon and A.J.L. Pombeiro, *J. Organomet. Chem.*, 1991, **402**, C23.

22 P.B. Hitchcock, M.F. Meidine and J.F. Nixon, *J. Organomet. Chem.*, 1987, **333**, 337.

23 S.I. Al-Resayes, P.B. Hitchcock, J.F. Nixon and D.M.P. Mingos, *J. Chem. Soc. Chem. Commun.*, 1985, 365.

24 a) B. Breit, U. Bergstrasser, G. Maas and M. Regitz, *Angew. Chem., Int. Ed. Engl.*, 1992, **31**, 1055.

b) B. Breit, A. Hoffmann, U. Bergstrasser, L. Ricard, F. Mathey and M. Regitz, *Angew. Chem., Int. Ed. Engl.*, 1994, **33**, 1491.

c) B. Breit and M. Regitz, *Chem. Ber.*, 1996, **129**, 489.

d) A. Hoffmann, S. Leininger, M. Regitz, *J. Organomet. Chem.*, 1997, **539**, 61.

e) A. Hoffmann, A. Mack, R. Goddard, P. Binger, M. Regitz, *Eur. J. Inorg. Chem.*, 1998, **11**, 1597.

25 a) N.E. Schore, *Chem. Rev.*, 1988, **88**, 1081.

b) G.W. Parshall, Homogeneous Catalysis, Wiley, 1980, p166.

26 T. Wettling, G. Wolmershäuser, P. Binger and M. Regitz, *J. Chem. Soc., Chem. Commun.*, 1990, 1541.

27 a) P.B. Hitchcock, M.J. Maah and J.F. Nixon, *J. Chem. Soc., Chem. Commun.*, 1986, 737.

b) P. Binger, R. Milczarek, R. Mynott, M. Regitz and W. Rösch, *Angew. Chem., Int. Ed. Engl.*, 1986, **25**, 644.

c) P. Binger, R. Milczarek, R. Mynott, C. Krüger, Y.-H. Tsay, E. Raabe and M. Regitz, *Chem. Ber.*, 1988, **121**, 637.

d) P. Binger, B. Biedenbach, R. Mynott, P. Betz and C. Krüger, *J. Chem. Soc., Dalton Trans.*, 1990, 1771.

28 P. Binger, B. Biedenbach, R. Mynott, C. Krüger, P. Betz and M. Regitz, *Angew. Chem., Int. Ed. Engl.*, 1988, **27**, 1158.

29 P. Binger, G. Glaser, S. Albus and C. Krüger, *Chem. Ber.*, 1995, **128**, 1261.

30 S. Creve, M.T. Nguyen and L.G. Vanquickenborne, *Eur. J. Inorg. Chem.*, 1999, 1281.

31 a) P. Binger, B. Biedenbach, C. Krüger and M. Regitz, *Angew. Chem., Int. Ed. Engl.*, 1987, **26**, 764.

b) E. Negishi, F.E. Coderbaum and T. Takashi, *Tetrahedron Lett.*, 1986, **27**, 2829.

c) V. Shibbe and G. Erker, *J. Organomet. Chem.*, 1983, **241**, 15.

32 B. Geissle, S. Barth, U. Bergsträsse, M. Slang, J. Durkin, P.B. Hitchcock, M. Hofmann, P. Binger, J.F. Nixon, P. von Ragué Schlenyer and M. Regitz, *Angew. Chem., Int. Ed. Engl.*, 1995, **34**, 484.

33 P.B. Hitchcock, M.J. Maah, J.F. Nixon and C.J. Woodward, *J. Chem. Soc., Chem. Commun.*, 1987, 844.

34 M. Green, P.B. Hitchcock, M.J. Maah and J.F. Nixon, *J. Organomet. Chem.*, 1994, **466**, 153.

35 G. Becker, W. Becker, P. Knebel, H. Schmidt, M. Mildenbrand and M. Westerhausen, *Phosphorus Sulfur*, 1987, **30**, 349.

36 R. Milczarek, W. Rüsseler, P. Binger, K. Jonas, K. Angermund, C. Krüger and M. Regitz, *Angew. Chem., Int. Ed. Engl.*, 1987, **26**, 908.

37 P. Binger, J. Haas, P. Betz and C. Krüger, *Chem. Ber.*, 1995, **128**, 737.

38 A.R. Barron and A.H. Cowley, *Angew. Chem., Int. Ed. Engl.*, 1987, **26**, 907.

39 P.B. Hitchcock, C. Jones, J.F. Nixon, *Angew. Chem., Int. Ed. Engl.*, 1994, **33**, 463.

40 P. Binger, S. Leininger, J. Stannek, B. Gabor, R. Mynott, J. Bruckmann and C. Krüger, *Angew. Chem., Int. Ed. Engl.*, 1995, **34**, 2227.

41 P. Binger, G. Glasser, B. Gabur and R Mynott, *Angew. Chem., Int. Ed. Engl.*, 1995, **34**, 81.

42 P. Kramkowski and M. Scheer, *Angew. Chem., Int. Ed.*, 1999, **38**, 3183.

43 M. Driess, D.H.U.H. Pritzkow, H. Schaufele, U. Zenneck, M. Regitz and W. Rösch, *J. Organomet. Chem.*, 1987, **334**, C35.

44 F.G.N. Cloke, K.R. Flower, P.B. Hitchcock and J.F. Nixon, *J. Chem. Soc., Chem. Commun.*, 1995, 1659.

45 A.G. Avent, F.G.N. Cloke, K.R. Flower, P.B. Hitchcock, J.F. Nixon and D.M. Vickers, *Angew. Chem., Int. Ed. Engl.*, 1994, **33**, 2330.

46 P.L. Arnold, G.N. Cloke, P.B. Hitchcock, J.F. Nixon, *J. Am. Chem. Soc.*, 1996, **118**, 7630.

47 P. Binger, R. Milczarek, R. Mynott and M. Regitz, *J. Organomet. Chem.*, 1987, **323**, C35.

48 P. Binger, B. Biedenbach, R. Mynott and M. Regitz, *Chem. Ber.*, 1988, **121**, 1455.

49 P.Binger, J. Haas, A.T. Herrmann, F. Langhauser, C. Krüger, *Angew. Chem., Int. Ed. Engl.*, 1991, **30**, 310.

50 M.H. Araujo, P.B. Hitchcock, J.F. Nixon, M.D. Vargas, *J. Brazil. Chem. Soc.*, 1998, **9**, 563.

51 D. Bohm, F. Knoch, S. Kummer, U. Schmidt and U Zenneck, *Angew. Chem., Int. Ed. Engl.*, 1995, **34**, 198.

2 Phosphaalkyne Coupling Reactions at Molybdenum Centres

2.1 Phosphaalkyne Cyclodimerisations at Molybdenum Centres

2.1.1 Introduction

The propensity of phosphaalkynes to dimerise at unsaturated metal centres to form η^4-1,3-diphosphacyclobutadiene complexes is well known (see Section 1.3.1.1). A number of examples of this reaction occurring at molybdenum centres have been documented. The reaction of $[Mo(CO)_3(MeCN)_3]$ with *tert*-butylphosphaalkyne, as carried out by Scheer and Krug,[1] gives a mixture of three products, two of which contain η^4-1,3-diphosphacyclobutadiene rings (Scheme 2.1).

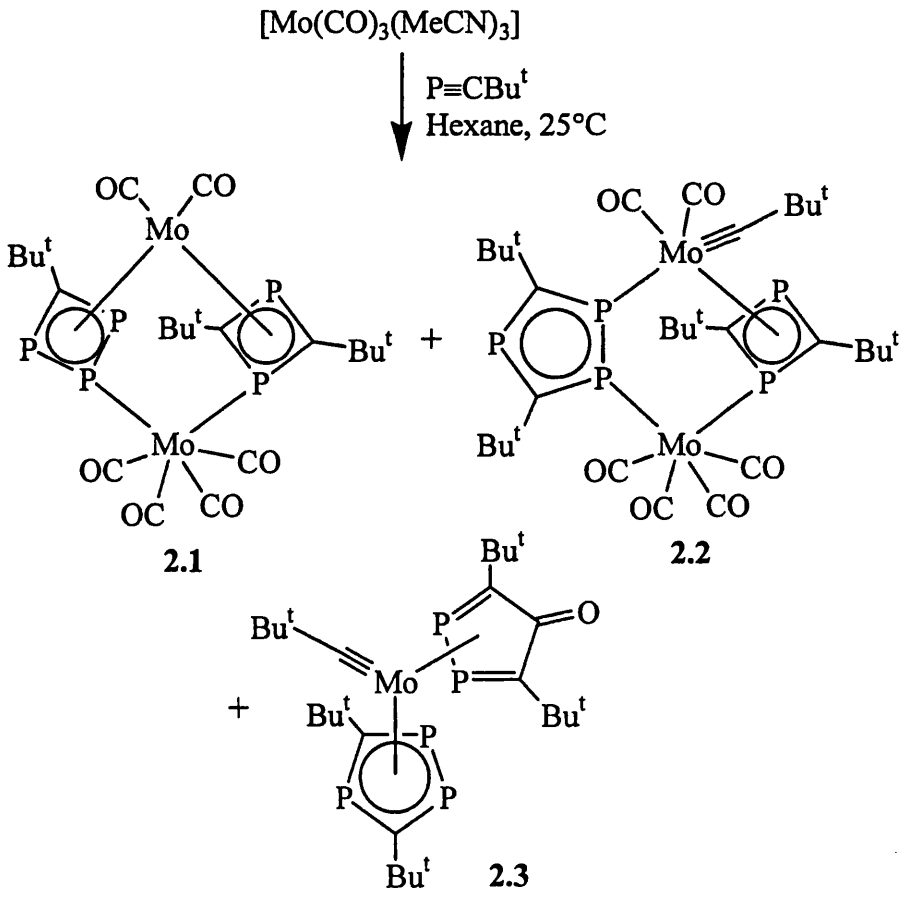

Scheme 2.1

These products are presumably formed by reorganisation reactions (see Section 1.3.1.3) at the molybdenum centre, as there are no longer the same number of *tert*-butyl groups as phosphorus atoms. Complex **2.1** can also be formed as a side product in the trimerisation of *tert*-butylphosphaalkyne with $[Mo(CO)_3(\eta^6\text{-}C_7H_8)]$ (see Section 1.3.1.2).[2]

The tris-diphosphacyclobutadiene molybdenum complex **2.4** be made can in low yield (< 5%) by reacting *tert*-butylphosphaalkyne with molybdenum vapour (Scheme 2.2).[3] This reaction is notable, as in most other reactions of metal vapours with *tert*-butylphosphaalkyne reorganisation products are formed.

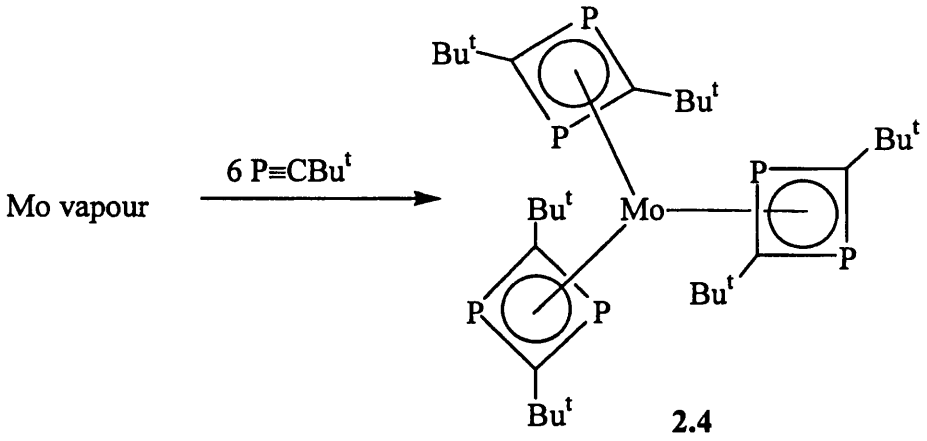

Scheme 2.2

The reaction of $[Mo(CO)_2(MeCN)_2(\eta^5\text{-}C_9H_7)][BF_4]$ with *tert*-butylphosphaalkyne, as carried out by Green and co-workers, gave as the major product the complex $[Mo(CO)_2(\eta^4\text{-}1,3\text{-}P_2C_2Bu^t_2)(\eta^5\text{-}C_9H_7)][BF_4]$, **2.5**.[4] In solution the 1,3-diphosphacyclobutadiene ligand is coordinated in the η^4 mode, but in the crystal structure the heterocyclic ring is coordinated in an η^3 manner to the metal centre, acting as a phosphavinyl ligand. The phosphorus atom not involved in the bonding to the metal is coordinated to one of the fluorine atoms from the BF_4^- counter ion (Figure 2.1).

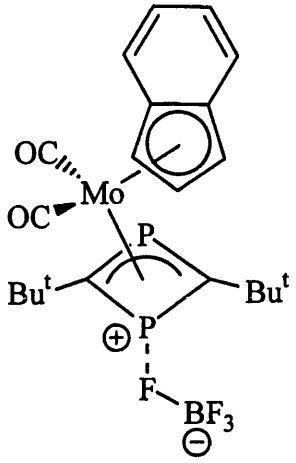

Figure 2.1 - Structure of complex **2.5** in the solid state

2.1.2 Results and Discussion

The reaction of $[MoCl(CO)_3(\eta^5\text{-}C_5H_5)]$ with an alkyne under reflux conditions in a non-polar solvent was reported in 1975 by Davidson and Sharp,[5] and later elaborated upon by Davidson and co-workers in 1976.[6] The products varied with the alkyne used and the reaction conditions (Scheme 2.3).

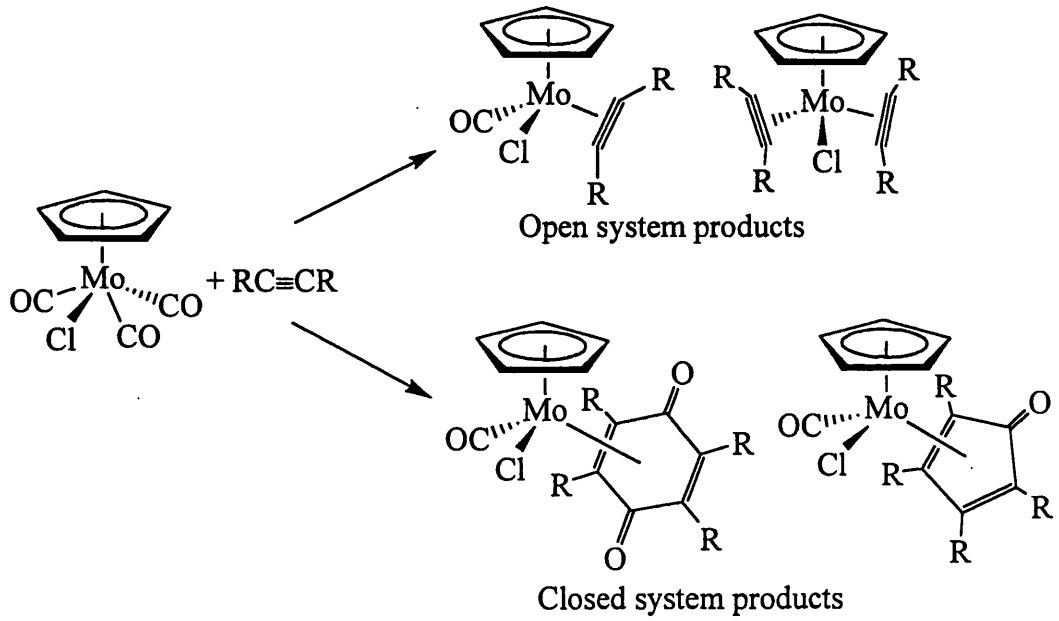

Scheme 2.3

In an open system the initial kinetic products were the η^2(4e) alkyne complexes [MoCl(CO){η^2(4e)-alkyne}(η^5-C_5H_5)]. These, upon exposure to prolonged heating and excess alkyne, reacted further to give the bis(alkyne) complexes [MoCl{η^2(3e)-alkyne}$_2$(η^5-C_5H_5)] where the two alkyne ligands donate 6 electrons between them. These compounds were originally considered to be 16 electron complexes, until X-ray crystallographic structure determinations and ^{13}C NMR studies revealed the η^2(4e) nature of the alkyne ligands. If the reaction was carried out in a closed system, then the products included 1,4-benzoquinone and cyclopentadienone derivatives formed by coupling reactions between the alkyne and a carbon monoxide molecule.

We were interested to see what the effect of changing the alkynes in the reactions described above to *tert*-butylphosphaalkyne would be. From the reactions with alkynes it might be expected that an η^2(4e)-phosphaalkyne complex, [MoCl(CO){η^2(4e)-P≡CBu^t}(η^5-C_5H_5)] would be formed. However, given the propensity of coupling reactions which *tert*-butylphosphaalkyne undergoes at transition metal centres it was suspected that this might not be the case. It was considered that a more likely product would be the η^4-1,3-diphosphacyclobutadiene complex [MoCl(CO)(η^4-1,3-$P_2C_2Bu^t_2$)(η^5-C_5H_5)], formed by a formal [2+2] cycloaddition reaction of two phosphaalkyne molecules.

2.1.2.1 Synthesis of [MoCl(CO)(η^4-1,3-$P_2C_2Bu^t_2$)(η^5-C_5R_5)] (R = H or Me)

One equivalent of P≡CBu^t was added to a pentane solution of [MoCl(CO)$_3$(η^5-C_5H_5)] and heated to reflux for 78 hours in an open system. Removal of solvent *in vacuo* gave a dark orange powder, which was shown, by ^{1}H and ^{31}P{^{1}H} NMR to be a 1:1 mixture of starting material and an unknown product.

Repeating the reaction with 2.1 equivalents of P≡CBu^t resulted in the precipitation of a dark green powder. The solvent was decanted from this precipitate, and cooled to –20°C, which yielded a second batch of green precipitate. The precipitates were combined, redissolved in CH_2Cl_2, and separated on a cooled (0°C) column (10 x 1 cm) packed with a Florisil/pentane slurry using CH_2Cl_2 as the eluant. A green band remained at the top of the column whilst an orange band was collected. The solvent

was removed *in vacuo*, and the orange powder recrystallised by slow diffusion of hexane into a CH_2Cl_2 solution to give orange crystals of complex $[MoCl(CO)(\eta^4\text{-}1,3\text{-}P_2C_2Bu^t_2)(\eta^5\text{-}C_5H_5)]$, **1**, in moderate yield (35%). In contrast to the reactions with alkynes described in Section 2.1.1, repeating the reaction in a closed reaction vessel gave the same product in a similar yield. This compound was characterised on the basis of multinuclear NMR, infrared spectra and elemental analysis.

Repeating the reaction as described above for **1** using a pentane solution of $[MoCl(CO)_3(\eta^5\text{-}C_5Me_5)]$ resulted in the formation of the orange complex $[MoCl(CO)(\eta^4\text{-}1,3\text{-}P_2C_2Bu^t_2)(\eta^5\text{-}C_5Me_5)]$, **2**, in good yield and after a far shorter reaction time (24 hours). This compound was characterised on the basis of multinuclear NMR, infrared spectra and elemental analysis. As for **1**, if the experiment is carried out in a closed tube the same product is produced in similar yield. The two reactions are shown in Scheme 2.4.

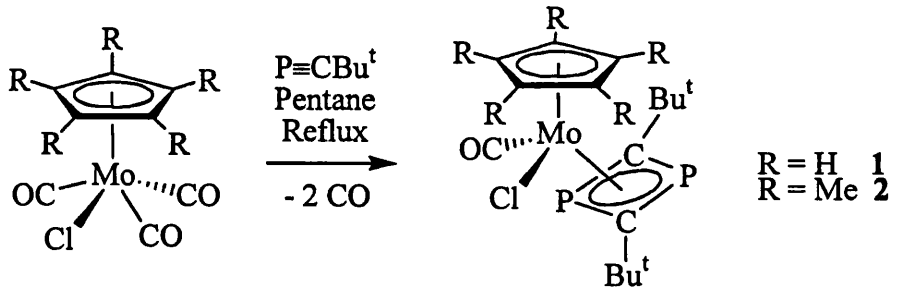

Scheme 2.4

The $^{31}P\{^1H\}$ NMR spectrum of **1** in CD_2Cl_2 shows two signals for the phosphorus atoms at 86.9 and 71.1 ppm. Likewise, in the $^{31}P\{^1H\}$ NMR spectrum of **2** in CD_2Cl_2, signals are seen at 101.7 and 74.4 ppm. Similarly, two different singlets are seen in the ^1H NMR spectrum of both complexes for the two *tert*-butyl groups (0.89 and 0.69 ppm for **1**, 0.86 and 0.82 ppm for **2**). The $^{13}C\{^1H\}$ NMR spectrum of **2** shows different environments for the two carbons in the 1,3-diphosphacyclobutadiene ring (107.7 and 101.2 ppm) and the appended *tert*-butyl groups. The signals for the η^4-1,3-diphosphacyclobutadiene ring carbon atoms in complex **1** are obscured by solvent peaks, but different environments are seen for the *tert*-butyl groups. The infrared spectra for **1** and **2** show single frequencies in the

C≡O stretching region at 1988 and 1961 cm^{-1} respectively, which were assigned to the metal carbonyl ligands.

The occurrence of two different environments in the NMR spectra for the phosphorus atoms, ring carbons and *tert*-butyl groups is a consequence of the asymmetry, introduced by the carbonyl and chloride ligands, at the metal centre. This demonstrates that the rotation of the 1,3-diphosphacyclobutadiene ring is slow on the NMR timescale at room temperature and 400 MHz. At higher temperatures, the η^4-1,3-diphosphacyclobutadiene ligand in **1** does begin to rotate on the NMR timescale, with the onset of coalescence of the *tert*-butyl signals being observed in the ^1H NMR spectrum at 60°C and 400 MHz.

Observations of this type have previously been precluded by the relatively high symmetry of the associated metal fragments in other 1,3-diphosphacyclobutadiene complexes. The only other examples where this have been observed are in **2.4** and **2.6**,[7] where it is believed that steric congestion around the metal centre inhibits the rotation of the 1,3-diphosphacyclobutadiene ring.

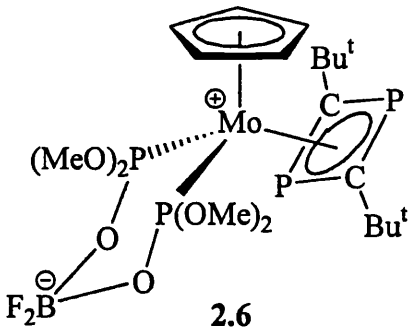

2.6

Figure 2.2

2.1.2.2 X-Ray Crystal Structure of [MoCl(CO)(η^4-1,3-$P_2C_2Bu^t_2$)(η^5-C_5Me_5)], 2

Complex **2** was recrystallised by a slow layer diffusion of pentane into a CH_2Cl_2 solution at room temperature to give crystals suitable for X-ray crystallographic studies. The crystal structure confirmed the formation of the η^4-1,3-

diphosphacyclobutadiene ligand (Figure 2.3). Selected bond lengths and angles are given in Table 2.1.

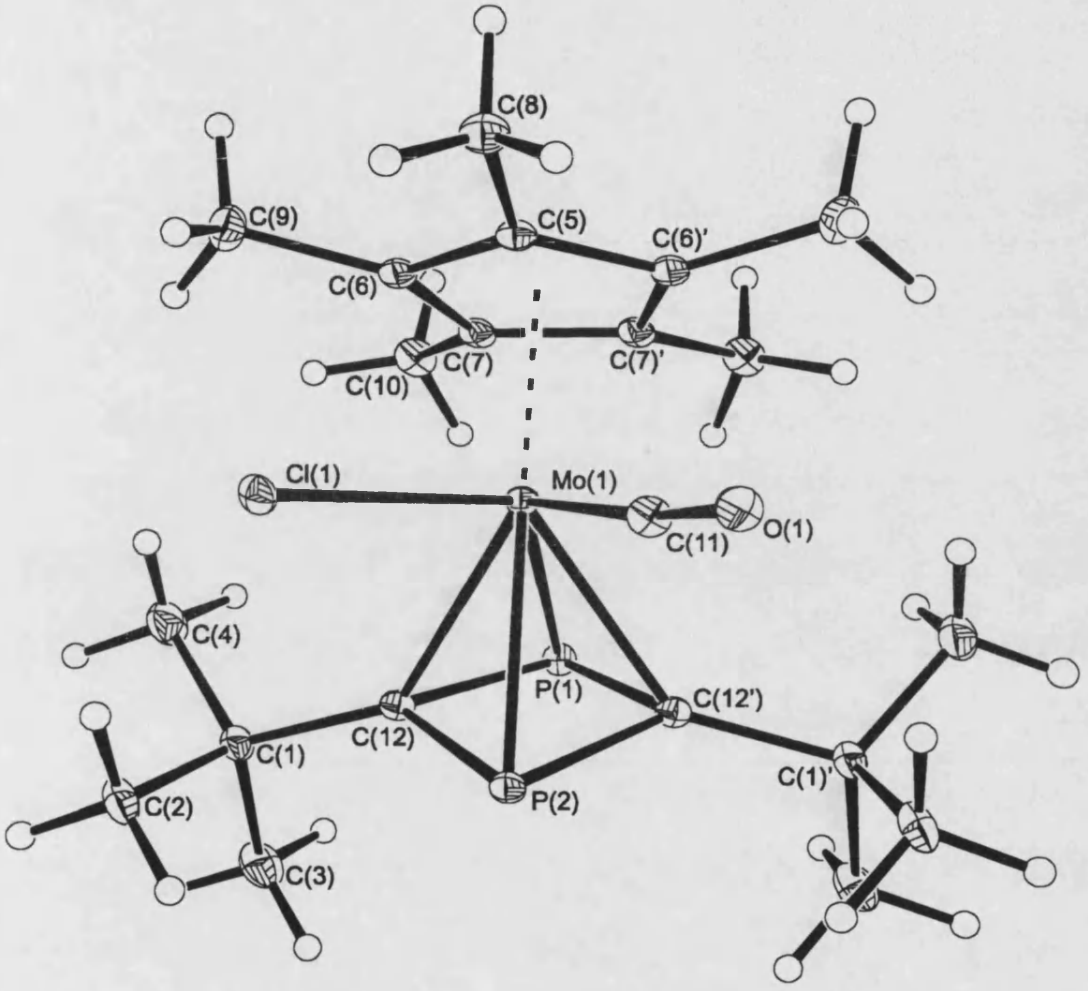

Figure 2.3: Molecular structure of $[MoCl(CO)(\eta^4\text{-}1,3\text{-}P_2C_2Bu^t_2)(\eta^5\text{-}C_5Me_5)]$, **2**

P(2)-C(12)	1.795(2)	P(1)-C(12)	1.784(2)
Mo-P(1)	2.5015(9)	Mo-P(2)	2.5057(7)
Mo-C(12)	2.339(2)	Mo-Cl(1)	2.521(2)
Mo-C(11)	1.919(7)		
C(12)-P(1)-C(12')	83.35(13)	C(12)-P(2)-C(12')	82.73(13)
P(1)-C(12)-P(2)	96.59(10)		

Table 2.1 Selected bond lengths (Å) and angles (°) for **2**

The asymmetric unit in this structure consists of one half of a molecule, the remaining portion being generated *via* a mirror plane intrinsic in the space group symmetry on which atoms Mo(1), C(5), C(8), P(1) and P(2) are located. As a consequence, the chloride and carbonyl ligand atoms are disordered.

A search of the CDS database[8] reveals that the C-P distances [P(1)-C(12) = 1.784(2) Å, P(2)-C(12) = 1.795(2) Å] lie within the known range for η^4-1,3-diphosphacyclobutadiene rings [1.747(8) – 1.860(5) Å]. Similarly, the PCP [96.59(10)°] and CPC angles [83.35(13) and 82.73(13)°] observed in the structure of **2** are within the previously observed ranges for these values [PCP = 93.2(4) – 99.4(1)°, CPC = 80.4(1) – 83.9(2)]. The Mo-P distances [Mo-P(1) = 2.5015(9), Mo-P(2) = 2.5057(7)] lie within the range for such distances in η^4-1,3-diphosphacyclobutadiene molybdenum complexes [2.496(2) – 2.552(1) Å], as do the Mo-C bond distances [Mo-C(12) = 2.339(2), compared to 2.255(4) – 2.535(4) Å]. The other bond lengths and angles in the complex are within the accepted ranges for their values.

The disorder in the molecule prevents any information being obtained on how the presence of the asymmetric metal centre affects the crystal structure. The distances and angles from P(1) are similar to those from P(2), within experimental error.

2.1.2.3 Reaction of [MoCl(CO)(η^4-1,3-$P_2C_2Bu^t_2$)(η^5-C_5H_5)], 1, with H_2O

Whilst attempting to obtain crystals suitable for structural analysis, a solution of **1** in CD_2Cl_2 was seen to precipitate red crystals. An X-ray crystallographic study on these revealed that they were not **1**, but a new complex [MoCl(CO){η^3,λ^3,λ^5-$PC_2Bu^t_2PH(OH)$}(η^5-C_5H_5)], **3**. Two molecules were seen in the asymmetric unit. The structure of one of these molecules is shown in Figure 2.4 and selected bond length and angles from both molecules are given in Table 2.2. It can be seen that the analogous distances and angles for the two molecules are similar, except for slight

differences in the Mo-P distances. Therefore it may be assumed that the two molecules have the same structure.

In this complex one of the phosphorus atoms has undergone formal oxidative addition of H_2O to produce an $\eta^3,\lambda^3,\lambda^5$-phosphaphosphonietinyl complex (Scheme 2.5). The water is believed to have originated from imperfectly dried solvent.

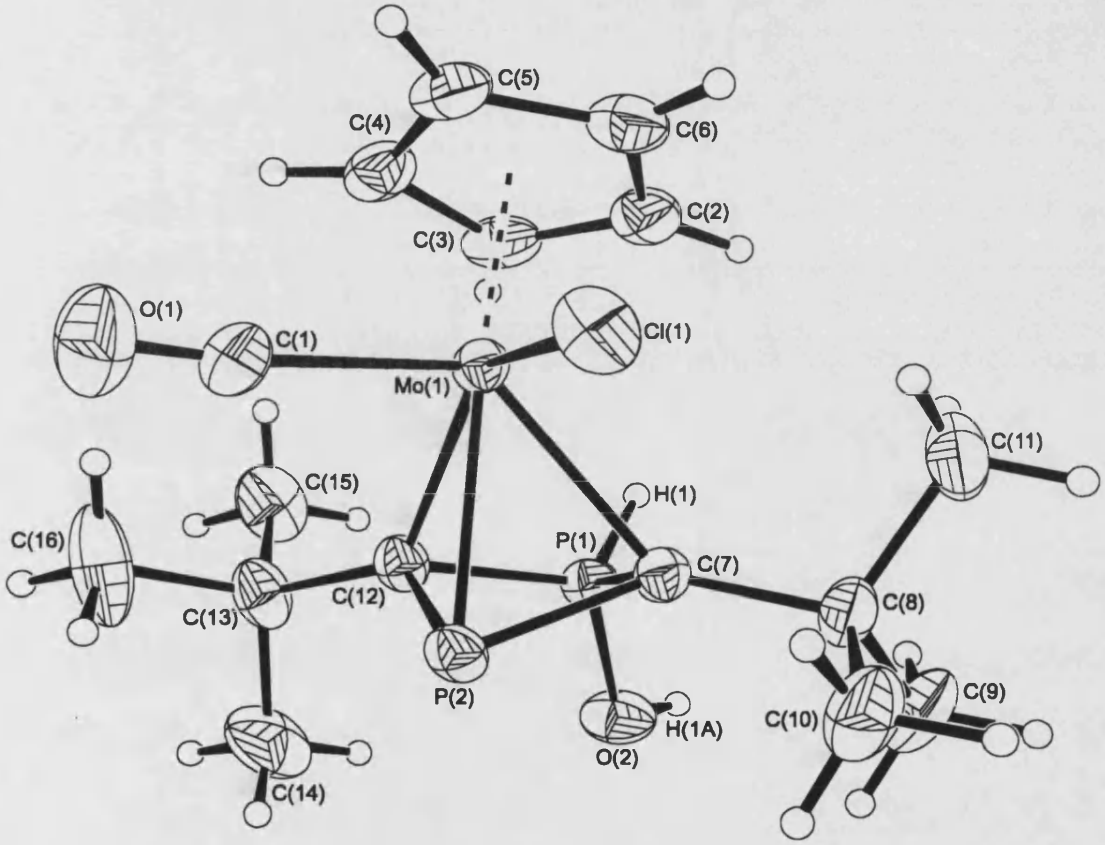

Figure 2.4: Structure of $[MoCl(CO)\{\eta^3,\lambda^3,\lambda^5\text{-}P_2C_2Bu^t_2PH(OH)\}(\eta^5\text{-}C_5H_5)]$, **3**

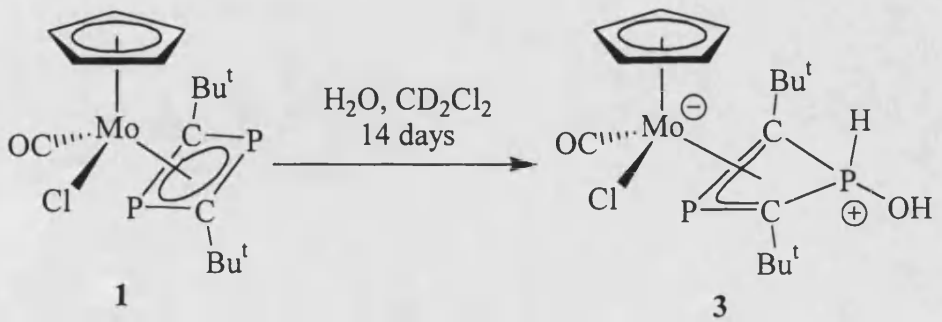

Scheme 2.5

It is apparent that phosphorus atoms P(1) and P(3) are no longer coordinated to the metal by the Mo-P distances [Mo(1)-P(1) = 2.8751(14) Å, Mo(2)-P(3) = 2.8664(11) Å]. Moreover, P(1) is sited out of the plane of the η^3-phosphaallyl group [C(12)-P(2)-C(7)] by 0.74 Å. Similarly, P(3) is situated out of the [C(23)-P(3)-C(28)] plane by 0.72 Å. The phosphorus atoms also bear hydroxy groups [P(1)-O(1) = 1.581(3) Å, P(3)-O(4) = 1.587(3) Å] and P-H bonds. All the hydroxy and phosphorus bound hydrogens were located in the difference map and refined without constraints. The remaining bond lengths and angles are consistent with the description of **3** as an $\eta^3,\lambda^3,\lambda^5$-phosphaphosphphonietinyl complex.

Mo(1)-P(1)	2.8751(14)	Mo(2)-P(3)	2.8664(11)
Mo(1)-P(2)	2.4178(11)	Mo(2)-P(4)	2.4290(14)
Mo(1)-C(7)	2.300(3)	Mo(2)-C(23)	2.317(3)
Mo(1)-C(12)	2.279(4)	Mo(2)-C(28)	2.278(4)
P(1)-C(7)	1.743(3)	P(3)-C(23)	1.740(4)
P(1)-C(12)	1.744(4)	P(3)-C(28)	1.747(4)
P(2)-C(7)	1.839(3)	P(4)-C(23)	1.832(3)
P(2)-C(12)	1.847(3)	P(4)-C(28)	1.849(3)
P(1)-O(2)	1.584(3)	P(3)-O(4)	1.587(3)
C(7)-P(1)-C(12)	86.6(2)	C(23)-P(3)-C(28)	86.6(2)
C(7)-P(2)-C(12)	80.9(2)	C(23)-P(4)-C(28)	81.0(2)
P(1)-C(7)-P(2)	90.5(2)	P(3)-C(23)-P(4)	90.9(2)
P(1)-C(12)-P(2)	90.1(2)	P(3)-C(28)-P(4)	90.1(2)
C(7)-P(1)-O(2)	118.4(2)	C(23)-P(3)-O(4)	118.2(2)
Mo(1)-P(1)-O(2)	162.88(12)	Mo(2)-P(3)-O(4)	163.48(11)

Table 2.2 : Selected bond lengths (Å) and angles (°) for **3**

If the structures of complexes **2** and **3** are compared, it may be seen that the η^3-phosphaallyl group is bound closer to the molybdenum centre in **3** than the η^4-1,3-diphosphacyclobutadiene ligand in **2**. As a result of the distortion of the 4 membered ring in complex **3**, the P-C bond lengths involving P(1) and P(3) are longer than

those in complex **2**, whilst those involving the atoms P(2) and P(4) are shorter. The C-P-C angles involving the oxidised phosphorus atoms [P(1) and P(3)] are longer than those observed in complex **2**, whilst the other C-P-C angles are shorter, as are the P-C-P angles.

From a bonding perspective, **3** can be viewed in terms of the two canonical forms **A** and **B** (see Figure 2.5); one in which there is a formal bond between Mo and P(1) (**A**), or a zwitterionic alternative in which there is no bond between these two atoms (**B**). On the basis of the long Mo(1)-P(1) and Mo(2)-P(3) distances coupled with the fact that in the IR spectrum of **3**, the carbonyl group stretch is observed at 67 cm^{-1} lower frequency compared to **1**, which is consistent with a negative charge on the molybdenum atom, it is thought that **B** best represents the mode of bonding in **3**. In either canonical form P(1) may be regarded as being formally phosphorus(V).

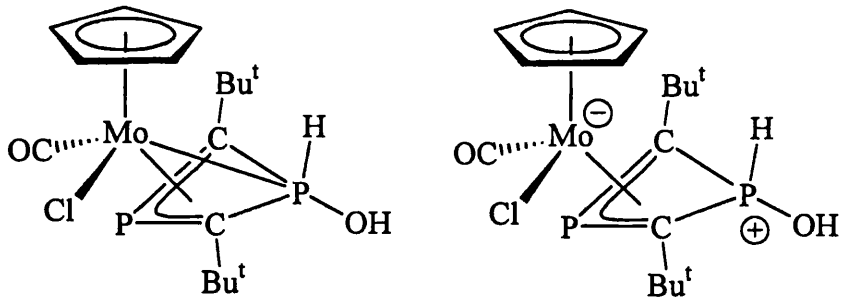

Figure 2.5

Further evidence for the structure of **3** comes from the comparison of the solid state structures of **3** and the related zwitterionic complex **2.5** (see Section 2.1.1). A comparison of the bond lengths and angles in the two complexes (Table 2.3) shows good similarities. Only the analogous Mo-P distances are not directly comparable with each other (within experimental limits). This may be because of the change in charge on the metal centres (-1 for **3**, neutral for **2.5**).

In the ^1H NMR spectrum of **3**, the phosphorus bound hydrogen is observed as a doublet of doublets at 8.11 ppm ($^1J_{HP}$ = 499.0 Hz, $^3J_{HP}$ = 4.1 Hz). The hydroxyl proton is not observed, presumably due to fast exchange in solution. In the proton-coupled ^{31}P NMR spectrum two different phosphorus environments are observed at

8.9 and –15.8 ppm, both significantly shifted to higher field from those seen for **1**. The lower field resonance is split as a doublet, with the large coupling constant being the same as that seen for the phosphorus bound hydrogen in the ^{1}H NMR spectrum ($^1J_{PH}$ = 499.0 Hz). This confirms the presence of a P-H bond.

3		**2.5**	
Mo(1)-P(1)	2.8751(14)	Mo(1)-P(1)	2.904(2)
Mo(1)-P(2)	2.4178(11)	Mo(1)-P(2)	2.450(2)
Mo(1)-C(7)	2.300(3)	Mo(1)-C(2)	3.320(6)
Mo(1)-C(12)	2.279(4)	Mo(1)-C(1)	2.308(7)
P(2)-C(7)	1.839(3)	P(2)-C(2)	1.824(8)
P(1)-C(7)	1.743(3)	P(1)-C(2)	1.766(6)
P(2)-C(12)	1.847(3)	P(2)-C(1)	1.823(8)
P(1)-C(12)	1.744(4)	P(1)-C(1)	1.739(9)
C(7)-P(1)-C(12)	86.6(2)	C(1)-P(1)-C(2)	84.9(3)
C(7)-P(2)-C(12)	80.9(2)	C(1)-P(2)-C(2)	80.9(3)
P(1)-C(7)-P(2)	90.5(2)	P(1)-C(1)-P(2)	91.9(4)
P(1)-C(12)-P(2)	90.1(2)	P(1)-C(2)-P(2)	91.0(3)
C(7)-P(1)-O(2)	118.4(2)	C(1)-P(1)-F(2)	117.5(4)

Table 2.3: Comparison of bond lengths between complexes **3** and **2.5**

The infrared spectrum of **3** displayed a single band in the C≡O stretching region at 1921 cm^{-1}, a movement to lower frequency of 67 cm^{-1} from the band observed for complex **1**.

It was found that **1** undergoes reaction with water (slowly with atmospheric, circa 2 days on addition of 10 equivalents) to afford complex **3**, in essentially quantitative yield. In sharp contrast complex **2** is remarkably stable to attack by water. Deuterated benzene solutions of **2** remain unchanged (by ^{1}H and ^{31}P{^{1}H} NMR spectroscopy) on exposure to atmospheric water for 2 weeks, whilst heating the complex to reflux in THF with an excess of water for 24 hours also leaves **2** unreacted.

2.1.2.4 *Reaction of [MoCl(CO)(η^4-1,3-$P_2C_2Bu^t_2$)(η^5-C_5H_5)], 1, with MeOH*

In an analogous manner to the formation of **3**, the reaction of **1** with MeOH affords the complex [MoCl(CO){η^3,λ^3,λ^5-$PC_2Bu^t_2PH(OMe)$}(η^5-C_5H_5)], **4**, in ~90% yield after 7 days (Scheme 2.6) as red crystals which precipitate out of solution. Side products left in the solution include **3** and at least two other unidentified compounds. Complex **4** was characterised by multinuclear NMR and infrared spectra.

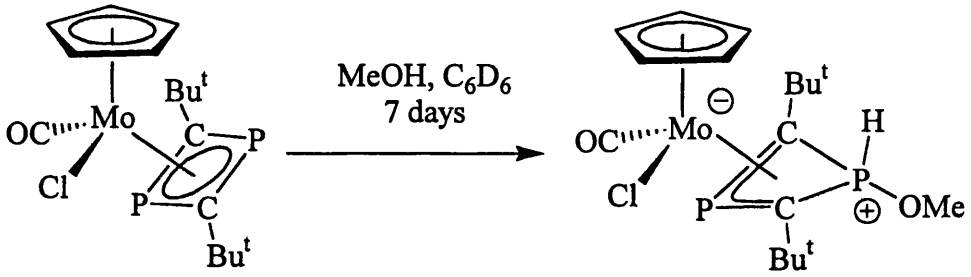

1 **4**

Scheme 2.6

The ^1H and ^{31}P NMR spectra for **4** are similar to those for **3**. The proton coupled ^{31}P NMR shows two signals at 10.6 and –16.7 ppm, the lower field signal split as a doublet ($^1J_{HP}$ = 496.3 Hz). The same coupling constant is observed in the ^1H NMR spectra for the signal which corresponds to the phosphorus bound proton, which is found at 8.00 ppm. The methoxy group is seen as a doublet at 3.90 ppm ($^3J_{HP}$ = 12.1 Hz). The infrared spectra of **4** shows a single band in the C≡O stretching region at 1889 cm^{-1}, a movement to lower frequency of 99 cm^{-1} from the resonance seen in **1**.

2.1.2.5 *Reaction Mechanism for Formation of [MoCl(CO){η^3,λ^3,λ^5-$PC_2Bu^t_2PH(OR)$}(η^5-C_5H_5)] (R = H or Me)*

As previously stated, the formulation of compounds **3** and **4** corresponds to the selective oxidative [P(III) → P(V)] addition of water or methanol respectively to one of the phosphorus centres present in the η^4-1,3-diphosphacyclobutadiene complex **1**.

Such behaviour in η^4-1,3-diphosphacyclobutadiene complexes has not previously been observed.

There are three possible mechanisms by which these reactions may proceed. They are shown in Scheme 2.7. Pathway **A** proceeds *via* an initial deprotonation of H_2O or MeOH, followed by nucleophilic attack by HO^- or MeO^- on the resulting [1,3-$PC_2P(H)]^+$ ring. Pathway **B** involves an initial nucleophilic attack by ROH to form an anionic intermediate, whilst in pathway **C**, the process is concerted, relying on hydrogen bonding.

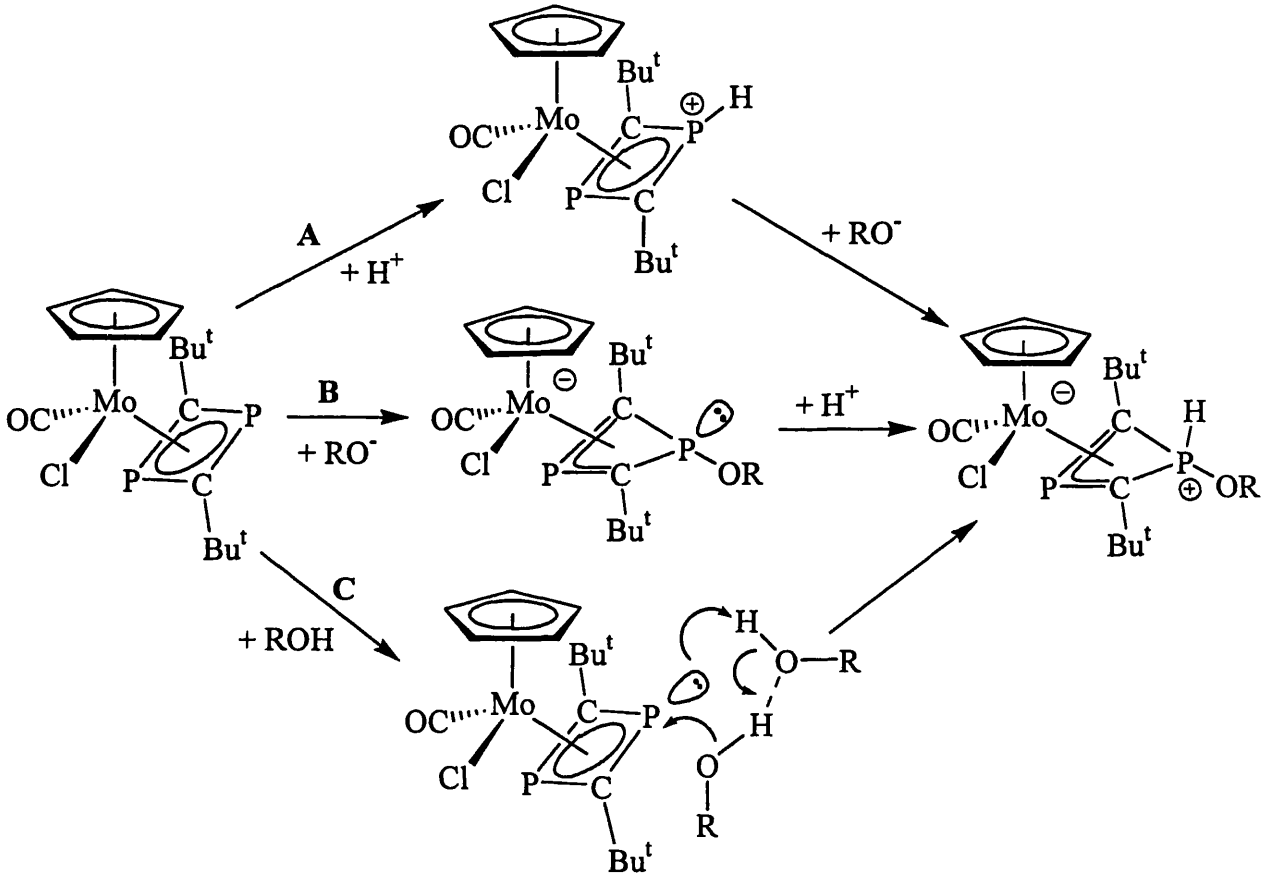

Scheme 2.7

NMR experiments carried out within our group have revealed a large positive kinetic isotope effect $k_D/k_H \approx 3.6$ [$t_{½}$ (H_2O) = 5.5 h, $t_{½}$ (D_2O) = 20 h]. This would indicate that an O-H bond is broken in the rate determining step of the reaction, and so is in accord with all three of the proposed mechanisms.

Although it has been previously shown that one of the phosphorus lone pairs of a coordinated 1,3-diphosphacyclobutadiene ring can coordinate onto transition metal Lewis acid fragments,[9] it seems unlikely that the formation of **3** or **4** proceeds *via* mechanism **A**, as this would require the η^4-1,3-diphosphacyclobutadiene ligand to be a strong enough base to deprotonate water.

Supporting evidence for pathway **B** comes from the solid state structure of **2.5**, in which the BF_4^- anion is bonded to one of the phosphorus centres resulting in the formation of the zwitterionic species shown in Figure 2.1. Whereas in solution the BF_4^- anion rapidly dissociates from **2.5**, in the case of the formation of **3** and **4**, *trans*-nucleophilic attack on the phosphorus centre is followed by the subsequent addition of H^+ at the same site.

Additional support for pathway **B** comes from the zwitterionic complex **2.7**, generated from a putative intermediate resulting from the attack of PF_6^- at a coordinated η^4-1,3-diphosphacyclobutadiene ring (Scheme 2.8).[10]

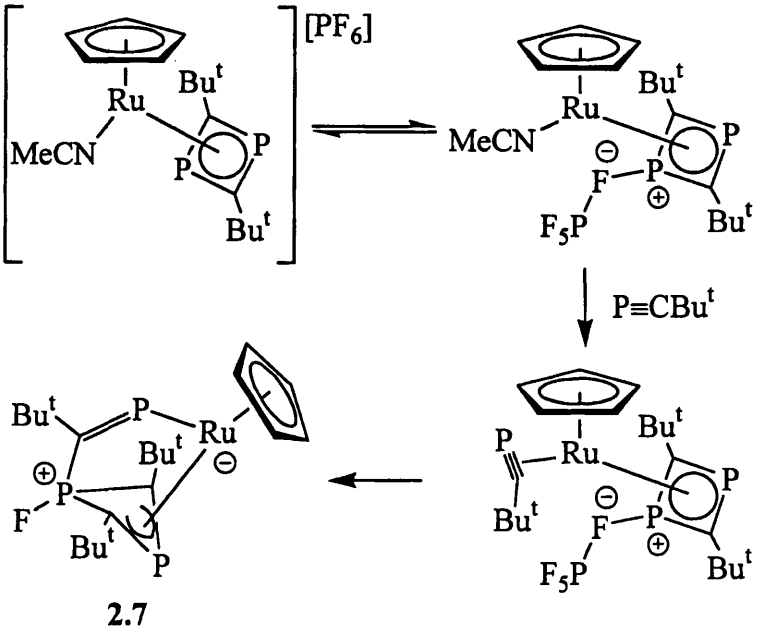

2.7

Scheme 2.8

2.1.3 Suggested Further Work

As the reaction of ROH with a η^4-1,3-diphosphacyclobutadiene ring was previously unrecorded, this reaction deserves further investigation. To that end, it is suggested that the reaction is repeated with other known complexes of the 1,3-diphosphacyclobutadiene ligand, in order to see if this is a general reaction or special case. New 1,3-diphosphacyclobutadiene complexes analogous to **1** and **2** can also be synthesised from $[WCl(CO)_3(\eta^5\text{-L})]$, by a photochemical reaction, or from the isoelectronic $[ReCl_2(CO)_2(\eta^5\text{-L})]$. These may then also be reacted with ROH.

The reaction itself between **1** and ROH could be investigated further. A wide variety of alcohols could be used, especially to create complexes with interesting structural aspects. The reaction between **1** and an aliphatic diol might be expected to give a dinuclear complex, with the alcohol bridging between two molybdenum centres. Alternatively, if catechol were used, the products might show unusual intramolecular hydrogen bonding.

The reactions of **1** with reagents related to ROH might also bear investigation. For example thiols and primary amines and phosphines might be expected to give analogous products.

2.2 Alkyne – Phosphaalkyne Cotrimerisations at Molybdenum Centres

2.2.1 Introduction

Metal mediated coupling reactions between alkynes and phosphaalkynes are relatively uncommon. In general, when a mixture of an alkyne and a phosphaalkyne is reacted in the presence of a metal centre, the alkyne molecules will couple with each other, whilst the same occurs with the phosphaalkyne molecules. However, a number of examples of alkyne-phosphaalkyne coupling reactions have been discovered (See Section 1.3.2). Of these, three examples of alkyne-phosphaalkyne cotrimerisation are known.

The iron complex $[Fe(C_2H_4)_2(\eta^6\text{-}C_6H_5Me)]$ has been shown to react with *tert*-butylphosphaalkyne to produce a 1,3-diphosphacyclobutadiene complex, plus reorganisation products.[11] However, if the iron complex is reacted at low temperature first with a terminal alkyne, and then with 4 equivalents of phosphaalkyne, a cotrimerisation can occur. The product, complex **2.8**, is shown in Scheme 2.9. The mechanism of the reaction is believed to involve a [2+2+2] cyclisation, and it may be significant that the substituted alkynic carbon is always adjacent to a phosphorus. Reacting the complex with $FeCl_3$ or halogenated hydrocarbons can remove the 1,3-diphosphabenzene from the metal.

Binger and co-workers have published an account of a cotrimerisation reaction between an alkyne and two phosphaalkyne molecules on a rhodium centre.[12] The product, **2.9**, has a structure resembling that of the ruthenium complex **2.7**, which is the product of a phosphaalkyne trimerisation.

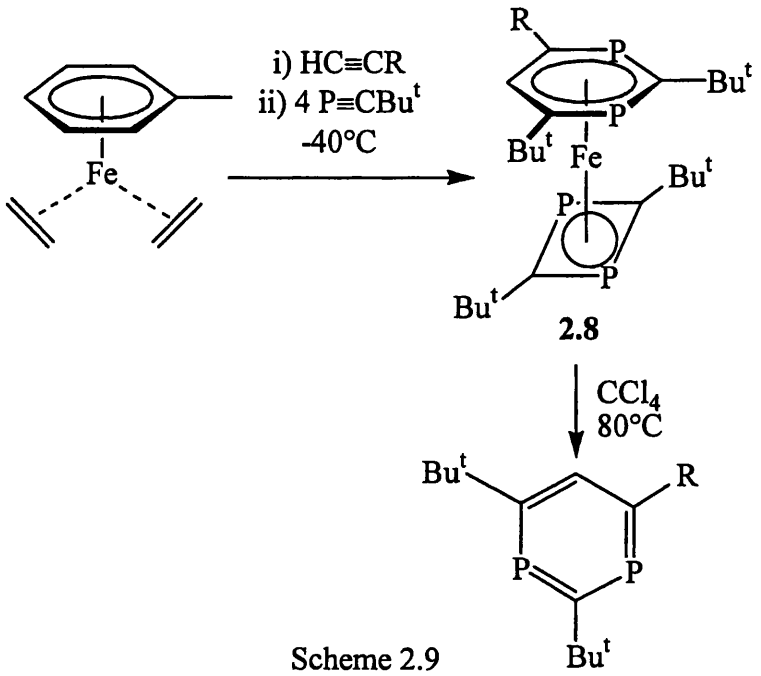

Scheme 2.9

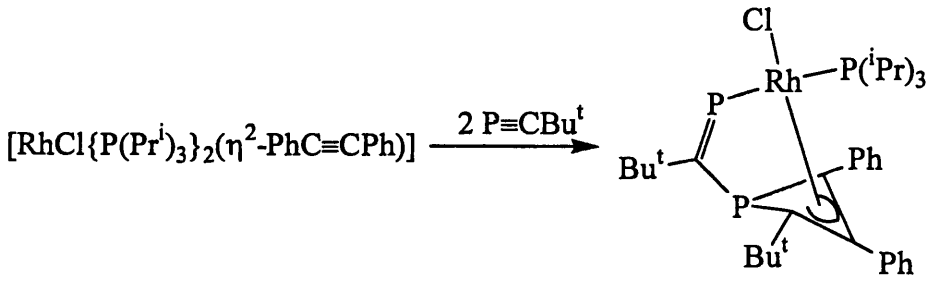

Scheme 2.10 **2.9**

In an attempt to prepare a complex containing both alkyne and phosphaalkyne ligands, analogous to those formed by the reaction of $[MoCl(CO)_3(\eta^5\text{-}C_5H_5)]$ with alkynes (see Section 2.1.1), a chloride ion was abstracted from the complex $[MoCl(CO)\{\eta^2(4e)\text{-}PhC{\equiv}CPh\}(\eta^5\text{-}C_5H_5)]$ with $TlPF_6$ in the presence of *tert*-butylphosphaalkyne.[13] If one equivalent of phosphaalkyne was used, a 1:1 mixture of starting material and a product were seen. When two equivalents of phosphaalkyne were used, the 16 electron carbene complex **2.10** was obtained in reasonable purity (Scheme 2.11).

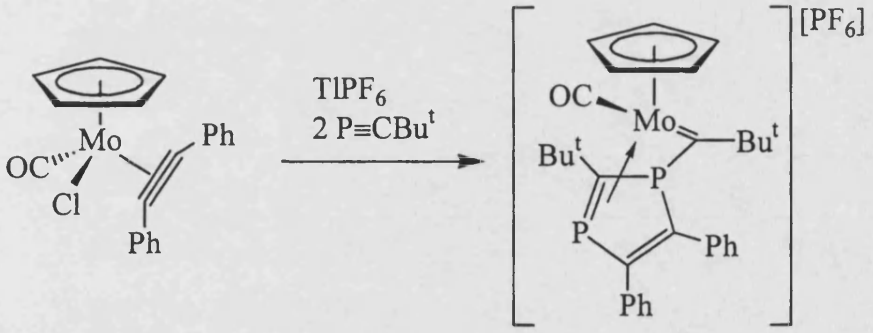

Scheme 2.10 **2.9**

An X-ray crystallographic study showed that only one of the two double bonds in the pendant 1,3-diphosphacyclopentadiene ring was coordinated to the metal (Figure 2.5). Presumably the restriction of the conformation of the ring caused by the presence of the carbene bond precludes the C=C bond from approaching near enough to allow coordination [Mo(1)-C(11) = 3.450(7), Mo(1)-C(12) = 3.443(6) Å].

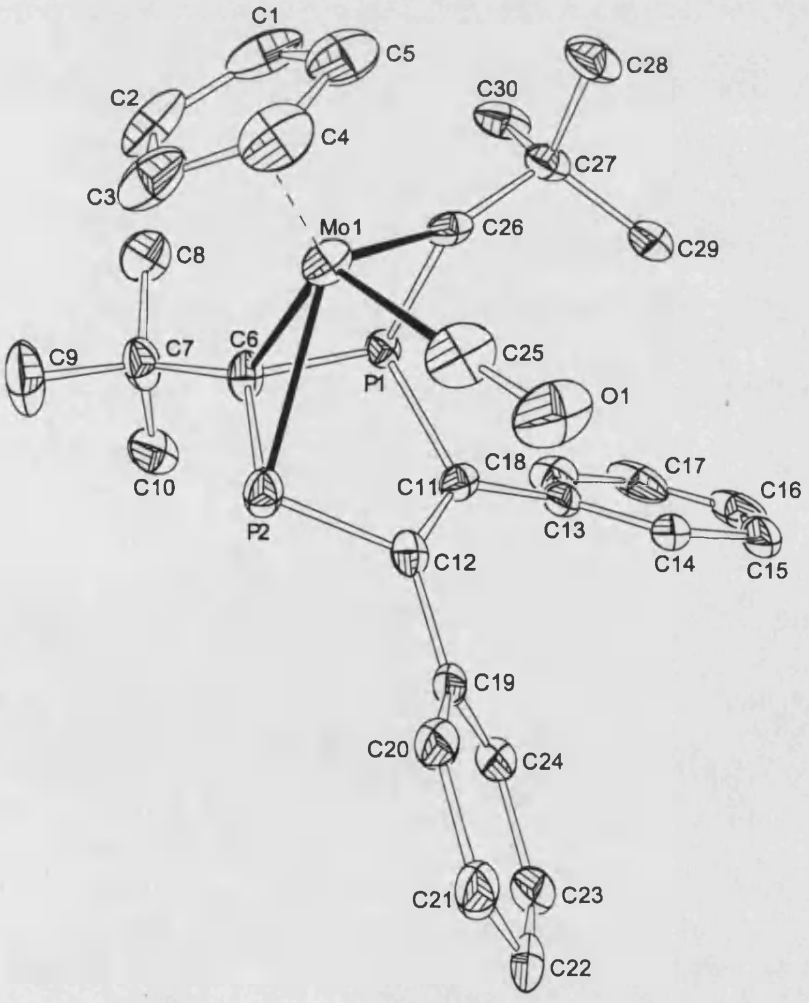

Figure 2.6: Structure of cation of complex **2.10**

Carrying out the same reaction with the unsymmetrical alkyne 1-phenylprop-1-yne complex gave the analogous complex **2.11** shown in Scheme 2.12. However, it was observed by $^{31}P\{^1H\}$ and ^1H NMR spectroscopy that only one of the two possible structural isomers, which vary by placement of the phenyl and methyl groups, had formed, though it was not possible to distinguish which had been produced.

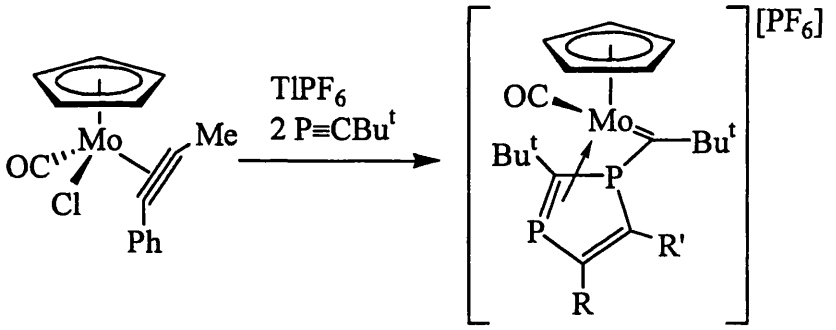

$R \neq R'$ = Ph or Me

2.11

Scheme 2.12

Due to the rapid decomposition of the products, it proved impossible to record $^{13}C\{^1H\}$ NMR spectra of these complexes. This decomposition may be due to the presence of thallium residues in the final product. This suggestion was reinforced by the observation that if reaction times longer than 30 minutes were used, decomposition of the products was seen to occur.

2.2.2 Results and Discussion

2.2.2.1 Introduction

It was decided to investigate the formation of complexes related to **2.10** and **2.11**. The primary interest was to discover a way of producing complexes of this type which did not involve the use of thallium salts, which were believed to be involved in the rapid decomposition of the products.

It has previously been shown that the reaction of $[MoX(CO)\{\eta^2(4e)\text{-}PhC{\equiv}CPh\}(\eta^5\text{-}C_5H_5)]$ with silver salts in the presence of ethene results in the formation of the

cationic ethene complexes $[Mo(CO)(\eta^2\text{-}C_2H_4)\{\eta^2(4e)\text{-}PhC{\equiv}CPh\}(\eta^5\text{-}C_5H_5)]^+$, **2.12**.[14] The labile ethene ligand may then be replaced by a range of other ligands (Scheme 2.13). Therefore, it was reasoned that **2.12** could act as an alternative precursor for the formation of **2.10** and **2.11**. It could be expected that rapid replacement of the ethene by the *tert*-butylphosphaalkyne would occur, followed by a further reaction with a second equivalent of phosphaalkyne to give the desired complexes (Scheme 2.14). This would avoid any decomposition reactions resulting from the presence of trace amounts of thallium containing impurities.

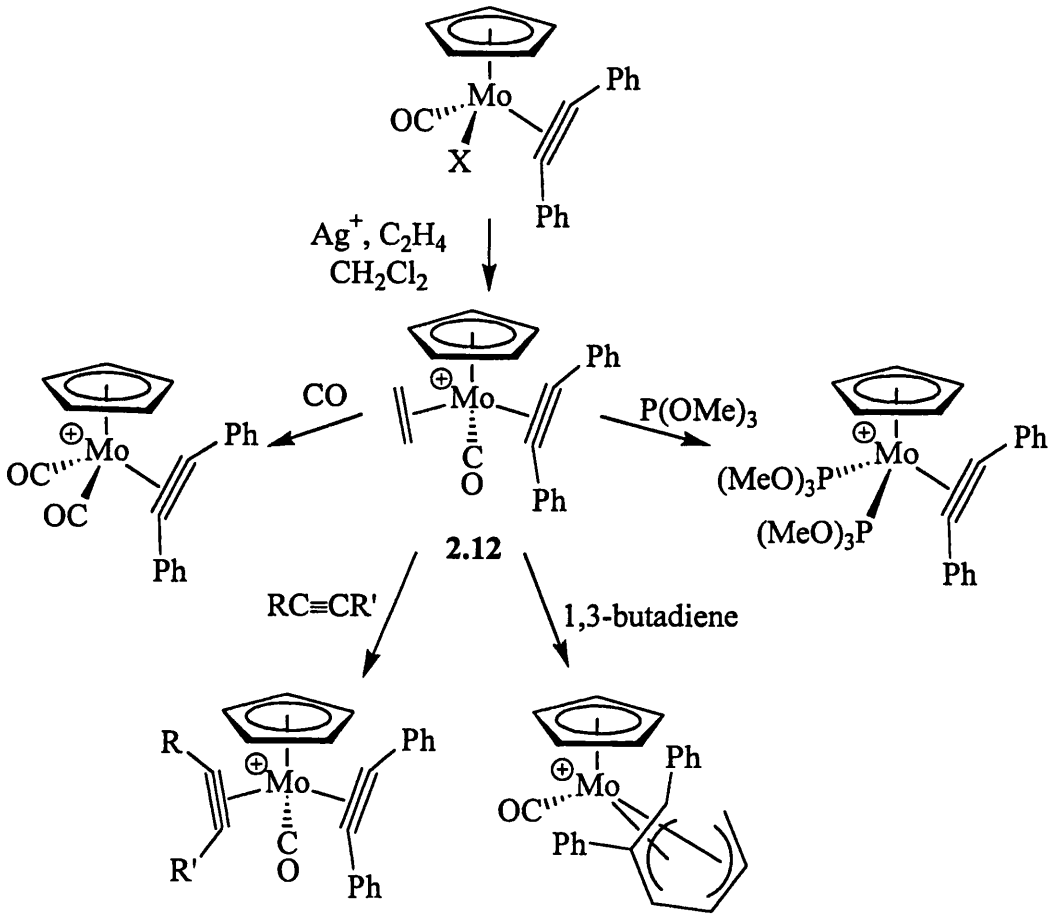

Scheme 2.13

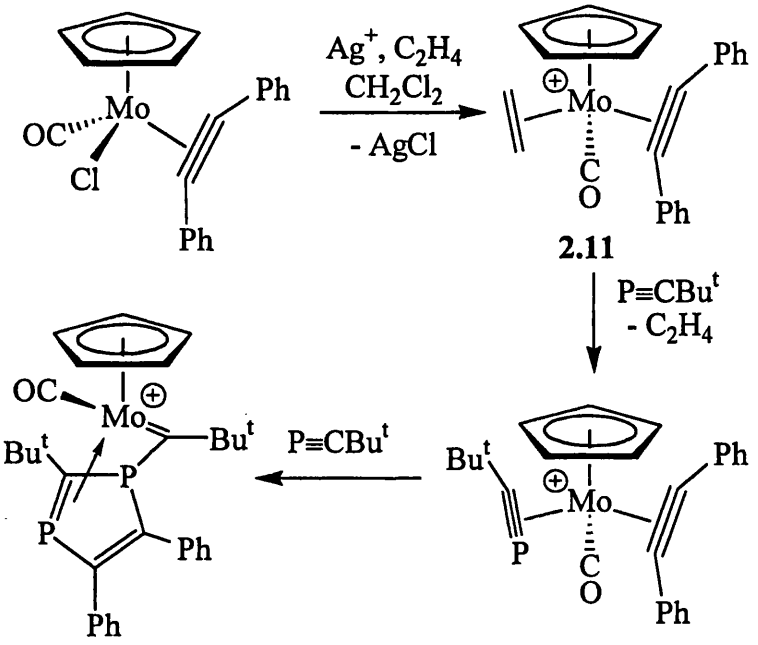

Scheme 2.14

2.2.2.2 Reaction of [MoCl(CO){η^2(4e)-PhC≡CR}(η^5-C_5H_5)] (R = Ph or Me) with $AgBF_4$, Ethene and *tert*-Butylphosphaalkyne

To a solution of the alkyne complex [MoCl(CO){η^2(4e)-PhC≡CPh}(η^5-C_5H_5)] in CH_2Cl_2 saturated with ethene was added with one equivalent of $AgBF_4$ with exclusion of light. After 15 minutes the originally green solution had turned red, and a white precipitate of AgCl had formed. The solution was filtered through a Celite pad under an atmosphere of ethene to remove the silver salt to give a red solution of [Mo(CO)(η^2-C_2H_4){η^2(4e)-PhC≡CPh}(η^5-C_5H_5)][BF_4], **5**, which was identified by the C≡O stretch in its infrared spectrum (1950 cm^{-1} in CH_2Cl_2). This ethene complex was not isolated, but instead the solution was treated with 2.1 equivalents of *tert*-butylphosphaalkyne. After stirring for 30 minutes an infrared spectra showed no trace of complex **5**. Removal of the solvents *in vacuo* gave the product [Mo(η^5-C_5H_5)(CO)(=C{Bu^t}P{η^2-C(Bu^t)=P}C{Ph}=C{Ph})][BF_4], **6**, as a red oil and in moderate yield (60%). This compound was characterised on the basis of multinuclear NMR and infrared spectroscopy and compared to the hexafluorophosphate derivative already known. The reaction scheme and structure of the product is shown in Scheme 2.15.

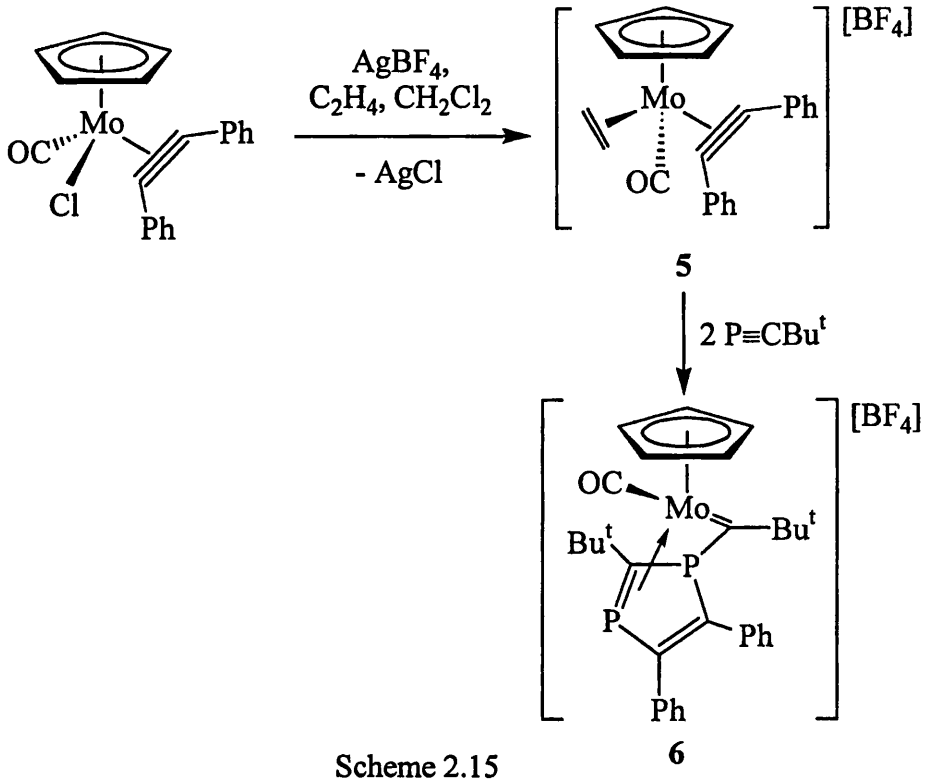

Scheme 2.15

The infrared spectrum of **6** as a solution in CH_2Cl_2 showed a single peak in the carbonyl C≡O stretching region. The high value of ν_{CO} (2053 cm^{-1}) implies that the metal is electron deficient, as in a 16-electron complex. The $^{31}P\{^1H\}$ NMR spectrum of **6** showed two resonances at 48.7 and –87.7 ppm, which were mutually coupled ($^2J_{PP}$ = 19.9 Hz). The ^1H NMR spectra showed two distinct *tert*-butyl resonances at 1.90 and 1.14 ppm. Unfortunately, it was not possible to record a full $^{13}C\{^1H\}$ NMR spectra, though the resonances for the η^5-C_5H_5 ring, the carbonyl group, the phenyl groups and the *tert*-butyl groups were located. The remaining, quaternary sp^2 hybridised, carbons were expected to show coupling to at least one phosphorus atom each, but due to the low intensity of their signals they were not observed.

The mechanism for this reaction was unclear, so the reaction was repeated using the molybdenum complex of the unsymmetrical alkyne 1-phenylprop-1-yne (PhC≡CMe). It was thought that the positioning of the phenyl and methyl groups in the final complex would give an insight into the reaction's mechanism.

The reaction was repeated as for **6**, using the complex $[MoCl(CO)\{\eta^2(4e)\text{-}PhC{\equiv}CMe\}(\eta^5\text{-}C_5H_5)][BF_4]$, and proceeding via the ethene complex $[Mo(CO)(\eta^2\text{-}C_2H_4)\{\eta^2(4e)\text{-}PhC{\equiv}CMe\}(\eta^5\text{-}C_5H_5)][BF_4]$, **7**. The product $[Mo(CO)(=C\{Bu^t\}P\{\eta^2\text{-}C(Bu^t)=P\}C\{R\}=C\{R'\})(\eta^5\text{-}C_5H_5)][BF_4]$ (R ≠ R' = Ph or Me), **8**, was isolated in moderate yield as a red oil. This compound was characterised on the basis of multinuclear NMR and IR spectra. The reaction is shown in Scheme 2.16.

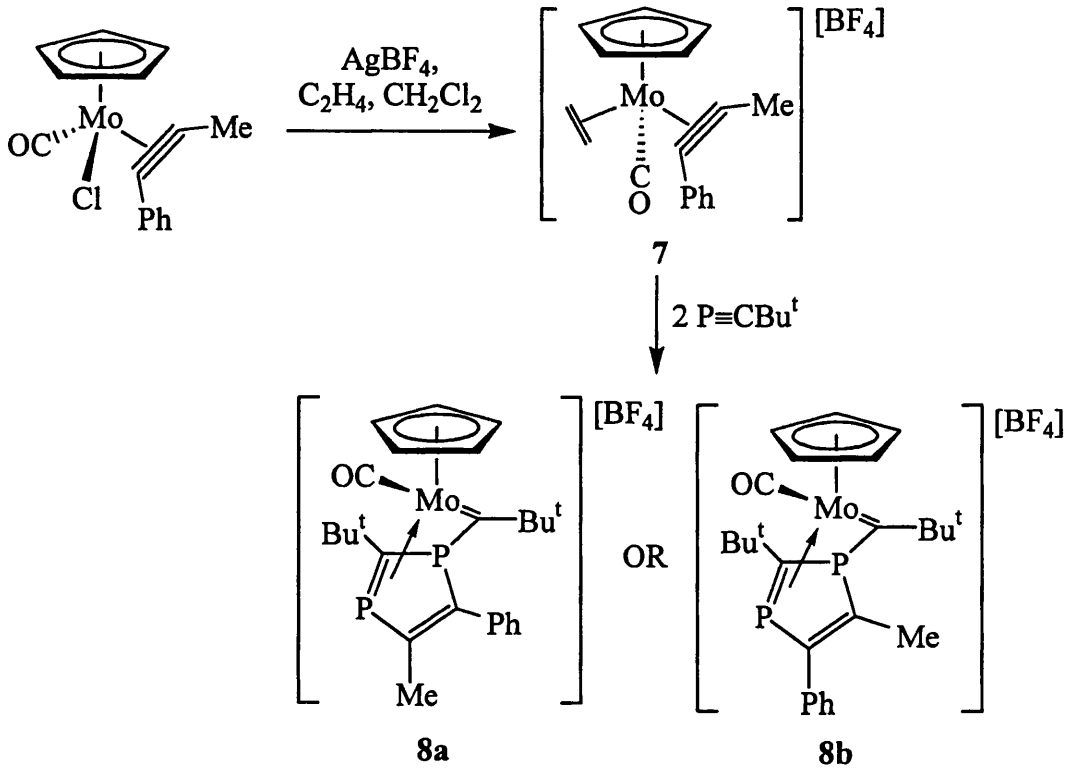

Scheme 2.16

As for complex **6**, two mutually coupled resonances ($^2J_{PP}$ = 20.1 Hz) were seen in the $^{31}P\{^1H\}$ NMR at 38.7 and –91.7 ppm. The ^1H NMR spectrum showed one $\eta^5\text{-}C_5H_5$ and methyl resonance (at 5.65 and 1.76 ppm respectively), indicating that only one structural isomer had formed. As for complex **6**, a full $^{13}C\{^1H\}$ NMR spectrum could not be recorded due to the low intensity of the quaternary carbon signals, but single resonances for methyl and $\eta^5\text{-}C_5H_5$ groups were seen, confirming that only one product was formed. The infrared spectrum recorded in a CH_2Cl_2 solution showed a single peak at high frequency (ν_{CO} = 2051 cm^{-1}) similar to that for **6**.

Despite repeated attempts by slow diffusion of non-polar solvents into CH_2Cl_2 and THF solutions, it proved impossible to recrystallise complex **8** to give X-ray quality crystals. Instead, oily solids were produced. This was unfortunate, as it means that the precise structure of the complex cannot be determined by crystallographic methods However, it may be possible to use NMR spectroscopy techniques such as Nuclear Overhauser Effect spectroscopy to determine which of the two possible structures is formed.

In contrast to the hexafluorophosphate derivatives made using thallium salts, complexes **6** and **8** showed improved stability. Whilst complexes **2.9** and **2.10** had decomposed completely after a matter of hours, samples of **6** and **8** were observed (by ^1H and $^{31}P\{^1H\}$ NMR} to begin decomposition after 7 days and to be completely decomposed after 4 weeks. The reaction time used in the synthesis of **6** and **8** also did not need the same degree of accuracy required for their hexafluorophosphate derivatives **2.8** and **2.9**. Whilst using a reaction time longer than 30 minutes in the preparation of the latter complexes led to rapid decomposition, no such sensitivity was seen with the analogous tetrafluoroborate complexes.

An NMR experiment was carried out on the formation of **6** by adding *tert*-butylphosphaalkyne to a CD_2Cl_2 solution of **5** at -78°C contained in an NMR tube. Allowing the solution to warm to room temperature whilst monitoring the reaction by $^{31}P\{^1H\}$ and ^1H NMR indicated that the reaction occurs at -40°C. At this temperature, the peaks due to the starting material **5** slowly disappeared to be replaced with peaks due to **6**. No other peaks, which would have been due to reaction intermediates, were seen.

2.2.2.3 Sterically Hindered Analogues of Complex 6 as Tools in Determining Reaction Mechanism

It was thought that by increasing the steric bulk of the η^5-ligand, intermediates in the formation of complexes analogous to **6** might be isolated, or stabilised enough to survive on the NMR timescale. To that end it was decided to use a cyclopentadienyl

ring with a bulky substituent group as the η^5-ligand. The substituent group used was a *tert*-butyl group due to the expected large effect of such a bulky group, and the ease with which it could be made *via* 6,6-dimethylfulvene.

2.2.2.4 Preparation of [MoCl(CO)$_3$(η^5-C$_5$H$_4$Bu^t)]

To a cooled solution (-78°C) of 6,6-dimethylfulvene in THF was added one equivalent of methyl lithium. On warming to room temperature the yellow solution darkened to an orange colour. The solvents were removed *in vacuo* to give an orange residue of [Li][$C_5H_4Bu^t$]. This was not purified, but redissolved in THF and used in the literature preparation of [MoCl(CO)$_3$(η^5-C_5H_5)] in place of NaCp. The resulting complex [MoCl(CO)$_3$(η^5-$C_5H_4Bu^t$)], **9**, was purified by recrystallisation from a slow diffusion of hexane into a CH_2Cl_2 solution to isolate the product as an orange powder in moderate yield (38%). The reactions are shown in Scheme 2.17. Complex **9** was characterised by multinuclear NMR and infrared spectroscopy.

The ^{1}H NMR spectrum of **9** displayed two different resonances split as multiplets for the protons on the η^5-bonded ring at 5.60 and 5.42 ppm. A singlet was seen at 1.28 ppm which was assigned to the *tert*-butyl group. In the $^{13}C\{^1H\}$ NMR spectrum two peaks were observed in the metal carbonyl region at 242.8 and 225.6 ppm. Three different resonances were displayed for carbons in the η^5-bonded ring at 131.7, 96.4 and 92.6 ppm. The peak for the quaternary carbon from the *tert*-butyl group was displayed at 32.0 ppm, whilst that for the CH_3 components of the group was observed at 31.4 ppm. The infrared spectrum of **9** as a solution in CH_2Cl_2 has three bands in the C≡O stretching region at 2050, 1975 and 1951 cm^{-1}.

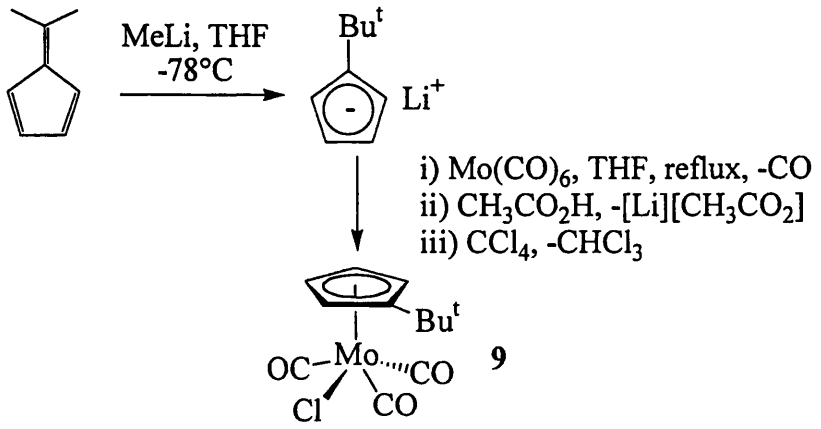

9

Scheme 2.17

2.2.2.5 *Preparation of [MoCl(CO){η^2(4e)-PhC≡CPh}(η^5-$C_5H_4Bu^t$)]*

Diphenylacetylene was added to a pentane solution of [MoCl(CO)$_3$(η^5-$C_5H_4Bu^t$)], **9**, and the reaction mixture heated at reflux for 24 hours. The red colour of the solution faded, and a green precipitate formed. The solvents were decanted and the precipitate recrystallised by a slow diffusion of hexane into a CH_2Cl_2 solution to give [MoCl(CO){η^2(4e)-PhC≡CPh}(η^5-$C_5H_4Bu^t$)], **10**, as a green powder in good yield (88%). The reaction is shown in Scheme 2.18. The complex was characterised by multinuclear NMR and infrared spectroscopy.

The ^{1}H NMR spectrum showed two different resonances split as multiplets for the ring protons on the η^5-$C_5H_4Bu^t$ group at 5.51 and 5.43 ppm. A single resonance for the *tert*-butyl group at 1.15 ppm was also observed. The $^{13}C\{^1H\}$ NMR spectra showed three different resonances for carbons in the η^5-bonded ring as expected at 97.6, 92.5 and 88.5 ppm. The infrared spectrum of **10**, recorded in CH_2Cl_2 solution, displayed a single band in the C≡O stretching region at 1938 cm^{-1}.

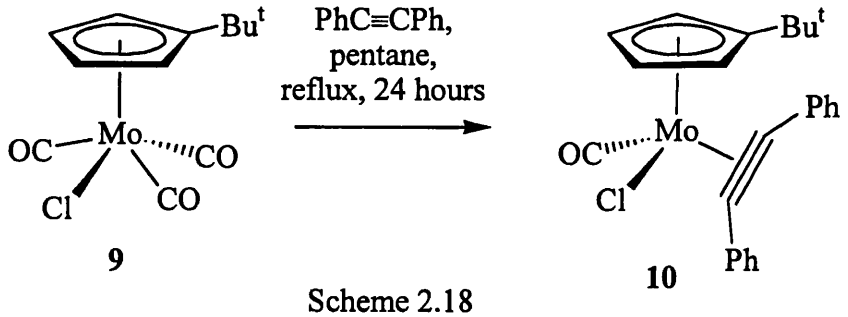

Scheme 2.18

2.2.2.6 *Reaction of [MoCl(CO){η^2(4e)-PhC≡CPh}(η^5-$C_5H_4CBu^t$)] with $AgBF_4$, ethene and tert-Butylphosphaalkyne*

The reaction was repeated as for **6**, using the complex **10** and proceeding via the ethene complex [Mo(CO)(η^2-C_2H_4){η^2(4e)-PhC≡CMe}(η^5-$C_5H_4Bu^t$)][BF_4], **11**. The product [Mo(CO)(=C{Bu^t}P{η^2-C(Bu^t)=P}C{Ph}=C{Ph})(η^5-$C_5H_4Bu^t$)][BF_4], **12**, was isolated as a green oil in moderate yield (50%). Characterisation was carried out by

multinuclear NMR and infrared spectroscopy. The reaction is shown in Scheme 2.19. As for **6** and **8**, despite repeated attempts using a wide variety of solvents, it proved impossible to obtain X-ray quality crystals, the complex remaining as a green oil.

As for complex **6**, two mutually coupled resonances ($^2J_{PP}$ = 19.5 Hz) were seen in the $^{31}P\{^1H\}$ NMR spectrum at 51.3 and –93.4 ppm. The ^1H spectrum was as expected, with distinct signals for all three *tert*-butyl groups at 1.95, 1.28 and 1.12ppm. One set of signals (2 multiplets at 5.60 and 5.42ppm) were seen for the ring protons from the η^5-$C_5H_4Bu^t$ ligand. As for **6** and **8**, it was not possible to assign a full $^{13}C\{^1H\}$ NMR spectrum due to the low intensity of the quaternary carbon signals, but resonances were seen for the carbonyl group, phenyl groups, η^5-$C_5H_4Bu^t$ ligand and the *tert*-butyl groups. The infrared spectrum, recorded in CH_2Cl_2, showed a single peak at 2044 cm^{-1}.

Despite the expected effect of the bulky *tert*-butyl substituent group on the η^5-ring, no sign of any reaction intermediates was seen in the final reaction mixture. A variable temperature NMR experiment, carried out in the same way as for complex **6** gave an identical result. The reaction started to occur at -40°C, whilst no peaks due to intermediates were observed in either the $^{31}P\{^1H\}$ or ^1H NMR spectra.

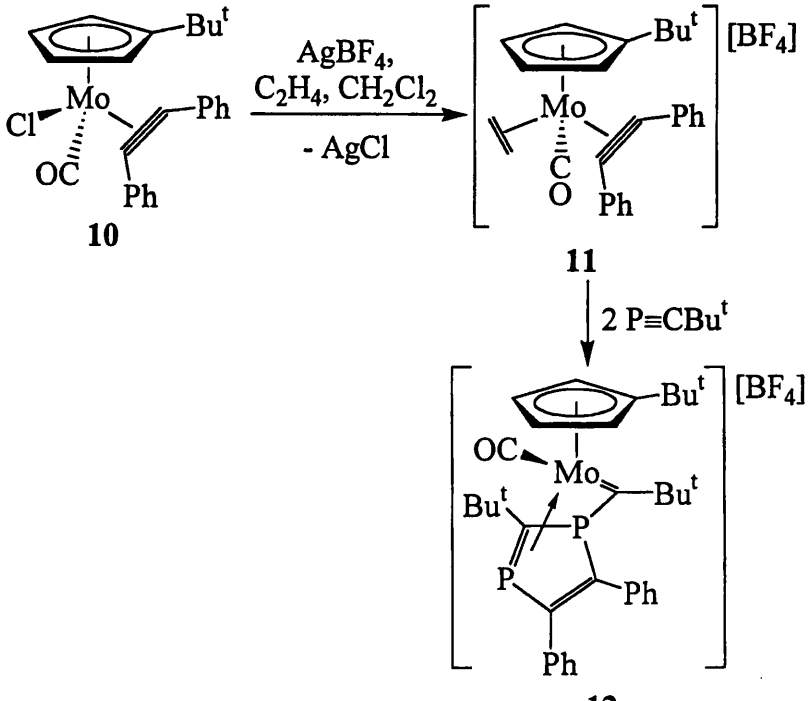

Scheme 2.19

2.2.2.7 *Proposed Mechanism for the Reaction of [Mo(CO)(η^2-C_2H_4){η^2(4e)-PhC≡CR}(η^5-L)][BF_4] with tert-Butylphosphaalkyne*

Although the lack of data on the intermediates prevents any definite conclusions being made, a possible mechanism (Scheme 2.19) for the reactions of the complexes [Mo(CO)(η^2-C_2H_4){η^2(4e)-PhC≡CR}(η^5-L)][BF_4], with *tert*-butylphosphaalkyne may be formulated by examining other known coupling reactions of alkynes and phosphaalkynes at metal centres.

Presumably the first step in the reactions is the formation of intermediate **A**, whose analogous bis(alkyne) complexes can be prepared in the same manner. It is then logical to suppose that a coupling reaction occurs to give the 16-electron complex **B**. In the initial stages of the reaction there is a resembence to the formation of the zirconocene complex **2.13** which was made by Binger and co-workers in the reaction shown in Scheme 2.20.[15]

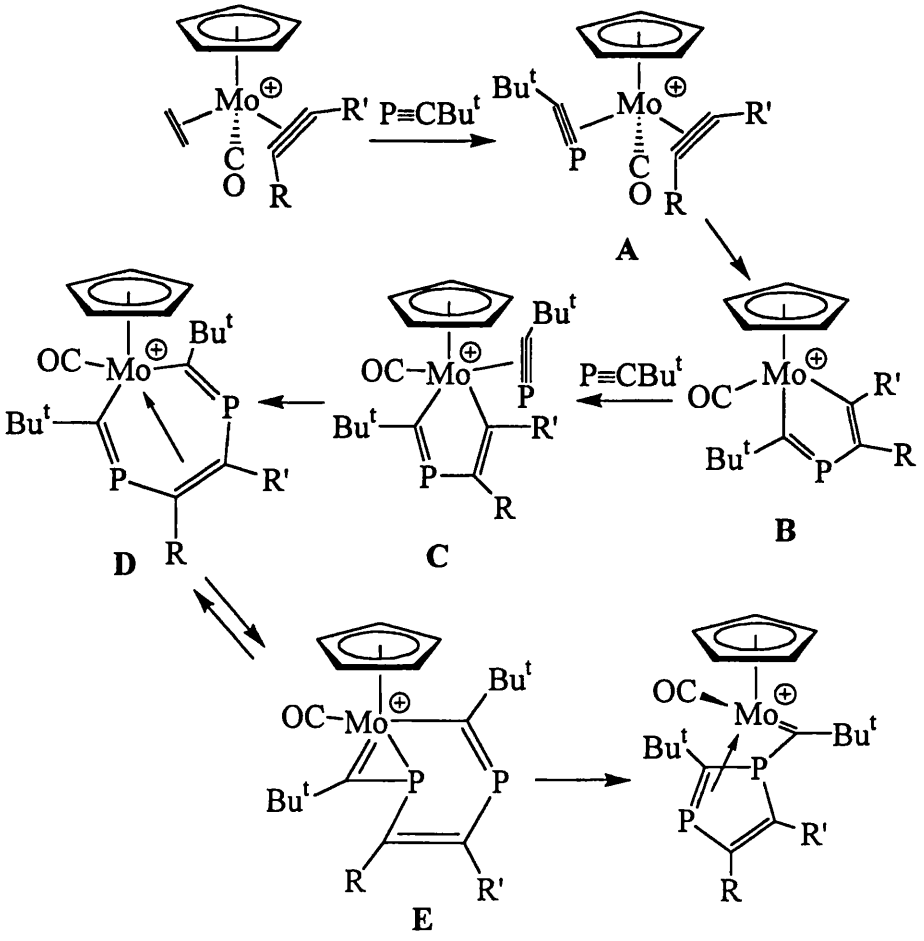

Scheme 2.19

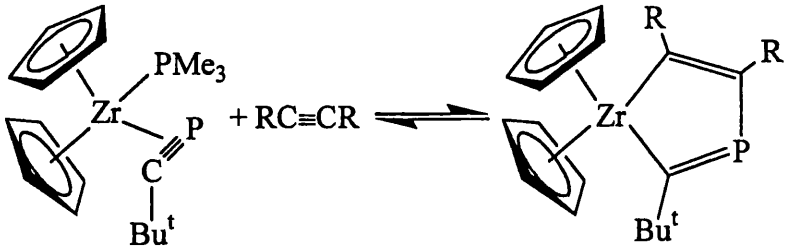

Scheme 2.20 **2.13**

As **B** is a 16-electron complex, another molecule of phosphaalkyne can coordinate, giving **C**. A second coupling reaction may then occur to give the metallacycloheptatriene complex **D**. If the double bond from the alkyne fragment coordinates to the metal, **D** is an 18-electron complex analogous to complex **2.14** which has been synthesised by Davidson and co-workers (Scheme 2.21).[16]

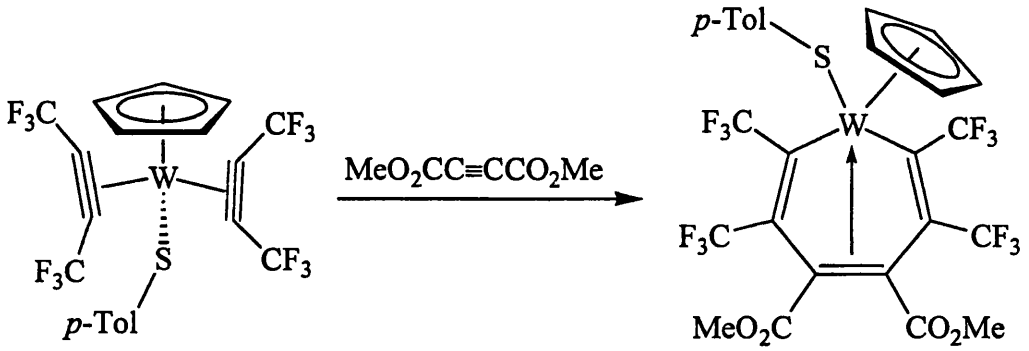

Scheme 2.21 **2.14**

Intermediate **D** may rearrange to give the η^2, 3 electron phosphaallyl complex **E**. This intermediate is similar to the η^2, 3 electron vinyl complex **2.15** already made within the group by reacting a cationic η^2(4e) alkyne complex with K[BHBu$^s_3$] as shown in Scheme 2.22.[17]

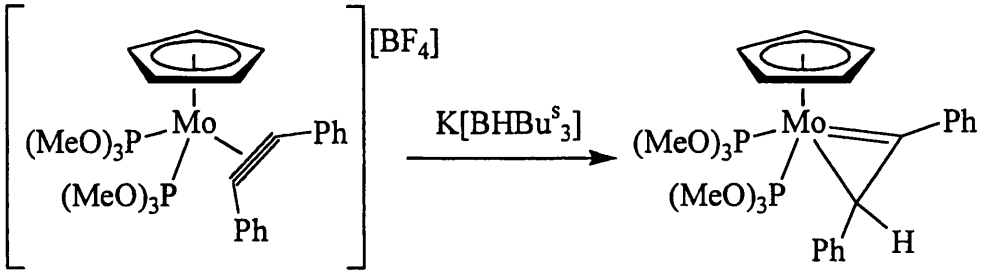

Scheme 2.22 **2.15**

The final step in the mechanism is a reductive elimination, where Mo-P and Mo-C bonds are broken and a C-P bond is made. It may be that the driving force behind this step is the release of strain from the 3 membered ring present in intermediate **E**.

2.2.2.8 Reaction of 6 with DIBAL-H

The characterisation of **6** as a 16-electron complex, caused by the inability of both double bonds in the pendant diphosphacyclopentadiene ring to coordinate to the metal is of interest. It was thought that if the geometric constraints imposed by the sp^2 carbene carbon were removed, it would be possible for both double bonds to coordinate, thus generating an 18-electron complex. To this end, a source of 'H^-' was used to carry out a nucleophilic attack on the carbene carbon, to convert it into a sp^3 hybridised atom.

The addition of one equivalent of Bu^i_2AlH (DIBAL-H) to a THF solution of **6** with stirring resulted in the formation of the red complex $[Mo(CO)(-CH\{Bu^t\}P\{\eta^2\text{-}C(Bu^t)=P\}\{\eta^2\text{-}C(Ph)=C(Ph)\})(\eta^5\text{-}C_5H_5)]$, **13**, in good yield (80 %). This compound was characterised on the basis of multinuclear NMR and infrared spectra, and is shown in Scheme 2.23.

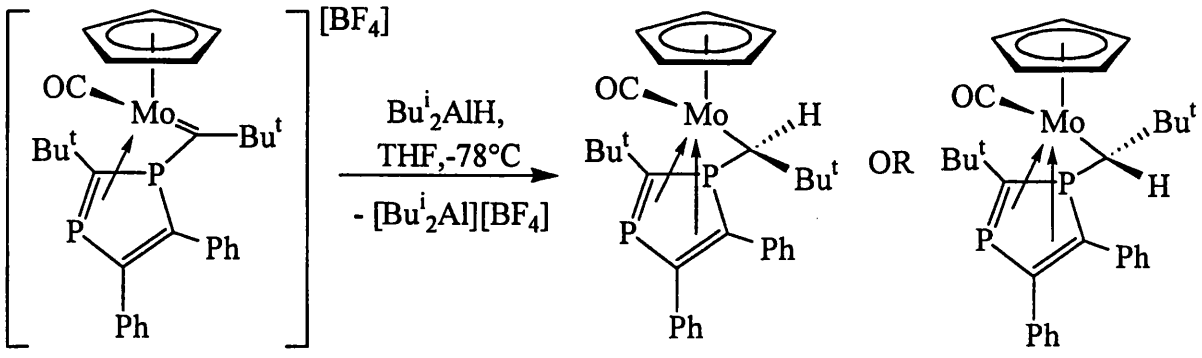

Scheme 2.23

The $^{31}P\{^1H\}$ NMR spectrum of **13** shows a pair of mutually coupled signals ($^2J_{PP}$ = 23.1 Hz) at 21.8 and –70.8 ppm. Compared to the spectra for **6**, **8** and **12**, the higher

field signal has shifted appreciably to lower field ($\Delta\delta \approx +20$ ppm), and *vice versa* ($\Delta\delta \approx -20$ ppm) while the coupling constant has increased slightly. The $^{13}C\{^1H\}$ NMR spectrum displayed the previously reported signals, plus a doublet ($^1J_{CP} = 29.6$ Hz) at 24.0 ppm due to the carbon bound to the molybdenum centre. A large shift was seen in the frequency of the carbonyl peak in the infrared spectra ($\nu_{CO} = 1882$ cm^{-1}, $\Delta\nu_{CO} = -170$ cm^{-1}).The ^1H NMR spectrum showed little change except for a new doublet ($^2J_{HP} = 7.6$ Hz) at 8.58 ppm corresponding to this new hydrogen atom. The value of the chemical shift for this peak discounts the possibility of an agostic interaction between the molybdenum and the new hydrogen atom, which might otherwise have been considered.

The significant shift of the carbonyl peak in the infrared spectrum is probably larger than could be explained by a simple change of charge on the metal centre. Therefore, we have proposed the structure shown above where both double bonds are now able to coordinate to the metal centre, making **13** an 18 electron complex. The combined effect of the change in charge plus the increase in electron density on the metal might then account for the large shift in the C≡O stretching frequency.

It may be surmised that the geometric constraints invoked by the presence of the sp^2 carbene carbon are released upon its conversion to a sp^3 carbon centre. This would therefore allow both double bonds in the pendant 1,3-diphosphacyclopentadiene ring to coordinate, giving an 18-electron complex. In contrast to the 16-electron complex, **13** decomposed within 3 days, due to unknown causes.

2.2.3 Suggested Further Work

It is proposed to perform one electron reductions on the 16 electron complexes **6**, **8** and **12** using cobaltocene followed by one electron oxidations with a ferrocenium salt. The purpose of these experiments is to investigate the stability of the 17 electron complexes.

It is important that the mechanism for the reactions of *tert*-butylphosphaalkyne with the complexes $[Mo(CO)(\eta^2\text{-}C_2H_4)\{\eta^2(4e)\text{-}PhC{\equiv}CR\}(\eta^5\text{-}L)][BF_4]$ is further investigated. Most especially, the structure of complex **8** needs to be found, as the positioning of the alkyne substituents may provide important information as to the governing factors in the reaction. To that end, it is proposed to react **8** with $[W(CO)_5(thf)]$, or other suitable complexes. The resulting bimetallic complexes may prove easier to crystallise than the initial compounds. The same method may be employed for complex **13**.

To date, the only alkyne complexes investigated have been those with either diphenylacetylene or 1-phenyl-1-propyne as the alkyne. By using a wider variety of alkynes, it may be that intermediates from the reaction can be isolated. Using primary alkynes might provide useful NMR data on the structure of the products, as the pattern of H/P coupling will be different depending upon which isomer is formed.

Using phosphaalkynes other than $P{\equiv}CBu^t$ may also be useful in analysis of the probable reaction mechanisms. Reactions involving phosphaalkynes with substiutuent groups even bulkier than *tert*-butyl (eg 2,4,6–$C_6H_2Bu^t_3$) may not progress to completion and the reaction intermediates for the reaction with *tert*-butylphosphaalkyne may thus be determined.

2.3 Conclusions

The reaction between the complexes $[MoCl(CO)_3(\eta^5\text{-}C_5R_5)]$ and *tert*-butylphosphaalkyne produces the η^4-1,3-diphosphacyclobutadiene complexes $[MoCl(CO)(\eta^4\text{-}1,3\text{-}P_2C_2Bu^t_2)(\eta^5\text{-}C_5R_5)]$ (R = H **1**, or Me **2**) in moderate and good yield respectively. Two different environments are observed for each of the phosphorus and carbon atoms in the 1,3-diphosphacyclobutadiene rings due to the asymmetry of the metal centre, and slow rotation of the ring on an NMR timescale. A crystal structure determination was carried out on **2**, confirming its identity.

Whilst complex **2** is remarkably stable to the ambient environment, **1** undergoes reaction with R'OH (R = H or Me) to give the complexes [MoCl(CO){η^3,λ^3,λ^5-$PC_2Bu^t_2PH(OR')$}(η^5-C_5H_5)] (R' = H **3**, or Me **4**) in almost quantitative yield. An X-ray crystallographic study of **3** indicates that one of the phosphorus atoms has undergone a formal oxidation to give a zwitterionic η^3,λ^3,λ^5-phosphaphosphonietinyl complex.

The reactions of [MoCl(CO){η^2(4e)-PhC≡CR}(η^5-L)][BF_4] (L = C_5H_5, $C_5H_4Bu^t$, R = Ph or Me) with $AgBF_4$, ethene and *tert*-butylphosphaalkyne to give the complexes [Mo(CO)(=C{Bu^t}P{η^2-C(Bu^t)=P}C{R}=C{R'})(η^5-L)][BF_4] (**6** L = C_5H_5, R = R' = Ph; **8** L = C_5H_5, R ≠ R' = Ph or Me; **12** L = $C_5H_4CMe_3$, R = R' = Ph) *via* the intermediates [Mo(CO)(η^2-C_2H_4){η^2(4e)-PhC≡CR}(η^5-L)][BF_4]. Only one of the two possible isomers of **8** is observed. The 16-electron complexes **6**, **8** and **12** are seen to be considerably more stable than their hexafluorophosphate derivatives.

The pendant 1,3-diphosphacyclopentadiene ring of complexes **6**, **8** and **12** only use one of their two double bonds to coordinate to the metal centre. This is believed to be due to the constrains invoked by the Mo=C bond. The reaction of **6** with DIBAL-H results in the addition of 'H^-' to the carbene carbon, releasing these constraints and resulting in the formation of the complex [Mo(CO)(-CH{Bu^t}P{η^2-C(Bu^t)=P}{η^2-C(Ph)=C(Ph)})(η^5-C_5H_5)], **13**, where it is thought both double bonds coordinate to the molybdenum centre, making **13** an 18-electron complex.

2.4 References

1 M. Scheer and J. Krug, *Z. Anorg. Alleg. Chem.*, 1998, **624**, 399.

2 A.R. Barron and A.H. Cowley, *Angew. Chem. Int. Ed. Engl.*, 1987, **26**, 907.

3 F.G.N. Cloke, K.R. Flower, P.B. Hitchcock and J.F. Nixon, *J. Chem. Soc. Chem. Commun.*, 1994, 489.

4 M. Green, P.B. Hitchcock, M.J. Maah and J.F. Nixon, *J. Organomet. Chem.*, 1994, **466**, 153.

5 J.L. Davidson and D.W.A. Sharp, *J. Chem. Soc. Dalton Trans.*, 1975, 2531.

6 J.L. Davidson, M. Green, F.G.A. Stone and A.J. Welch, *J. Chem. Soc. Dalton Trans.*, 1976, 738.

7 G. Brauers, *PhD thesis*, University of Bath, 1993.

8 a) D.A. Fletcher, R.F. McMeeking and D. Parkin, *J. Chem. Inf. Comput. Sci.*, 1996, **36**, 746.

b) F.H. Allen and O. Kennard, *Chem. Des. Automat. News*, 1993, **8**, 31.

9 a) P.B. Hitchcock, M.J. Maah, J.F. Nixon and C.J. Woodward, *J. Chem. Soc. Chem. Commun.*,1987, 844.

b) P. Binger, R. Milczarek, R. Mynott, M. Regitz and W. Rösch, *Angew. Chem. Int. Ed. Engl.*, 1986, **25**, 644.

c) P. Binger, R. Milczarek, R. Mynott, C. Krüger, Y.-H. Tsay, G. Raabe and M. Regitz, *Chem. Ber.*, 1988, 121, 637.

10 P.B. Hitchcock, C. Jones and J.F. Nixon, *Angew. Chem. Int. Ed. Engl.*, 1994, **33**, 463.

11 D. Böhm, F. Knoch, S. Kummer, U. Schmidt and U. Zenneck, *Angew. Chem. Int. Ed. Engl.*, 1995, **34**, 198.

12 P. Binger, J. Haas, A.T. Herrmann, F. Langhauser and C. Krüger, *Angew. Chem. Int. Ed. Engl.*, 1991, **30**, 310.

13 N. Carr and M. Green, *Unpublished results*.

14 C. Carfanga, M. Green, K.R. Nagle, D.J. Williams, C.M. Woodhouse, *J. Chem. Soc. Dalton. Trans.*, 1993, 1761.

15 P. Binger, B. Biedenbach, A.T. Herrmann, F. Langhauser, P. Betz, R. Goddard and C. Krüger, *Chem. Ber.*, 1990, **123**, 1617.

16 N.M. Agh-Atabay, J.L. Davidson, U. Dullweber, G. Douglas, K.W. Muir, *J. Chem. Soc. Dalton. Trans.*, 1999, 3883.

17 S.R. Allen, R.G. Beevor, M. Green, N.C. Norman, A.G. Orpen and I.D. Williams, *J. Chem. Soc. Dalton. Trans.*, 1985, 435.

3 Phosphines in Transition Metal Chemistry

3.1 Introduction

Phosphines have long been of interest as ligands in both organometallic and coordination chemistry. This is in no small part due to the importance of their transition metal complexes as catalysts in industrially important processes such as hydrogenation and hydroformylation. An important feature of phosphines as ligands is in the ease by which their steric and electronic properties can be altered, hence affecting their coordination properties. Section 3.2 covers the theory behind these properties, and some of the commercial uses to which transition metal phosphine complexes are put. The synthesis of phosphines is reviewed in Section 3.3, while functionalised phosphines, a popular area of research is covered in Section 3.4. The chemistry of *N*-pyrrolyl phosphines, and especially *N*-pyrrolyl ketophosphines, an area of particular interest to the group, is covered in Section 3.5.

3.2 Transition Metal Phosphine Chemistry

3.2.1 Phosphine-Transition Metal Interactions

The M-P bond in a metal phosphine complex is formed when electron density from the lone pair of electrons is donated to an empty d-type orbital on the metal. An additional component is the back bonding from filled d-type orbitals on the metal to empty σ^* orbitals on the phosphorus (Figure 3.1). Therefore, the ability of phosphines and transition metals to form stable complexes of the type $L_nM\text{-}PR_3$ is determined to a large extent by the donor-acceptor properties of the phosphine and metal centre, modulated by steric influences.

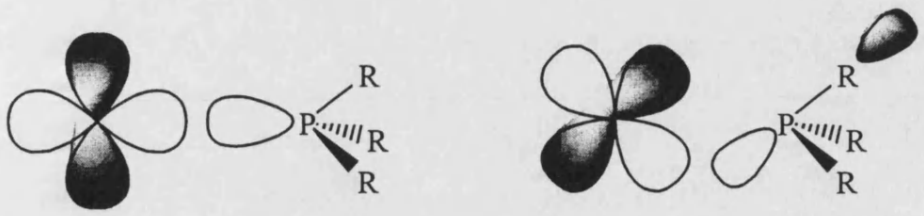

M(σ) ← lone pair M(dπ) → σ*

Figure 3.1: Orbital interactions between a metal and a phosphine, PR_3

The major factors that determine the behaviour of a phosphine are the σ-donor character, the π-acceptor character, and the steric effect of the substituent R groups. For bi- or polydentate phosphines, the bite angle is also important.

3.2.1.1 σ-Donor Effects

The donation of electron density from the lone pair of electrons on the phosphorus to the metal may be viewed as a donor covalent bond with the phosphorus providing both electrons. Hence the phosphine is acting as a Lewis base, and its ability to act as a σ-donor can be gauged by the pKa of its conjugate acid. In general, electron-releasing substituents will increase the electron availability on the phosphorus, resulting in a higher pKa and better σ-donor character. This was illustrated by Goel with a series of *para*-substituted phenyl phosphines, $P(4\text{-}C_6H_4R)_3$, as shown in Table 3.1.[1]

R	NMe_2	OMe	Me	H	F	Cl
pKa	8.65	4.57	3.84	2.73	1.97	1.03

Table 3.1: pKa values for *para*-substituted phosphines

Overall, phosphines follow the general trend in σ-donor ability:-

$$PBu^t_3 > PMe_3 > PMe_2Ph > PPh_2Me > PPh_3 > PH_3 > PF_3$$

3.2.1.2 π-Acceptor Effects

Initial models of the back donation from a transition metal to a coordinated phosphine utilised empty 3d orbitals on the phosphorus atom as recipients of the electron density. However, more recent calculations[2] have shown that this would be energetically unfavourable, and the phosphorus d orbitals are too diffuse to have any appreciable interaction with the metal orbitals. It is now thought that the orbitals on the phosphorus used to accept the electron density during back donation are the P-R antibonding σ* orbitals.

In general, phosphines follow the trend in π-acceptor behaviour:-

$$PF_3 > PH_3 > PPh_3 > PPh_2Me > PMe_2Ph > PMe_3 > PBu^t_3$$

3.2.1.3 Steric Effects: The Cone Angle Concept

The physical bulk of the substituents on a phosphine can exclude other ligands from the area close to the phosphine. In 1970 Tolman introduced the concept of the 'Cone Angle',[3] later amplified by him in 1977.[4] The Tolman Cone Angle is defined as the angle at the metal atom of the cone swept out by the van der Waals radii of the substituent groups on the phosphorus. This is shown in Figure 3.2. The actual value of the angle depends in part on the M-P distance, and so is different for each metal. The Tolman Cone Angles are calculated with nickel as the metal centre.

Although the Tolman Cone Angle is a useful concept in understanding the spatial/steric effects of phosphine ligands, it is not a perfect simulation of reality. The substituent groups do not sweep out a perfect cone, and are able to mesh together, like cogs. There are other concepts such as CARP and ERCODE which may be used to describe the same effect and which give a more accurate picture,[5] but as these are more complicated to calculate, the Cone Angle concept is still often used.

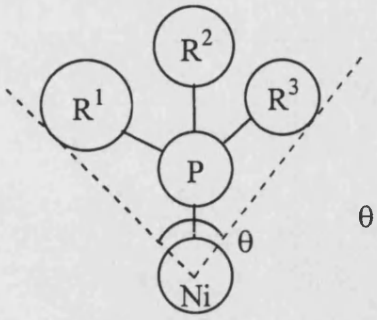

Figure 3.2: Derivation of Tolman Cone Angle

The bulkier the substituent groups, the larger will be the Cone Angle and the more steric crowding there will be at the metal centre. In addition, the size of the phosphine substituents can also have an influence on the electronic properties of the metal. An increase in bulk of the substituents increases the interbond angles, leading to an increase in the 'p character' of the phosphorus' lone pair of electrons. Selected values for the Tolman Cone Angle θ are given in Table 3.2.

Phosphine	Tolman Cone Angle / °
PH_3	87
PMe_3	118
PMe_2Ph	122
PBu^n_3	132
PPh_2Me	136
PBu^s_3	143
PPh_3	145
PBu^t_3	182

Table 3.2: Tolman Cone Angles for selected phosphines

3.2.1.4 Phosphine Electronic and Steric Effects – Their Influence on Transition Metal Complexes

The influence of the electronic effects of phosphines on their transition metal complexes is relatively straightforward. Strong σ-donors will donate more electron density to the metal than weaker donors, whilst strong π-acceptors will remove more electron density form the metal centre than weaker π-acceptors. Therefore, phosphines which are strong σ-donors will stabilise electron poor metal complexes, whilst strongly π-accepting phosphines will stabilise electron rich metal complexes.

The differing electronic effects of phosphines can also be seen if the metal complex has a coordinated carbonyl group. The nickel complexes $[Ni(CO)_3L]$, where L is a phosphine were used by Tolman to generate the phosphine electronic parameter ν.[4] This parameter is equal to the C-O stretch of the A_1 carbonyl group in the nickel complexes, and provides an overall view of the electronic properties of a phosphine. Selected values are given in Table 3.3.

It can be seen that phosphines which are good π-acceptors [such as $P(OPh)_3$ and PF_3] move ν and ν_{CO} to higher wavenumbers, whereas the phosphines which are good σ-donors (such as the trialkyl phosphines) shift ν and ν_{CO} to lower wavenumbers.

Phosphine	ν / cm^{-1}
PBu^t_3	2056.1
PMe_3	2064.1
PMe_2Ph	2065.3
PPh_2Me	2067.0
PPh_3	2068.9
PH_3	2083.2
PCl_3	2097.0
PF_3	2110.8

Table 3.3: Values of electronic parameter ν for selected phosphines

Another visible expression as to the π-acceptor character of phosphines is the M-P bond distance in their transition metal complexes. Phosphines with greater π-accepting ability have a shorter M-P bond length. The rhodium complexes $[RhCl(CO)L_2]$ also show this to good effect. When L is tris(*N*-pyrrolyl)phosphine (poor σ-donor / good π-acceptor) the M-P distance is 2.282(1) Å, whilst when L is tris(*N*-pyrrolidinyl)phosphine (good σ-donor / poor π-acceptor) the M-P distance is 2.333(1) Å.[6]

The effect of the steric bulk of a tertiary phosphine may be seen in many ways. For example, sterically demanding phosphines such as PBu^t_2Me promote spatially less demanding features such as hydride formation and coordinatively unsaturated metal centres. Such phosphines also favour internal C-metallation reactions.

3.2.2 Commercial Importance of Transition Metal Phosphine Complexes

The first work to demonstrate the application of phosphine complexes to catalysis was published in 1948 by Reppe and co-workers.[7] This showed that triphenylphosphine complexes of nickel were effective catalysts for the polymerisation of olefinic and acetylenic substances. There thus resulted considerable industrial interest in the potential catalytic properties of phosphine complexes soluble in organic solvents. From this work the development of phosphine complexes as homogeneous catalysts began.

The volume of chemicals produced from homogeneous catalysis is still relatively small when compared to heterogeneous systems. However, the improved reactivity and selectivity of homogeneous systems mean that their value to both the petrochemical and pharmaceutical industries is immense. Phosphine containing homogeneous catalysts have been used in a wide range of chemical processes, including hydroformylation, hydrogenation and isomerisation.

In hydroformylation, an aldehyde is produced from the reaction of an olefin with CO and hydrogen gas, though formally the units H and HCO are added across the double

bond, thus giving the reaction its name. The rhodium phosphine complex $[RhH(CO)(PPh_3)_3]$ is used to catalyse this reaction in the Union Carbide hydroformylation process.[8] It has been found that by increasing the steric bulk of the phosphine, the production of unbranched products is favoured. This is because with the increased steric congestion around the metal centre, the formation of the least substituted alkyl or acyl complex is favoured, as these have less steric bulk than their more substituted analogues.

Hydroformylation may also be carried out with the cobalt complexes $[CoH(CO)_2L]$ where L is a phosphine.[9] A similar steric effect is seen in these catalysts, but there also exists an extra electronic effect. Catalysts containing poor σ-donor phosphines are shown to have higher turnovers, but lower relative yields of linear products. This is because the phosphines are less strongly bound to the metal and may be displaced under the atmosphere of CO to generate the complex $[CoH(CO)_3]$ which has been shown to be a more active, but less selective catalyst.

Hydrogenation is the addition of hydrogen to an unsaturated species such as olefins and alkynes. Probably the best known phosphine containing complex that can catalyse this reaction is Wilkinson's catalyst $[RhCl(PPh_3)_3]$.[10] This complex hydrogenates alkenes, alkynes and other unsaturated species at 25°C and a hydrogen pressure of 1 bar.

Enantioselective reactions, whereby an achiral species is converted into a chiral entity are of particular importance to the pharmaceutical industry. By using metal complexes with optically active phosphine ligands (particularly diphosphines) as the catalyst, asymmetry may be induced in the product.

An example of asymmetric hydrogenation is the synthesis of L-DOPA, a drug used in treating Parkinson's disease. Here the rhodium catalyst **3.1**, shown in Figure 3.3, contains an optically active tertiary phosphine, and has been used to give the desired product with an optical purity of over 90%.[11]

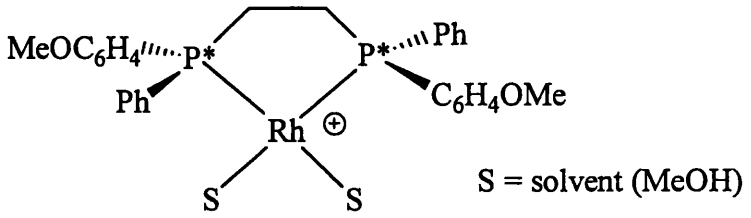

3.1

Figure 3.3: Catalyst used in commercial synthesis of L-DOPA

In alkene isomerisation, the C=C double bond migrates along the carbon chain due to the metal mediated transfer of hydrogen atoms. There are two possible mechanisms by which this reaction can proceed. The 'alkyl' mechanism involves a 1,2-hydrogen shift, whilst in the 'allyl' mechanism there is a 1,3-hydrogen shift. An example of a phosphine complex that works by the latter method is the cationic rhodium species $[Rh\{(S)\text{-BINAP}\}(cod)]^+$. This is used to catalyse the reaction shown, which is part of the commercial synthesis of L-menthol.[12]

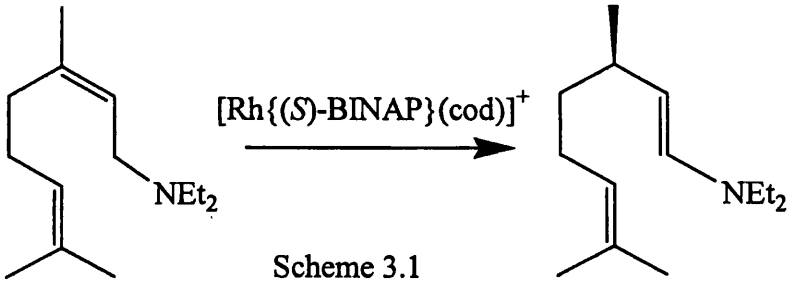

Scheme 3.1

3.3 Phosphine Synthesis[13]

By using the disconnection approach towards the formation of the C-P bonds in phosphines, three strategies for the synthesis of tertiary phosphines can be envisaged.

$C\text{-}P \Rightarrow C^- + P^+$, equivalent to M-C + P-X (1)

$C\text{-}P \Rightarrow C^+ + P^-$, equivalent to X-C + P-M (2)

Where M is a metal, and X is a halide.

$C\text{-}P \Rightarrow C\cdot + P\cdot$ (3)

Disconnection 1 shows the reaction of a nucleophilic carbon with an electrophilic phosphorus. An example is the reaction of a organometallic compound such as a Grignard reagent with a halophosphine (Scheme 3.2). With the ready availability of the starting materials, this is one of the most commonly used synthetic routes. A synthesis of PPh_2Me by this route is shown in Scheme 3.3.

$$3\ RMgBr + PX_3 \rightarrow R_3P + 3\ MgBrX$$
$$RMgBr + R'R''PX \rightarrow RR'R''P + MgBrX$$

Scheme 3.2

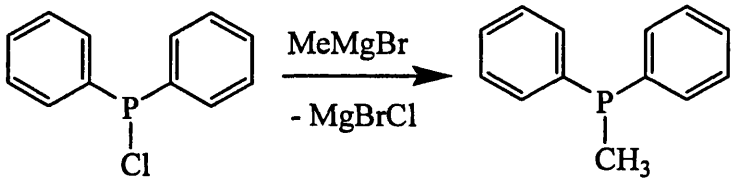

Scheme 3.3

Disconnection 2 can be considered as the reaction of an electrophilic carbon with a nucleophilic phosphorus. An example is the reaction of a metal phosphide with an organohalogen compound (Scheme 3.4). Although the synthetic steps are more complex than in the previous case, this is also a popular route in phosphine synthesis, particularly in the preparation of unsymmetrical and assymetric tertiary phosphines. The synthesis of (2-tetrahydrofurylmethyl)diphenylphosphine is shown in Scheme 3.5.[14]

$$PM_3 + 3\ RX \rightarrow R_3P + 3\ MX$$
$$RR'PM + R''X \rightarrow RR'R''P + MX$$

Scheme 3.4

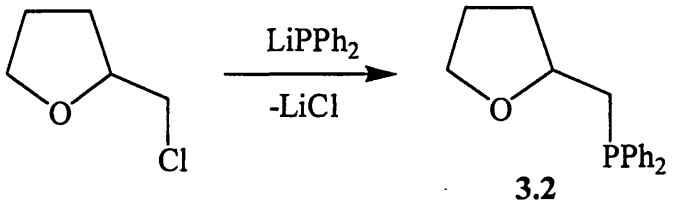

3.2

Scheme 3.5

Disconnection 3 represents the radical based reaction of carbon and phosphorus. In practice, this tends to be the radical addition of a phosphine to a species containing a carbon-carbon multiple bond, such as an alkene or alkyne. A typical mechanism is shown in Scheme 3.6. This route is much less commonly used than the other two, but is utilised in the synthesis of the fluorinated phosphine **3.3** in Scheme 3.7.[15]

$$R_2PH + \text{initiator} \rightarrow R_2P^{\cdot}$$

$$R_2P^{\cdot} + RCH{=}CH_2 \rightarrow R_2PCH_2C^{\cdot}HR$$

$$R_2PCH_2C^{\cdot}HR + R_2PH \rightarrow R_2PCH_2CH_2R$$

Scheme 3.6

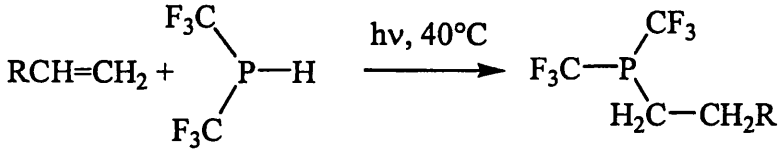

Scheme 3.7 **3.3**

A fourth possible route that may be employed is the reduction of a phosphine oxide or sulphide to the phosphine. A number of reducing agents may be used, but silanes (eg. $SiHCl_3$ and $R_{4-x}SiH_x$) are the most common as they are easy to use, effective for a wide range of phosphines, give clean stereochemistry and high yields. Adding a weak base to the reaction mixture removes any HCl formed. A general reaction is shown in Scheme 3.8.

$$R_3P{=}O + 2\ SiHCl_3 \rightarrow R_3P + SiCl_4 + H_2 + (Cl_2SiO)_n$$

$$R_3P{=}O + SiHCl_3 + Et_3N \rightarrow R_3P + (Cl_2SiO)_n + [R_3NH][Cl]$$

Scheme 3.8

An advantage of the use of silanes is that reduction may be carried out in the presence of functional groups otherwise susceptible to reactions with reducing agents such as

carbonyls, nitriles etc. An example of the synthesis of a phosphine containing ester groups by this method is shown in Scheme 3.9.[16]

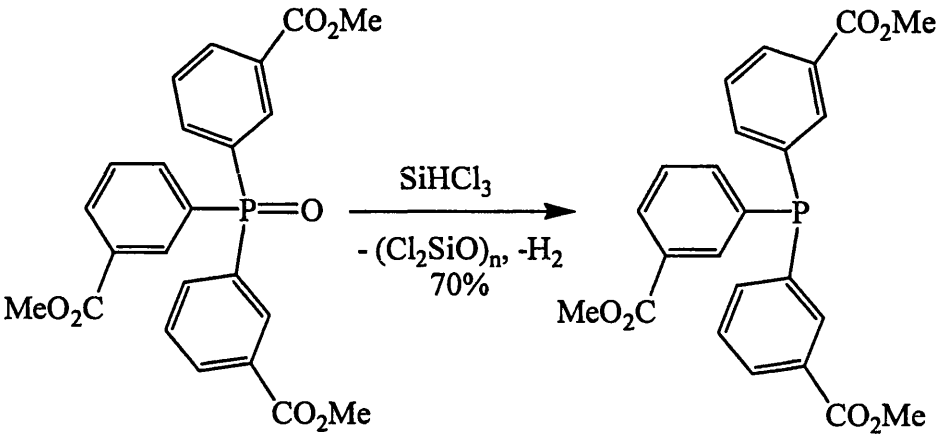

3.4

Scheme 3.9

3.4 Functionalised Phosphines[17]

Tertiary phosphines may have additional functional groups attached to them, that can also ligate to metal centres. These additional ligating groups are mostly based on heteroatoms such as oxygen, nitrogen and sulfur, or on carbon-carbon multiple bonds (Figure 3.4).

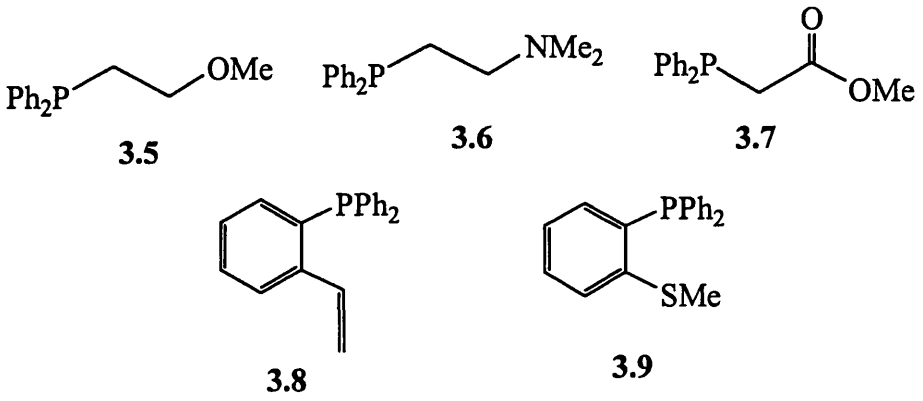

3.5 3.6 3.7

3.8 3.9

Figure 3.4: Examples of functionalised phosphines

Such functionalised phosphines can act as bidentate ligands, where both the phosphorus, and the functional group coordinate to a metal. In this respect, the length of the chain between the two groups is very important. Five- and six-membered

chelate rings are favoured, whilst four-membered rings are disfavoured because of their inherent strain. Seven- and higher-membered rings are energetically unfavourable due to both entropic and strain considerations.

The combination of a phosphorus atom which forms a relatively strong, substitutionally inert bond (especially to late transition metals) with a labile ligating group provides the potential for the ligand to exhibit hemilability.[18] In the absence of a strongly coordinating ligand or solvent, the weakly coordinating functional group on the phosphine can bind to the metal, thus acting as a bidentate ligand. However, if strongly coordinating species are introduced, the labile portion of the ligand may be displaced. The presence of the substitutionally inert metal-phosphorus bond keeps the labile group in close proximity to the metal, so allowing its recoordination once the strongly coordinating ligand has been removed. This process is shown schematically in Figure 3.5.

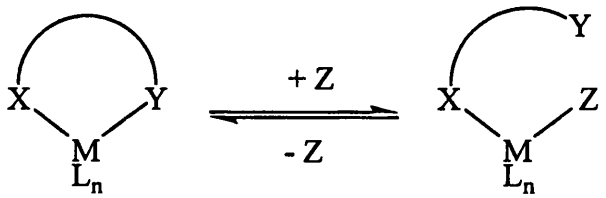

X = substitutionally inert group
Y = substitutionally labile group
Z = ligand or solvent

Figure 3.5: Hemilabile behaviour

The chelating hemilabile ligand can be viewed as protecting a vacant coordination site on the metal. This makes such systems very interesting due to their potential to act as catalysts, especially if the substrate for the reaction to be catalysed is strongly coordinating to the metal centre, whilst the product is weakly coordinating. During the reaction, the substrate coordinates to the metal centre, displacing the weakly coordinating end of the hemilabile ligand. After the reaction has occurred, the hemilabile ligand re-chelates, displacing the product. The catalyst can now react with another molecule of substrate to repeat the procedure. A stylised representation of this process is shown in Scheme 3.10.

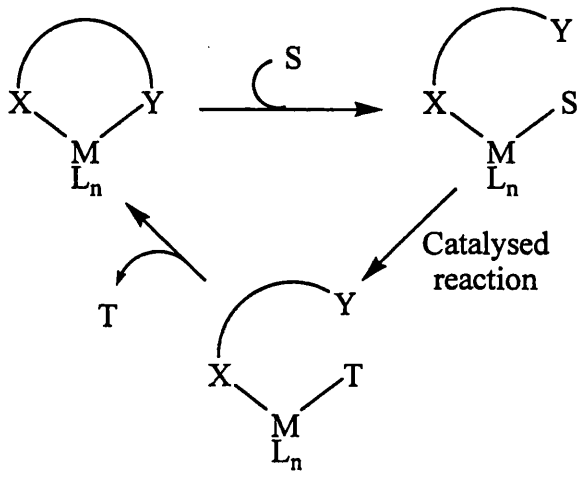

X = substitutionally inert group
Y = substitutionally labile group
S = substrate
T = product

Scheme 3.10

In addition to homogeneous catalysis, the mixing of donor groups to give hemilabile ligands is of particular interest in the fields of chemical sensing. For example, carbon monoxide may be detected electrochemically by using the rhodium phosphino-ether complex **3.10** in a titania or zirconia film.[19]

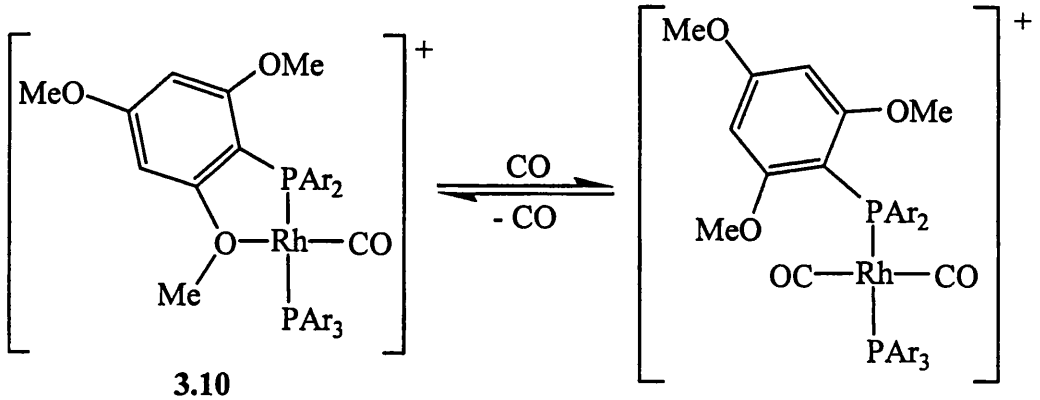

3.10

Ar = 2,4,6-$C_6H_2(OMe)_3$

Scheme 3.11

Ligands that contain both phosphorus and oxygen donor atoms are amongst the most studied groups of hemilabile ligands.[20] There is a considerable range of labile oxygen-containing functional groups that have been incorporated into hemilabile phosphorus-oxygen ligands. The most common of these are ether and keto-groups, but alcohols, esters, amides and phosphorus oxides are also well known. Compared to the

analogous phosphorus-oxygen based ligands, nitrogen-modified phosphines show a marked preference to form substitutionally inert chelates. This is due, in part, to the greater coordinating ability of most nitrogen-containing moieties as compared to oxygen groups to late transition metal centres. Those functional groups that do exhibit hemilability include amines, amides and imines.

3.4.1 Phosphino-ethers

The chemistry of ether-functionalised phosphines (or phosphino-ethers) has been intensively researched, notably by Lindner and co-workers.[20] The oxygen donor atom of the ether group may be incorporated into the phosphine as either a simple ether, or as part of a more complex macrocycle or polyether chain, in which two or more oxygen donor atoms are incorporated (Figure 3.6).

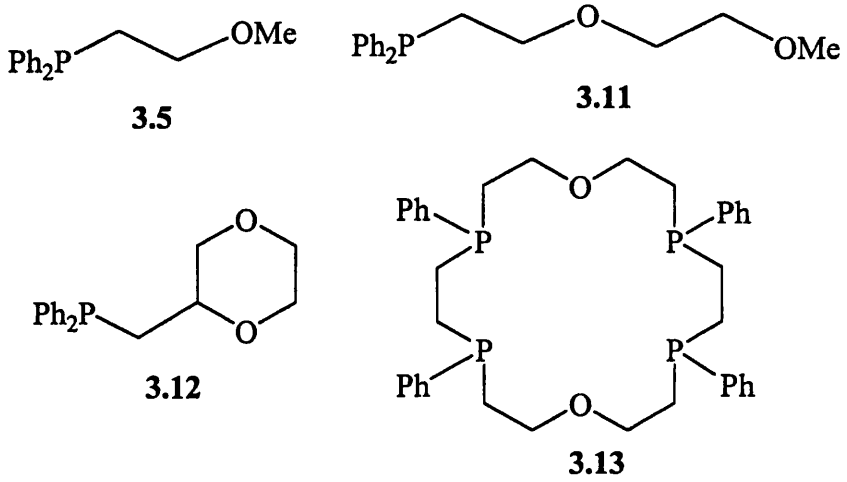

Figure 3.6: Examples of phosphino-ethers

Phosphino-ethers can be made by any of the methods described in Section 3.3, but the reaction of a halophosphine with the appropriate Grignard reagent (often made *in situ*) is most commonly used (Scheme 3.12).

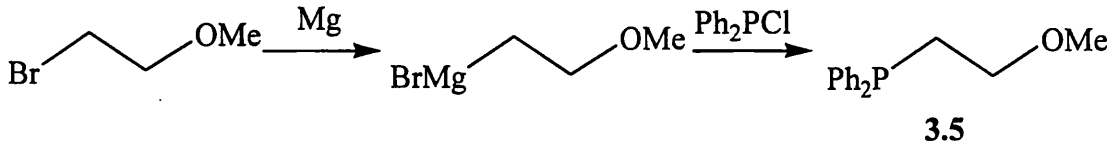

Scheme 3.12

Many transition metal complexes of ether-functionalised phosphines have been shown to be effective catalysts for various processes. For instance, rhodium[21] and cobalt[22] complexes have been shown to act as catalysts in the carbonylation of methyl iodide (Scheme 3.13). Rhodium[23] and palladium[24] complexes of ether-functionalised phosphines have also been shown to act as hydrogenation catalysts and amination catalysts.

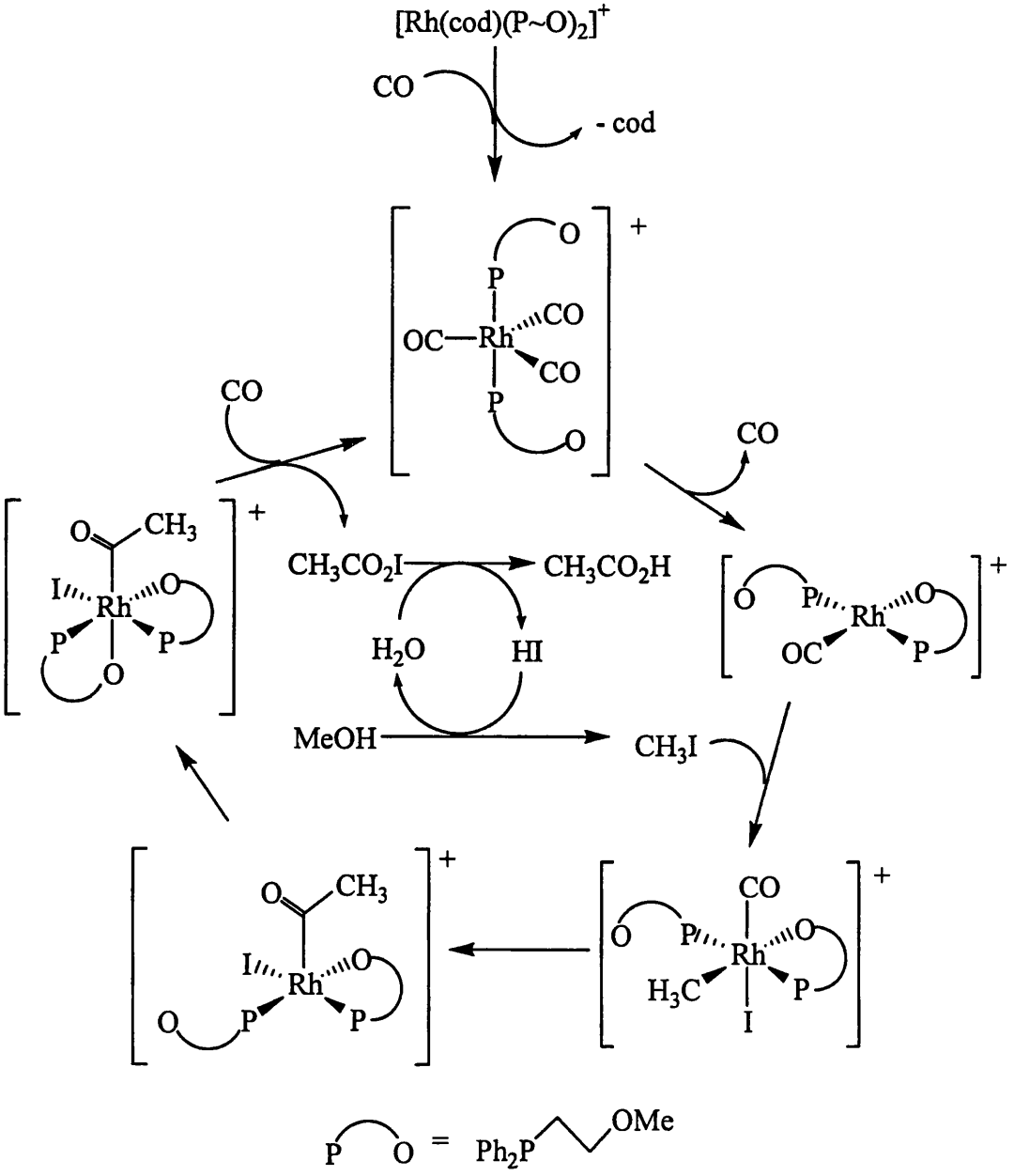

Scheme 3.13

More recently, the catalytic properties of supported ether-functionalised phosphine complexes have attracted interest.[25] Most notably, the supported palladium complex **3.14** shown in Figure 3.7 was shown to be an effective catalyst for the copolymerisation between carbon monoxide and ethylene in the absence of solvent.[26]

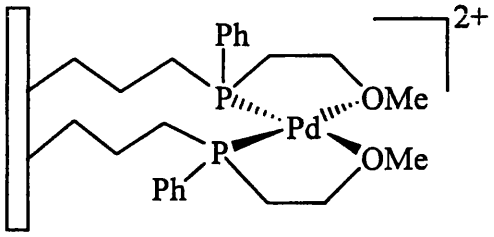

3.14

Figure 3.7: Supported palladium catalyst

Polyether-functionalised phosphines are also attracting interest for two main reasons. Firstly, with more than one oxygen donor atom, they can stabilise multiple coordination sites at a metal centre (Figure 3.8).[27] Secondly, the polyether chain can impart phase-transfer properties to a catalyst.[28]

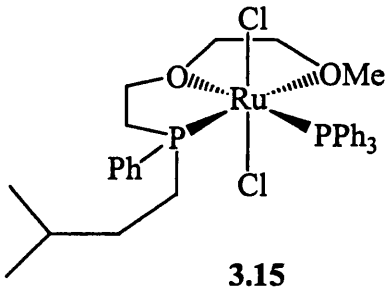

3.15

Figure 3.8: Polyether-functionalised phosphine complex

3.4.2 Ketophosphines and Phosphino-enolates

Phosphines containing a keto group have also attracted interest, particularly their complexes with late transition metals. There are a number of differences between ketophosphines and phosphino-ethers, mainly due to the carbonyl group on ketophosphines coordinating more strongly to late transition metals than the corresponding ether group.[29] This results in increased stability of their P,O

coordinated complexes compared to the analogous ether-functionalised phosphine complexes. An example of this increased stability involves the analogous complexes $[Rh\{PPh_2CH_2C(O)Ph\text{-}P,O\}_2][PF_6]$, **3.16**, and $[Rh(PPh_2CH_2CH_2OCH_3\text{-}P,O)_2][BPh_4]$, **3.17**. Whilst **3.16** is stable at room temperature, **3.17** is unstable above -30°C. As a result of this increased carbonyl oxygen – metal bond strength, a number of ketophosphine complexes have been observed to be stereochemically rigid on the NMR timescale at room temperature. This is in contrast to the equivalent ether functionalised phosphine complexes which exhibit fluxionality under the same conditions.[30]

The most commonly used variety of ketophosphines are β-ketophosphines. These may be made by the reaction of a chlorophosphine with the requisite enolate (Scheme 3.14).[31] These ligands form 5-membered rings upon chelation.

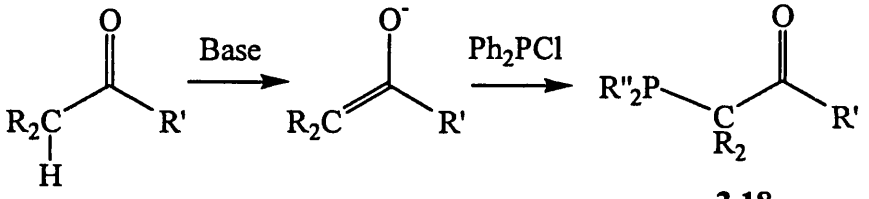

Scheme 3.14 **3.18**

Both Shaw and Cole-Hamilton (with their respective co-workers) have made chiral ketophosphines in this way, based upon camphor (Scheme 3.15).[32]

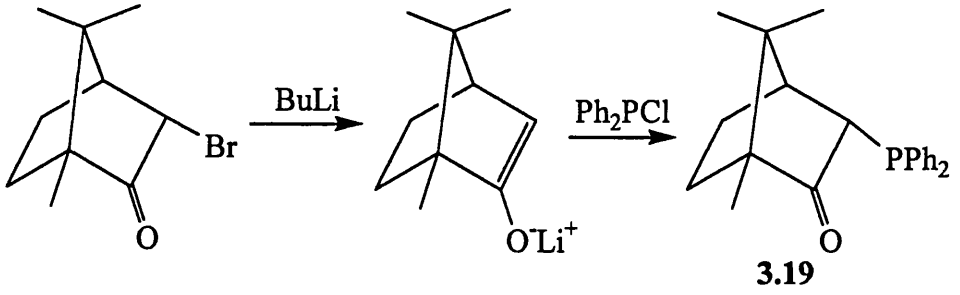

3.19

Scheme 3.15

The reaction of an enone with Ph_2PLi followed by quenching with water gives as the product a γ-ketophosphine (Scheme 3.16).[33] These can be reacted with metal centres to form six-membered chelate rings.

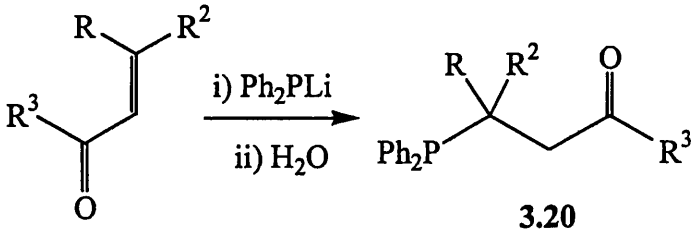

3.20

Scheme 3.16

A large amount of work has been carried out on the transition metal complexes of ketophosphines. The majority has been performed using β-ketophosphines and metals from groups 8-10.

The infrared spectra of ketophosphine complexes is a valuable tool in determining the coordination mode of the ligand. Most free ketophosphines have a carbonyl stretching frequency in the region 1680-1640 cm^{-1}. When the ketophosphine is coordinated to a metal *via* the phosphorus only, this stretching frequency does not change to any great extent. However, when chelation occurs, there is an decrease in the bond order of the carbonyl bond thus lowering its stretching frequency to typically within the range 1580-1520 cm^{-1}.

Coordinated ketophosphines have the ability to react with bases to produce phosphino-enolates. The decrease in bond order of the CO bond decreases the stretching frequency once more, to somewhere in the region 1500-1430 cm^{-1}. Phosphino-enolates tend not to be hemilabile, though an exception is complex **3.21**, where the two isomers equilibrate slowly on the NMR timescale at -10°C (Scheme 3.17).[34]

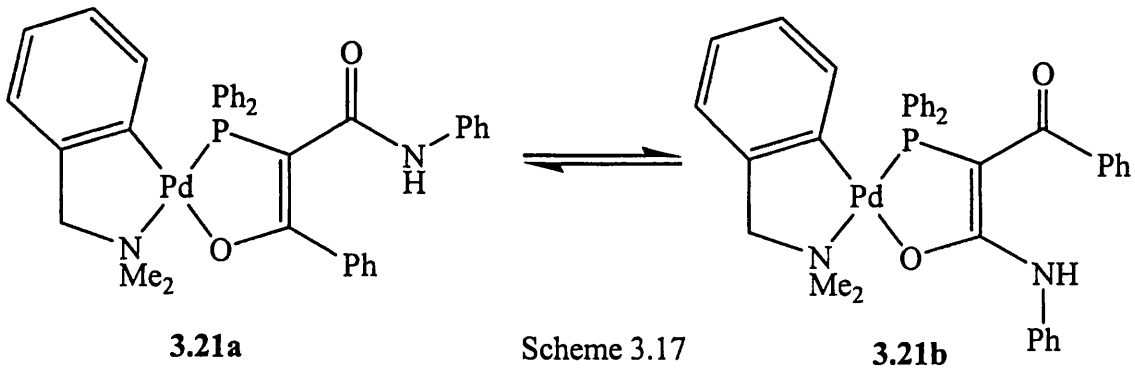

3.21a Scheme 3.17 **3.21b**

Often the phosphino-enolate complexes can be reacted with an acid to reform the ketophosphine complexes. An example is shown in Scheme 3.18.[35]

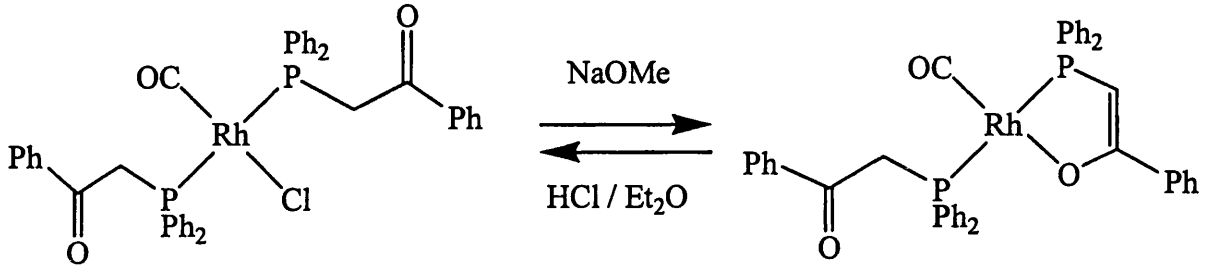

3.22 Scheme 3.18 **3.23**

An alternative method of making phosphino-enolate complexes is the oxidative addition of a P-aryl bond from a phosphorus ylide across a transition metal complex. This has so far only been seen for Ni^0 complexes, an example of which is shown in Scheme 3.19.[36]

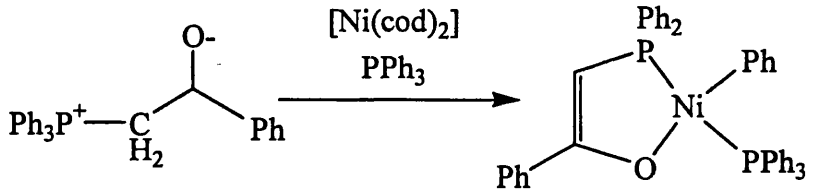

Scheme 3.19 **3.24**

Such nickel phosphino-enolate complexes are used as catalysts in the Shell Higher Olefin Process.[37] In this, ethene is oligomerised to give a mixture of α-olefins. The phosphino-enolate ligand has been shown to control the activity and selectivity of the catalyst, and therefore there has been a lot of interest in altering the structure of the ligand. A particular aim is to increase the relative yield of the shorter chain α-olefins, which are commercially more valuable. To this end, Braunstein and co-workers produced the nickel catalyst shown in Figure 3.9, where the enolate oxygen can partake in intramolecular hydrogen bonding with an amine group.[38] As a result of this, there is a decrease in electron density at the nickel centre and β-hydrogen elimination is facilitated. This catalyst maintains the high activity of **3.24** but the products it produces show a marked shift towards C_{4-8} linear α-olefins.

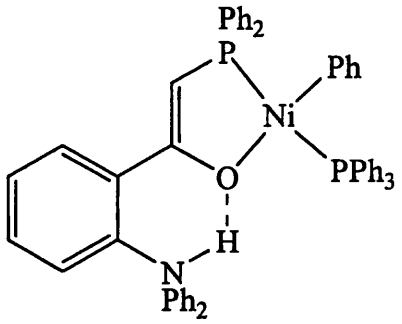

3.25

Figure 3.9: Adapted nickel SHOP catalyst

3.4.3 Amidophosphines

Phosphines functionalised with amide groups can coordinate to metal centres through the phosphorus and oxygen atoms, in much the same way as keto-phosphines.[39] However, they also have the potential to coordinate *via* their nitrogen atoms, thus acting as P,N ligands.[40] The phosphines **3.26** and **3.27**, developed by Braunstein and co-workers, are good examples of the former type. The phosphines **3.28** and **3.29** developed by Hedden, Roundhill and co-workers, provide good examples of the latter.

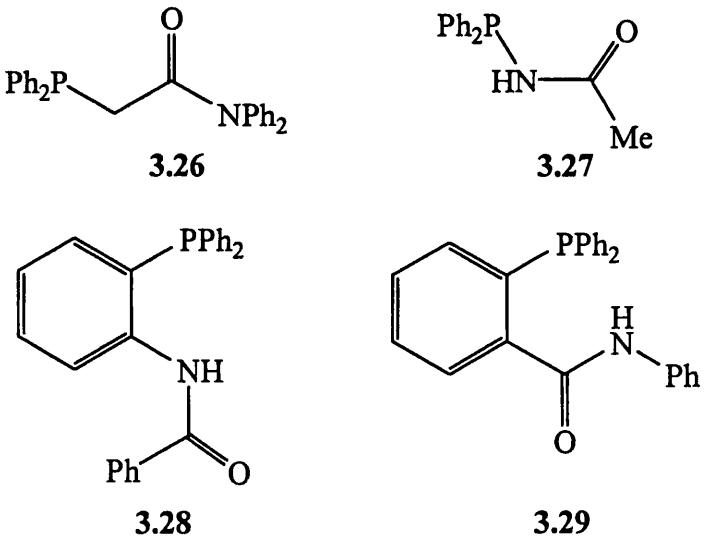

3.26 **3.27**

3.28 **3.29**

Figure 3.10: Examples of amidophosphines

The predominant factors in determining which atom bonds to the metal centre are the ring size, and the relative stability of the M-N and M-O bonds. Of those

amidophosphines shown above, **3.27** coordinates predominantly through the oxygen atom to create a 5-membered chelate ring, rather than the nitrogen which would involve the formation of a strained three membered ring. In contrast, phosphine **3.287** would form an disfavoured 7-membered ring as a P,O ligand, as so acts as a P,N ligand. The chelate ring size does not alter for amidophosphines **3.26** and **3.29** depending on which donor atom is used, and so the relative stability of the M-O and M-N bonds are more important. Late transition metal centres like Pd(0) prefer the 'softer' sp^3 hybridised nitrogen atoms, whilst earlier transition metal centres such as Re(III) prefer the 'harder' sp^2 hybridised oxygen atoms.

Work by Braunstein and co-workers indicates that the amidophosphine $Ph_2PNHC(O)Me$, **3.27**, acts as a better chelating ligand than the analogous ketophosphine $Ph_2PCH_2C(O)Ph$, **3.40**.[41] This may be observed in the complexes $[Pd(CH_3)L_2][PF_6]$, where L is **3.40** and/or **3.27**. Both the complexes $[Pd(CH_3)\{Ph_2PCH_2C(O)Ph\text{-}P\}\{Ph_2PCH_2C(O)Ph\text{-}P,O)][PF_6]$ and $[Pd(CH_3)\{Ph_2PNHC(O)Me\text{-}P\}\{Ph_2PNHC(O)Me\text{-}P,O\}][PF_6]$ are fluxional, whereas the mixed phosphine complex $[Pd(CH_3)\{Ph_2PCH_2C(O)Ph\text{-}P\}\{Ph_2PNHC(O)Me\text{-}P,O\}][PF_6]$ is not.

A recent paper has been published by Kuriyama and Tomioka in which a chiral amidophosphine-rhodium(I) complex is used to catalyse the asymmetric 1,4-addition of arylboronic acids to cyclohexenone.[42] The reaction is shown in Scheme 3.20.

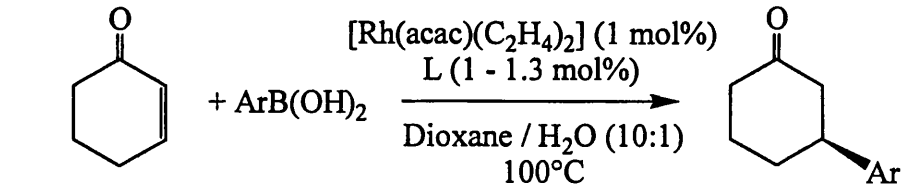

Ar = Ph, 4-C_6H_4Me, 2-C_6H_4Me, 3-C_6H_4OMe,

Yield = 98 - 99%
ee = 91 - 96%

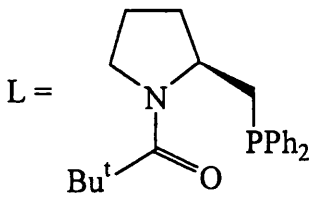

Scheme 3.20

As with the O-bound amidophosphines, the N-bound amidophosphines have been shown to exhibit hemilability. For example, Roundhill and co-workers showed that in the complex **3.31**, the free and coordinated amido groups exchanged at temperature over 75°C.[40a]

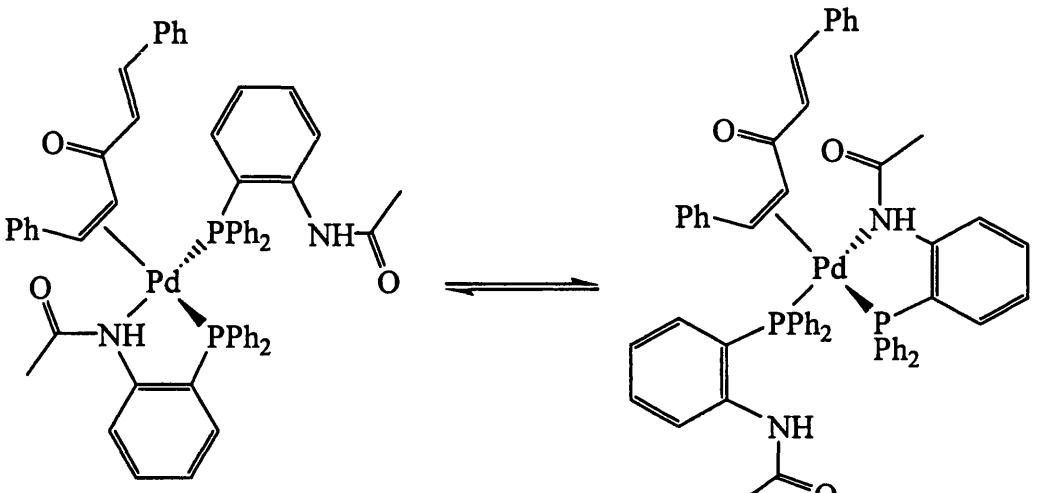

3.31a **3.31b**

Figure 3.11: Fluxionality in amidophosphine complex **3.31**

In the complex **3.32**, which contains a P-N coordinated imidophosphine, the nitrogen atom was shown to be displaced from the metal centre in the presence of acetonitrile.[40b] The imido group dissociates from the metal, and rearranges to form an amido group. Upon removal of acetonitrile, the original chelating imidophosphine complex reforms.

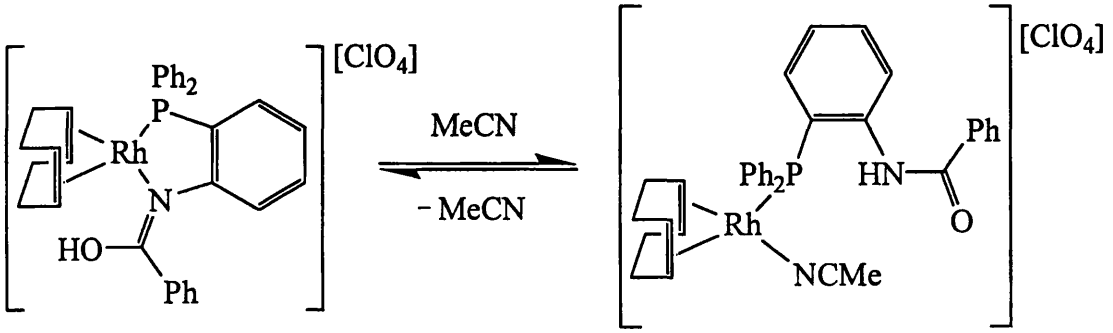

3.32 Scheme 3.21 **3.33**

As with ketophosphines, most of the work carried out on the transition metal complexes of amide functionalised phosphines has been with metals from groups 8-

10. However, Braunstein and co-workers have recently begun to investigate their behaviour with earlier transition metals.[43]

3.4.4 Aminophosphines

Aminophosphine complexes were amongst the first examples of hemilabile phosphine ligands on transition metal complexes. One of the earliest demonstrations of a hemilabile functionalised phosphine was the reaction of complex **3.34** with SCN^-, as carried out by Mann and Watson.[44] The chelating amino group was displaced from the metal centre in favour of the thiocyanate ligand, as shown in Scheme 3.22.

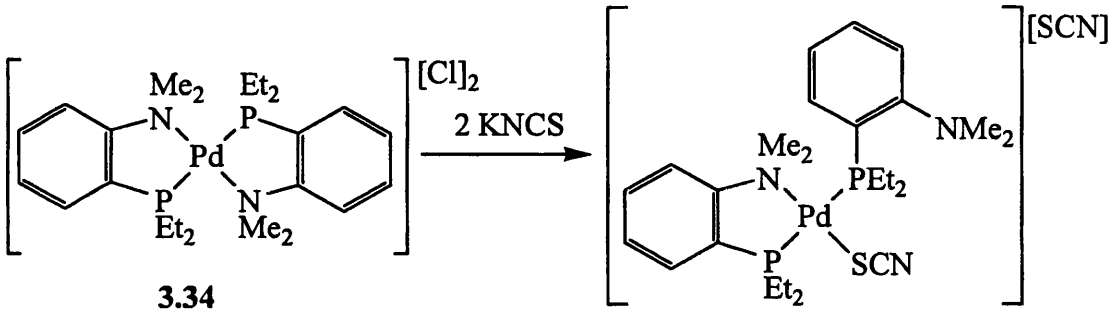

3.34 **3.35**

Scheme 3.22

In contrast to the analogous phosphino-ether ligands which usually react in a hemilabile fashion, the nitrogen donors of aminophosphines are not always displaced upon addition of small molecules to their complexes. For example, Rauchfuss and co-workers showed that CO displaces the ether groups from complex **3.36**, whilst the amino groups in the analogous complex **3.37** are substitutionally inert under comparable conditions (Scheme 3.23).[45]

Hemilabile aminophosphines complexes have been shown to have potential catalytic implications.[46] For example, the amination of aryl halides has been shown to be catalysed by a palladium(II) complex, as shown in Scheme 3.24.[23b]

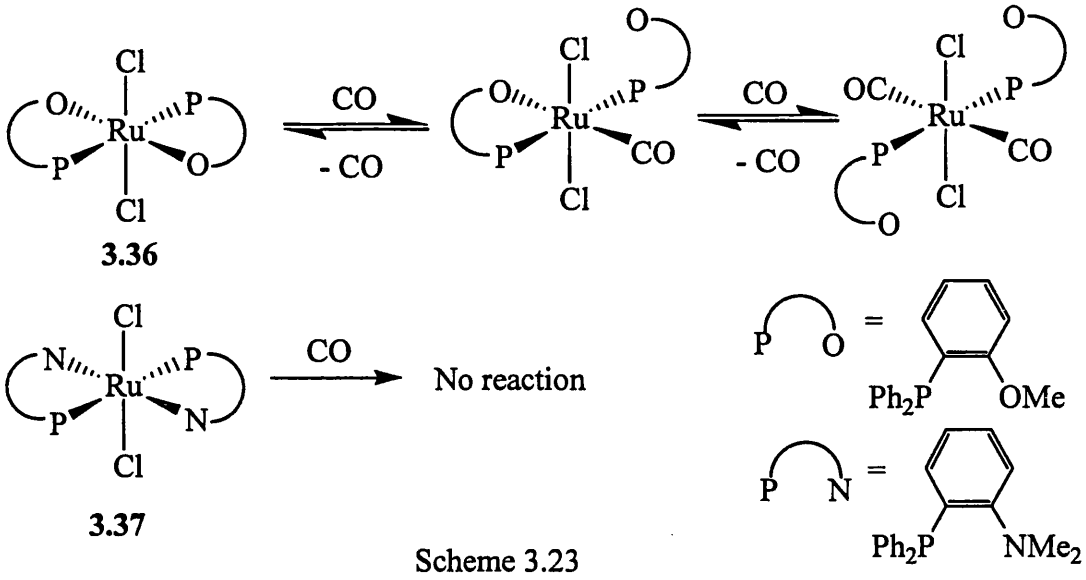

Scheme 3.23

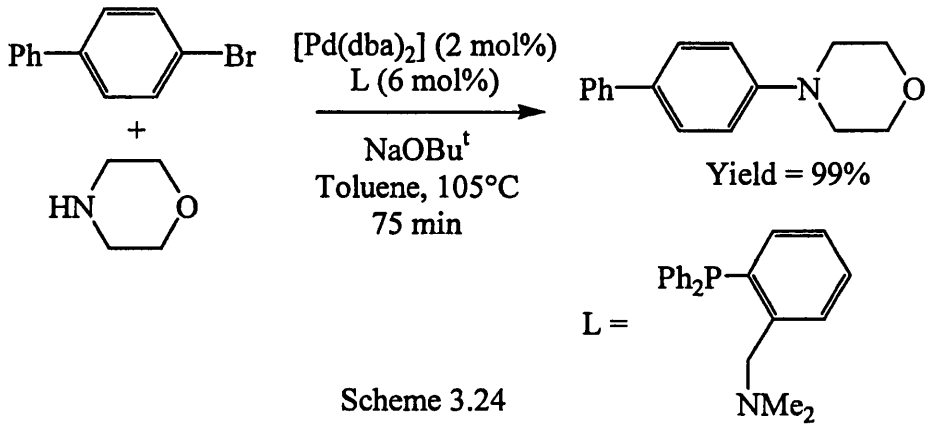

Scheme 3.24

3.5 *N*-Pyrrolyl Phosphines

The chemistry of *N*-pyrrolyl substituted phosphines has been the subject of recent investigation.[6,47] This is due to their exceptional π-acceptor properties, which can exceed those of phosphites such as $P(OPh)_3$. Delocalisation of the nitrogen lone pair into the 5-membered ring (Scheme 3.25) contributes to the strong electron withdrawing properties of the *N*-pyrrolyl group, which results in the phosphines acting as relatively poor σ-donors and as good π-acceptors.

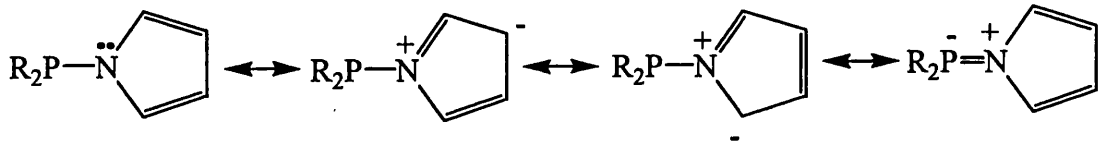

Scheme 3.25

N-Pyrrolyl phosphines can be easily made by reacting pyrrole directly with a chlorophosphine in the presence of triethylamine (Scheme 3.26). The mild reaction conditions allow the potential for incorporating a variety of functional groups into the phosphine.[48]

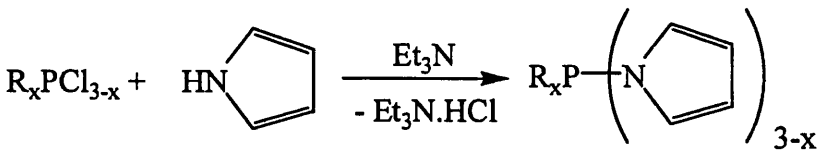

R = Ph, NC_4H_4

3.38

Scheme 3.26

Complexes containing *N*-pyrrolyl substituted phosphines have been shown to be of relevance to catalysis. Examples are the rhodium(I) tri(*N*-pyrrolylphosphine) complexes **3.39** and **3.40** which have been used to catalyse the hydroformylation of hex-1-ene[49] and the hydrogenation of olefins and arenes.[50]

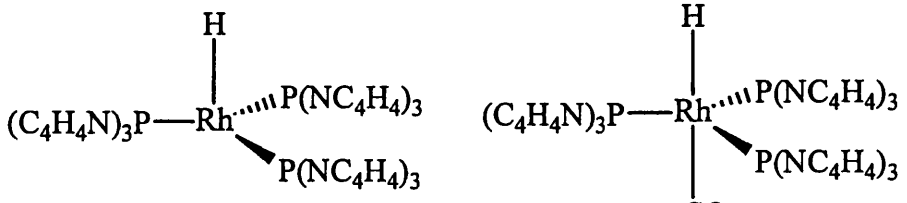

3.39

3.40

Figure 3.12: Catalytically active tris(N-pyrrolyl)phosphine complexes

3.5.1 *N*-Pyrrolyl Keto Phosphines

The chemistry of 2-acetyl-*N*-pyrrolyl phosphine, **3.41**, on transition metal centres has recently been investigated.[51] The ligand itself can be synthesised using the method shown in Scheme 3.28. Triethylamine is used to deprotonate 2-acetylpyrrole, which is then reacted with an equimolar quantity of Ph_2PCl. This reaction produces good yields but suffers from a slow completion time (2 days). Replacement of NEt_3 by the stronger base 1,8-diazabicyclo[5.4.0]undec-7-ene (DBU) decreases the reaction time to a few hours, but purification of the product is more difficult.

An important point to note is that resonance within the pyrrolyl ring can extend to the carbonyl group, producing an enolate canonical form (Figure 3.13).

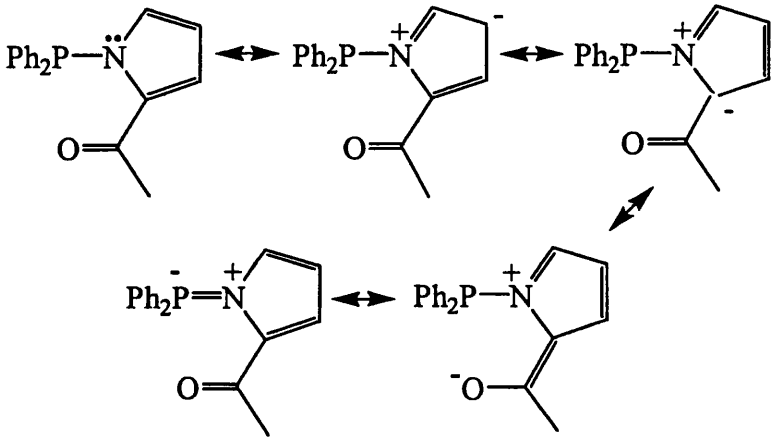

Figure 3.13: Resonance in *N*-pyrrolyl phosphine **3.41**

The chemistry of phosphine **3.41** has been studied on a number of transition metal centres. The reaction between $[M(dmba)(\mu\text{-}Cl)]_2$ (M = Pt or Pd) and **3.41** gives the ketophosphine complexes $[M(dmba)\{Ph_2PNC_4H_3C(O)CH_3\}Cl]$, **3.42**, where **3.41** is bound only through the phosphorus. The chlorine can be abstracted from these complexes to give the *P,O*-coordinated ketophosphine complexes **3.43**, as shown in Scheme 3.27.

In an attempt to gauge the hemilability of the ketophosphine, reactions of the platinum complex **3.43a** with a range of potential ligands, including diphenylacetylene, acetonitrile, carbon monoxide and xylyl isocyanide were attempted. Of these, only the last gave any reaction, forming the product **3.44**.

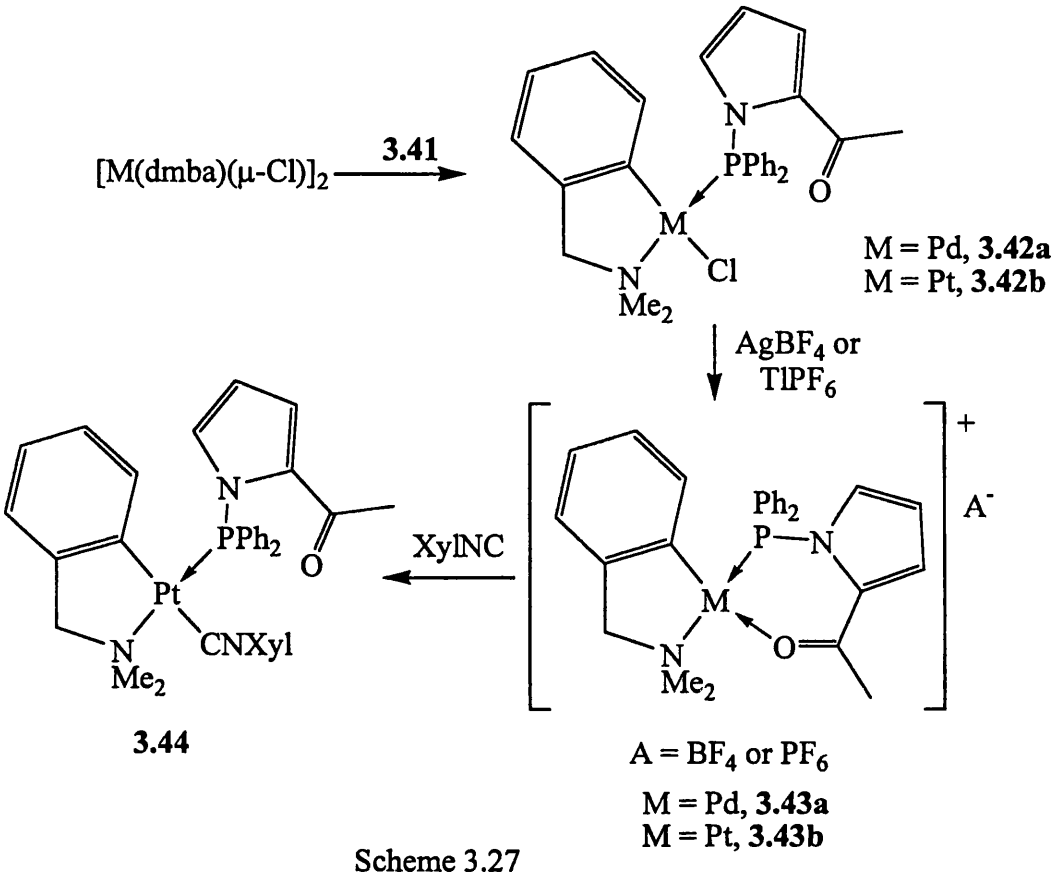

Scheme 3.27

When the rhodium dimer $[Rh(\mu\text{-}Cl)(CO)_2]_2$ is reacted with two equivalents of **3.41**, the product is the P,O-coordinated ketophosphine complex **3.45**, as shown in Scheme 3.28. The ketophosphine exhibits hemilability in this complex, reversibly forming complex **3.46** upon addition of carbon monoxide.

If the dimer $[Rh(\mu\text{-}Cl)(CO)_2]_2$ is reacted with four equivalents of the ketophosphine, then the product is the complex **3.47**. This was seen to react with trace amounts of water to hydrolyse the P-N bond, giving the novel rhodium dimer **3.48**. A single crystal X-ray study showed that the $Ph_2P\text{-}O\text{-}PPh_2$ bridging ligands are *trans* to each in the axial positions. In the equatorial plane, the chlorides and carbonyl ligands are disordered between the bridging and terminal positions.

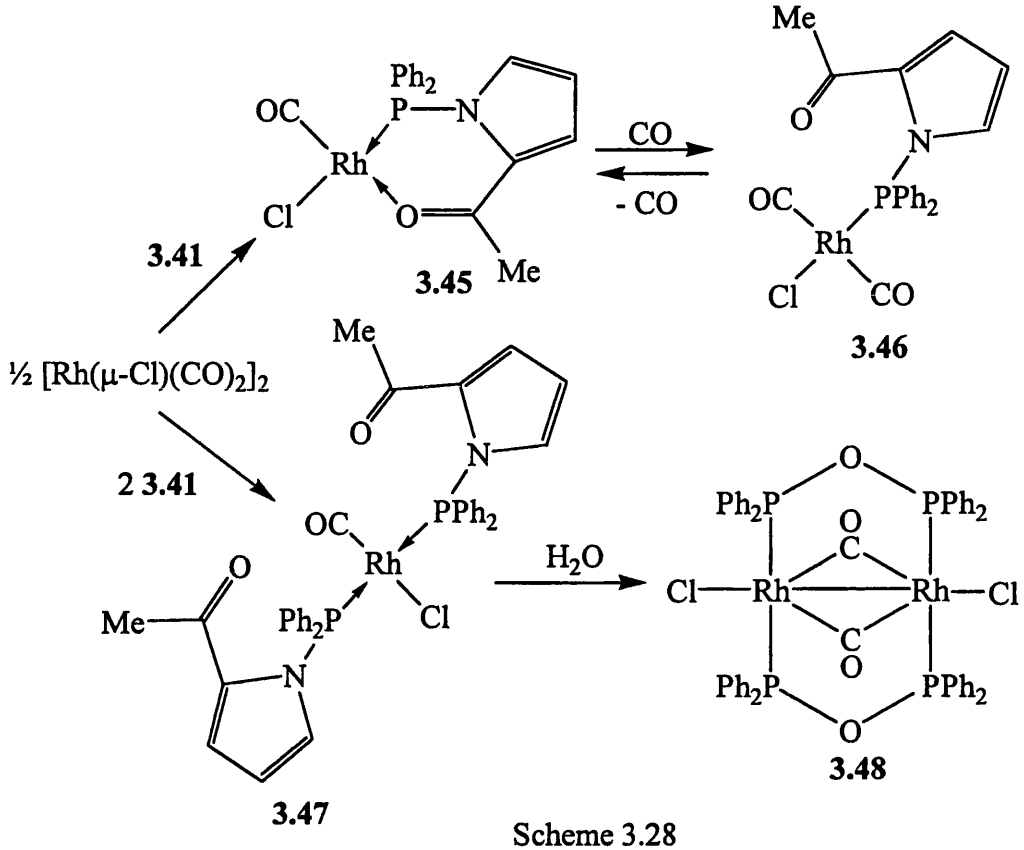

Scheme 3.28

3.6 Summary

Phosphines have proved to be a versatile family of ligands which may be prepared by a variety of routes. The electronic and steric properties of phosphine ligands may be tailored to affect the chemistry of their metal complexes, some of which have found commercial use as homogeneous catalysts.

Functionalised phosphines are an important area of research in part due to their potential to act as hemilabile ligands. The hemilability of the phosphine has been shown to be of interest in homogeneous catalysis, chemical sensing and the stabilisation of reactive metal species. A variety of functionalised phosphines may be made, but those that most commonly exhibit hemilability are those with either an oxygen or nitrogen donor atom. These include phosphinoethers, ketophosphines, amidophosphines and aminophosphines.

The chemistry of *N*-pyrrolyl phosphines, and more especially the hemilabile *N*-pyrrolyl ketophosphines, has been the subject of recent investigation. Preliminary results indicate that this is a rich field for investigation.

3.7 References

1 R.G. Goel and T. Allman, *Can. J. Chem*, 1982, **60**, 716.

2 L.M. Venanzi, *Chem. Ber.*, 1968, **4**, 162.

3 C.A. Tolman, *J. Am. Chem. Soc*, 1970, **92**, 2953.

4 C.A. Tolman, *Chem. Rev.*, 1977, **77**, 313.

5 a) M.G. Choi and T.L.Brown, *Inorg. Chem.*, 1993, **32**, 5603.

b) T.L. Brown and K.J. Lee, *Coord. Chem. Rev.*, 1993, **128**, 89.

c) T.K. Woo and T. Ziegler, *Inorg. Chem.*, 1994, **33**, 1857.

d) M. Chin, G.L. Durst, S.R. Head, P.L. Bock and J.A. Mosbo, *J. Organomet. Chem.*,1994, **470**, 73.

e) J.M. Smith, B.C. Taverner and N.J. Coville, *J. Organomet. Chem.*, 1997, **530**, 131.

f) R.J. Bubel, W. Douglass and D.P.White, *J. Comp. Chem.*, 2000, **21**, 239.

6 K.G. Moloy and J.L. Petersen, *J. Am. Chem. Soc.*, 1995, **117**, 7896.

7 W. Reppe and W.J. Schweckendick, *Annalen*, 1948, **560**, 104.

8 G.W. Parshall, *Homogeneous Catalysis,* Wiley-Interscience, New York, 1980.

9 C. Masters, *Homogeneous Transition Metal Catalysts*, Chapman & Hall, London and New York, 1981.

10 a) J.F. Young, F.H. Jardine, J.A. Osborn and G. Wilkinson, *J. Chem., Soc. Chem. Commun.*, 1965, 131.

b) D. Evans, J.A. Osborn, F.H. Jardine and G. Wilkinson, *Nature*, 1965, **208**, 1203.

c) R.S. Coffey and Imperial Chemical Industries, *Brit Pat. 1*, 1965, **121**, 642.

11 a) W.A. Knowles, *Acc. Chem. Res.*, 1983, **16**, 106.

b) J. Halpern, *Pure Apll. Chem.*, 1983, **55**, 99.

12 a) K. Tani, T. Yamagata, S. Otsuka, S. Akutagawa, H. Kumobayashi, T. Taketomi, H. Takaya, A. Miayshita and R. Noyori, *J. Chem. Soc., Chem. Commun.*, 1982, 600.

b) K. Tani, T. Yamagata, S. Akutagawa, H. Kumobayashi, T. Taketomi, H. Takaya, A. Miayshita, R. Noyori and S. Otusuka, *J. Am. Chem. Soc.*, 1984, **106**, 5208.

c) K. Tani, T. Yamagata, Y. Tatsuno, Y. Yamagata, T. Tomita, S. Akutagawa, H. Kumobayashi and S. Otusuka, *Angew. Chem., Int. Ed. Engl.*, 1985, **24**, 217.

13 a) L. Maier, *Organic Phosphorus Compounds*, ed. G.M. Kosolapoff and L. Maier, Wiley-Interscience, 1972.

b) D.G. Gilheany and C.M. Mitchell, *The Chemistry of Organophosphorus Compounds*, ed. F.R. Hartley, Wiley, 1990.

14 E. Lindner, H. Rauleder, C. Scheytt, H.A. Meyer, W. Hiller, R. Fawzi and P. Wegner, *Z. Naturforsch Teil B*, 1984, **39**, 632.

15 R. Fields, R.N. Hazseldine and J. Kirman, *J. Chem. Soc, Chem. Commun.*, 1970 197.

16 G.P. Schiemenz and H.-U. Siebeneick, *Chem. Ber.*, 1969, **102**, 1883.

17 C.S. Slone, D.A. Weinberger and C.A. Mirkin, *Prog. Inorg. Chem.*, 1999, **48**, 233.

18 P. Braunstein and F. Naud, *Angew. Chem., Int. Ed.*, 2001, **40**, 680.

19 J.I. Dulebohn, S.C. Haefner, K.A. Berglund and K.R. Dunbar, *Chem. Mater.*, 1992, **4**, 506.

20 A. Bader and E. Lindner, *Coord. Chem. Rev.*, 1991, **108**, 27.

21 E. Lindner and B. Andres, *Chem. Ber.*, 1988, **121**, 829.

22 E. Lindner, A. Sickinger and P. Wegner, *J. Organomet. Chem.*, 1988, **349**, 75.

23 a) L. Horner and G. Simons, *Z. Naturforsch Teil B*, 1984, **39**, 497.

b) X. Bei, T. Uno, J. Norris, H.W. Turner, W.H. Weinberg, A.S. Guram, and J.L. Petersen, *Organometallics*, 1999, **18**, 1840.

24 E. Lindner, R. Speidel, R. Fawzi and W. Hiller, *Chem. Ber.*, 1990, **123**, 2255.

25 E. Lindner, M. Kemmler, T. Schneller and H.A. Mayer, *Inorg. Chem.*, 1995, **34**, 5489.

26 E. Lindner, R. Schreiber, T. Schneller, P. Wegner, H.A. Mayer, W. Göpel and C. Ziegler, *Inorg. Chem.*, 1996, **35**, 514.

27 E. Valls, J. Suades, B. Donadieu and R. Mathieu, *Chem. Commun.*, 1996, 771.

28 S. Sabata, J. Vcelák and J. Hetflejs, *Collect. Czech. Chem. Commun.*, 1995, **60**, 127.

29 P. Braunstein, Y. Chauvin, J. Nähring, A. DeCian, J. Fischer, A. Tiripicchio and F. Ugozzoli, *Organometallics*, 1996, **15**, 5551.

30 E. Lindner, K. Gierling, B. Keppler and H.A. Mayer, *Organometallics*, 1997, **16**, 3531.

31 a) S.-E. Bouaoud, P. Braunstein, D. Grandjean. D. Matt and D. Nobel, *Inorg. Chem.*, 1986, **25**, 3765.

b) P. Braunstein, T.M.G. Carneiro, D. Matt, F. Balegroune and D. Grandjean, *J. Organomet. Chem.*, 1989, **367**, 117.

32 a) D.A Knight, D.J. Cole-Hamilton, D. Cupertino, M. Harman and M. Hursthouse, *Polyhedron*, 1992, **11**, 1987.

b) D.A. Knight, D.J. Cole-Hamilton, D. Cupertino, *J. Chem. Soc., Dalton Trans.*, 1990, 3051.

c) S.D. Perera and B.L. Shaw, *J. Organomet. Chem.*, 1991, **402**, 133.

33 B. Demerseman, B. LeLagadec, B. Guilbert, C. Renouard, P. Crochet and P.H. Dixneuf, *Organometallics*, 1994, **13**, 2269.

34 P. Braunstein, S.-E. Bouaoud, D. Grandjean, D. Matt and D. Nobel, *J. Chem. Soc., Chem. Commun.*, 1987, 488.

35 H.D. Empsall, S. Johnson and B.L. Shaw, *J. Chem. Soc., Dalton Trans.*, 1980, 302.

36 W. Keim, A. Behr, B. Gruber, B. Hoffman, F.H. Kowaldt, U. Kürschrer, B. Limbäcker and F.P. Sistig, *Organometallics*, 1986, **5**, 2356.

37 a) W. Keim, *Angew. Chem., Int. Ed. Engl.*, 1990, **29**, 235.

b) P. Braunstein, Y. Chauvin, S. Mercier, L. Saussine, A. DeCian and J. Fischer, *J. Chem. Soc., Chem. Commun.*, 1994, 2203.

38 a) U. Klablunde, T.H. Tulip, D.C. Roe and S.D. Ittel, *J. Organomet. Chem.*, 1987, **334**, 141.

b) U. Klablunde and S.D. Ittel, *J. Mol. Catal.*, 1987, **41**, 123.

39 a) C. Weiser, D. Matt, J. Fischer and A. Harriman, *J. Chem. Soc., Dalton Trans.*, 1997, 2391.

b) J. Andrieu, P. Braunstein, A. Tiripicchio and F. Ugozzoli, *Inorg. Chem.*, 1996, **35**, 5975.

c) J. Andrieu, P. Braunstein and A.D. Burrows, *J. Chem. Res.*, 1993, 380.

d) T. Hosokawa, Y. Wakabayashi, K. Hosokawa, T. Tsuji and S.-I. Murahashi, *Chem. Commun.*, 1996, 859.

40 a) S. Park, D. Hedden, A.L. Rheingold and D.M. Roundhill, *Organometallics*, 1986, **5**, 1305.

b) D. Hedden and D.M. Roundhill, *Inorg. Chem.*, 1986, **25**, 9.

c) D. Hedden, D.M. Roundhill, W.C. Fultz and A.L. Rheingold, *J. Am. Chem. Soc.*, 1984, **106**, 5014.

41 P. Braunstein, C. Frison, X. Morise and R.D. Adams, *J. Chem. Soc., Dalton Trans.*, 2000, 2205.

42 M. Kuriyama and K. Tomioka, *Tetrahedron Lett.*, 2001, **42**, 921.

43 J.M. Camus, D. Morales, J. Andrieu, P. Richard, R. Poli, P. Braunstein and F. Naud, , *J. Chem. Soc., Dalton Trans.*, 2000, 2577.

44 F.G. Mann and H.R. Watson, *J. Chem. Soc.*, 1957, 3950.

45 T.B. Rauchfuss, F.T. Patino and D.M. Roundhill, *Inorg. Chem.*, 1975, **14**, 652.

46 a) K. Burgess, M.J. Ohlmeyer and K.H. Whitmire, *Organometallics*, 1992, **11**, 3588.

b) D.M. Roundhill, R.A. Bechtold and S.G.N. Roundhill, *Inorg. Chem.*, 1980, **19**, 284.

47 S. Serron, S.P. Nolan and K.G. Moloy, *Organometallics*, 1996, **15**, 4301.

48 A. Huang, J.E. Marcone, K.L. Mason, W.J. Marshall and K.G. Moloy, *Organometallics*, 1997, **16**, 3377.

49 A.M. Trzeciak, T. Glowiak, R. Grzybeck and J.J. Ziółkowski, *J. Chem. Soc., Dalton Trans.*, 1997, 1831.

50 A.M. Trzeciak, T. Glowiak and J.J. Ziółkowski, *J. Organomet. Chem.*, 1998, **552**, 159.

51 M.T. Palmer, *PhD thesis*, University of Bath, 2000.

4 Keto- and Amido-phosphines Coordinated to Molybdenum Centres

4.1 Introduction

Phosphines functionalised with a carbonyl group, either as a ketophosphine or an amidophosphine, have attracted considerable interest, most notably from Braunstein and co-workers,[1] for their ability to act as hemilabile ligands. The majority of studies with these ligands have concentrated on late transition metals. There has been to date only one structure published of each of these types of phosphine coordinated to a group 6 metal.

A tungsten ketophosphine complex was prepared by Shaw and co-workers in 1984 and crystallographically characterised.[2] The β-ketophosphine $Ph_2PCH_2C(O)Ph$ (L^2) is formed *in situ* by the route shown in Scheme 4.1.

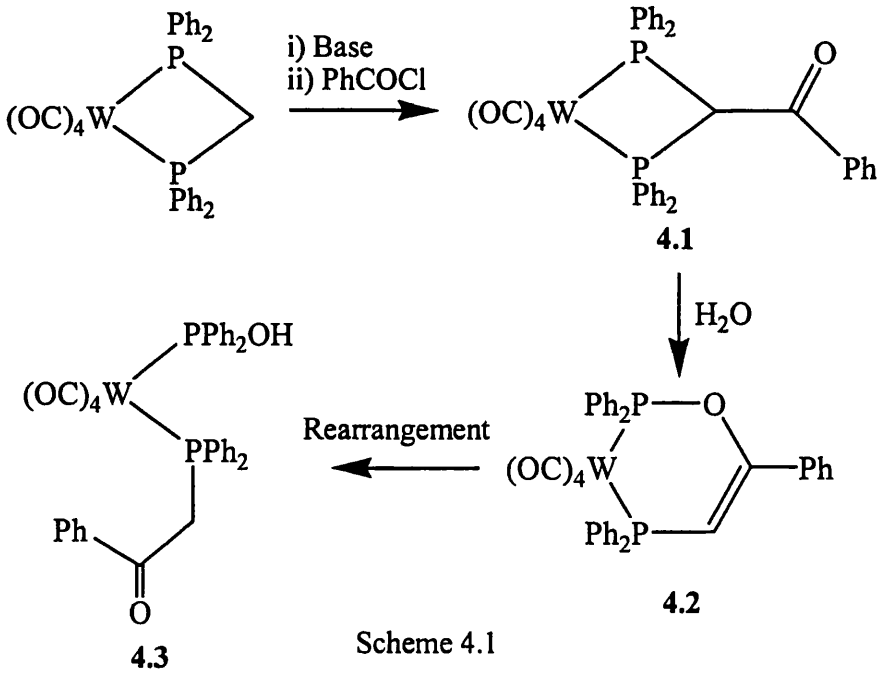

Scheme 4.1

Very recently, Green and co-workers have presented a preliminary account[3] of molybdenum η^6-arene complexes with the same β-ketophosphine, L^2, although in this case L^2 is prepared separately and not formed *in situ*.

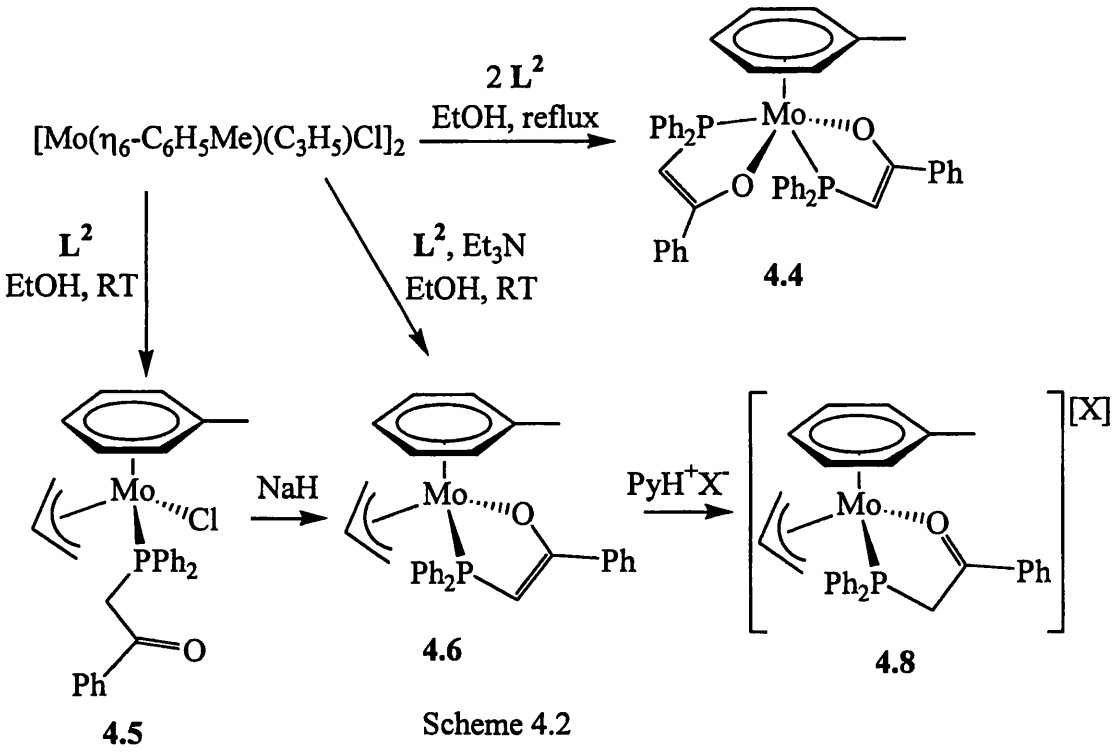

Scheme 4.2

Braunstein and co-workers have recently reported the synthesis of molybdenum half-sandwich complexes of the amidophosphine $Ph_2PCH_2C(O)NPh_2$ ($\mathbf{L^3}$).[4] These were made by direct reaction between $\mathbf{L^3}$ and $[MoCl_4(\eta^5\text{-}C_5Me_5)]$ (Scheme 4.3), cleavage of the molybdenum dimer $[Mo(\mu\text{-}Cl)_2(\eta^5\text{-}C_5H_5)]_2$ in the presence of $\mathbf{L^3}$ (Scheme 4.4), or by oxidative cleavage of the $\eta^5\text{-}C_5Me_5$ analogue (Scheme 4.5).

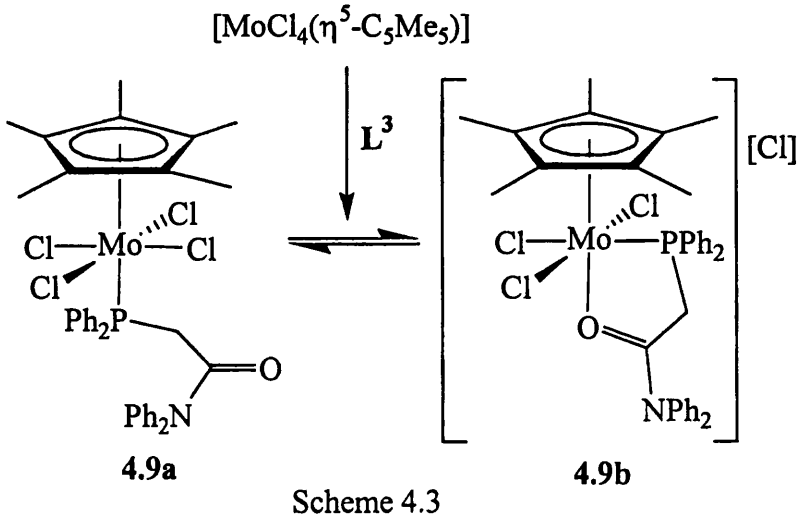

Scheme 4.3

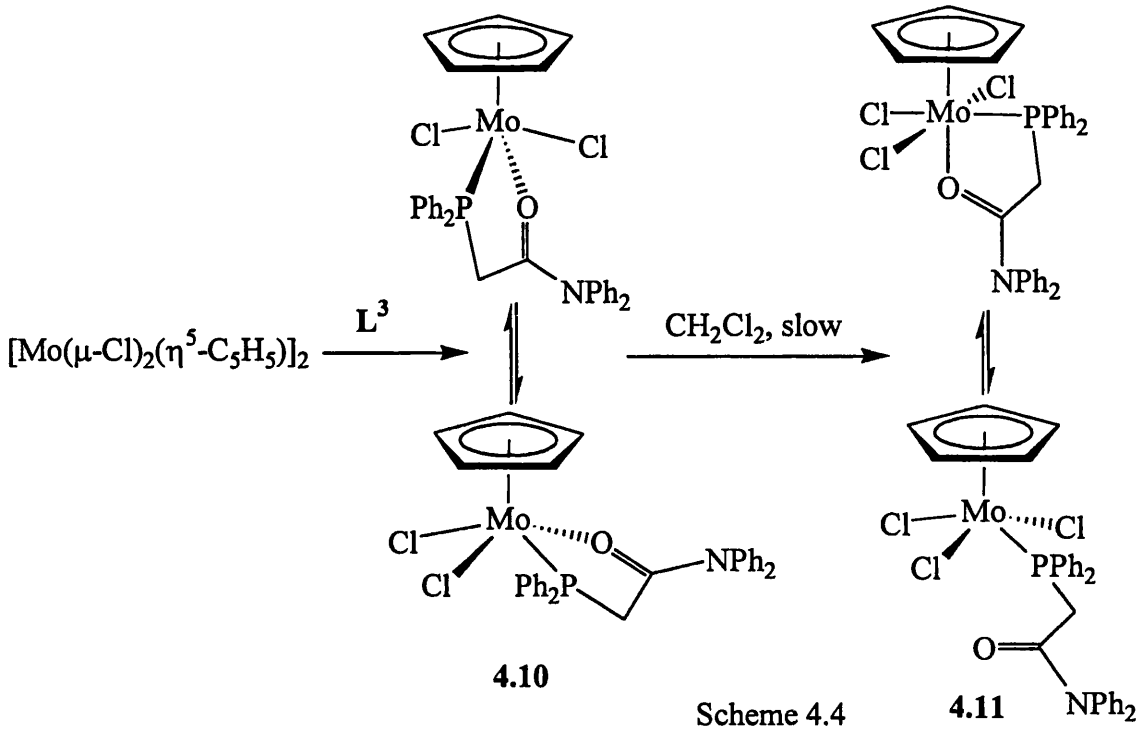

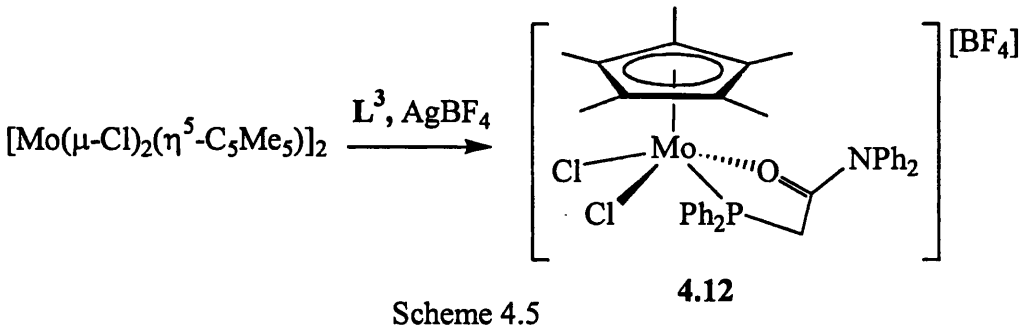

There have been only two published examples of *N*-pyrrolyl phosphines coordinated to group 6 metal centres, both by Moloy and co-workers.[5] Both involve chelating diphosphines, which when reacted with $Mo(CO)_6$ gave the complexes shown in Figure 4.1.

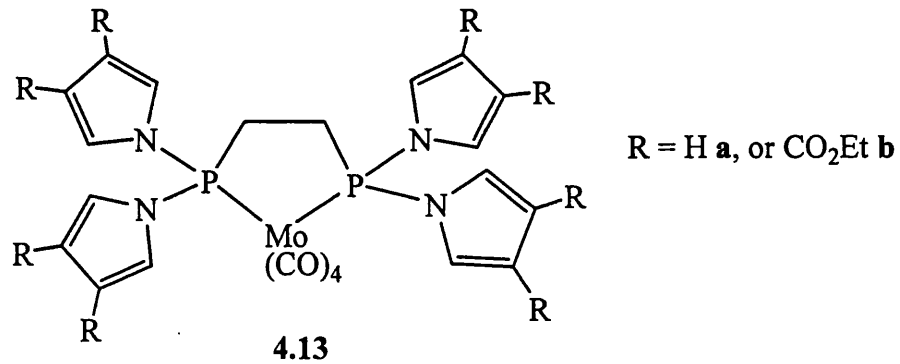

Figure 4.1: Structure of published molybdenum *N*-pyrrolyl phosphine complexes

4.2 Results and Discussion

4.2.1 Aims of research

Although the chemistry of keto- and amido-phosphines with late transition metal centres has been well developed, the analogous chemistry of these ligands with earlier transition metals has yet to be covered in any depth. Similarly the chemistry of *N*-pyrrolyl phosphines, although attracting interest with mid to late transition metals,[6] has not been widely investigated with earlier transition metal centres.

The synthesis of the novel *N*-pyrrolyl ketophosphine, $\mathbf{L^1}$, has recently been developed within the group, and some experiments carried out on late transition metal centres (see Section 3.5.1). It was therefore decided to investigate the reactions of this ligand, together with the more well-known ligands $\mathbf{L^2}$ and $\mathbf{L^3}$, on half-sandwich molybdenum(II) centres.

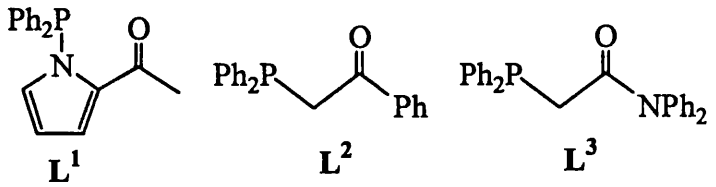

$\mathbf{L^1}$ $\mathbf{L^2}$ $\mathbf{L^3}$

Figure 4.2: Phosphines investigated

4.2.2 Crystal Structure of $\mathbf{L^1}$

One of the aspects of the chemistry of the *N*-pyrrolyl ketophosphine $\mathbf{L^1}$ is the existence of an enolate canonical form, due to the delocalisation of the lone pair of electrons through the ring system and into the ketone group. This is shown in Scheme 4.6.

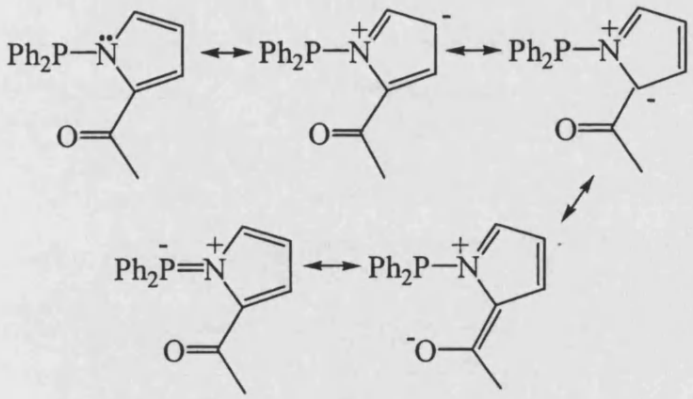

Scheme 4.6

It is therefore important to obtain the crystal structure of the free ligand, so that comparisons may be made with the ligand when it is coordinated (especially in a bidentate manner) to metal centres.

The *N*-pyrrolyl ketophosphine $\mathbf{L^1}$ was synthesised by reacting 2-acetylpyrrole with NEt_3, and then one equivalent of PPh_2Cl. The crude product was purified by recrystallisation from a layer diffusion of hexane into a THF solution to give crystals suitable for X-ray crystallographic studies. The molecular structure of $\mathbf{L^1}$ is shown in Figure 4.3, whilst selected bond lengths and angles are shown in Table 4.1.

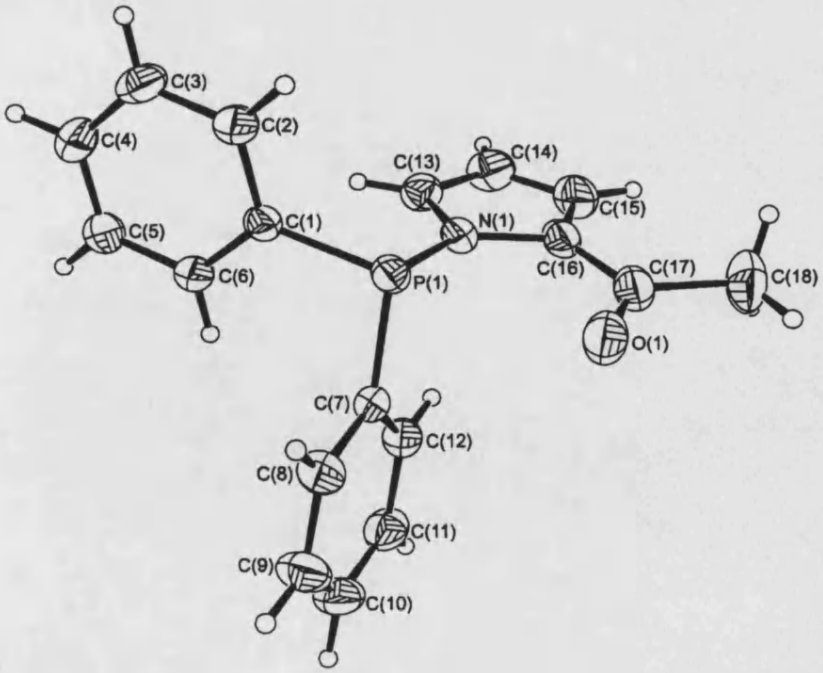

Figure 4.3: Molecular structure of $Ph_2PNC_4H_3C(O)Me$, $\mathbf{L^1}$

The P-N distance in $\mathbf{L^1}$ of 1.7637(14) Å is longer than in tri(*N*-pyrrolyl)phosphine [1.701(4) Å], and is consistent with no double bond character in the P-N bond, in contrast to the aminophosphines PPh_2NHR [P-N lengths = 1.696(3) – 1.730(2) Å].[7] The sum of the angles around the nitrogen atom is 360°, and indicates that the atom is sp^2 hybridised. Since there is no N-P double bond character, this denotes the delocalisation of the lone pair of the nitrogen into the pyrrolyl ring sytem.

P(1)-N(1)	1.7637(14)	C(17)-O(1)	1.216(2)
N(1)-C(13)	1.365(2)	N(1)-C(16)	1.388(2)
C(13)-C(14)	1.358(3)	C(14)-C(15)	1.380(3)
C(15)-C(16)	1.375(3)	C(16)-C(17)	1.441(3)
C(17)-C(18)	1.504(3)		
C(13)-N(1)-P(1)	126.74(12)	C(16)-N(1)-P(1)	125.48(12)
C(13)-N(1)-C(16)	107.45(15)	C(16)-C(17)-C(18)	118.0(2)
C(16)-C(17)-O(1)	121.11(18)	C(18)-C(17)-O(1)	120.8(2)

Table 4.1: Selected bond lengths (Å) and angles (°) for $\mathbf{L^1}$

4.2.3 Reactions of $[MoCl(CO)_3(\eta^5\text{-}C_5R_5)]$ (R = H or Me) with $\mathbf{L^1}$, $\mathbf{L^2}$ and $\mathbf{L^3}$

The molybdenum system chosen to react with the functionalised phosphines $\mathbf{L^1}$, $\mathbf{L^2}$ and $\mathbf{L^3}$ was that of the half-sandwich cyclopentadienyl complexes $[MoCl(CO)_3(\eta^5\text{-}C_5R_5)]$ (R = H or Me). These were chosen as the substitution of one or more carbonyl groups by ligands under mild conditions is already well known for these complexes (See Section 2.1). It was expected that in a reaction with one equivalent of functionalised phosphine, at least one carbonyl would be displaced.

If one carbonyl was displaced, then the functionalised phosphine would coordinate through the phosphorus atom to give the complexes $[MoCl(CO)_2(L\text{-}P)(\eta^5\text{-}C_5R_5)]$ (L = $\mathbf{L^1}$, $\mathbf{L^2}$ or $\mathbf{L^3}$; R = H or Me), **4.14**. There are two possible structural isomers for such complexes. In the *lat* isomer, the two remaining carbonyl ligands are adjacent to

each other, whilst in the *diag* isomer they are opposite to each other. This is shown in Scheme 4.7.

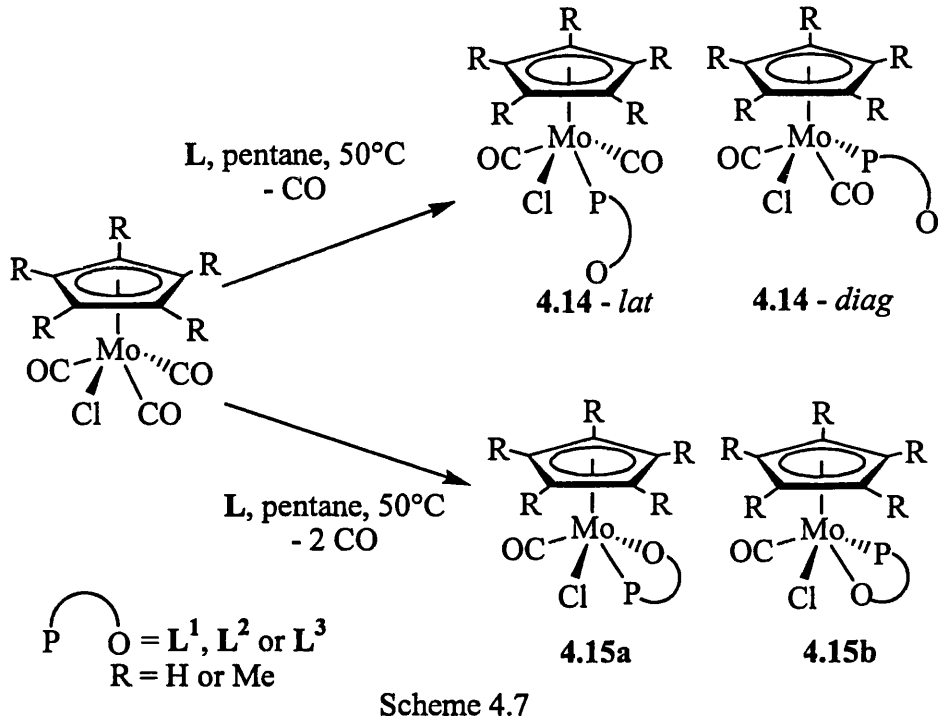

Scheme 4.7

If two carbonyl ligands were displaced, then the functionalised phosphine could coordinate through both the phosphorus and oxygen atoms to give the complexes [MoCl(CO)(L-*P,O*)(η^5-C_5R_5)] (L = **L**^{1}, **L**^{2} or **L**^{3}; R = H or Me), **4.15**. Again there are two possible structural isomers. In isomer **a** the phosphorus is adjacent to the chlorine atom, whilst in isomer **b** the phosphorus is opposite to the chlorine. This is also shown in Scheme 4.7.

4.2.3.1 Reaction of [MoCl(CO)$_3$(η^5-C_5H_5)] with $Ph_2PNC_4H_3C(O)Me$, L^1

Addition of 1.1 equivalents of **L**^{1} to a hexane solution of [MoCl(CO)$_3$(η^5-C_5H_5)] and heating at reflux for 18 hours resulted in formation of an orange precipitate. The crude product was separated by filtration and recrystallised by slow diffusion of toluene into a CH_2Cl_2 solution to give the complex [MoCl(CO)$_2$(**L**^{1}-*P*)(η^5-C_5H_5)], **14**, in good yield (80%). The compound was characterised on the basis of elemental analysis, an X-ray crystallographic study, multinuclear NMR and infrared

spectroscopy. Repeating the experiment with two equivalents of $\mathbf{L^1}$ gave the same organometallic product.

The $^{31}P\{^1H\}$ NMR spectrum of **14**, recorded in $CDCl_3$, displayed a single phosphorus resonance at 112.2 ppm. This represents a significant movement from the chemical shift of the free ligand ($\Delta\delta$ = +55.8 ppm). The ^1H NMR spectrum was as expected with distinctive signals for the pyrrolyl and methyl protons. The infrared spectra, recorded in CH_2Cl_2, displayed a strong band at 1654 cm^{-1}, which was assigned to the C=O stretch of the ketone group. The small change in frequency from that of the free ligand [ν_{CO} = 1643 cm^{-1}, $\Delta\nu_{CO}$ = +11 cm^{-1}] is consistent with an uncoordinated carbonyl group. The bands due to the C≡O stretch of the metal carbonyls were observed at 1970 and 1888 cm^{-1}.

The $^{13}C\{^1H\}$ NMR spectrum of **14** displayed two metal-carbonyl resonances at 254.2 and 242.9 ppm, together with the expected signals for the cyclopentadienyl ring and $\mathbf{L^1}$. The carbonyl signals were observed as doublets, with one coupling constant much larger than the other ($^2J_{CP}$ = 31.4 and < 2 Hz respectively). The signal due to the carbonyl carbon on $\mathbf{L^1}$ was observed as a singlet at 185.5 ppm. The $^{13}C\{^1H\}$ NMR data suggests that **14** exists solely in the *lat*-isomer in a similar manner to $[MoCl(CO)_2(PPh_3)(\eta^5\text{-}C_5H_5)]$, as if the complex had been in the *diag* arrangement, the two metal carbonyls would be equivalent, and so only one signal would have been observed. The reaction is shown in Scheme 4.8.

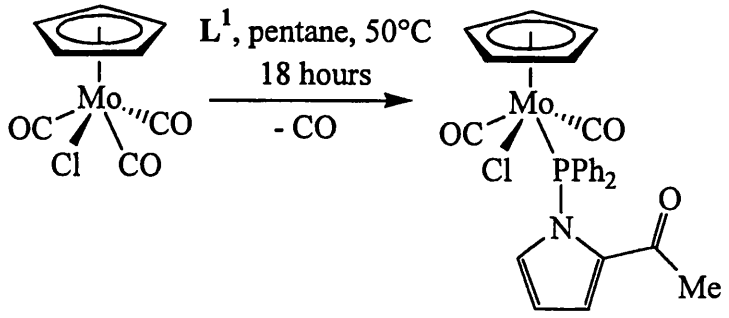

Scheme 4.8 **14**

4.2.3.2 X-Ray Crystal Structure of [MoCl(CO)$_2$(L^1-P)(η^5-C_5H_5)], 14

Complex **14** was recrystallised by a slow diffusion of toluene into a CH_2Cl_2 solution to give crystals suitable for an X-ray structural analysis. The molecular structure of **14** is shown in Figure 4.4, whilst selected bond lengths and angles are given in Table 4.2.

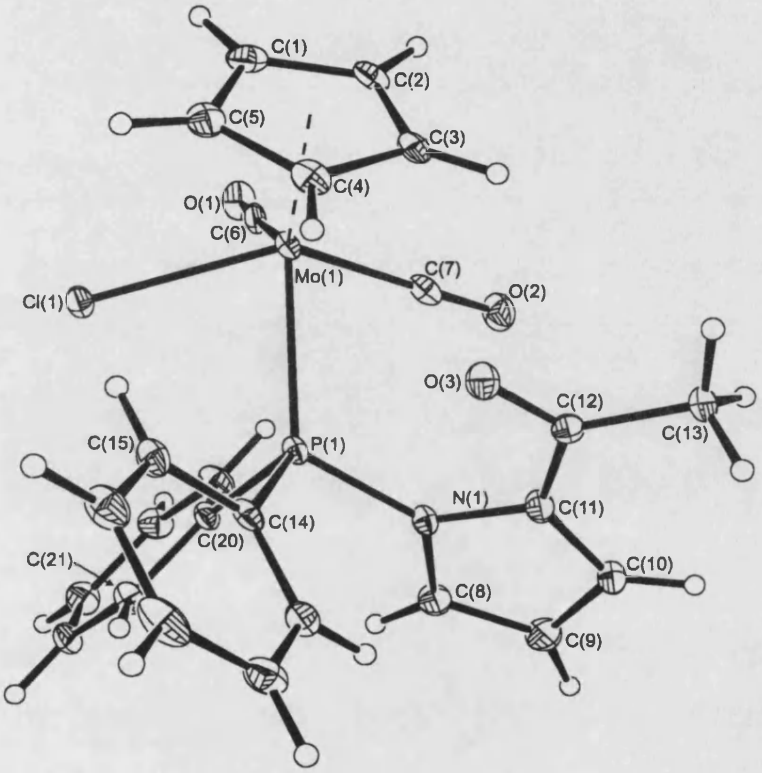

Figure 4.4: Molecular structure of [MoCl(CO)$_2$(**L**^{1}-*P*)(η^5-C_5H_5)], **14**

The crystal structure confirmed the *lat* arrangement of the metal-carbonyl ligands. The complex adopts a pseudo square pyramidal metal geometry, with the *lat* carbonyls, and chlorine and phosphorus atoms forming the base of the pyramid, and the cyclopentadienyl ring the apex.

Comparison of the bond lengths and angles within the coordinated phosphine with those found in free **L**^{1} indicates that the bond lengths are similar to each other (within experimental limits). The C-N-P angles around the nitrogen atoms are different, but in both cases add up to 360°, so it may be assumed that there is no change in the hybridisation of the nitrogen atom.

Mo(1)-P(1)	2.5176(16)	Mo(1)-Cl(1)	2.4991(16)
Mo(1)-C(6)	1.961(5)	Mo(1)-C(7)	1.969(6)
P(1)-N(1)	1.748(4)	C(17)-O(1)	1.222(6)
N(1)-C(8)	1.383(7)	N(1)-C(11)	1.407(6)
C(8)-C(9)	1.355(8)	C(9)-C(10)	1.395(8)
C(10)-C(11)	1.366(8)	C(11)-C(12)	1.451(7)
C(12)-C(13)	1.495(7)		
C(6)-Mo(1)-C(7)	76.0(2)	Cl(1)-Mo(1)-P(1)	76.42(5)
C(6)-Mo(1)-Cl(1)	80.03(15)	C(7)-Mo(1)-Cl(1)	134.99(15)
C(6)-Mo(1)-P(1)	111.62(16)	C(7)-Mo(1)-P(1)	77.86(16)
C(8)-N(1)-P(1)	125.5(4)	C(11)-N(1)-P(1)	128.3(3)
C(8)-N(1)-C(11)	106.1(4)	N(1)-C(11)-C(12)	122.2(5)
C(11)-C(12)-O(3)	121.0(5)		

Table 4.2 Selected bond lengths (Å) and angles (°) for **14**

A search of the CDS database[8] reveals one other structure of the formula $[MoCl(CO)_2P(\eta^5\text{-}C_5R_5)]$ (P = phosphine, R = H or Me). This is the chiral phosphine complex $[MoCl(CO)_2\{R\text{-}Ph_2PN(Me)CH(Ph)Me\}(\eta^5\text{-}C_5R_5)]$, **4.16**.[9] A comparison of selected bond lengths and angles is made in Table 4.3.

It may be seen that the bond lengths of the two complexes are similar, except for the Mo-P distances. This is shorter in **14** [2.5176(16) Å cf. 2.58(1) Å], possibly due to a stronger Mo-P bond caused by an larger π-acceptor effect from the N-pyrrolyl phosphine over the phosphinoamine. The Mo-P distance in **14** is longer than those observed in complex **4.13b** [2.471(2) – 2.430(2) Å], though as both the two phosphines, and the environments of the metal centres are considerably different, no conclusions should be made.

The Cl-Mo-P angle is less in **14** [76.42(5)°] than in **4.16** [85.2(5)°]. There is a corresponding increase in the size of the C-Mo-C angles [76.0(2)° for **14**, 74.5(2.6)°] for **4.16**]. This variation would indicate that the steric interactions between the

phosphine and the chlorine atom are reduced, presumably as a result of a reduction in the steric bulk of the phosphine.

14		**4.16**	
Mo(1)-P(1)	2.5176(16)	Mo-P	2.58(1)
Mo(1)-Cl(1)	2.4991(16)	Mo-Cl	2.49(2)
Mo(1)-C(6)	1.961(5)	Mo-C	1.89(6)
Mo(1)-C(7)	1.969(6)		
C(6)-Mo(1)-C(7)	76.0(2)	C-Mo-C	74.5(2.6)
Cl(1)-Mo(1)-P(1)	76.42(5)	Cl-Mo-P	85.2(2)
C(6)-Mo(1)-Cl(1)	80.03(15)	C-Mo-Cl	81.1(2.6)
C(7)-Mo(1)-Cl(1)	134.99(15)		136.3(1.8)
C(6)-Mo(1)-P(1)	111.62(16)	C-Mo-P	80.7(1.4)
C(7)-Mo(1)-P(1)	77.86(16)		125.9(2)

Table 4.3: Comparison of bond lengths (Å) and angles (°) for complexes **14** and **4.16**

4.2.3.3 Reaction of [MoCl(CO)$_3$(η^5-C$_5$Me$_5$)] with Ph$_2$PNC$_4$H$_3$C(O)Me, L^1

The reaction between $\mathbf{L^1}$ and [MoCl(CO)$_3$(η^5-C$_5$Me$_5$)], carried out as for **14**, resulted in the formation of an orange precipitate. After recrystallisation (slow diffusion of toluene into a CH_2Cl_2 solution) [MoCl(CO)$_2$(*P*-$\mathbf{L^1}$)(η^5-C$_5$Me$_5$)], **15**, was isolated in good yield (90%). This complex was characterised on the basis of elemental analysis, multinuclear NMR and infrared spectroscopy. The reaction is shown in Scheme 4.9. Repeating the reaction with two equivalents of $\mathbf{L^1}$ gave the same product.

As for **1**, the $^{31}P\{^1H\}$ NMR spectrum for **15**, recorded in $CDCl_3$, displayed a single resonance at 58.6 ppm, which in contrast to **14**, was not very different than that for the free ligand. Three multiplets were observed for the pyrrolyl protons in the ^1H NMR at 7.12, 6.39 and 6.22 ppm, as well as peaks for the methyl, η^5-C$_5$Me$_5$ and

phenyl groups. The $^{13}C\{^1H\}$ NMR spectrum displayed a singlet for the carbonyl carbon of the ketone group at 188.1 ppm, plus doublets for the metal-bound carbonyls at 246.3 ($^2J_{CP}$ = 30.5 Hz) and 227.4 ppm ($^2J_{CP}$ = <5 Hz).

The C=O stretching frequency for the ketone was observed in the infrared spectra (recorded in CH_2Cl_2) at 1658 cm^{-1}, consistent with its uncoordinated nature. The bands due to the C≡O stretching of the metal carbonyls were observed at 1964 and 1880 cm^{-1}. The slight movement to lower frequencies from those observed for complex **14** are due to the presence of the η^5-C_5Me_5 ring, which donates more electron density to the metal, thus increasing the back bonding in the carbonyl ligands.

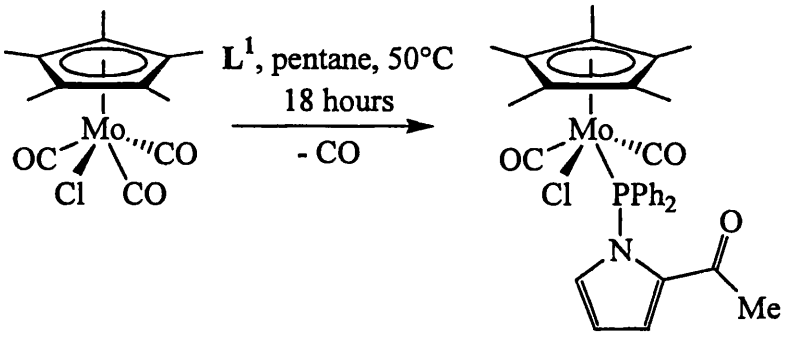

Scheme 4.9 **15**

4.2.3.4 Reactions of [MoCl(CO)$_3$(η^5-C_5R_5)] (R = H or Me) with $Ph_2PCH_2C(O)Ph$, L^2

The reaction between [MoCl(CO)$_3$(η^5-C_5H_5)] and L^2, carried out in the same manner as for **14**, produced an orange precipitate. This was recrystallised by slow diffusion of toluene into a CH_2Cl_2 solution to give [MoCl(CO)$_2$(L^2-*P*)(η^5-C_5H_5)], **16**, as the product in good yield (91%). This complex was characterised on the basis of elemental analysis, multinuclear NMR and infrared spectroscopy. The reaction is shown in Scheme 4.10.

The $^{31}P\{^1H\}$ NMR spectrum, run in $CDCl_3$, displayed a single peak at 48.2 ppm. This represents a significant downfield shift ($\Delta\delta$ = +65.3 ppm) from the signal

observed for the free ligand (–17.1 ppm). The infrared spectrum of a CH_2Cl_2 solution of **16** displayed a strong band for ν_{CO} at 1656 cm^{-1}, which was assigned to the ketone group. The small change in frequency from that of the free ligand (ν_{CO} = 1670 cm^{-1}, $\Delta\nu_{CO}$ = -14 cm^{-1}) is, as with **14**, consistent with an uncoordinated carbonyl group. The bands due to the C≡O stretch of the metal carbonyls were observed at 1970 and 1888 cm^{-1}.

The resonances in the $^{13}C\{^1H\}$ NMR spectrum of **16** for the metal carbonyls were observed as two doublets at 256.8 ($^2J_{CP}$ = 29.5 Hz) and 243.6 ppm ($^2J_{CP}$ = 8.2 Hz), thus indicating a *lat* arrangement of metal carbonyl ligands as observed in **14**. The ketone carbonyl centre was observed as a doublet at 195.2 ppm due to coupling through the carbon chain ($^2J_{CP}$ = 9.7 Hz), as was the signal for the methylene carbon at 36.4 ppm ($^1J_{CP}$ = 20.4 Hz).

The methylene protons were observed in the ^1H NMR spectrum as a pair of doublet of doublets at 4.41 ($^2J_{HH}$ = 15.6 Hz, $^2J_{HP}$ = 9.9 Hz) and 4.14 ppm ($^2J_{HH}$ = 15.6 Hz, $^2J_{HP}$ = 7.9 Hz). This coupling pattern is observed as the *lat* arrangement of metal carbonyl ligands at the molybdenum centre causes the complex to be asymmetric, and the two methylene protons to be inequivalent. The doublets of doublets were also distorted due to second order effects.

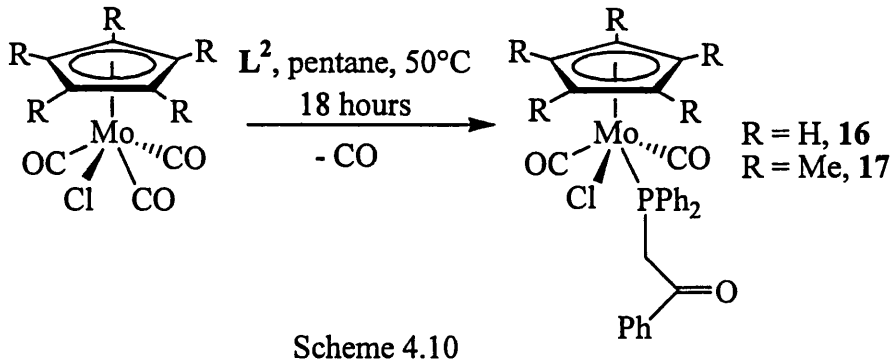

Scheme 4.10

When the reaction was repeated using $[MoCl(CO)_3(\eta^5\text{-}C_5Me_5)]$ and the same conditions, an orange precipitate was produced. This was recrystallised by slow diffusion of toluene into a CH_2Cl_2 solution to give the dark orange product $[MoCl(CO)_2(L^2\text{-}P)(\eta^5\text{-}C_5Me_5)]$, **17**, in good yield (85%). This compound was

characterised on the basis of multinuclear NMR and infrared spectroscopy. The reaction is shown in Scheme 4.10.

The signal for the coordinated ketophosphine was observed in the $^{31}P\{^{1}H\}$ NMR spectra (run in $CDCl_3$) at 45.4 ppm, which represents a significant movement in the chemical shift of the ligand upon coordination ($\Delta\delta$ = +62.5 ppm). In the infrared spectrum of a CH_2Cl_2 solution of **17** the band corresponding to the C=O stretch of the ketone was displayed at 1656 cm^{-1}, consistent with the phosphorus only coordination of the ketophosphine. Bands observed at 1960 and 1879 cm^{-1} were assigned to the C≡O stretch of the metal carbonyl ligands.

The $^{13}C\{^{1}H\}$ NMR spectrum of **17** displayed a pair of doublets for the metal carbonyl centres at 259.0 ($^{2}J_{CP}$ = 27.1 Hz) and 246.2 ppm ($^{2}J_{CP}$ = 5.4 Hz). The ketone carbonyl was observed as a doublet at 195.2 ppm ($^{2}J_{CP}$ = 8.1 Hz), whilst the doublet for the methylene carbon was observed at 34.1 ($^{1}J_{CP}$ = 13.6 Hz). The ^{1}H NMR spectra displayed the methylene protons as a pair of doublets of doublets at 4.64 ($^{2}J_{HH}$ = 14.9 Hz, $^{2}J_{HP}$ = 8.1 Hz) and 3.73 ppm ($^{2}J_{HH}$ = 14.9 Hz, $^{2}J_{HP}$ = 7.0 Hz). These were distorted due to second order effects.

4.2.3.5 Reactions of $[MoCl(CO)_3(\eta^5\text{-}C_5R_5)]$ (R = H or Me) with $Ph_2PCH_2C(O)NPh_2$, L^3

Using the same conditions as in the preparation of **14**, the reactions between $[MoCl(CO)_3(\eta^5\text{-}C_5R_5)]$ (R = H or Me) and $\mathbf{L^3}$ gave orange precipitates. These, when recrystallised by slow diffusion of toluene into CH_2Cl_2 solutions, gave as the products the complexes $[MoCl(CO)_2(\mathbf{L^3}\text{-}P)(\eta^5\text{-}C_5R_5)]$, (R = H **18**, Me **19**) in good yields (93 and 87% respectively). These compounds were characterised on the basis of elemental analysis, multinuclear NMR and infrared spectroscopy.

In the $^{31}P\{^{1}H\}$ NMR spectra (run in $CDCl_3$) of both **18** and **19** single peaks were observed at 52.1 ppm. This represents a significant downfield shift ($\Delta\delta$ = +66.7 ppm) from the signal for the free ligand, which is observed at −14.6 ppm.

The infrared spectrum of **18** displayed a strong band for ν_{CO} at 1666 cm^{-1}, which was assigned to the ketone group. The small change in frequency from that of the free ligand (ν_{CO} = 1670 cm^{-1}, $\Delta\nu_{CO}$ = −3 cm^{-1}) is consistent with an uncoordinated carbonyl group, as is the band observed in the infrared spectrum of **19** (ν_{CO} = 1669 cm^{-1}, $\Delta\nu_{CO}$ = −1 cm^{-1}). The bands for the C≡O stretch of the metal carbonyl ligands were observed at 1964 and 1872 cm^{-1} for **18**, and at 1944 and 1860 cm^{-1} for **19**.

The signals for the metal carbonyl centres in the $^{13}C\{^1H\}$ NMR spectrum of **18** were observed as two doublets at 257.5 ($^2J_{CP}$ = 19.5 Hz) and 243.7 ppm ($^2J_{CP}$ = 6.7 Hz). The methylene carbon was observed as a doublet at 35.7 ppm ($^1J_{CP}$ = 25.7 Hz). Unlike complexes **16** and **17**, the amide carbonyl centre was observed as a singlet at 167.3 ppm.

The $^{13}C\{^1H\}$ NMR spectrum of **19** displayed doublets at 258.6 ($^2J_{CP}$ = 18.4 Hz) and 245.8 ppm ($^2J_{CP}$ = 4.8 Hz) for the metal carbonyls. The methylene carbon was observed as a doublet ($^2J_{CP}$ = 26.0 Hz) at 31.9 ppm. As in **18**, the carbonyl carbon from the ketone group was observed as a singlet at 167.4 ppm.

As in complexes **16** and **17**, the methylene protons were observed in the ^1H NMR spectrum of **18** as a distorted pair of doublet of doublets at 3.51 ($^2J_{HH}$ = 16.0 Hz, $^2J_{HP}$ = 11.7 Hz) and 3.33 ppm ($^2J_{HH}$ = 16.0 Hz, $^2J_{HP}$ = 6.9 Hz). The ^1H NMR spectrum of **19** displayed similar resonances at 3.84 ($^2J_{HH}$ = 16.0 Hz, $^2J_{HP}$ = 8.0 Hz) and 3.29 ppm ($^2J_{HH}$ = 16.0 Hz, $^2J_{HP}$ = 6.5 Hz).

From their $^{13}C\{^1H\}$ and ^1H NMR spectra, it may therefore be deduced that complexes **18** and **19** have analogous structures to **14** with a *lat* arrangement of the carbonyl ligands. The reactions are shown in Scheme 4.11.

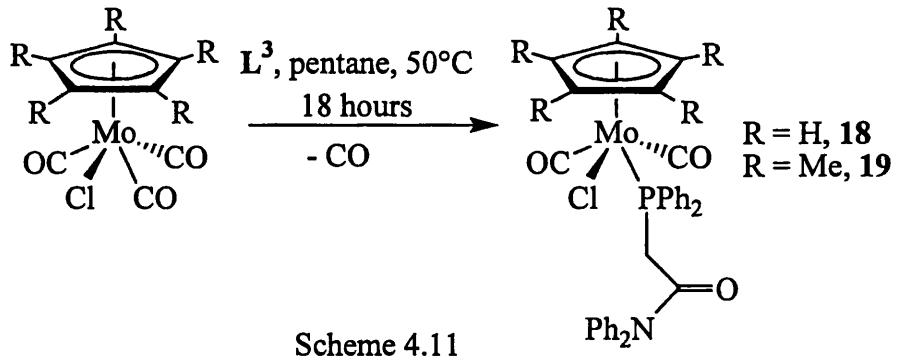

Scheme 4.11

4.2.4 Reactions of Complexes 14 – 19 with $AgBF_4$

As prolonged refluxing of the complexes **14 - 19** did not displace a second molecule of carbon monoxide (which would have led to the neutral complexes **4.14** where the functionalised phosphines are acting as bidentate ligands) it was decided to abstract the chloride from the complexes with silver salts, to attempt the preparation of the cationic complexes $[Mo(CO)_2(\mathbf{L}\text{-}P,O)(\eta^5\text{-}C_5R_5)]^+$ (L = $\mathbf{L^1}$, $\mathbf{L^2}$ or $\mathbf{L^3}$, R = H or Me). As complexes **14 - 19** all exist in the *lat* isomeric form it was considered most likely that the initial kinetic product would retain this conformation. The *diag* structure, as observed for complex **4.10** (in equilibrium with the *lat* isomer), might then be formed either in equilibrium with the *lat* isomer, or as the product. Although orbitally disfavoured, this conformation would be sterically less congested, and therefore more likely to occur with the η^5-C_5Me_5 derivatives.

For complexes **18** and **19** there was also the possibility of $\mathbf{L^3}$ acting as a P,N ligand and undergoing coordination *via* the nitrogen of the amide group. However this was considered unlikely on both electronic and steric considerations.

4.2.4.1 Reaction of $AgBF_4$ with $[MoCl(CO)_2(L^1\text{-}P)(\eta^5\text{-}C_5H_5)]$, 14

Addition of one equivalent of $AgBF_4$ to a solution of **14** in CH_2Cl_2 resulted in the formation of silver chloride. The reaction was monitored by infrared spectroscopy and observed to have gone to completion in 20 minutes. The solution was filtered

through Celite and the solvent removed from the filtrate *in vacuo* to give a red powder. This was recrystallised by slow diffusion of toluene into a CH_2Cl_2 solution to give $[Mo(CO)_2(\mathbf{L^1}\text{-}P,O)(\eta^5\text{-}C_5H_5)][BF_4]$, **20**, as red crystals in good yield (82%). This compound was characterised on the basis of elemental analysis, multinuclear NMR and infrared spectroscopy. The reaction is shown in Scheme 4.12.

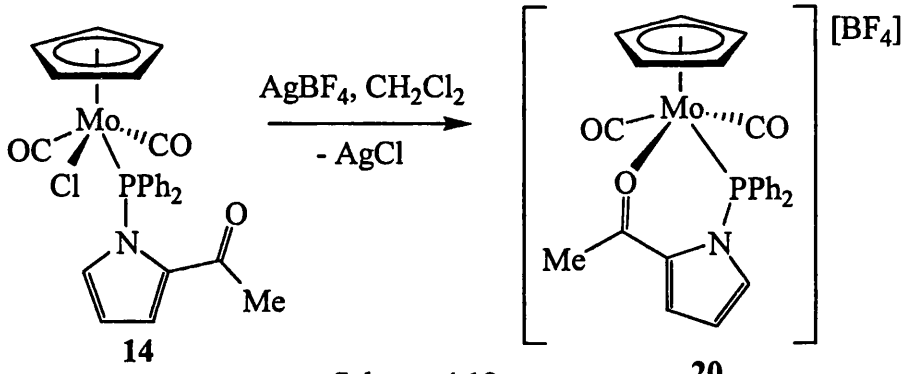

Scheme 4.12

The $^{31}P\{^1H\}$ NMR spectrum of **20** in $CDCl_3$ displayed a single resonance at 114.6 ppm. This represents only a small downfield movement from **14** ($\Delta\delta$ = +2.4 ppm). However, the C=O stretching frequency of the ketone group was observed in the infrared spectra of a CH_2Cl_2 solution of **20** at 1553 cm^{-1}. This large shift from the peak observed in the spectra of **14** ($\Delta\nu_{CO} = -101$ cm^{-1}) is consistent with the decrease in bond order that occurs with the coordination of the ketone group, and thus indicates that the ketophosphine is now acting as a bidentate ligand. The C≡O stretching bands for the metal carbonyls were observed at 1997 and 1928 cm^{-1}.

The ^1H NMR spectrum of **20** displayed the expected peaks, with multiplets due to the pyrrolyl protons being observed at 7.29 and 6.56 ppm (the third being hidden under the phenyl resonances). The $^{13}C\{^1H\}$ NMR spectrum displayed two metal carbonyl signals, both split as doublets, at 248.0 ($^2J_{CP}$ = 30.0 Hz) and 240.0 ppm ($^2J_{CP}$ = 3.2 Hz). In contrast to the spectra for **14**, the ketone carbonyl signal was observed as a doublet ($^3J_{CP}$ = 6.8 Hz) and moved significantly downfield (δ = 199.3 ppm, $\Delta\delta$ = 14.2 ppm). The presence of two metal carbonyl resonances in the $^{13}C\{^1H\}$ NMR suggests that complex **20** has retained the *lat* conformation present in **14**. If **20** were in the *diag* conformation, the metal carbonyls would have been in the same environment and so the values for $^2J_{CP}$ would have been the same.

4.2.4.2 X-Ray Crystal Structure of [Mo(CO)$_2$(L^1-P,O)(η^5-C$_5$H$_5$)][BF$_4$], 20

Complex **20** was recrystallised by slow diffusion of toluene into a CH_2Cl_2 solution to give crystals suitable for an X-ray structural analysis. The molecular structure of **20** is shown in Figure 4.5, whilst selected bond lengths and angles are given in Table 4.4.

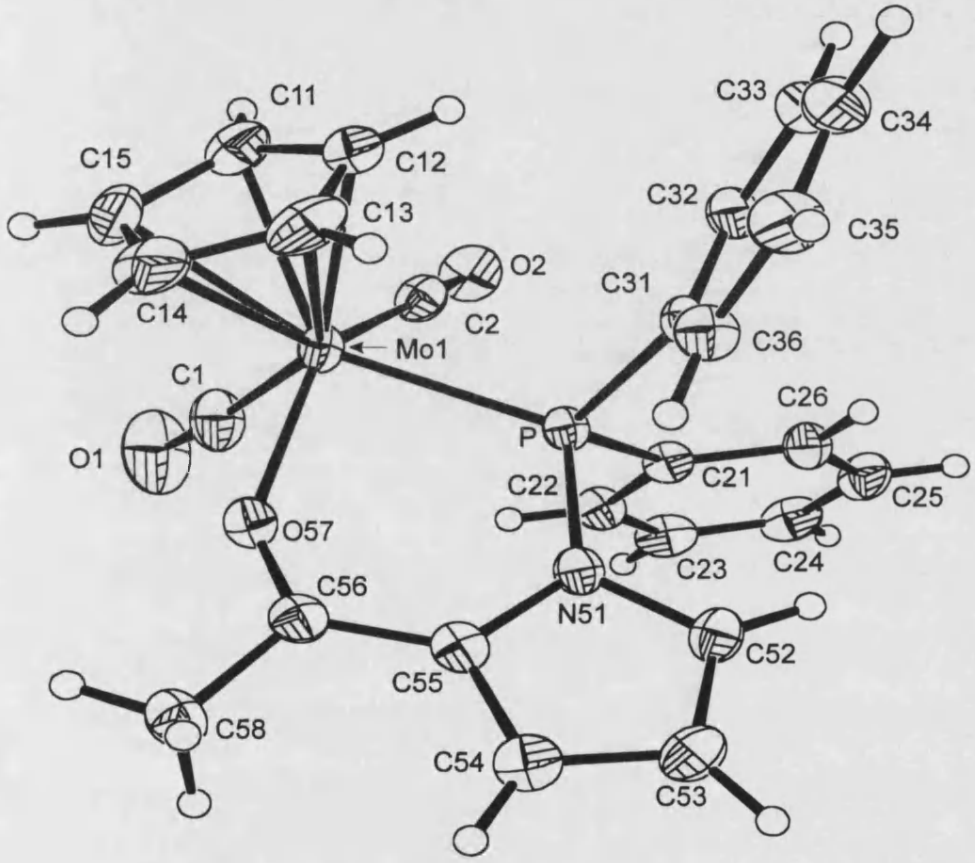

Figure 4.5: X-ray Crystal structure of [Mo(CO)$_2$(**L**^{1}-*P,O*)(η^5-C$_5$H$_5$)][BF$_4$], **20**

The crystal structure confirmed the *lat* arrangement of the metal carbonyl ligands. The complex adopts a pseudo square pyramidal metal geometry, with the *lat* carbonyls, and oxygen and phosphorus atoms forming the base of the pyramid, and the cyclopentadienyl ring the apex.

Mo-P	2.4399(6)	Mo-O(57)	2.1619(17)
Mo-C(1)	1.993(3)	Mo-C(2)	1.978(3)
P-N(51)	1.733(2)	C(56)-O(57)	1.251(3)
N(51)-C(52)	1.383(3)	N(51)-C(55)	1.406(3)
C(52)-C(53)	1.369(4)	C(53)-C(54)	1.395(4)
C(54)-C(55)	1.387(4)	C(55)-C(56)	1.427(3)
C(56)-C(58)	1.505(3)		
C(1)-Mo-O(57)	79.57(10)	C(2)-Mo-O(57)	139.64(9)
C(1)-Mo-P	117.29(9)	C(2)-Mo-P	78.06(7)
C(1)-Mo-C(2)	77.55(11)	O(57)-Mo-P	83.61(5)
C(52)-N(51)-P	124.18(16)	C(55)-N(51)-P	128.77(17)
C(52)-N(51)-C(55)	106.9(2)	N(51)-C(55)-C(56)	125.6(2)
C(55)-C(56)-O(57)	124.9(2)	C(56)-O(57)-Mo	141.33(15)

Table 4.4: Selected bond lengths (Å) and angles (°) for **20**

The C=O bond length of 1.251(3) Å is longer than that observed in the free ligand $\mathbf{L^1}$ and in complex **14** [1.216(2) and 1.222(6) Å respectively]. This suggests an decrease in bond order, though the bond is still shorter than expected for a C–O single bond [~1.333(6) Å]. The P-N bond length of 1.733(2) Å is similar to that observed in **14** [1.748(4) Å], but shorter than in the free phosphine $\mathbf{L^1}$ [1.7637(14) Å]. The Mo-P distance [2.4399(6) Å] is shorter than in **14** [2.5176(16) Å], but similar to those observed in complex **4.13** [2.430(2) – 2.471(2) Å].

The angles around the nitrogen atom in **20** are different from those in both the free phosphine and in complex **14**. However, the sum of the angles remains 360°, indicating that the lone pair of electrons is still delocalised within the pyrrolyl ring. The angle between the carbonyl groups is larger than in **14** [77.55(11)° cf. 76.0(2)°], presumably as the phosphine is closer to the metal centre.

As this is the first complex containing a *P,O*-coordinated ketophosphine on a molybdenum centre, there are no other directly related compounds for comparison.

However, by comparing the bite angle [O(57)-Mo-P = 83.61(5)°] with that from the molybdenum complex $[MoCl_3(O)\{Et_2PCH_2CH_2P(O)Et_2\text{-}P,O\}]$,[10] where the P,O-coordinated ligand also forms a six-membered chelate ring, the angles are observed to be similar (within experimental limits) [P-Mo-O = 83.0(2)°].

4.2.4.3 Reaction of $AgBF_4$ with $[MoCl(CO)_2(L^1\text{-}P)(\eta^5\text{-}C_5Me_5)]$, 15

Using the same method employed in the synthesis of **20**, though requiring a slightly longer reaction time of 1 hour, the reaction between **15** and $AgBF_4$ produced a red powder. This was recrystallised by slow diffusion of toluene into a CH_2Cl_2 solution to give the product $[Mo(CO)_2(\mathbf{L^1}\text{-}P,O)(\eta^5\text{-}C_5Me_5)][BF_4]$, **21**, as red crystals in good yield (83%). This complex was characterised on the basis of multinuclear NMR and infrared spectroscopy. The reaction is shown in Scheme 4.13.

The $^{31}P\{^1H\}$ NMR of **21** in $CDCl_3$ displayed a single resonance at 108.9 ppm. The significant downfield movement ($\Delta\delta$ = +50.3 ppm) of the resonance from that of the *P*-coordinated complex, **15**, is in direct contrast to the behaviour observed for the analogous complexes **14** and **20**.

The C=O stretching frequency of the ketone group was observed in the infrared spectrum of **21** at 1558 cm^{-1}, the large shift ($\Delta\nu_{CO}$ = -100 cm^{-1}) confirming coordination of the ketone. The bands due to the C=O stretching of the metal carbonyl ligands were observed at 1990 and 1916 cm^{-1}. The shift to higher frequencies from those bands seen in the infrared spectra of **14** demonstrate the cationic character of the complex, as with less electron density on the metal, back bonding to the carbonyl ligands is reduced.

The ^1H NMR spectra displayed the expected peaks, with multiplets due to the pyrrolyl protons being observed at 7.20, 7.16 and 6.59 ppm. The $^{13}C\{^1H\}$ NMR spectrum of **21** displayed two metal carbonyl signals, both split as doublets, at 244.4 ($^2J_{CP}$ = 28.0 Hz) and 225.9 ppm ($^2J_{CP}$ <2 Hz). The ketone carbonyl signal was observed as a doublet ($^3J_{CP}$ = 8.7 Hz) and moved significantly downfield (δ = 202.7

ppm, $\Delta\delta$ = 14.6 ppm). As for **20**, the $^{13}C\{^1H\}$ NMR spectrum of **21** confirms the retention of the *lat* conformation.

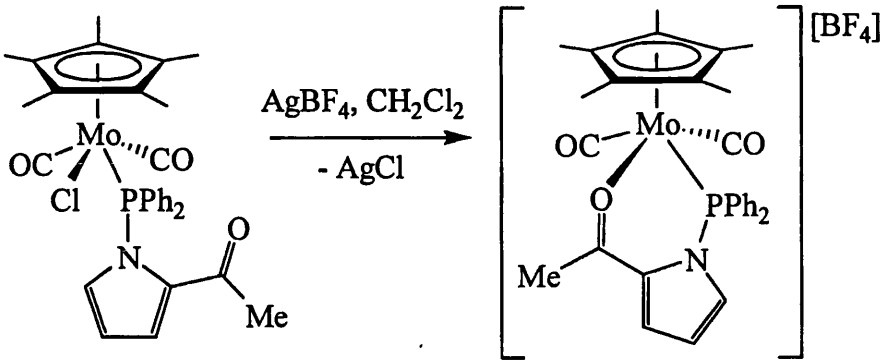

15 Scheme 4.13 **21**

4.2.4.4 Reactions of [MoCl(CO)$_2$(L^2-P)(η^5-C$_5$R$_5$)] (R = H 16, Me 17) with AgBF$_4$

Using the same conditions as in the preparation of **20**, complexes **16** and **17** were reacted with $AgBF_4$ to obtain red powders. These were recrystallised by slow diffusion of toluene into CH_2Cl_2 solutions to isolate the complexes $[Mo(CO)_2(\mathbf{L^2}\text{-}P,O)(\eta^5\text{-}C_5R_5)][BF_4]$ (R = H **22**, R = Me **23**) as red microcrystalline solids in good yields (~86%). These compounds were characterised on the basis of multinuclear NMR and infrared spectroscopy. Selected data is given in Tables 4.5 and 4.6, as is the analogous data complexes **16** and **17** to allow comparison.

The large shifts in the C=O stretching frequencies of the ketone groups ($\Delta\nu_{CO} \approx -100$ cm^{-1}) confirm the coordination of the oxygen to the molybdenum centre in both complexes **22** and **23**. Evidence is also observed in the significant downfield shift in the $^{13}C\{^1H\}$ NMR spectra of the resonances due to the ketone carbonyl carbons ($\Delta\delta \approx +20$ ppm).

The inequivalent methylene protons from the phosphine backbone observed in the ^1H NMR spectra of complexes **22** and **23** arise due to the constraints of the chelate ring. The resonances appear as doublets of doublets, distorted by second order effects.

Complex	δ(P) L^3 / ppm	ν_{CO}(>C=O) / cm^{-1}	ν_{CO}(M-CO) / cm^{-1}	δ(H) CH_2 / ppm	$^2J_{HH}$ / Hz	$^2J_{HP}$ / Hz
16	48.2	1656	1970	4.41	15.6	9.9
			1888	4.14	15.6	7.9
22	72.5	1556	1987	5.00	18.3	9.0
			1912	3.73	18.3	12.3
17	45.4	1656	1960	4.64	14.9	8.1
			1879	3.73	14.9	7.0
23	65.6	1559	1980	5.00	19.0	8.2
			1905	4.29	19.0	11.2

Table 4.5: Comparison of infrared, $^{31}P\{^1H\}$ and ^1H NMR spectroscopy data for complexes **16, 17, 22** and **23**

Complex	δ(C) M-CO / ppm	$^2J_{CP}$ / Hz	δ(C) >C=O / ppm	$^2J_{CP}$ / Hz	δ(C) CH_2 / ppm	$^1J_{CP}$ / Hz
16	256.8	29.5	195.2	9.7	36.4	20.4
	243.6	8.2				
22	247.0	29.7	216.1	10.4	44.7	28.3
	241.9	< 2				
17	259.0	27.1	195.2	8.1	34.1	13.6
	246.2	5.4				
23	251.3	27.2	214.8	12.5	44.5	26.5
	245.8	< 2				

Table 4.6: Comparison of $^{13}C\{^1H\}$ NMR data for complexes **16, 17, 22** and **23**

It may be deduced from the data that, as in complexes **20** and **21**, the *lat* arrangement of ligands has been retained for **22** and **23**. The reactions are shown in Scheme 4.14.

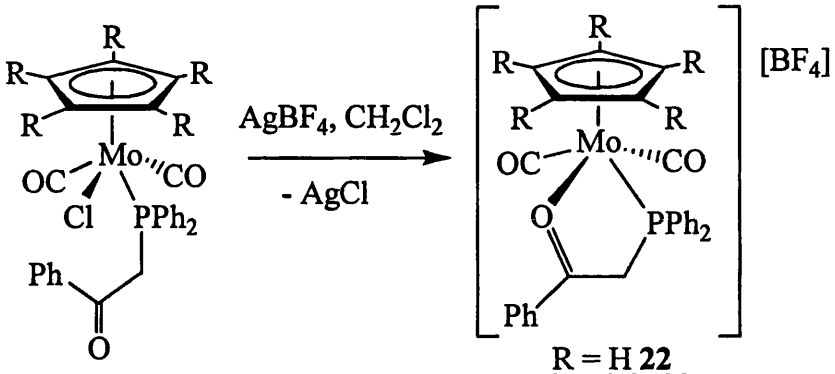

R = H **22**
R = Me **23**

Scheme 4.14

4.2.4.5 Reactions of [MoCl(CO)$_2$(L^3-P)(η^5-C$_5$R$_5$)] (R = H 18, Me 19) with AgBF$_4$

Using the same conditions as in the synthesis of **20**, the reactions between $AgBF_4$ and complexes **18** and **19** produced red powders. These were recrystallised by slow diffusion of toluene into CH_2Cl_2 solutions to give the products the complexes $[Mo(CO)_2(L^3\text{-}P,O)(\eta^5\text{-}C_5R_5)][BF_4]$ (R = **24**, R = Me **25**) as red microcrystalline solids in good yields (88 and 85% respectively). These compounds were characterised on the basis of multinuclear NMR (in $CDCl_3$) and infrared spectroscopy (as CH_2Cl_2 solutions). Selected data is given in Tables 4.7 and 4.8, as is the analogous data for complexes **18** and **19**, to allow comparison.

The large shifts in the C=O stretching frequency of the amide groups ($\Delta\nu_{CO} \approx -120$ cm^{-1}) is indicative of the coordination of the oxygen to the metal centre. No evidence was observed for the coordination of the nitrogen atom. As in complexes **22** and **23**, the methylene protons from the phosphine backbone were observed to be inequivalent, due to the constraints of the chelate ring.

Complex	δ(P) L^3 / ppm	ν_{CO}(>C=O) / cm^{-1}	ν_{CO}(M-CO) / cm^{-1}	δ(H) CH_2 / ppm	$^2J_{HH}$ / Hz	$^2J_{HP}$ / Hz
18	52.1	1666	1964, 1972	3.51 3.33	16.0 16.0	11.7 6.9
24	65.7	1542	1980, 1902	4.42 3.04	16.0 16.0	8.6 12.5
19	52.1	1669	1944, 1860	3.84 3.29	16.0 16.0	8.0 6.5
25	57.1	1547	1963, 1888	4.23 2.94	15.1 15.1	8.6 12.3

Table 4.7: Selected infrared, $^{31}P\{^1H\}$ and ^1H NMR spectroscopy data for complexes **18, 19, 24** and **25**.

Complex	δ(C) M-CO / ppm	$^2J_{CP}$ / Hz	δ(C) >C=O / ppm	$^2J_{CP}$ / Hz	δ(C) CH_2 / ppm	$^1J_{CP}$ / Hz
18	257.5 243.7	19.5 6.7	167.3	-	35.7	25.7
24	250.2 242.4	19.8 < 2	179.6	8.8	31.7	16.2
19	258.6 245.8	18.4 4.8	167.4	-	31.9	26.0
28	251.1 244.3	18.6 < 2	178.8	10.6	31.5	15.9

Table 4.8: Selected $^{13}C\{^1H\}$ NMR spectroscopy data for complexes **18, 19, 24** and **25**.

It may be deduced from the data that, as in complexes **20** and **21**, the *lat* arrangement of ligands has been retained for **24** and **25**. The reactions are shown in Scheme 4.15

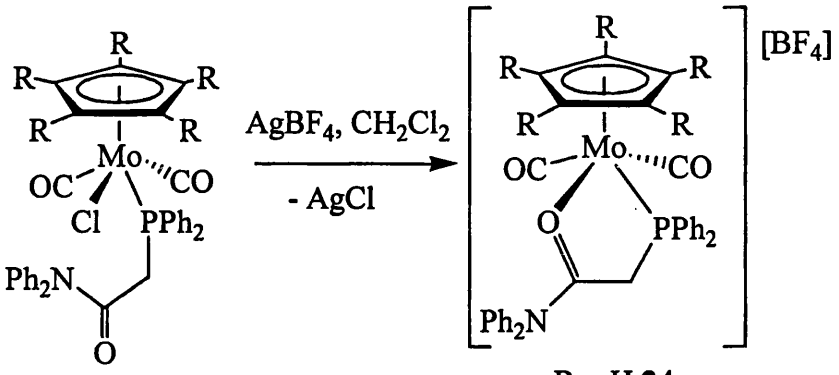

R = H **24**
R = Me **25**

Scheme 4.15

4.2.5 Reactions of $[Mo(CH_3)(CO)_3(\eta^5\text{-}C_5H_5)]$ with $HBF_4{\cdot}Et_2O$ and L (L = L^1 or L^2)

An alternative route was proposed for the synthesis of the *P,O*-coordinated ketophosphine complexes. The methyl group from the complex $[Mo(CH_3)(CO)_3(\eta^5\text{-}C_5H_5)]$ may be protonated by $HBF_4{\cdot}Et_2O$ to produce methane and the etherate complex $[Mo(CO)_3(OEt_2)(\eta^5\text{-}C_5H_5)][BF_4]$. This was expected to react with one equivalent of a ketophosphine **L** to produce the complexes $[Mo(CO)_3(\mathbf{L}\text{-}P)(\eta^5\text{-}C_5H_5)][BF_4]$ as an intermediate. This complex may then eliminate carbon monoxide to produce the complexes $[Mo(CO)_2(\mathbf{L}\text{-}P,O)(\eta^5\text{-}C_5H_5)][BF_4]$. The analogous reaction with alkynes displaces two carbonyl ligands to give the bis-alkyne complexes $[Mo(CO)(\eta^2\text{-alkyne})_2(\eta^5\text{-}C_5H_5)][BF_4]$, so it was considered likely that a carbonyl ligand would be displaced in the reactions with ketophosphines.

The addition of one equivalent of $HBF_4{\cdot}Et_2O$ to a CH_2Cl_2 solution of $[Mo(CH_3)(CO)_3(\eta^5\text{-}C_5H_5)]$ at −78°C led to the formation of a purple solution of $[Mo(CO)_3(OEt_2)(\eta^5\text{-}C_5H_5)][BF_4]$. Subsequent addition of one equivalent of $\mathbf{L}^1$ or $\mathbf{L}^2$, and stirring for 16 hours results in a change of colour in the solution to dark red. The solvents were removed from the solution *in vacuo*, and the resulting red powder recrystallised by slow diffusion of toluene into CH_2Cl_2 solutions to give the

complexes **20** and **22** in good yield (~86%). These complexes were characterised by $^{31}P\{^{1}H\}$ NMR and infrared spectroscopy, which displayed identical spectra to samples prepared by the route described in Sections 4.2.4.1 and 4.2.4.4. The reactions are shown in Scheme 4.16.

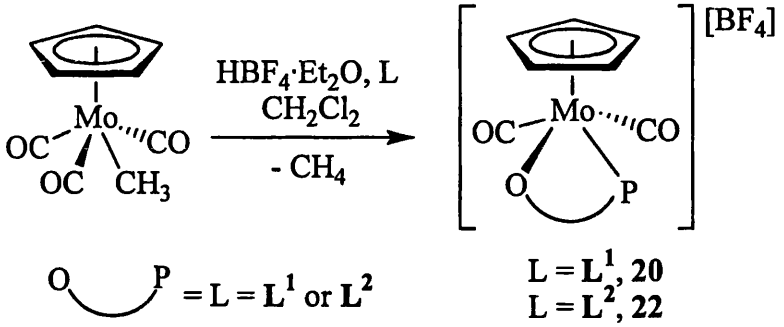

Scheme 4.16

This route was not adapted for the general synthesis of complexes of the type $[Mo(CO)_2(\mathbf{L}\text{-}P,O)(\eta^5\text{-}C_5R_5)][BF_4]$, due to the relative sensitivity of the starting materials $[Mo(CH_3)(CO)_3(\eta^5\text{-}C_5R_5)]$, compared with those used in the syntheses described earlier. However, it does allow an alternative synthesis of the *P,O*-coordinated complexes, and may prove useful, especially for thermally sensitive phosphines where the reaction in pentane at reflux might prove disadvantageous.

4.2.6 Deprotonation of Complexes 14 – 25

One of the most commonly performed reactions of coordinated β-keto- and amidophosphines is deprotonation by a base to form the phosphino-enolate complexes (Scheme 4.17). The methylene protons are so susceptible to attack by base that in the work carried out by Green and co-workers and shown in Scheme 4.2, the formation of an enolate occurred in the absence of a strong base to give complex **4.4**. Such reactions may be reversed by the addition of an acid to the enolate, which reprotonates the α-carbon centre.

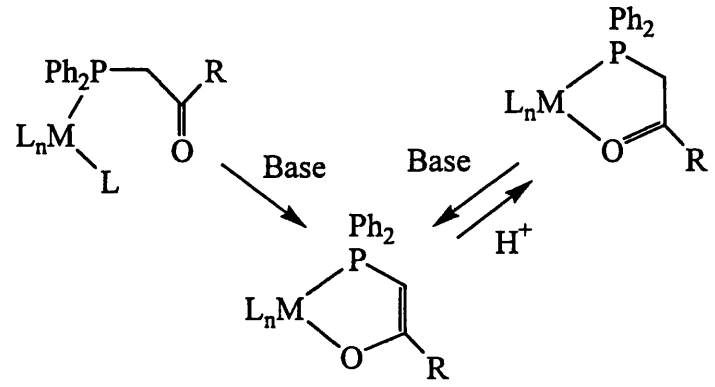

Scheme 4.17

Although the *N*-pyrrolyl phosphine $\mathbf{L^1}$ does not contain such a methylene group, deprotonation of the methyl group would also give a phosphino-enolate ligand. The

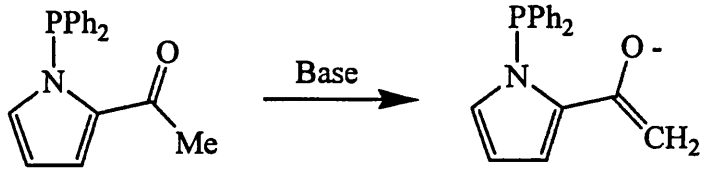

Scheme 4.18

It was thought that reacting complexes **14 – 19** with one equivalent of BuLi would produce the phosphino-enolate complexes, with loss of butane and LiCl. Similarly, the reaction of complexes **20 – 25** with a base such as Et_3N would produce the same, neutral phosphino-enolate complexes accompanied by formation of the salt $[Et_3NH][BF_4]$.

4.2.6.1 Reaction of BuLi with Complexes 14 - 19

One equivalent of a 1.6M solution of BuLi to a thf solution of complexes **14 - 19** at – 78°C, producing light orange solutions and fine white precipitates of LiCl upon warming to room temperature. The solutions were filtered through Celite, the solvents removed from the filtrate *in vacuo*, and the residues analysed by multinuclear NMR and infrared spectroscopy. These indicated that the reactions with complexes **14, 15** and **17-19** had formed multiple products which proved intractable.

However, the reaction with complex **16** gave only one product which was recrystallised by slow diffusion of hexane into a CH_2Cl_2 solution to give $[Mo(CO)_2\{Ph_2PCH{=}C(Ph)O\text{-}P,O\}(\eta^5\text{-}C_5H_5)]$, **26**, as an orange powder in good yield (86%). The complex was fully characterised by elemental analysis, multinuclear NMR and infrared spectroscopy. The reaction is shown in Scheme 4.19.

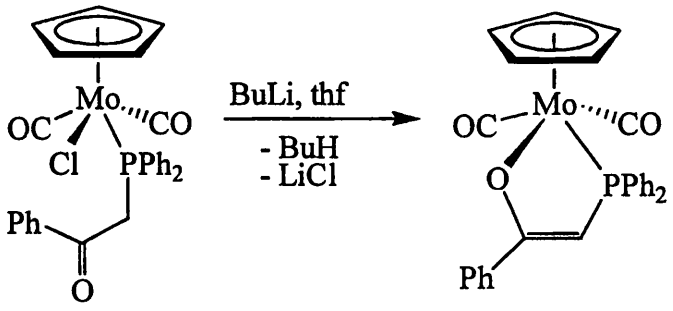

16 **26**

Scheme 4.19

The $^{31}P\{^1H\}$ NMR spectrum of **26** in $CDCl_3$ displayed a single peak at 68.4 ppm. This is a significant downfield shift from the *P*-coordinated complex **16** ($\Delta\delta$ = +20.2 ppm), and a small upfield shift from the *P,O*-coordinated complex **22** ($\Delta\delta$ = -4.1 ppm). The ^1H NMR spectrum no longer displays two inequivalent protons but instead, a single doublet with an integration value of one proton is observed at 5.19 ppm ($^2J_{HP}$ = 1.2 Hz).

The CO stretching frequency of the phosphine was observed to have shifted to a much lower frequency (ν_{CC+CO} = 1460, $\Delta\nu$ = –196 cm^{-1}) in the infrared spectrum of **26**. This indicates that there is no longer a C=O bond, but instead a conjugated C-O bond from the enolate.

The $^{13}C\{^1H\}$ NMR of **26** displayed two metal carbonyl signals, both split as doublets, at 253.2 ($^2J_{CP}$ = 29.7 Hz) and 242.7 ppm ($^2J_{CP}$ = 4.1 Hz). The β-carbon of the phosphine was observed as a doublet at 181.1 ppm ($^1J_{CP}$ = 30.1 Hz), while the α-carbon was observed as a doublet at 45.6 ppm ($^1J_{CP}$ = 69.7 Hz). The very large value for $^1J_{CP}$ is in agreement with the literature examples of this type of complex, and in line with the increased s orbital character of the carbon-phosphorus bond.

4.2.6.2 X-Ray Crystal Structure of [Mo(CO)$_2${Ph$_2$PCH=C(Ph)O-P,O}(η^5-C$_5$H$_5$)], 26

Crystals suitable for X-ray crystallographic studies were grown by a slow evaporation of a solution of **26** in deuterated chloroform. The molecular structure of **26** is shown in Figure 4.6, whilst selected bond distances and angles are given in Table 4.9. Proton H(9) was located in an advanced Fourier difference map.

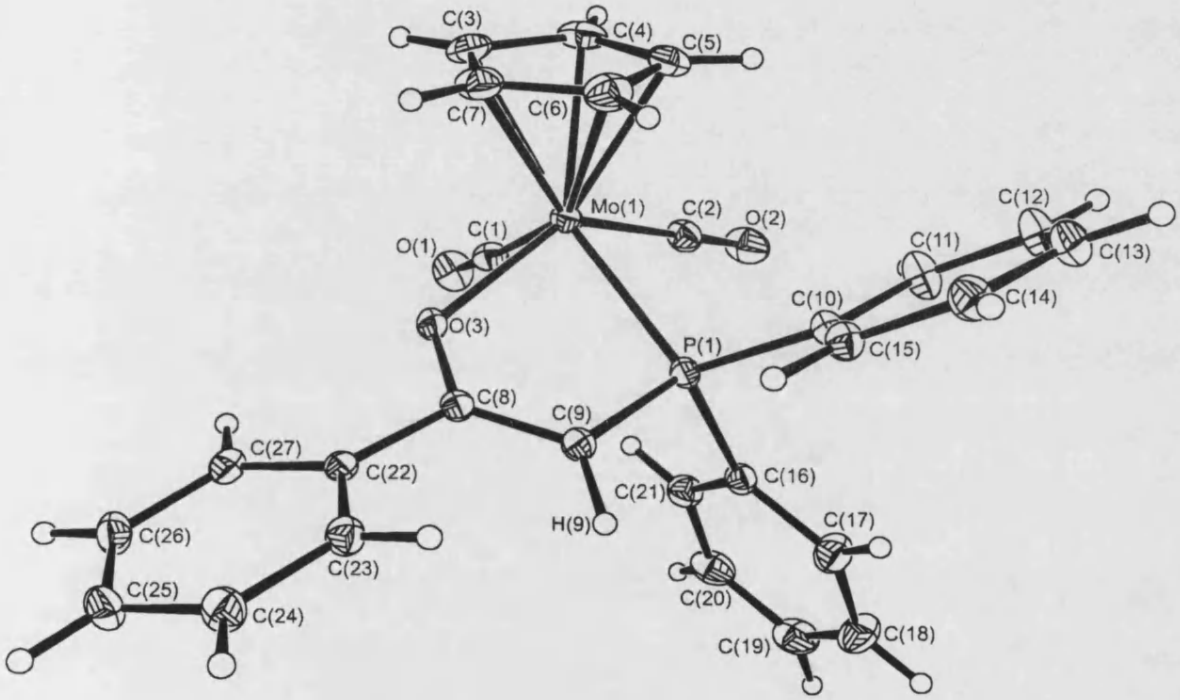

Figure 4.6: X-ray crystal structure of [Mo(CO)$_2${Ph$_2$PCH=C(Ph)O-*P,O*}(η^5-C$_5$H$_5$)], **26**

The complex adopts a pseudo square pyramidal metal geometry, with the *lat* carbonyls, and oxygen and phosphorus atoms forming the base of the pyramid, and the cyclopentadienyl ring the apex.

A search of the CDS database[8] reveals no other molybdenum phosphino-enolate complexes with which to compare 26. However, a comparison of the bond lengths and angles observed for **26** with those for complexes of phosphino-enolates and *P,O*-coordinated **L**^{2} on other metal centresreveal them to be typical for a phosphino-

enolate complex. The P-C bond length of 1.765(4) Å is significantly shorter than in any of the complexes where $\mathbf{L^2}$ is *P,O*-coordinated to the metal, as is the C(8)-C(9) bond length of 1.372(5). The C-O distance in **26** of 1.319(5) Å is again inside the previously observed range for a phosphino-enolate complex, though significantly longer than that expected for a ketophosphine complex.

Mo(1)-P(1)	2.4475(10)	Mo(1)-O(3)	2.151(2)
Mo(1)-C(1)	1.977(4)	Mo(1)-C(2)	1.974(4)
P(1)-C(9)	1.765(4)	C(9)-C(8)	1.372(5)
C(8)-O(3)	1.319(5)		
C(1)-Mo(1)-P(1)	114.62(12)	C(2)-Mo(1)-P(1)	78.77(12)
C(1)-Mo(1)-O(3)	84.22(13)	C(2)-Mo(1)-O(3)	137.53(14)
O(3)-Mo(1)-P(1)	76.54(7)	C(1)-Mo(1)-C(2)	75.43(17)
Mo(1)-P(1)-C(9)	101.28(13)	P(1)-C(9)-C(8)	113.7(3)
C(9)-C(8)-O(3)	123.5(3)	C(8)-O(3)-Mo(1)	121.1(2)

Table 4.9 Selected bond lengths (Å) and angles (°) for **26**

Bond / angle	**26**	CDS phosphino-enolate	CDS $\mathbf{L^2}$-*P,O*
P-C	1.765(4)	1.726(9) – 1.796(5)	1.835(5) – 1.862(9)
C-C	1.372(5)	1.336(13) – 1.421(9)	1.480(7) – 1.580(6)
C-O	1.319(5)	1.258(14) – 1.335(6)	1.223(14) – 1.252(6)
PCC	113.7(3)	111.3(5) – 117.5(2)	101.1(3) – 118.8(8)
CCO	123.5(3)	120.6(6) – 127.7(3)	118.3(5) – 120.1(10)
MPC	101.28(13)	96.7(4) – 101.7(3)	97.5(5) – 106.6(4)
MOC	121.2(2)	113.2(3) – 122.0(4)	120.6(8) – 124.7(3)

Table 4.10: Comparison of bond lengths (Å) and angles (°) between **26**, and CDS database values for complexes of phosphino-enolates and $\mathbf{L^2}$.

The range of bond angles as obtained from the CDS database for phosphino-enolate and ketophosphine complexes overlap to a considerable degree, and those angles seen for **26** are similar to both systems.

4.2.6.3 Reaction of Et_3N with Complexes 20 - 25

The addition of one equivalent of Et_3N to CH_2Cl_2 solutions of complexes **20 - 25** resulted in changes of colour in the solutions from red to orange and the formation of fine precipitates of $[Et_3NH][BF_4]$. The solutions were filtered through Celite and the solvents removed from the filtrates *in vacuo*. Initial analysis by ^1H and $^{31}P\{^1H\}$ NMR spectroscopy on the resulting orange residues revealed that for complexes **20, 21** and **23 - 25** multiple products had formed, which proved to be intractable. The reaction with complex **22** was observed to give a single product, which was recrystallised by diffusion of hexane into a CH_2Cl_2 solution to give **26** in very good yield (94%). The complex was characterised by $^{31}P\{^1H\}$ NMR and infrared spectroscopy which displayed identical spectra to those of samples prepared by the route described in Section 4.2.6.1. The reaction is shown in Scheme 4.20.

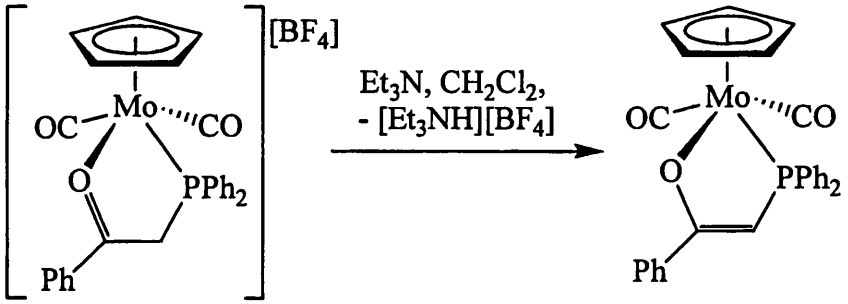

22 **26**

Scheme 4.20

4.2.6.4 Reaction of $[Mo(CO)_2\{Ph_2PCH=C(Ph)O\text{-}P,O\}(\eta^5\text{-}C_5H_5)]$, 13, with $HBF_4{\cdot}Et_2O$

The addition of one equivalent of $HBF_4{\cdot}Et_2O$ to a solution of the enolate complex **26** at –78°C, with subsequent warming to room temperature, resulted in a colour change

of orange to red. Removal of the solvents *in vacuo* followed by recrystallisation by diffusion of toluene into a CH_2Cl_2 solution led to the isolation of complex **22**. This was characterised by $^{31}P\{^1H\}$ NMR and infrared spectroscopy which displayed identical spectra to those from samples synthesised by the previously mentioned route (Section 4.2.4.4). The reaction is shown in Scheme 4.21.

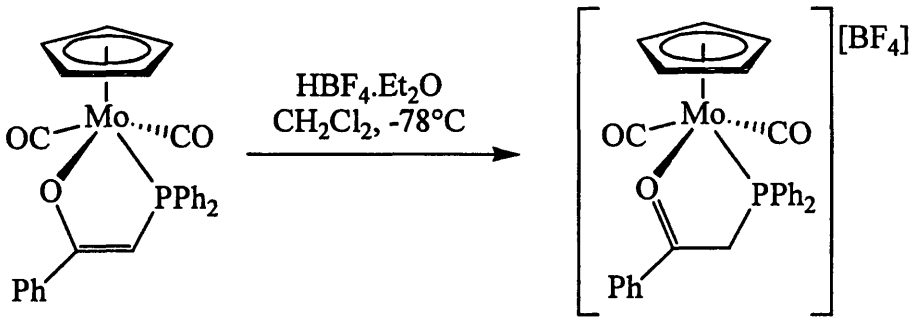

26 Scheme 4.21 **22**

4.2.7 Hemilability of Complexes 20 - 25

One of the most important aspects in the chemistry of *P,O*-coordinating functionalised phosphines is their ability to act as hemilabile ligands (see Section 3.4). It was decided to investigate the hemilability of the ligands $\mathbf{L^1}$, $\mathbf{L^2}$ and $\mathbf{L^3}$ by reacting the complexes **20 – 25** with different reagents that might be able to displace the oxygen atom from the molybdenum centre.

Reactions of the *P,O*-coordinated phosphine complexes **20 – 25** with a chloride anion were expected to recreate the *P*-coordinated complexes **14 – 19**, as is shown in Scheme 4.22.

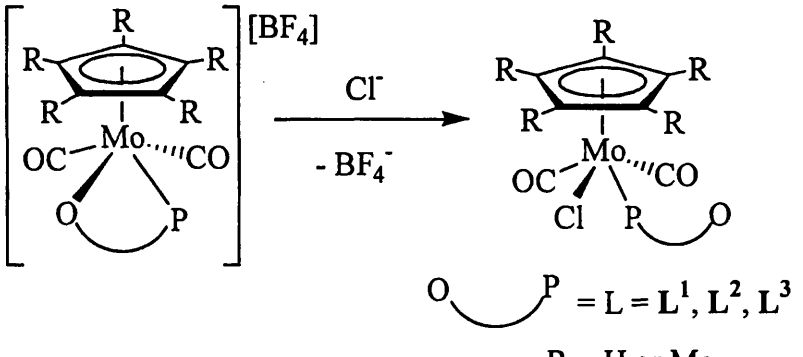

Scheme 4.22

Neutral ligands such a phosphines were expected to displace the oxygen from the molybdenum centre to give the complexes $[Mo(CO)_2(L\text{-}P)(A)(\eta^5\text{-}C_5R_5)][BF_4]$, where A is the new ligand. There are two possible conformations of the products of such reactions, either *lat* or *diag*. These reactions are shown in Scheme 4.23.

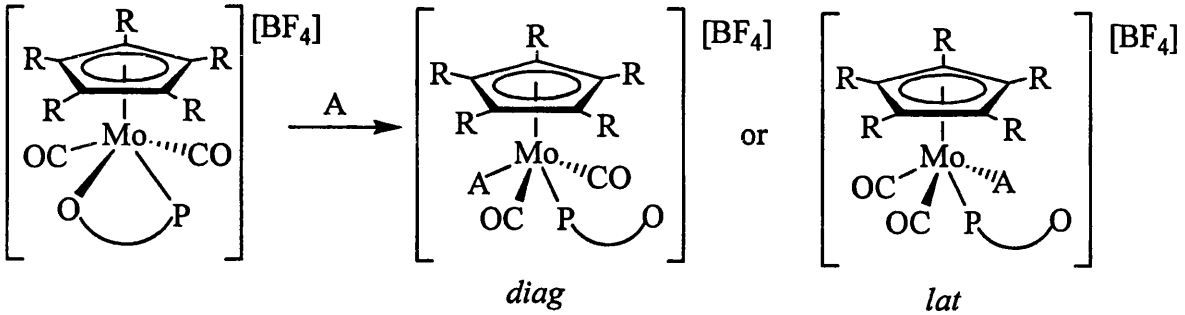

$O\frown P = L = L^1, L^2, L^3$

Scheme 4.23 R = H or Me

The ligands chosen to investigate were the phosphine series PPh_3, PPh_2Me, PMe_2Ph and PMe_3, which were expected to give valuable information about the relative electronic and steric effects for each of the functionalised phosphines. Similarly the bulky phosphine PCy_3, and the good π-acceptor ligand $P(OMe)_3$ were used to investigate this behaviour. The diphosphine ligand $Ph_2P(CH_2)_6PPh_2$ (dpph) was used to investigate whether it was possible to link two molybdenum centres, whilst the phosphine oxide $Ph_3P{=}O$ was used to investigate the feasibilty of replacing one oxygen donor atom with another. Reactions with MeC≡CMe and P≡CBu^t were attempted since it was expected that such ligands would not wish to remain as 2 electron donors, but would eliminate CO to give either η^2(4e)-alkyne, or 1,3-diphosphacyclobutadiene complexes respectively.

4.2.7.1 Reactions of Complexes 20 - 25 with [PhCH$_2$NEt$_3$][Cl]

Dichloromethane solutions of complexes **20 – 25** were reacted with one equivalent of the salt $[PhCH_2NEt_3][Cl]$, and the reactions monitored by infrared spectroscopy. In every case, the peaks due to the starting material were observed to disappear after 2 hours. Cooling the solutions to –20°C led to the formation of a fine white precipitate

of $[PhCH_2NEt_3][BF_4]$. The solutions were filtered, and the solvents removed from the filtrates *in vacuo* to give orange residues. These were recrystallised by slow diffusion of toluene into CH_2Cl_2 solutions to give complexes **14** – **19** as orange powders in good yields (76 – 93%). The products were characterised by $^{31}P\{^1H\}$ NMR and infrared spectroscopy, which displayed identical spectra to samples of the complexes prepared by the previously described routes (Sections 4.2.3.1 and 4.2.3.3 – 5). The reactions are shown in Scheme 4.24

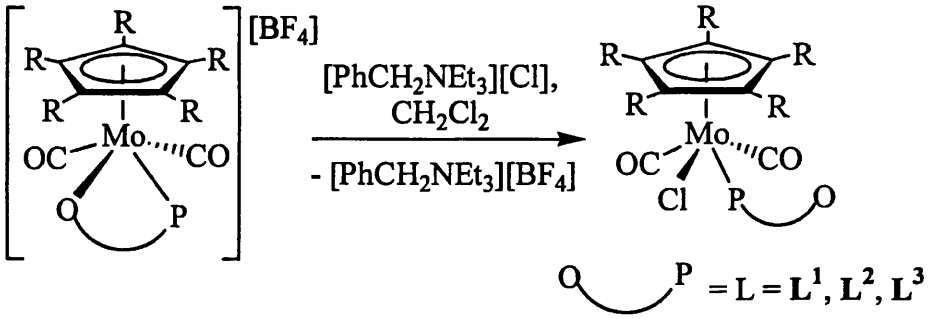

Scheme 4.24

4.2.7.2 Reactions of $[Mo(CO)_2(L^1\text{-}P,O)(\eta^5\text{-}C_5H_5)][BF_4]$, 20, with Neutral Ligands

One equivalent of PPh_3, PPh_2Me, PMe_2Ph, PMe_3, PCy_3, $P(OMe)_3$, dpph, MeC≡CMe, Ph_3P=O, and P≡CBu^t were added to solutions of **20** in CH_2Cl_2, and the reactions monitored by $^{31}P\{^1H\}$ NMR spectroscopy.

Even after 14 days, no products were observed in the reactions with PPh_3, dpph, PCy_3, MeC≡CMe, Ph_3P=O or P≡CBu^t. In the other reactions, after the reactions were observed to have gone to completion by $^{31}P\{^1H\}$ NMR spectroscopy, the solvents were removed *in vacuo*. Diffusion of hexane into CH_2Cl_2 solutions of the residues isolated the products as dark orange to red oils.

The reaction with PPh_2Me resulted in the formation of the red complex $[Mo(CO)_2(\mathbf{L^1}\text{-}P)(PPh_2Me)(\eta^5\text{-}C_5H_5)][BF_4]$, **27**, in good yield (90%). Likewise, the reactions with PMe_2Ph, PMe_3 and $P(OMe)_3$ produced the analogous products $[Mo(CO)_2(\mathbf{L^1}\text{-}P)(L)(\eta^5\text{-}C_5H_5)][BF_4]$ (L = PMe_2Ph **28**, PMe_3 **29**, $P(OMe)_3$ **30** in

similar yields. These complexes were characterised by multinuclear NMR and infrared spectroscopy. Selected data is given in Tables 4.11 and 4.12 with analogous data for complexes **14** and **20** included to allow comparison. The reactions are shown in Scheme 4.25.

Complex	Ligand	δ(P) L^1 / ppm	δ(P) L / ppm	$^2J_{PP}$ / Hz	ν_{CO}(>C=O) / cm^{-1}	ν_{CO}(M-CO) / cm^{-1}
14	-	112.2	-	-	1654	1970, 1880
20	-	114.6	-	-	1553	1997, 1928
27	PPh_2Me	122.5	40.6	20.9	1669	1978, 1900
28	PMe_2Ph	127.7	26.2	20.9	1669	1974, 1898
29	PMe_3	125.1	20.3	23.4	1664	1972, 1896
30	$P(OMe)_3$	121.1	168.7	23.5	1665	1966, 1889

Table 4.11: Selected $^{31}P\{^1H\}$ NMR and infrared spectroscopy data for complexes **14**, **20**, and **27-30**.

Complex		δ(C) M-CO /ppm	$^2J_{CP}$ /Hz	δ(C) >C=O /ppm	$^3J_{CP}$ /Hz
14		254.2 242.9	31.4 < 1	185.5 -	- -
20		248.0 240.0	30 3. 2	199.3 -	6.8 -
27	PPh_2Me	230.8*	29.2	185.1	-
28	PMe_2Ph	231.2*	29.2	184.7	-
29	PMe_3	231.1*	29.6	184.4	-
30	$P(OMe)_3$	223.6*	29.7	185.5	-

Table 4.12: Selected $^{13}C\{^1H\}$ NMR data for complexes **14**, **20**, and **27-30** (peaks marked * are triplets)

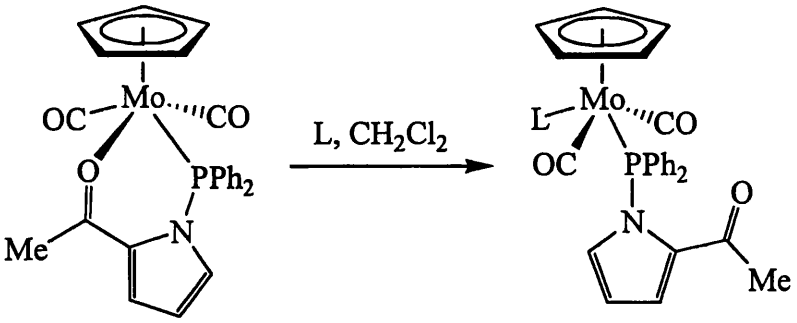

20

L = PPh_2Me, **27**
= PMe_2Ph, **28**
= PMe_3, **29**
= $P(OMe)_3$, **30**

Scheme 4.25

The carbonyl stretching frequencies in the infrared spectra for the ketone groups in complexes **27** – **30** lie within the range 1664 – 1669 cm^{-1}, and are in the region associated with the non-coordination of the ketone group. This indicates that the oxygen atoms from the ketone groups have been displaced from the molybdenum centres. The frequencies for the metal carbonyl groups on the metal centres show the expected trend to lower wavenumbers (From 1978 and 1900 cm^{-1} to 1966 and 1889 cm^{-1}) with increasing σ-donor/decreasing π-acceptor character of the introduced ligand.

The $^{31}P\{^1H\}$ NMR spectra of complexes **27** – **30** in $CDCl_3$ display two mutually coupled doublets, assigned as the two phosphine ligands. The values of $^2J_{PP}$ are in the range 20.9 – 23.5 Hz.

The ^1H NMR spectra display the methyl resonances for complexes **27** - **30** as doublets at 2.21 ($^2J_{HP}$ = 9.4 Hz), 1.96 ($^2J_{HP}$ = 9.9 Hz), 1.66 ($^2J_{HP}$ = 10.3 Hz) and 3.42ppm ($^2J_{HP}$ = 9.4 Hz) respectively. The appearance of the methyl peak for complex **28** as one doublet indicates that the arrangement of the two different phosphines is *diag*, as this provides a plane of symmetry, thus allowing the two methyl groups to be equivalent. If the complex was in the *lat* conformation, the two methyl groups would be inequivalent, and so two signals would be expected.

The $^{13}C\{^1H\}$ NMR spectra for complexes **27** - **30** displayed triplets at 230.8, 231.2, 231.0 and 223.6 ppm respectively, relating to the two symmetrical M-CO groups.

This indicates that the two carbon-phosphorus coupling constants must be within spectral resolution. An upfield shift was observed for the peaks corresponding to the ketone carbonyl carbons, and no phosphorus-carbon coupling was observed, consistent with the non-coordination of the ketone groups.

4.2.7.3 Reactions of [Mo(CO)$_2$(L^2-P,O)(η^5-C$_5$H$_5$)][BF$_4$], 22, with Neutral Ligands

One equivalent of PPh_3, PPh_2Me, PMe_2Ph, PMe_3, PCy_3, $P(OMe)_3$, dpph, $Ph_3P{=}O$, MeC≡CMe, and P≡CBu^t were added to solutions of complex **22** in CH_2Cl_2, and the reactions monitored by $^{31}P\{^1H\}$ NMR spectroscopy.

In the reactions with PCy_3, $Ph_3P{=}O$, MeC≡CMe, and P≡CBu^t, the only species observed in the $^{31}P\{^1H\}$ NMR spectra were the starting materials, even after a period of 14 days. The reaction with $P(OMe)_3$ resulted in the formation of multiple intractable products.

The reaction of **22** with PMe_3 resulted in the formation of a sticky white precipitate, and a colour change in the solution from red to orange. The solution was filtered off the precipitate, the solvents removed from the filtrate *in vacuo*, and the residue recrystallised by diffusion of hexane into a CH_2Cl_2 solution to generate orange crystals. These were characterised by $^{31}P\{^1H\}$ NMR and infrared spectroscopy, and proved to be not the expected product [Mo(CO)$_2$(L^2-*P*)(PMe_3)(η^5-C_5H_5)][BF_4], but instead the phosphino-enolate complex **26** in good yield and purity (85%). The white precipitate was therefore believed to be [PMe_3H][BF_4]. This reaction is shown in Scheme 4.26.

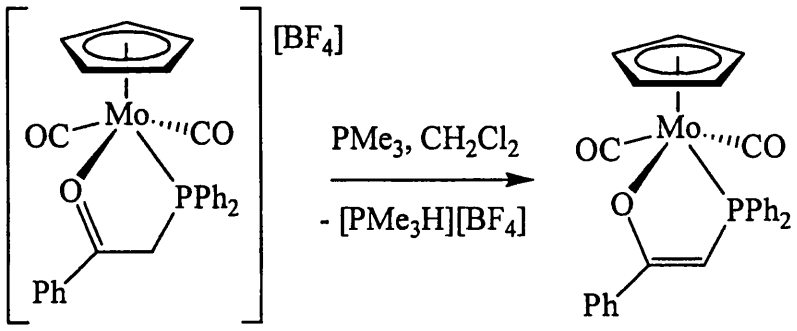

22 **26**

Scheme 4.26

The reaction of **22** with PPh_3 was observed by $^{31}P\{^1H\}$ NMR spectroscopy to have gone to completion in 7 days. The solvents were removed from the red solution *in vacuo*, and hexane diffused into a CH_2Cl_2 solution of the residue to isolate the red oily product $[Mo(CO)_2(\mathbf{L^2}\text{-}P)(PPh_3)(\eta^5\text{-}C_5H_5)][BF_4]$, **31**, in good yield (90%). Likewise, the reactions with PPh_2Me and PMe_2Ph produced the analogous complexes $[Mo(CO)_2(\mathbf{L^2}\text{-}P)(L)(\eta^5\text{-}C_5H_5)][BF_4]$ (L = PPh_2Me **32**, PMe_2Ph **33**), in similar yield, though in shorter times (3 days). The reaction with dpph gave the dinuclear complex $[\{Mo(CO)_2(\mathbf{L^2}\text{-}P)(\eta^5\text{-}C_5H_5)\}_2(dpph)][BF_4]_2$, **34**, in reasonable yield (60%). The complexes were characterised by multinuclear NMR (in $CDCl_3$) and infrared spectroscopy (in CH_2Cl_2). Selected data are given in Tables 4.13 and 4.14, as is the analogous data for complexes **16** and **22**, to allow comparison. The formation of complexes **31** - **34** are shown in Scheme 4.27.

Complex	Ligand	δ(P) $\mathbf{L^2}$ / ppm	δ(P) L / ppm	$^2J_{PP}$ / Hz	ν_{CO}(>C=O) / cm^{-1}	ν_{CO}(M-CO) / cm^{-1}
16		48.2	-	-	1656	1970, 1888
22		72.5	-	-	1556	1987, 1912
31	PPh_3	47.3	57.7	18.8	1684	1974, 1895
32	PPh_2Me	48.8	41.2	19.8	1665	1973, 1892
33	PMe_2Ph	52.1	25.6	21.0	1663	1972, 1890
34	dpph	48.6	47.3	18.5	1679	1969, 1889

Table 4.13 Selected $^{31}P\{^1H\}$ NMR and infrared spectroscopy data for complexes **16**, **22** and **31-34**.

As for complexes **27** – **30**, two mutually coupled ($^2J_{PP}$ = 18.5 – 21.0 Hz) doublets are seen in the $^{31}P\{^1H\}$ NMR spectra of complexes **31-34** in $CDCl_3$. The infrared spectra show a shift by the ketone C=O stretching frequency to regions associated with uncoordinated ketone groups, indicating that the added phosphines have displaced the ketone groups from the molybdenum centres. The frequencies for the metal carbonyl groups also show the same trend to lower wavenumbers with increasing σ-

donor/decreasing π-acceptor character of the introduced ligand (1974 and 1895 cm^{-1} to 1972 and 1890 cm^{-1}).

Complex	Ligand	δ(C$\underline{H_2}$) /ppm	$^2J_{HH}$ / Hz	$^2J_{HP}$ / Hz	δ(C) M-CO / ppm	$^2J_{CP}$ / Hz	δ(C) >C=O / ppm	$^3J_{CP}$ / Hz
16		4.41	15.6	9.9	256.8	29.5	195.2	9.7
		4.14	-	7.9	243.6	8.2	-	-
21		5.00	18.3	9.0	247.0	29.7	216.1	10.4
		3.73	-	12.3	241.9	< 2	-	-
31	PPh_2Me	4.62	-	8.3	233.9*	27.1	193.3	5.7
32	PMe_2Ph	4.42	-	8.6	234.1*	27.1	193.3	4.7
33	PMe_3	4.33	-	8.6	234.3*	27.6	193.0	3.7
34	dpph	4.50	-	8.2	234.1*	27.1	193.3	5.3

Table 4.14: Selected ^1H and $^{13}C\{^1H\}$ NMR data for complexes **16**, **22** and **31-34**. (peaks marked * are triplets)

The ^1H NMR spectra of complexes **32** and **33** display doublets at 2.23 ($^2J_{HP}$ = 9.0Hz) and 2.06ppm ($^2J_{HP}$ = 9.0Hz) respectively, which were assigned as the methyl groups on the phosphine ligands. As for complex **28**, the appearance of this signal as a doublet for complex **33** indicates a *diag* arrangement of ligands around the metal centre. The spectra of complex **34** shows multiplets at 3.66, 2.55 and 1.18 ppm which were assigned to the chain methylene groups in the dpph ligand.

The ^1H NMR spectra of complexes **31 - 34** display doublets at 4.62 ($^2J_{HP}$ = 8.3 Hz), 4.42 ($^2J_{HP}$ = 8.6 Hz), 4.33 ($^2J_{HP}$ = 8.6 Hz) and 4.50 ppm ($^2J_{HP}$ = 8.2 Hz) respectively. These signals were assigned as the methylene protons from the ketophosphine. Their appearance as doublets, rather than two doublet of doublets as in complex **21** provides additional evidence for the *diag* arrangement of ligands. As there is now a plane of symmetry through the molecule, the methylene protons are equivalent, and thus do not couple to each other.

The $^{13}C\{^1H\}$ NMR spectra for complexes **31 - 34** show triplets at 233.9, 234.1, 234.3 and 234.1 ppm respectively, relating to the two symmetrical M-CO groups. This indicates that the two carbon-phosphorus coupling constants must be very similar. An upfield shift was observed for the peaks corresponding to the ketone carbonyl carbons, consistent with its uncoordinated character.

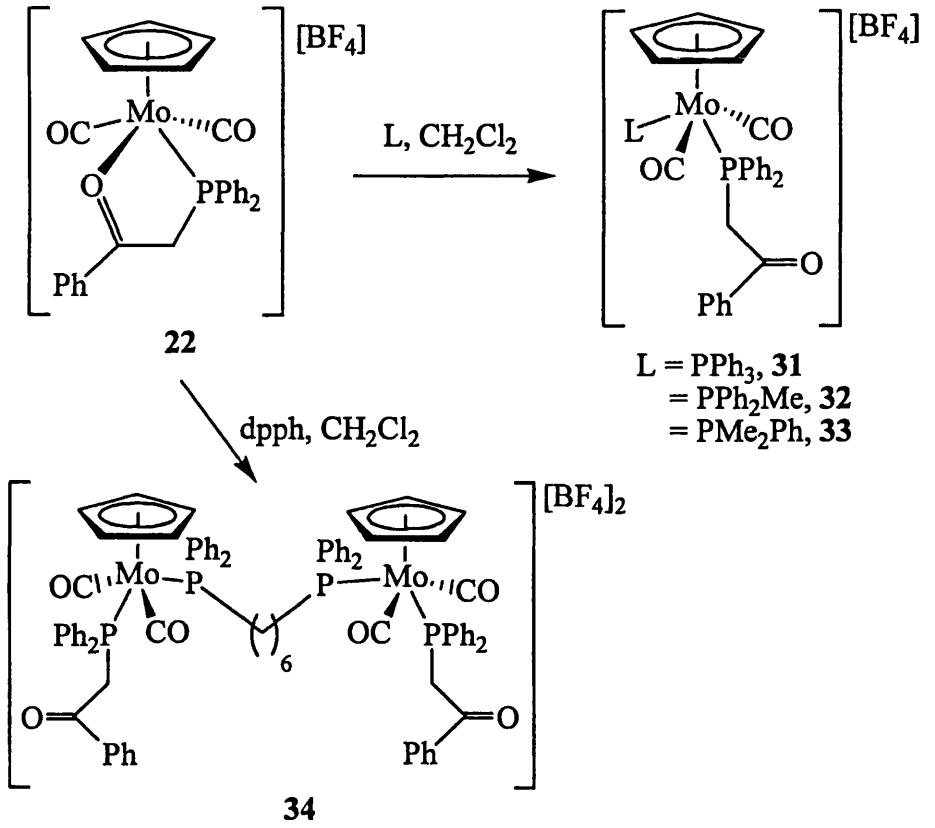

Scheme 4.27

4.2.7.4 Reactions of [Mo(CO)$_2$(L^3-P,O)(η^5-C$_5$H$_5$)][BF$_4$], 24, with Neutral Ligands

Solutions of complex **24** in CH_2Cl_2 were reacted with one equivalent of PPh_3, PPh_2Me, PMe_2Ph, PMe_3, PCy_3, $P(OMe)_3$, dpph, $Ph_3P{=}O$, MeC≡CMe, and P≡CBu^t, and the reactions monitored by $^{31}P\{^1H\}$ NMR spectroscopy.

In the reactions with but-2-yne, *tert*-butylphosphaalkyne, and triphenylphosphine oxide, the only species observed in the $^{31}P\{^1H\}$ NMR spectra were the starting

materials, even after a period of 14 days. The reactions with PCy_3, dpph and $P(OMe)_3$ resulted in the formation of multiple intractable products.

The reaction of **24** with PPh_3 was observed by $^{31}P\{^1H\}$ NMR spectroscopy to have gone to completion in 14 days. The solvents were removed from the red solution *in vacuo*, and a diffusion of toluene into a CH_2Cl_2 solution of the residue used to isolate the red oily product $[Mo(CO)_2(\mathbf{L^3}\text{-}P)(PPh_3)(\eta^5\text{-}C_5H_5)][BF_4]$, **35**, in good yield (90%). Likewise, the reactions with PPh_2Me, PMe_2Ph and PMe_3 produced the analogous complexes $[Mo(CO)_2(\mathbf{L^3}\text{-}P)(L)(\eta^5\text{-}C_5H_5)][BF_4]$ (L = PPh_2Me **36**, PMe_2Ph **37**, PMe_3 **38**), in similar yield, though in shorter time (3 days). The complexes were characterised by multinuclear NMR and infrared spectroscopy. Selected data are given in Tables 4.15 and 4.16, and compared against that for complexes **18** and **24**. The formation of complexes **35 - 38** is shown in Scheme 4.28.

Complex	Ligand	δ(P) $\mathbf{L^3}$ / ppm	δ(P) L / ppm	$^2J_{PP}$ / Hz	ν_{CO} >C=O / cm^{-1}	ν_{CO} M-CO / cm^{-1}
18		52.1	-	-	1666	1964, 1872
24		65.7	-	-	1542	1980, 1902
35	PPh_3	54.6	60.1	17.6	1663	1974, 1896
36	PPh_2Me	55.6	41.3	17.6	1663	1972, 1892
37	PMe_2Ph	55.8	26.5	21.0	1663	1968, 1888
38	PMe_3	55.6	22.5	21.1	1663	1968, 1888

Table 4.15: Selected $^{31}P\{^1H\}$ NMR and infrared spectroscopy data for complexes **18**, **24** and **35-38**.

It can be observed from the infrared spectra that the carbonyl stretching frequencies for the amide groups in complexes **35** – **38** are all 1663 cm^{-1}, and in the region associated with the non-coordination of the ketone group. This indicates that the oxygen atoms from the amide groups are no longer coordinated to the molybdenum centres. The frequencies for the carbonyl groups on the metal centres show the

expected trend to lower wavenumbers with increasing σ-donor/decreasing π-acceptor character of the introduced ligand (1974 and 1896 to 1968 and 1888 cm^{-1}).

Complex	Ligand	δ(C$\underline{H_2}$) / ppm	$^2J_{HH}$ / Hz	$^2J_{HP}$ / Hz	δ(C) M-CO / ppm	$^2J_{CP}$ / Hz	δ(C) >C=O / ppm	$^3J_{CP}$ / Hz
18		3.51	16.0	11.7	257.5	19.5	167.3	-
		3.33	-	6.9	243.7	6.7	-	-
24		4.42	16.0	8.6	250.2	19.8	179.6	8.8
		3.04	-	12.5	242.4	<2	-	-
35	PPh_3	3.65	-	7.8	234.8*	17.4	165.0	-
36	PPh_2Me	3.72	-	7.8	235.2*	17.5	165.1	-
37	PMe_2Ph	3.81	-	8.2	235.3*	17.6	164.9	-
38	PMe_3	3.85	-	8.2	235.7*	17.6	165.1	-

Table 4.16 Selected ^1H and ^{13}C NMR data for complexes **18**, **24** and **35-38**. (Signals marked * are triplets)

The $^{31}P\{^1H\}$ NMR spectra of complexes **36**, **37** and **38** in $CDCl_3$, display a pair of mutually coupled ($2J_{PP}$ = 17.6 – 21.1 Hz) doublets, assigned to the two phosphine ligands. The ^1H NMR spectra display doublets at 2.16 ($^2J_{HP}$ = 9.4 Hz), 2.04 ($^2J_{HP}$ = 9.9 Hz) and 1.70 ppm ($^2J_{HP}$ = 10.2 Hz) respectively, which were assigned as the methyl groups on the phosphine ligands. As for complexes **28** and **33**, the appearance of this signal as a doublet for complex **37** indicates a *diag* arrangement of ligands around the metal centre.

As for complexes **31 - 34**, the amidophosphine methylene protons for complexes **35 - 38** may be observed in the ^1H NMR as doublets at 3.65 ($^2J_{HP}$ = 7.8 Hz), 3.72 ($^2J_{HP}$ = 7.8 Hz), 3.81 ($^2J_{HP}$ = 8.2 Hz) and 3.85 pm ($^2J_{HP}$ = 8.4 Hz) respectively. This provides additional evidence for a *diag* arrangement of ligands around the molybdenum centre.

The $^{13}C\{^1H\}$ NMR spectra for complexes **35 - 38** show triplets at 234.8, 235.2, 235.3 and 235.7 ppm respectively, relating to the two symmetrical M-CO groups. This indicates that the two carbon-phosphorus coupling constants must be very similar. An upfield shift was observed for the peaks corresponding to the ketone carbonyl carbons, consistent with the non-coordination of the amide groups.

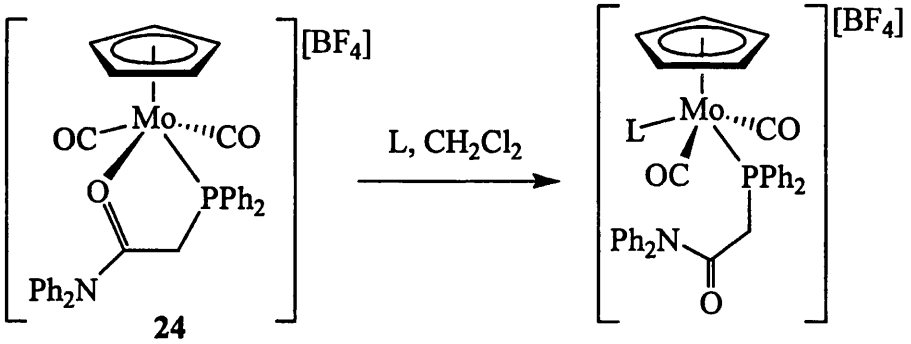

L = PPh_3, **35**
= PPh_2Me, **36**
= PMe_2Ph, **37**
= PMe_3, **38**

Scheme 4.28

4.2.7.5 Reactions of [Mo(CO)$_2$(L-P,O)(η^5-C$_5$Me$_5$)][BF$_4$] (L = L^1 21, L^2 23, L^3 25) with Neutral Ligands

One equivalent of PPh_3, PPh_2Me, PMe_2Ph, PMe_3, dpph, PCy_3, $P(OMe)_3$, $Ph_3P{=}O$, MeC≡CMe, and P≡CBu^t were added to deuterated chloroform solutions of complexes **21**, **23** and **25** and the reactions monitored by $^{31}P\{^1H\}$ NMR spectroscopy. Even after 14 days the only species observed were the starting materials.

4.2.7.6 Summary of Hemilability Investigations

The results of the reactions described in sections 4.2.7.1 → 4.2.7.3 are summarised below in Table 4.17.

From these results it may be deduced that these reactions of complexes **20**, **22** and **24** are sterically controlled. The *N*-pyrrolyl ketophosphine **L^1** is the bulkiest

functionalised phosphine of the three, and its complex **20** does not react at all with PPh_3. The β-ketophosphine $\mathbf{L^2}$ and the β-amidophosphine $\mathbf{L^3}$ have less steric bulk around the phosphorus, and their complexes **22** and **24** are observed to react with PPh_3. The reaction with complex **24** may proceed more slowly (as observed also in the reactions with PPh_2Me and PMe_2Ph) due to the introduction of the NPh_2 moiety with greater steric bulk in place of a single phenyl group. In view of this it is perhaps surprising that reactions did occur between complex **24** and PCy_3, the most sterically demanding of the ligands employed, albeit to give multiple intractable products.

This theory of steric control is further borne out by both the *diag* conformation of the products **37 – 38**, and the lack of reaction by the neutral ligands employed with the η^5-C_5Me_5 complexes **21, 23** and **25**.

		Complex		
Reactant	Cone angle / °	**20**	**22**	**24**
PCy_3		No reaction	No reaction	M/P
PPh_3	145	No reaction	**31**	**35**
PPh_2Me	136	**27**	**32**	**36**
$PPhMe_2$	122	**28**	**33**	**37**
PMe_3	118	**29**	**26**	**38**
$P(OMe)_3$	107	**30**	M/P	M/P
dpph		No reaction	**34**	M/P

Table 4.17: Results of hemilability investigations (M/P = multiple intractable products)

The *diag* arrangement of phosphines around the molybdenum centre will reduce the steric interactions between the bulky ligands. A search of the CDS database revealed that of the six structures known for the cations $[M(CO)_2P^1P^2(\eta^5\text{-}C_5R_5)]^+$, where M is a group 6 metal, P^1 and P^2 are phosphines or phosphites, and R = H or Me, five are in the *diag* form. The only example found in the database for the *lat* conformation is a chromium complex observed by Salsini and co-workers where both structural

isomers were formed. When P^1 and P^2 are either end of a bridging bisphosphine ligand however, the *lat* conformation was formed in all cases, presumably because the *diag* arrangement would cause too much strain in the chelate ring.

It is supposed that the greater bulk around the metal centres in complexes **21**, **23** and **25**, as provided by the more sterically demanding η^5-C_5Me_5 ring, prevents the reactions with the neutral ligands from taking place. The chloride ion, which is far smaller than any of the other ligands, is presumably the only one that can coordinate without creating unfavourable steric interactions. This might also explain why the products from the reactions of **20** – **25** with $[PhCH_2NEt_3][Cl]$ are all in the *lat* form, as the lesser steric influence of the chlorine could allow this sterically more demanding, conformation to form.

Given the time constraints it was not possible to conduct a mechanistic study on the formation of complexes **27** – **38**. However, it is likely that the general mechanism follows that shown in Scheme 4.29, where the initial step is the reversible dissociation of the keto group from the metal centre to give a 16-electron intermediate. This would then react with the neutral ligand L, forming the product. To minimise unfavourable interactions, L might be expected to approach the metal centre on the side opposite from the bulky phosphine, coordinating between the carbonyl groups and thus giving the *diag* conformation seen in the products.

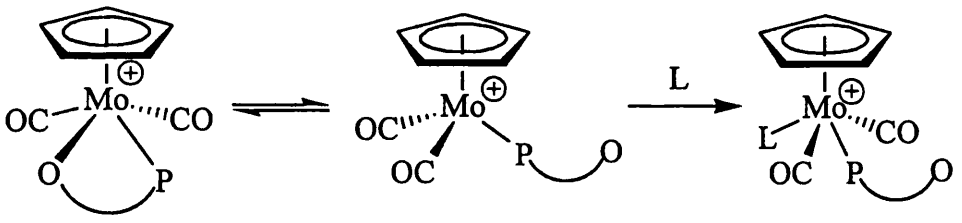

Scheme 4.29 $= L^1, L^2, L^3$

4.2.6 Future Work

The chemistry of keto- and amidophosphines on molybdenum centres has proved to a rich area of study. In view of this, it is suggested that the work be expanded to cover other early transition metal centres.

A number of questions have been left unanswered by this work, and deserve further investigation. The synthesis of a phosphino-enolate might have been expected to have been a facile reaction for those complexes containing ligands $\mathbf{L^2}$ and $\mathbf{L^3}$, and indeed might have happened. However, the number of by-products in the reactions prevented a full investigation being made. Therefore, it is suggested that the reactions between the complexes $[Mo(CO)_2(L\text{-}P,O)(\eta^5\text{-}C_5R_5)][BF_4]$ (L = $\mathbf{L^2}$ or $\mathbf{L^3}$, R = H or Me) and a base are repeated using NaH as the base. This has been used to good effect in previously published work.[11]

The complexes **27 – 38**, obtained by reacting complexes **20**, **22** and **24** with neutral ligands, were designated as having a *diag* structure on the basis of their multinuclear NMR spectra. It is desirable that a crystal structure be obtained of one or more of these complexes to confirm this, and to allow comparisons of bond lengths and angles. The reactions with complexes **21**, **23** and **25**, which were believed to not progress due to inherently unfavourable steric interactions in the possible products, also deserve further study. If steric interactions are preventing the reactions from progressing, using a smaller neutral ligand, such as an isocyanide, may lead to the isolation of a product. A thorough mechanistic study needs to be made on all these reactions.

In view of the commercial applications of transition metal complexes with hemilabile ligands, a comparison needs to be made between the behaviour of the keto- and amidophosphines $\mathbf{L^1}$, $\mathbf{L^2}$ and $\mathbf{L^3}$, and that of analogous phosphino-ethers on molybdenum centres. particular attention should be paid to their respective hemilabile characters.

4.3 Conclusions

The reaction between the complexes $[MoCl(CO)_3(\eta^5\text{-}C_5R_5)]$ and the *N*-pyrrolyl ketophosphine $\mathbf{L^1}$ produces the complexes $[MoCl(CO)_2(\mathbf{L^1}\text{-}P)(\eta^5\text{-}C_5R_5)]$ (R = H **14**, or Me **15**) in very good yield. Repeating the reactions with $\mathbf{L^2}$ and $\mathbf{L^3}$ produced the analogous complexes $[MoCl(CO)_2(\mathbf{L^2}\text{-}P)(\eta^5\text{-}C_5R_5)]$ (R = H **16**, or Me **17**) and $[MoCl(CO)_2(\mathbf{L^3}\text{-}P)(\eta^5\text{-}C_5R_5)]$ (R = H **18**, or Me **19**) respectively. Complexes **16** - **19** show inequivalent methylene protons in their ^1H NMR spectra, implying a *lat* arrangement of ligands around the metal centre, as did the presence of two metal carbonyl signals in the ^{13}C NMR spectra. An X-ray crystallographic study on **14** confirmed this structure.

The reactions of complexes **14** and **15** with $AgBF_4$ produce the complexes $[Mo(CO)_2(\mathbf{L^1}\text{-}P,O)(\eta^5\text{-}C_5R_5)][BF_4]$ (R = H **20**, or Me **21**) in good yield. Repeating the reactions with complexes **16** and **17** gave $[Mo(CO)_2(\mathbf{L^2}\text{-}P,O)(\eta^5\text{-}C_5R_5)][BF_4]$ (R = H **22**, or Me **23**), whilst the analogous reactions of **18** and **19** produced the complexes $[Mo(CO)_2(\mathbf{L^3}\text{-}P,O)(\eta^5\text{-}C_5R_5)][BF_4]$ (R = H **24**, or Me **25**). The ^1H NMR spectra of complexes **22** – **25** still display inequivalent methylene protons, which now arise due to the constraints of the chelate ring. An X-ray crystallographic study on **20** confirmed the structure, and the retention of the *lat* arrangement of ligands. Complexes **20** and **22** were also made by the alternative method of reacting $[Mo(CH_3)(CO)_3(\eta^5\text{-}C_5H_5)]$ with $HBF_4{\cdot}Et_2O$, and then adding the required ketophosphines.

When complex **16** was reacted with BuLi, the phosphino-enolate complex $[Mo(CO)_2\{Ph_2PCH{=}C(Ph)O\text{-}P,O\}(\eta^5\text{-}C_5H_5)]$, **26**, was formed. This complex was also produced by reacting complex **22** with Et_3N. An X-ray crystallographic study on **26** confirmed the structure. Reacting **26** with HBF_4 resulted in the reformation of complex **22**. Complexes **14**, **15** and **17** - **19** did react with BuLi, but to form multiple intractable products.

The reaction of complexes **20** – **25** with $[PhCH_2NEt_3][Cl]$ results in the displacement of the carbonyl group form the metal centre, opening the chelate ring and regenerating complexes **14** – **19** respectively.

The reaction of complex **20** with PPh_2Me, PMe_2Ph, PMe_3 and $P(OMe)_3$ resulted in the formation of $[Mo(CO)_2(P\text{-}\mathbf{L^1})(L)(\eta^5\text{-}C_5H_5)][BF_4]$ (L = PPh_2Me **27**, PMe_2Ph **28**, PMe_3 **29**, $P(OMe)_3$ **30**). Analysis of the NMR spectra for the complexes indicated a *diag* arrangement of ligands around the metal centre.

Complex **22** reacts with PPh_3, PPh_2Me and PMe_2Ph to give products analogous to **27** with the general formulae $[Mo(CO)_2(P\text{-}\mathbf{L^2})(L)(\eta^5\text{-}C_5H_5)][BF_4]$ (L = PPh_3 **31**, PPh_2Me **32**, $PPhMe_2$ **33**). The same reaction with dpph gives the dimeric complex $[\{Mo(CO)_2(P\text{-}\mathbf{L^2})(\eta^5\text{-}C_5H_5)\}_2(dpph)][BF_4]_2$, **34**. In contrast, the reaction with PMe_3 led to the deprotonation of the β-ketophosphine leading to the formation of the phosphino-enolate complex **26**. The reaction with $P(OMe)_3$ gave multiple intractable products.

Complex **24** reacts with PPh_3, PPh_2Me, PMe_2Ph and PMe_3 to give to give products analogous to **27** with the general formulae $[Mo(CO)_2(P\text{-}\mathbf{L^3})(L)(\eta^5\text{-}C_5H_5)][BF_4]$ (L = PPh_3 **35**, PPh_2Me **36**, PMe_2Ph **37**, PMe_3 **38**). The analogous reactions with $P(OMe)_3$, dpph and PCy_3 gave multiple intractable products.

No reactions were observed with complexes **20**, **22** and **24** with $MeC{\equiv}CMe$, $P{\equiv}CBu^t$ or $Ph_3P{=}O$. No reaction was observed with their $\eta^5\text{-}C_5Me_5$ analogues **21**, **23** and **25** with any of the neutral ligands tested.

4.4 References

1 a) S.-E. Bouaoud, P Braunstein, D. Grandjean, D. Matt and D. Nobel, *Inorg. Chem.*, 1986, **25**, 3765.

b) P. Braunstein, D. Matt, D. Nobel, F. Balegroune, S.-E. Bouaoud, D. Grandjean and J. Fischer, *J. Chem. Soc., Dalton Trans.*, 1988, 353.

c) P. Braunstein, Y. Chauvin, J. Nähring, A. DeCian, J. Fischer, A. Tiripicchio and F. Ugozzoli, *Organometallics*, 1996, **15**, 5551.

d) J. Andrieu, P. Braunstein, F. Naud and, R.D. Adams, *J. Organomet. Chem.*, 2000, **601**, 43.

2 S. Al-Jibori, M. Hall, A.T. Hutton and B.L. Shaw, *J. Chem. Soc., Dalton Trans.*, 1984, 863.

3 N.G. Jones, M.L.H. Green, X. Morise, L. Rees and D. Watkin, *34th International Conference on Coordination Chemistry*, Edinburgh, 2000, poster abstract P0453.

4 J.M. Camus, D. Morales, J. Andrieu, P. Richard, R. Poli, P. Braunstein and F. Naud, *J. Chem. Soc., Dalton Trans.*, 2000, 2577.

5 a) A. Huang, J.E. Marcone, K.L. Mason, W.J. Marshall, K.G. Moloy, S. Serron and S.P. Nolan, *Organometallics*, 1997, **16**, 3377.

b) K.G. Moloy and J.L. Petersen, *J. Am. Chem. Soc.*, 1995, **117**, 7696.

6 a) A.J. Arce, A.J. Deeming, Y. De Sanctis, S.K. Johal, C.M. Martin, S. Shinhmar, D.M. Speel and A. Vassas, *Chem. Commun.*, 1998, 233.

b) S. Serron, S.P. Nolan, Y.A. Abramov, L. Brammer and J.L. Petersen, *Organometallics*, 1998, **17**, 104.

7 a) S.M. Aucott, A.M.Z. Slawin and J.D. Woolins, *J. Chem. Soc., Dalton Trans.*, 2000, 2559.

b) T.G. Wetzel, S. Dehnen and P.W. Roesky, *Angew. Chem., Int. Ed.*, 1999, **38**, 1086.

c) N. Poetschke, M. Nieger, M.A. Khan, E. Niecke and M.T. Ashby, *Inorg. Chem.*, 1997, **36**, 4087.

d) P. Braunstein, L. Frison, X. Morise and R.D. Adams, *J. Chem. Soc., Dalton Trans.*, 2000, 2205.

e) A.D. Burrows, M.T. Palmer and M.F. Mahon, *J. Chem. Soc., Dalton Trans.*, 2000, 1669.

8 a) D.A. Fletcher, R.F. McMeeking and D. Parkin, *J. Chem. Inf. Comput. Sci.*, 1996, **36**, 746.

b) F.H. Allen and O. Kennard, *Chem. Des. Automat. News*, 1993, **8**, 31.

9 G.M. Reisner, I Bernal, H. Brummer, M. Muschiol and B. Siebrecht, *J. Chem. Soc., Chem. Commun.*, 1978, 691.

10 M.A. Bakar, A. Hills, D.L. Hughes and G.J. Leigh, *J. Chem. Soc., Dalton Trans.*, 1989, 1417.

5 Reactions of Phosphaalkynes with Palladium Clusters

5.1 Introduction

5.1.1 Reactions of Phosphaalkynes with Transition Metal Clusters

Compared to the depth of investigation into the chemistry of phosphaalkynes on mono- or dinuclear metal centres (see Chapter 1), the chemistry of these ligands with metal clusters is relatively unexplored.

In contrast to the wealth of carbonyl clusters reported to react with alkynes,[1] the anionic complexes $[M_3H(CO)_{11}]^-$ (M = Fe, Ru) are the only examples known to undergo ligand substitution reactions with phosphaalkynes.[2] The products, shown in Scheme 5.1 are μ_3,η^2-phosphaalkyne complexes.

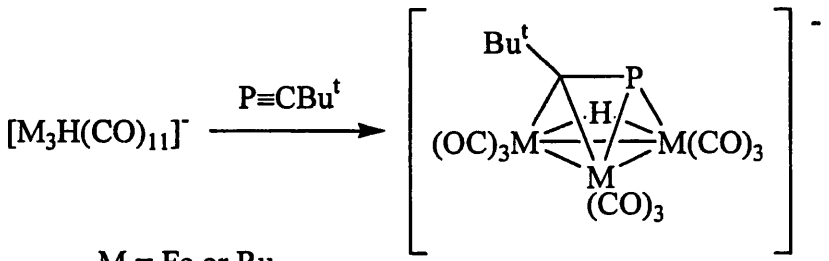

5.1

Scheme 5.1

Those reactions of phosphaalkynes with metal clusters that have been carried out are generally characterised by the insertion of the phosphaalkyne into a metal ligand bond. Most common of these reactions is the insertion of a phosphaalkyne into a M-CO bond from a metal carbonyl cluster to form a phosphinidene complex.

The complexes $[M_3(CO)_{12}]$ (M = Ru or Os) react with *tert*-butylphosphaalkyne to give the *nido*-clusters $[M_3\{\mu_3\text{-}PC(CO)Bu^t\}_2(CO)_9]$, **5.2**.[3] The ruthenium complex **5.2a** can react with an excess of $[Ru_3(CO)_{12}]$ to give the *closo*-cluster $[Ru_4\{\mu_3\text{-}PC(CO)Bu^t\}_2(\mu\text{-}CO)(CO)_{10}]$, **5.3**.[4] These reactions are shown in Scheme 5.2

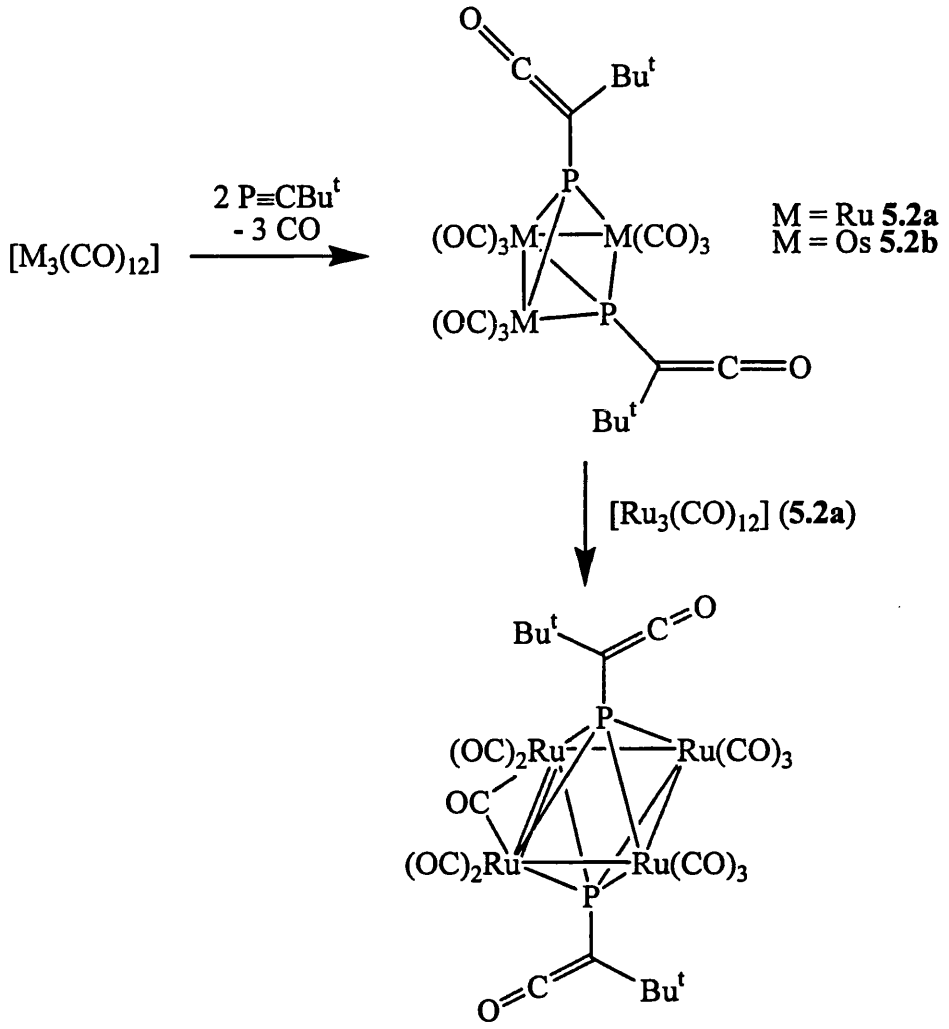

Scheme 5.2 **5.3**

The reaction with $[Ru_3(\mu\text{-dppm})(CO)_{10}]$, which is characterised by its enhanced reactivity over the unsubstituted complex gives a product analogous to **5.2a**.[5] Similar reactions are also known with other ruthenium carbonyl clusters.[6]

Under photochemical conditions, 3 equivalents of *tert*-butylphosphaalkyne react with the iron cluster $[Fe_3(CO)_9(\mu_3\text{-}PBu^t)(\mu_3\text{-Se})]$ to produce the complex shown in Scheme 5.3 in 36% yield.[7] The reaction is believed to proceed *via* an initial insertion of one molecule of phosphaalkyne to give **5.4**, followed by addition of another two phosphaalkyne molecules to give **5.5**.

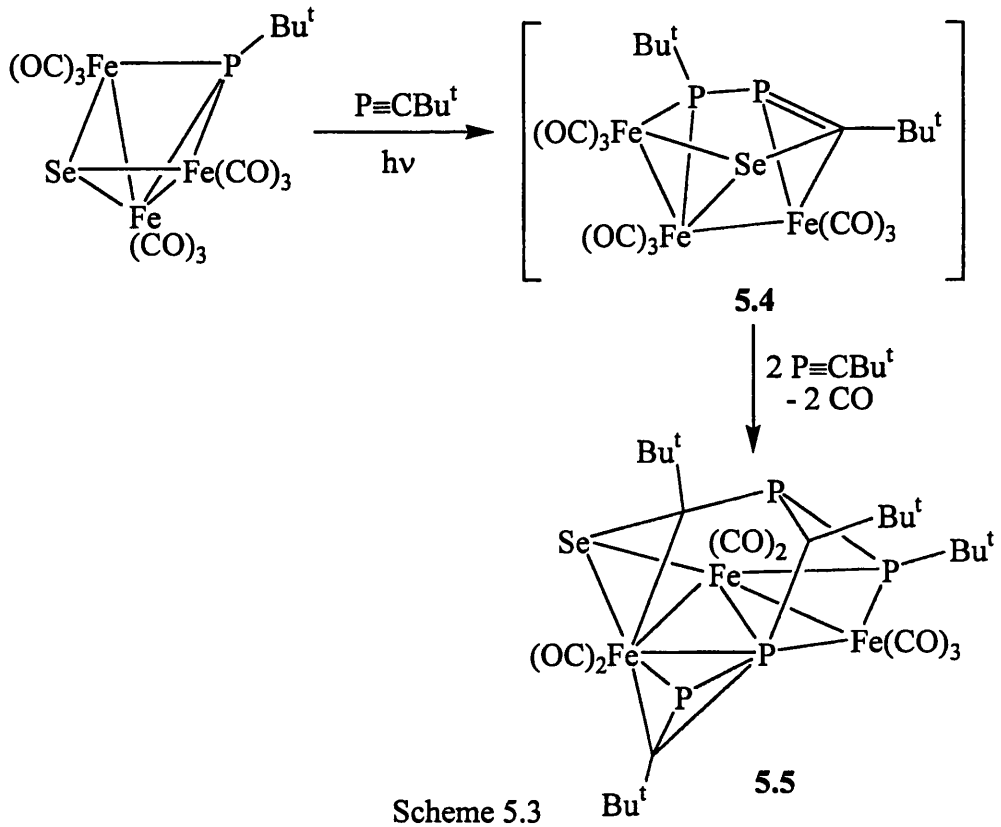

Scheme 5.3

The triiron cluster $[Fe_3(CO)_9(\mu_3\text{-}CF)_2]$ reacts with *tert*-butylphosphaalkyne to give the cluster **5.6**.[8] The central 5 membered ring is planar, and so may be considered a 1-ferra-3-phosphacyclopentadiene ring. This reaction is shown in Scheme 5.4

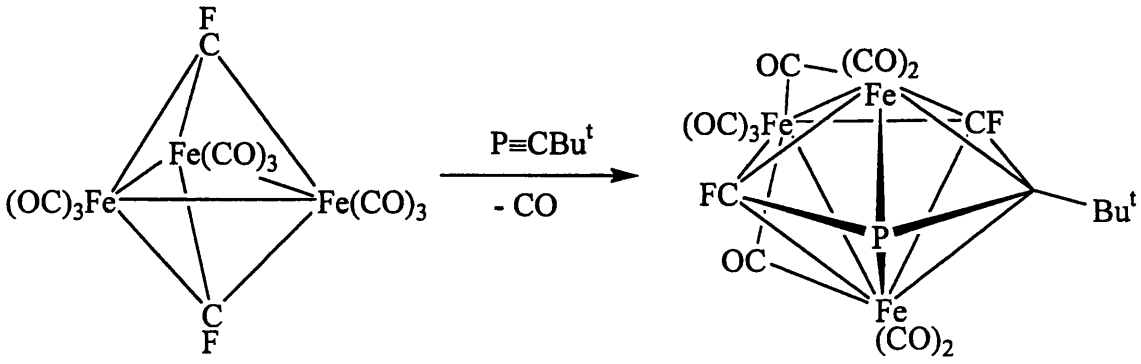

Scheme 5.4 **5.6**

5.1.2 Proposed Research

We were interested to investigate the reactivity of *tert*-butylphosphaalkyne with the coordinatively unsaturated palladium *triangulo* cluster **5.7**, which is shown in Figure 5.1.

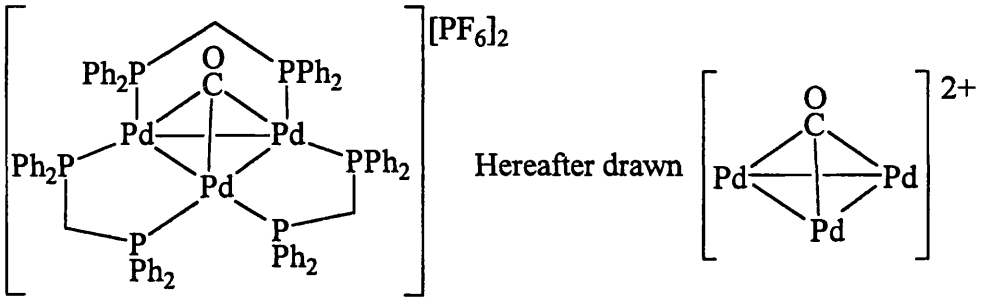

Figure 5.1: Structure of $[Pd_3(\mu_3\text{-}CO)(\mu\text{-dppm})][PF_6]_2$, **5.7**

This cluster, which contains three Pd-Pd bonds, has been shown to react with a number of ligands to give a range of different products (Scheme 5.5).[9] In most cases the ligands add to the face of the cluster opposite to that coordinated to the carbonyl ligand. The exceptions to this are isocyanide ligands which displace the carbonyl.

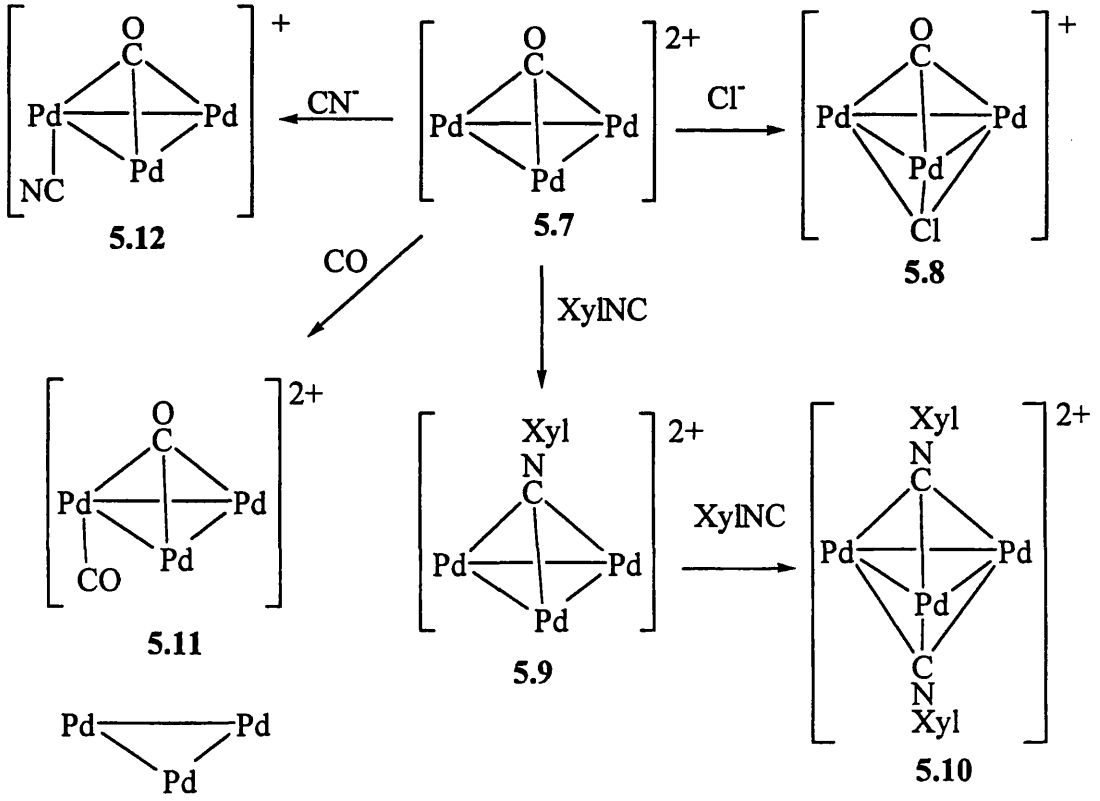

Scheme 5.5

As the triangular cluster is surrounded by bridging bis(diphenylphosphino)methane ligands, the Pd_3 core is sterically very hindered. Approach by a ligand is only possible perpendicular to the plane of the triangle, if the palladium triangle is to be retained. Similar chemistry is displayed by the platinum analogue $[Pt_3(\mu_3\text{-}CO)(\mu\text{-}dppm)_3]^{2+}$, **5.14**, as shown in Scheme 5.6.

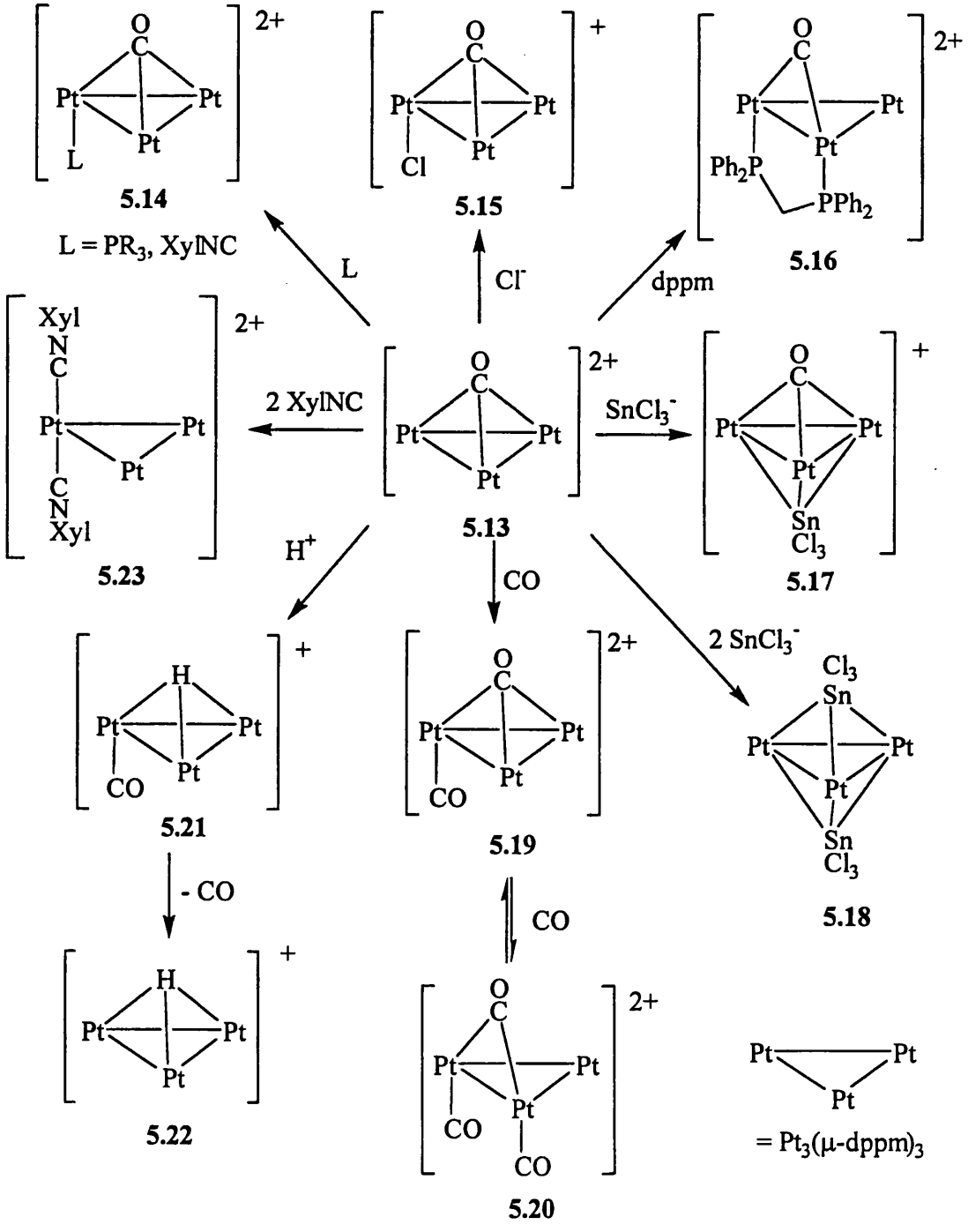

Scheme 5.6

Ethyne and electron-poor alkynes react with these trimetallic clusters by inserting between the metal-metal bonds.[10] The products are those shown in Scheme 5.7

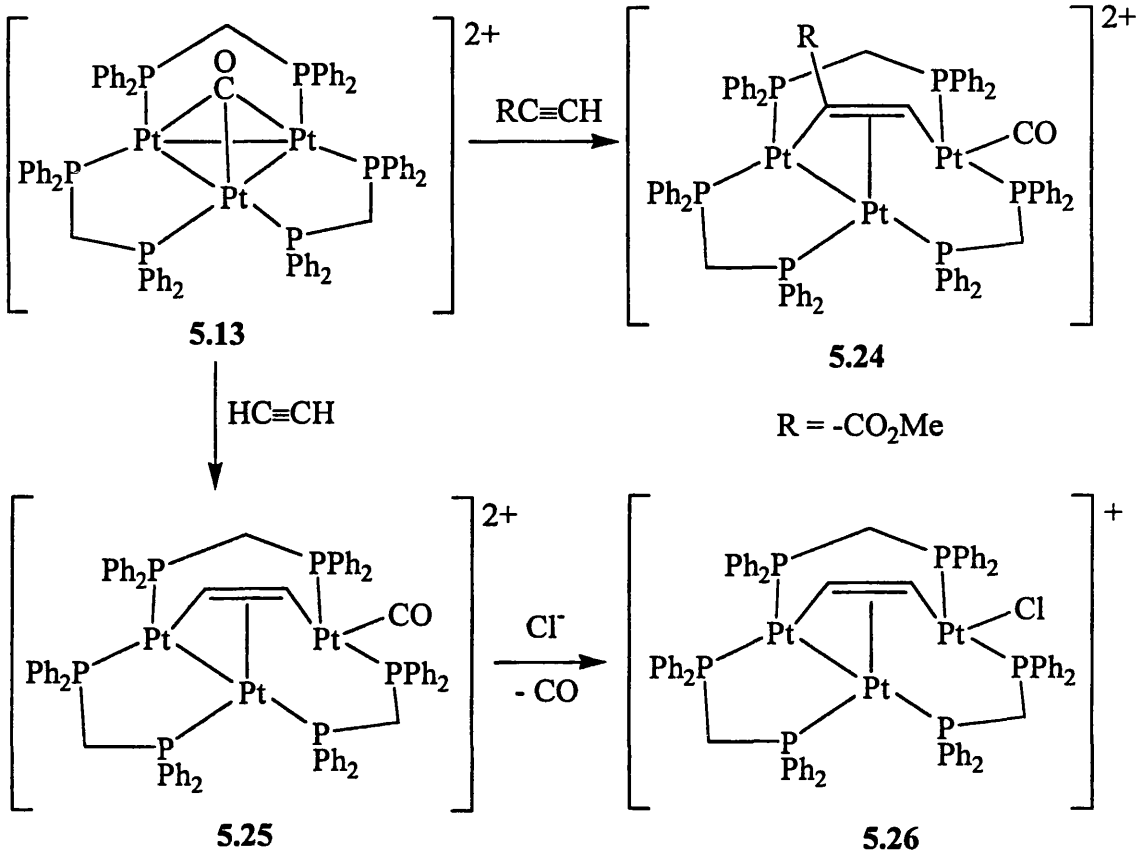

5.13 **5.24** **5.25** **5.26**

R = -CO_2Me

Scheme 5.7

It was anticipated that reacting **5.7** with one equivalent of *tert*-butylphosphaalkyne would result in the formation of one or more possible products. If the phosphaalkyne inserts into the palladium-palladium bond in the same way as the electron-poor alkynes in Scheme 5.7, it might be expected that the product from the reaction of *tert*-butylphosphaalkyne and **5.7** would be the complex **5.27**, as shown in Figure 5.2. It can be see that there are two possible structural isomers for this proposed product, that differ in the orientation of the phosphaalkyne. These complexes have a cluster valence electron count of 46 under the Wade-Mingos-Lauher rules.[11]

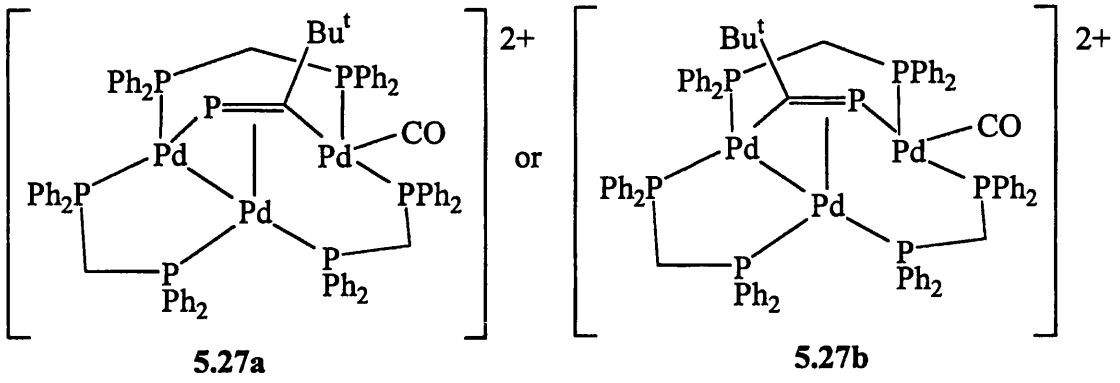

Figure 5.2: Possible products from insertion reaction of P≡CBu^t with **5.7**

If the phosphaalkyne were to react in a similar way as in the synthesis of complex **5.1**, the putative product would be the μ_3-σ:σ:η^2-phosphaalkyne complex **5.28**, as shown in Figure 5.3. Another possible outcome of the reaction is the formation of an μ_3-σ:η^2:η^2-phosphaalkyne complex **5.29**.

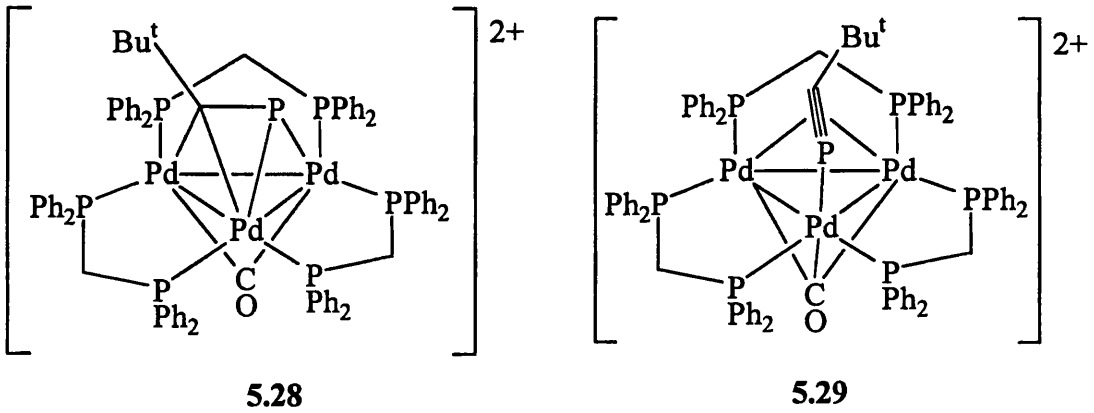

Figure 5.3: Putative μ_3-σ:σ:η^2- and μ_3-σ:η^2:η^2-phosphaalkyne complexes

As the bulky phenyl groups are arranged in tori above and below the palladium trimer (as shown in Figure 5.4), it may be that the phosphaalkyne would not be able to coordinate in an η^2-manner, due to the adverse steric interactions. A further possible product therefore was an η^1-phosphaalkyne complex. This could either be in a μ_3-manner as seen in the palladium xylyl isocyanide complex **5.9** (Scheme 5.5), or to just one metal, in a similar manner to the xylyl isocyanide ligands in the platinum complex **5.21** (see Scheme 5.6). These putative products are shown in Figure 5.5.

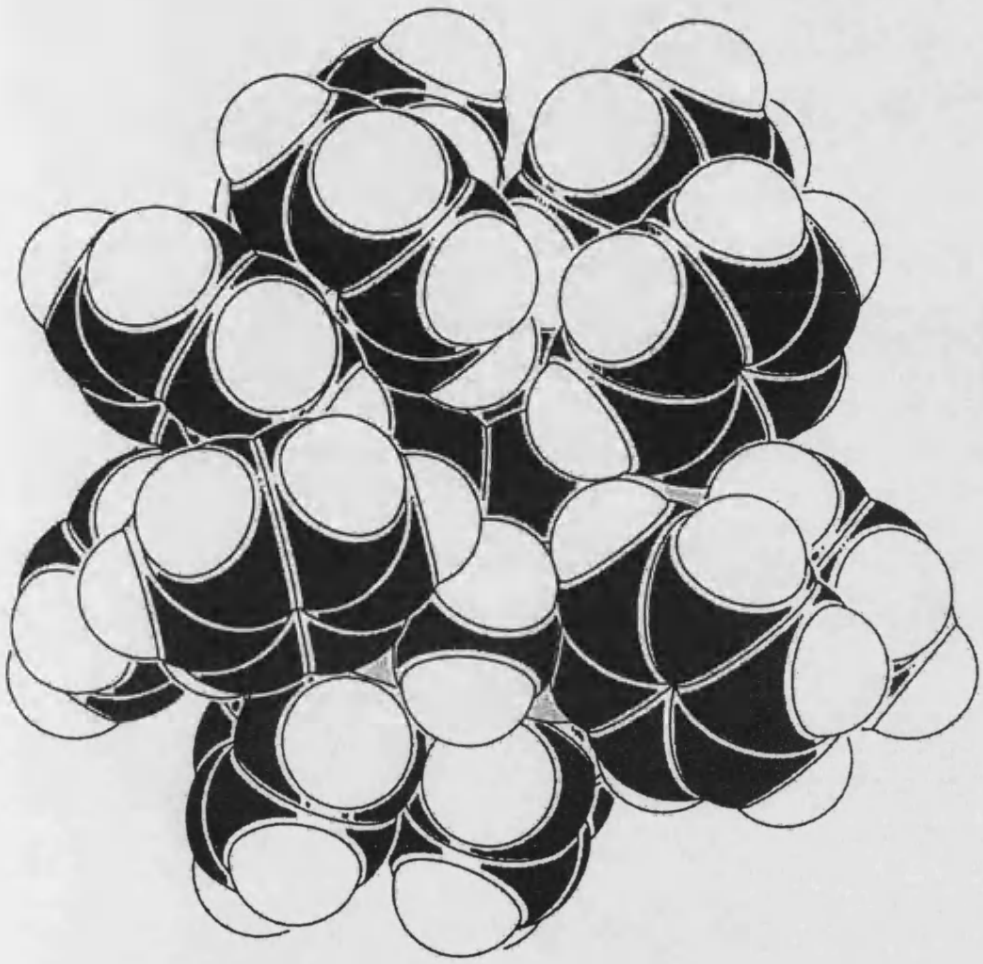

Figure 5.4: Space filling diagram of vacant coordination site in **5.7**

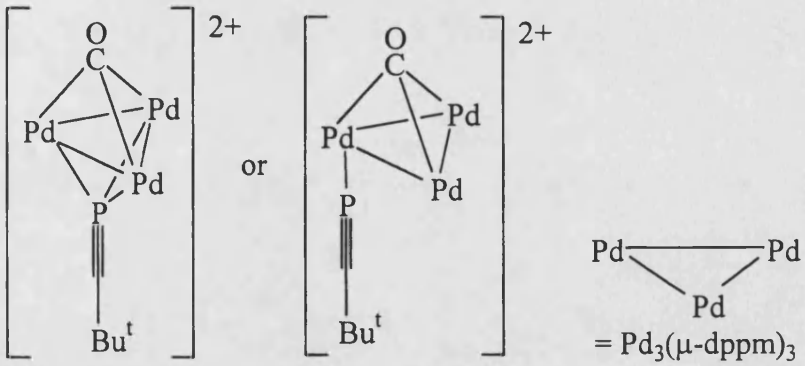

5.30 **5.31**

Figure 5.5: Putative η^1-phosphaalkyne complexes

5.2 Results and Discussion

5.2.1 Reaction between $[Pd_3(\mu_3\text{-}CO)(\mu\text{-}dppm)_3][PF_6]_2$ and *tert*-Butylphosphaalkyne

One equivalent of *tert*-butylphosphaalkyne was added to an acetone solution of $[Pd_3(\mu_3\text{-}CO)(\mu\text{-}dppm)_3][PF_6]_2$, and the reaction followed by $^{31}P\{^1H\}$ NMR and infrared spectroscopy. After two days the only peak observed in the infrared spectrum in the carbonyl stretching region was that of the starting material, albeit in reduced intensity with respect to the C-H stretching peaks. The $^{31}P\{^1H\}$ NMR spectra displayed four resonances. One of these was a singlet at –0.23 ppm assigned to the dppm ligands from the starting material **5.7**, while another was the septet ($^1J_{PF}$ = 710 Hz) at –142.8 ppm from the PF_6^- anion. Neither of the two remaining resonances were due to free *tert*-butylphosphaalkyne (-69.2 ppm), one being at very high field, the other being close to the dppm peak from the starting material. This latter peak integrated to the same value as that for the remaining starting material, **5.7**.

On the basis of this spectroscopic data which suggested half the starting material **5.7** remained unreacted, a second equivalent of *tert*-butylphosphaalkyne was added to the reaction mixture. After further 2 days, there was no evidence for the presence of **5.7** in the infrared spectrum. The solvents were removed *in vacuo*, and the resulting green oil recrystallised by diffusion of toluene into an acetone solution to give the complex $[Pd_3(\mu\text{-}dppm)_3(P{\equiv}CBu^t)_2][PF_6]_2$, **39**, as green crystals in virtually quantitative yield. The compound was characterised by multinuclear NMR spectroscopy.

The $^{31}P\{^1H\}$ NMR spectra of **39** in deuterated acetone displayed a triplet ($^2J_{PP}$ = 21.7 Hz) at –6.3 ppm and a septet at –121.4 ppm ($^2J_{PP}$ = 21.7 Hz). A further septet resulting from the PF_6^- anion was observed at –142.8 ppm ($^1J_{PF}$ = 710 Hz). Integration of the resonances revealed that the triplet was three times the intensity of both septets. Therefore, it may be assumed that the triplet corresponds to the six phosphorus atoms of the three bridging dppm ligands, and that these are coupled to

phosphorus atoms from two equivalent phosphaalkyne ligands whose signal appears at very high field.

The ^{1}H NMR spectra displays the methylene, *tert*-butyl and phenyl groups, in the ratio 1:3:10, which is correct for a complex of the formulation $[Pd_3(\mu\text{-dppm})_3(PCBu^t)_2][PF_6]_2$. The $^{13}C\{^{1}H\}$ NMR displays resonances for the phenyl groups at 133.3 - 129.0 ppm, while the *tert*-butyl groups are observed as a singlet at 32.5 ppm. A single triplet ($^{1}J_{CP}$ = 117.0 Hz) is observed for the methylene carbons at 31.4 ppm, whilst the resonance for the sp hybridised carbons in the phosphaalkyne molecules was observed as a virtual triplet (J_{CP} = 59.9 Hz) at 214.8 ppm. This virtual triplet is caused by a $^{1}J_{CP}$ coupling (between the carbon and the phosphorus from the same molecule of phosphaalkyne) merging with a $^{3}J_{CP}$ coupling (between the carbon and the phosphorus from the other phosphaalkyne molecule).

The equivalence of the dppm ligands rules out the formation of an insertion product (**5.27**), as does the stoichiometry of the reaction. Similarly these arguments also rule out the putative μ_3,η^2-phosphaalkyne complex **5.28**. A bis-$\eta^1\eta^2\eta^2$-phosphaalkyne complex similar to **5.29** with two phosphaalkyne ligands, one on either face of the Pd_3 triangle would show equivalent dppm ligands if it were fluxional, with the phosphaalkyne ligands able to rotate. However, a cluster of this type would disobey the Wade-Mingos-Lauher rules for cluster complexes. Furthermore, in all three cases, the chemical shift of the of the phosphaalkyne in the $^{31}P\{^{1}H\}$ NMR might be expected to be at far lower fields than is actually seen. Therefore, it seems likely that **39** is a bis-η^1-phosphaalkyne complex.

There are several possible structural isomers for **39**. The two with the most precedence are shown in Figure 5.6. Structure **A** is similar to that found in the palladium bis(xylyl isocyanide) complex **5.11**, in that both phosphaalkynes are coordinated in a μ_3 fashion. Structure **B** is similar to the platinum complex **5.26**, where both ligands are η^1-coordinated to a single metal centre. For **B** to generate the NMR spectra seen, with equivalent dppm ligands, the complex would have to be fluxional with the two phosphaalkyne ligands spending equal amounts of time on each palladium atom.

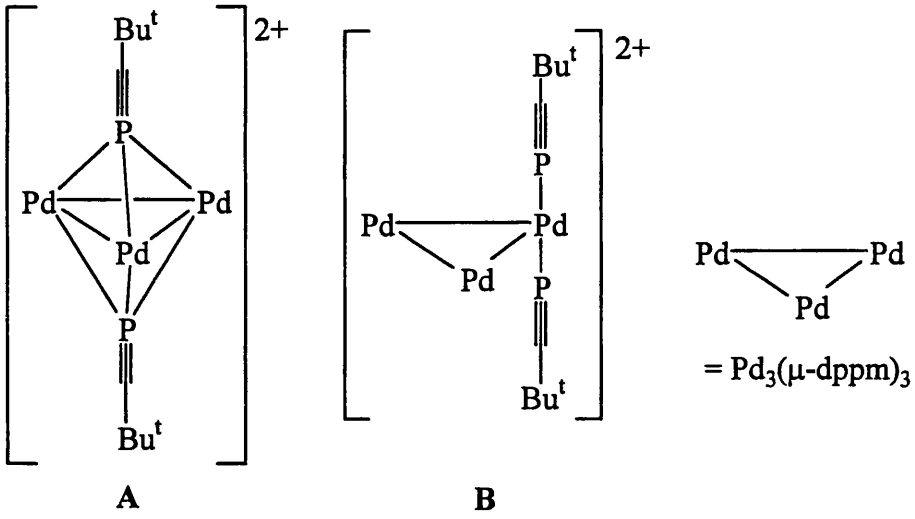

Figure 5.3: Possible structures for **39**

A variable temperature $^{31}P\{^{1}H\}$ NMR experiment was carried out, in which a solution of **39** in deuterated acetone was cooled to –80°C, to investigate the possibility of fluxionality in the complex. Both the dppm and phosphaalkyne resonances remained unchanged between 20 and –60°C. Between –60 and –80°C there was a degree of broadening, though it was unclear whether this was the result of reduced fluxionality or due to solvent effects. A similar effect was seen in the ^{1}H NMR spectrum at the same temperature. Without a X-ray crystal structure determination study it is therefore impossible to determine precisely the structure of **39**. Repeated attempts to obtain X-ray quality crystals failed, despite using a variety of solvents.

5.2.2 Formation of $[Pd_3\{(CH_3)_2CO\}(\mu_3\text{-}PCH_2Bu^t)(\mu\text{-dppm})_3][PF_6]_2$, 40

Whilst attempting to obtain crystals of **39** suitable for structural analysis by slow diffusion of toluene into an acetone solution, red crystals were seen to precipitate. An X-ray crystallographic study on these revealed that they were not **39**, but a new complex $[Pd_3\{(CH_3)_2CO\}(\mu_3\text{-}PCH_2Bu^t)(\mu\text{-dppm})_3][PF_6]_2$, **40**. The structure of the cation in **40** is shown in Figures 5.4 and 5.5, and selected bond lengths and angles are given in Table 5.1.

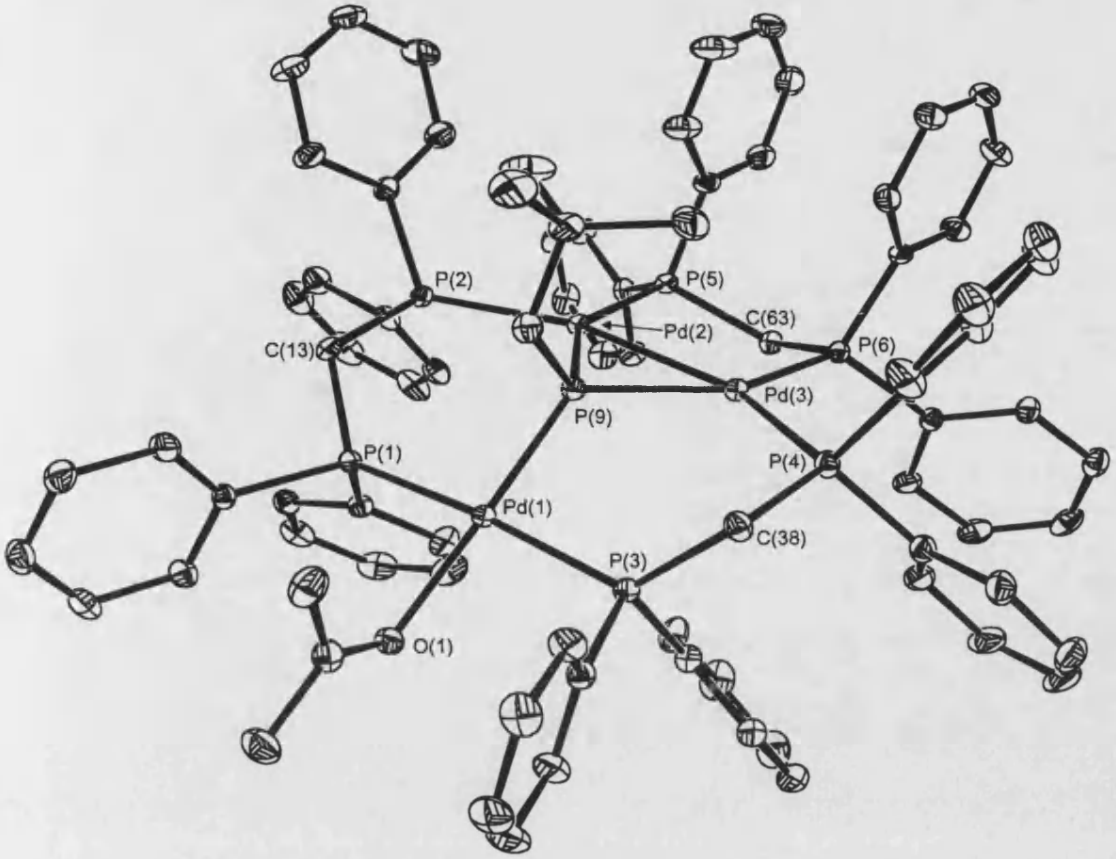

Figure 5.4: Structure of $[Pd_3(\mu\text{-dppm})_3(\mu^3\text{-}PCH_2Bu^t)\{(CH_3)_2CO\}]^{2+}$ cation observed in **40**.

The structure is broadly symmetrical, with an approximate mirror plane running along the O(1)-Pd(1)-P(9) axis and through the midpoint of the Pd(2)-Pd(3) bond. This is not however a crystallographic mirror plane, and the two sides of the cluster are not equivalent.

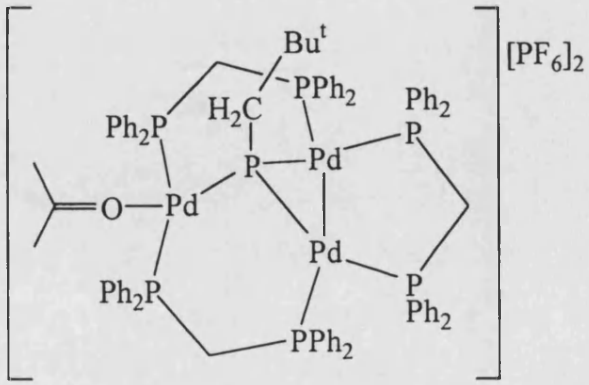

Figure 5.5: Structure of **40**

Pd(2)-P(9)	2.2435(7)	Pd(3)-P(9)	2.2541(7)
Pd(1)-P(9)	2.2748(7)	Pd(2)-Pd(3)	2.6977(3)
Pd(1)-O(1)	2.236(2)	P(9)-C(76)	1.865(3)
O(1)-C(81)	1.248(4)		
P(1)-Pd(1)-P(9)	92.17(3)	P(3)-Pd(1)-P(9)	102.01(3)
P(1)-Pd(1)-O(1)	88.45(6)	P(3)-Pd(1)-O(1)	87.44(6)
P(9)-Pd(1)-O(1)	176.17(7)	P(1)-Pd(1)-P(3)	173.38(3)
P(2)-Pd(2)-P(9)	102.34(3)	P(5)-Pd(2)-P(9)	148.26(3)
Pd(3)-Pd(2)-P(9)	53.326(19)	P(2)-Pd(2)-P(5)	109.39(3)
P(2)-Pd(2)-Pd(3)	155.59(2)	P(5)-Pd(2)-Pd(3)	94.933(18)
P(4)-Pd(3)-P(9)	102.01(3)	P(6)-Pd(3)-P(9)	146.20(3)
Pd(2)-Pd(3)-P(9)	52.963(19)	P(4)-Pd(3)-P(6)	111.79(3)
P(4)-Pd(3)-Pd(2)	154.97(2)	P(6)-Pd(3)-Pd(2)	93.238(19)
Pd(1)-P(9)-Pd(2)	122.71(3)	Pd(1)-P(9)-Pd(3)	121.59(3)
Pd(2)-P(9)-Pd(3)	73.71(2)	Pd(1)-P(9)-C(76)	97.24(10)
Pd(2)-P(9)-C(76)	121.28(11)	Pd(3)-P(9)-C(76)	122.16(10)
P(9)-C(76)-C(77)	119.9(2)	Pd(1)-O(1)-C(81)	120.8(2)

Table 5.1 Selected bond lengths (Å) and angles (°) for **40**

It can be observed that two Pd-Pd bonds have been broken by the insertion of a bridging phosphinidene ligand. The Pd(2)-Pd(3) length of 2.6977(3) Å is longer than in the starting material **5.7** [2.576(1) - 2.610(2) Å], but is consistent with it being a Pd-Pd single bond. The other two Pd-Pd distances are 3.953(3) and 3.965(3) Å, and so are too long to be significant interactions. All three palladium atoms have a distorted square planar geometry. This distortion is more pronounced for Pd(2) and Pd(3) than for Pd(1), and more resembles the arrangement in the starting material[12] and the Pd(I) dimer $[Pd_2(SC_6F_5)(PPh_3)(\mu\text{-}SC_6F_5)(\mu\text{-dppm})]$.[13] The O(1)-Pd(1)-P(9) angle is 176.17(7)°, whilst the P(1)-Pd(1)-P(3) angle is 173.38(3)°, a small deviation from the square planar value of 180°. The cis angles deviate similarly by a small amount from a square planar geometry value of 90° [P(1)-Pd(1)-P(9) = 92.17(3)°,

P(3)-Pd(1)-P(9) = 102.01(3)°, P(1)-Pd(1)-O(1) = 88.45(6)° and P(3)-Pd(1)-O(1) = 87.44(6)°].

The core of the complex may be visualised as two planes. One plane contains the Pd(1), P(1), P(3), O(1) and P(9) atoms, the other contains the Pd(2), Pd(3), P(5), P(6) and P(9) atoms. The angle between the two planes is 34.2°. This is in contrast to the starting material **5.7** where all the palladium and phosphorus atoms lie in the same plane.

The P(9)-C(76) bond, previously the triple bond of a phosphaalkyne, is observed to be 1.865(3) Å in length. This is considerably longer than the C≡P bond length in free *tert*-butylphosphaalkyne of 1.536(2)Å, and is typical of a P-C single bond length. The two hydrogen atoms on C(76) were located in the difference map, and refined without constraints.

The methylene carbons C(13) and C(38) from two of the bridging dppm ligands lie out of the plane of the three palladium atoms, on the same side as the phosphinidene ligand. By contrast, the methylene carbon C(63) lies below the plane. In both cases, this is presumably to minimise steric interactions between the phenyl groups of the phosphines and the *tert*-butyl group of the phosphinidene.

A related complex to **40** has been seen in the reaction of the primary phosphine $PhPH_2$ with the platinum cluster $[Pt_3(\mu_3\text{-}CO)(\mu\text{-}dppm)_3][PF_6]_2$, **5.13**, as carried out by Puddephatt and co-workers.[10] The initial reaction results in the formation of complex **5.32**, but loss of H_2 leads to the formation of **5.33**. This in turn can react with two electron donor ligands to produce complex **5.34**, as shown in Scheme 5.13.

Other analogous products are formed in the reactions of the complexes $[M_3(\mu_3\text{-}CO)(\mu\text{-}dppm)_3][PF_6]_2$ (M = Pd or Pt) with H_2E (E = S or Se), also carried out by Puddephatt and co-workers.[14] The products, and those from analogous work with thiols[15] are shown in Scheme 5.9.

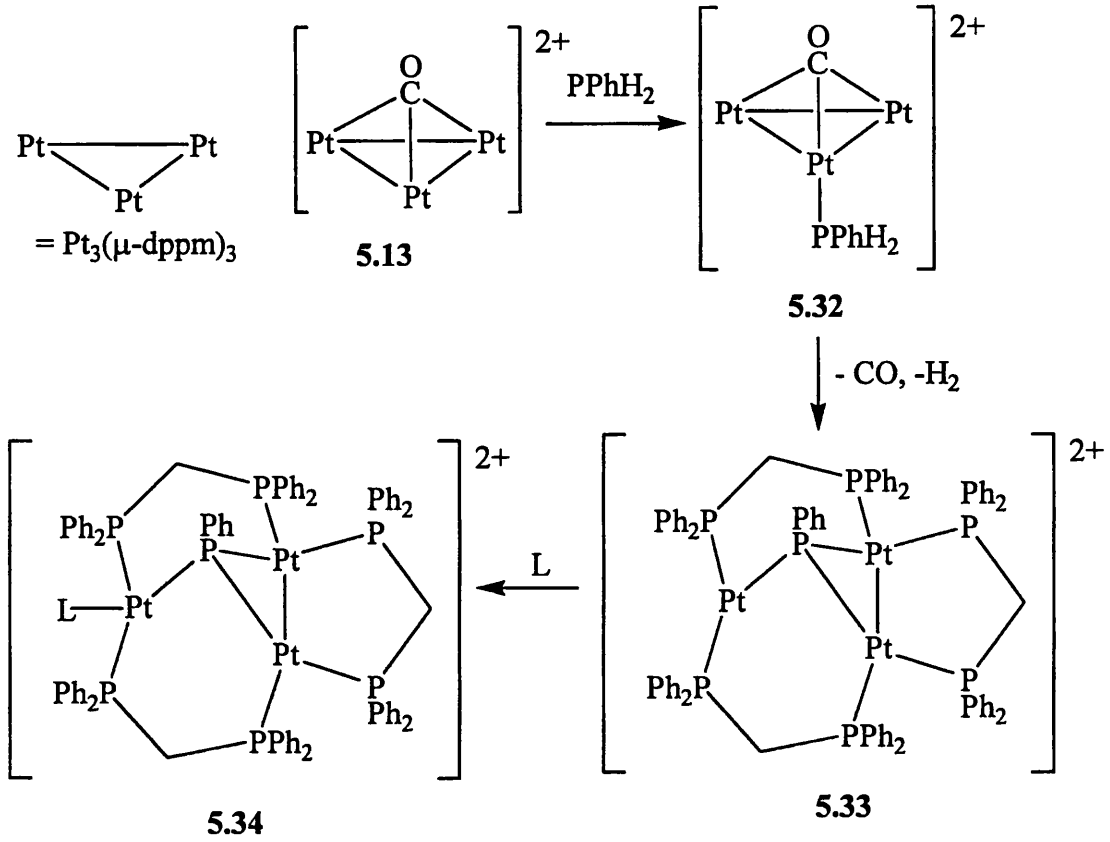

Scheme 5.8

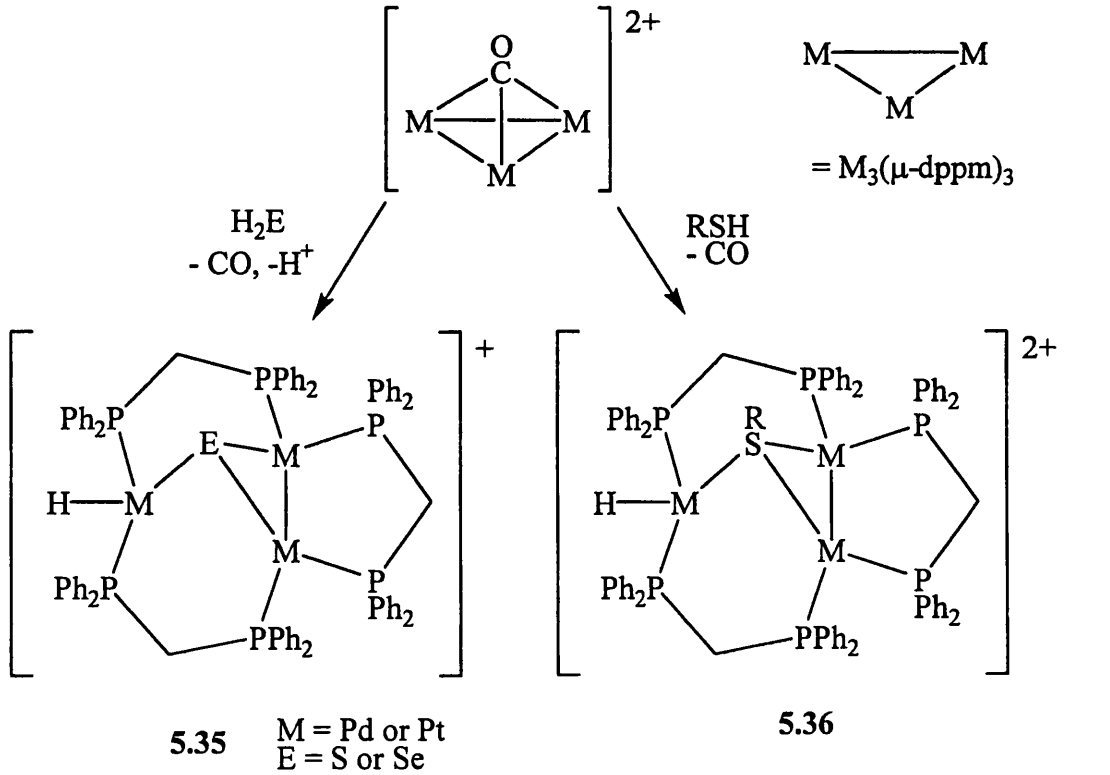

Scheme 5.9

If the complex $[Pd_3(\mu_3\text{-}CO)(\mu\text{-}dppm)_3][PF_6]_2$, **5.9**, is reacted with thiocyanide, then the analogous product to the μ_3-isocyanide complex **5.10** is formed.[16] However, this μ_3-thiocyanide complex, **5.37**, loses carbon monoxide to give the complex **5.38**, as shown in Scheme 5.9.

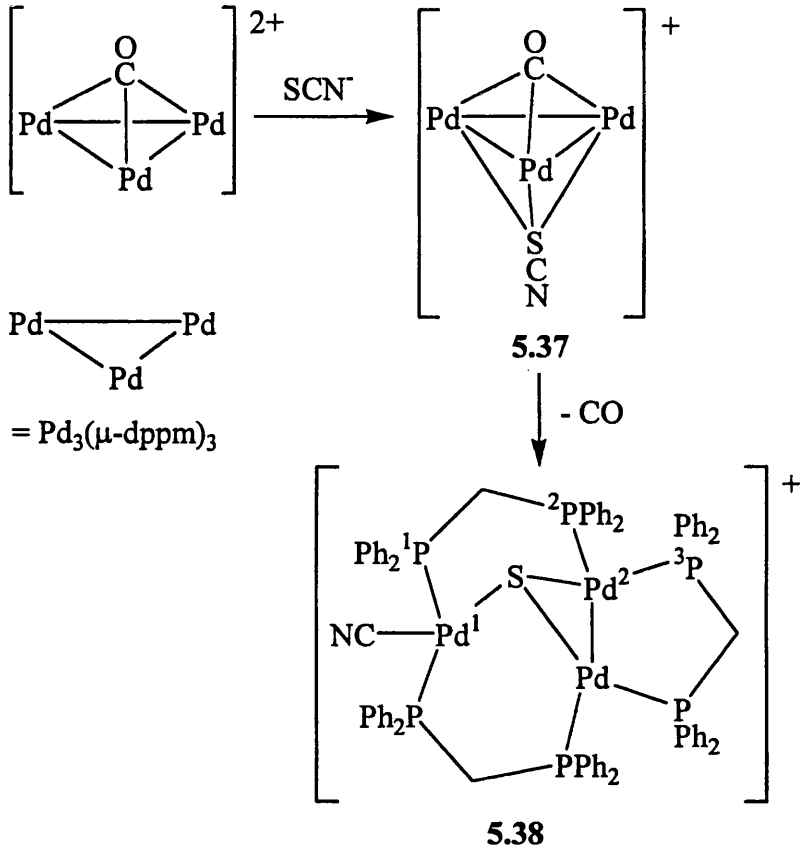

Scheme 5.9

A crystal structure determination has been carried out on complex **5.38**.[16] Table 5.2 compares selected bond lengths and angles with those from complex **40**. The plane angles are the angles between the two planes in the centre of the complexes. For **40** these planes are formed by the atoms Pd(1), P(1), P(3), O(1) and P(9) in one case and Pd(2), Pd(3), P(5), P(6) and P(9) in the other. In complex **5.38**, one plane contains the atoms Pd(1), P(1), P(1'), C(1) and S(1), while the other contains the atoms Pd(2), Pd(2'), P(3), P(3') and S(1).

The structure of **5.38** is more symmetrical than that found for **40**, and contains a mirror plane running through the cyanide ligand, Pd(1), the sulfur atom, midway through the Pd-Pd bond and through the methylene carbon of a dppm ligand. The

palladium atoms are arranged in an isosceles triangle, with the sulfur atom capping one face.

40		**5.38**	
Pd(2)-Pd(3)	2.6977(3)	Pd(2)-Pd(2')	2.579(1)
Pd(1)···Pd(2)	3.953(6)	Pd(1)···Pd(2)	3.508(1)
Pd(1)···Pd(3)	3.965(3)		
Pd(1)-P(9)	2.2748(7)	Pd(1)-S(1)	2.297(3)
Pd(2)-P(9)	2.2435(7)	Pd(2)-S(1)	2.297(3)
Pd(3)-P(9)	2.2541(7)		
P(9) above Pd_3 plane	0.82	S(1) above Pd_3 plane	1.31
Pd(1)-P(9)-Pd(2)	122.71(3)	Pd(1)-S(1)-Pd(2)	99.6
Pd(1)-P(9)-Pd(3)	121.59(3)		
Pd(2)-P(9)-Pd(3)	73.71(2)	Pd(2)-S(1)-Pd(2')	68.30
P(2)-Pd(1)-P(3)	173.38(3)	P(1)-Pd(1)-P(1')	162.1(1)
O(1)-Pd(1)-P(9)	176.17(7)	C(1)-Pd(1)-S(1)	176.0(4)
Plane angles	34.2	Plane angles	68.6

Table 5.2 Comparison of selected bond lengths (Å) and angles (°) for complexes **40** and **5.38**

It can be seen that the phosphinidine phosphorus in complex **40** exhibits less deviation from the plane of palladium atoms than the sulfur atom in complex **5.38**. All the Pd-Pd lengths in **40** are longer than their analogous lengths in **5.38**, whilst the bond angles are also larger. The angle between the two planes in the complexes is also far less in **40** than in **5.38**. The geometry of ligands around the isolated palladium is closer to square planar in **40** than in **5.38**. However, it cannot be ruled out that these differences are not due to the difference in charge between the two complexes.

Nixon and co-workers have previously reported the reaction of the iridium cluster $[Ir_4H(CO)_{10}(\mu\text{-}PPh_2)]$ with the phosphaalkyne complex $[Pt(\eta^2\text{-}P{\equiv}CBu^t)(dppe)]$ results in the formation of the μ_4-phosphinidene complex **5.41** as a minor product.[17] Comparison of the phosphinidene P-C bond lengths in complexes **40** and **5.39** indicate that they are similar [1.865(3) cf. 1.83(4)Å]. The synthesis of **5.39** is shown in Scheme 5.10.

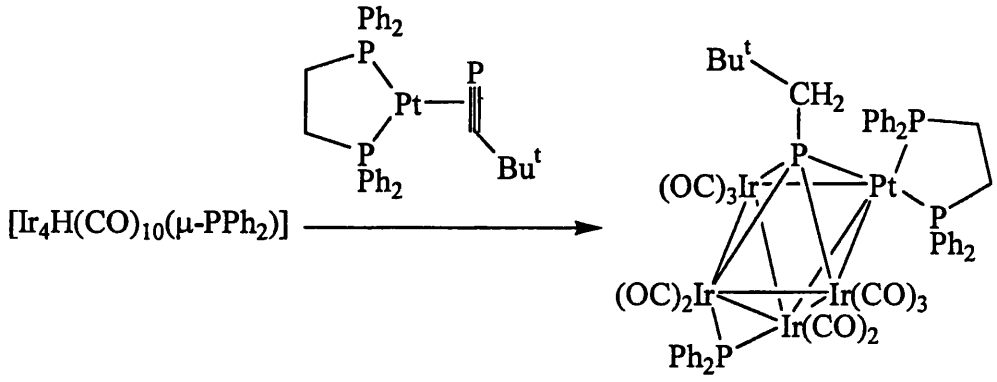

5.39

Scheme 5.10

Attempts to obtain the ^1H and $^{31}P\{^1H\}$ NMR spectra of **40** had only limited success, due to the low solubility of the complex. In the $^{31}P\{^1H\}$ NMR spectrum, complex multiplets were observed at 24-29, –6 and –32 ppm, but the clarity was such that it was not possible to discern coupling constants. In the ^1H NMR spectra, peaks assigned to the phenyl and *tert*-butyl groups were observed at 7.75 – 6.74 ppm and 1.96 ppm respectively and were integrated to give the correct ratio of 6.7:1. The signals corresponding to the dppm methylene protons were observed as broad multiplets at 2.91 and 2.78 ppm. It was not possible to assign resonances to the phosphinidene methylene group with any degree of certainty.

5.2.4 Mechanism for Formation of 40

Complex **40** was the only isolated product from the decomposition of **39**. Although a molecule of *tert*-butylphosphaalkyne is displaced during its formation, analysis by $^{31}P\{^1H\}$ and ^1H NMR on the remaining supernatant solution indicates no free phosphaalkyne is present. Instead, multiple products are observed which proved

intractable. Due to the lack of data on the fate of the displaced phosphaalkyne molecule, or on the other products of the reaction, it is impossible to state with certainty the mechanism for the formation of **40**. It must be deemed likely though that imperfectly dried solvent was the cause of the reaction. In this case, it might be assumed that the source of the two hydrogen atoms on the phosphinidene ligand is a water molecule. The oxygen atom from the same water molecule is presumably in one of the other products of the reaction, as is the second phosphaalkyne molecule.

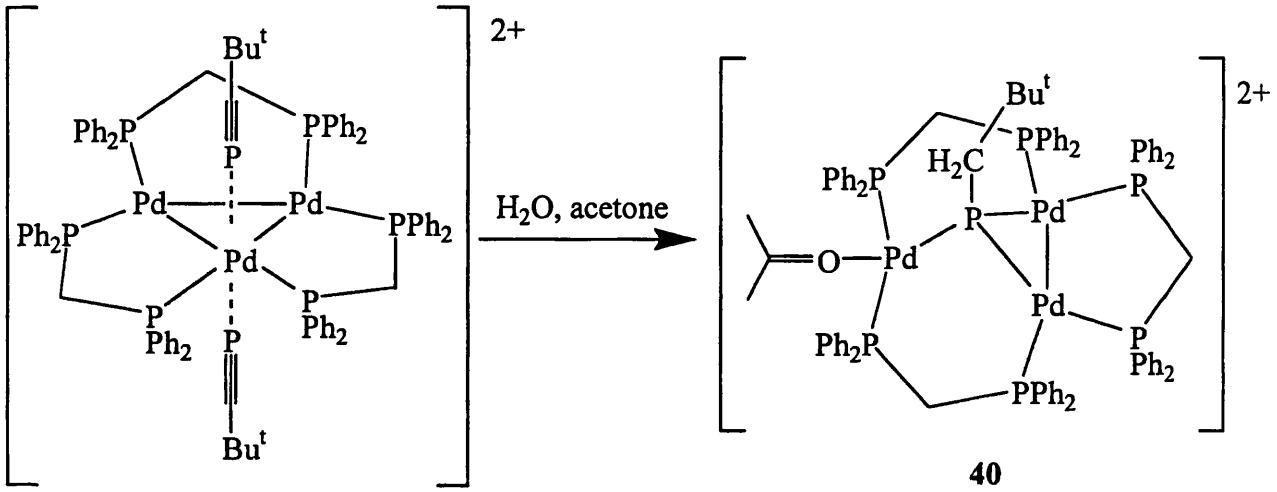

39 **40**

Scheme 5.18

5.3 Suggested Further Work

It should be noted that these reactions were discovered towards the end of my period of experimental work. Therefore it was not possible to fully complete all the research that was possible. The most important piece of future work to be carried out in this area is to obtain an X-ray crystal structure of **39**, in order to fully establish its structure. To facilitate this, it may be necessary to synthesise analogues of **39** with different anions as it has not proved possible to obtain crystals of sufficient quality using hexafluorophosphate.

In order to gain more evidence for the proposed reaction of water with **39** to produce the phosphinidene complex **40**, it is suggested that **39** be deliberately reacted with a stoichiometric amount of water. Following the reaction by spectroscopic methods

would allow some kinetic data on the reaction to be gathered. Repetition of the reaction using D_2O, in addition to giving a value for the kinetic isotope effect, would allow the source of the two new hydrogen atoms on the phosphinidene ligand to be determined. If they do originate from a reaction of a η^1-phosphaalkyne with water, then deuterium atoms will be incorporated in the product. It would then be possible to observe those by spectroscopic methods.

Repeating the synthesis of **39** using different phosphaalkynes (eg 1-adamantyl or mesitylphosphaalkyne) might affect the reactivity of the η^1-phosphaalkyne ligands, both as a result of the different substituent groups, and also as the larger substituent groups might prevent the approach of water molecules. Such complexes might also prove easier to crystallise than **39**.

The platinum analogue of the starting material, $[Pt_3(\mu\text{-dppm})_3(\mu_3\text{-CO})][PF_6]_2$, **5.13**, might be expected to react with *tert*-butylphosphaalkyne, though not necessarily to give precisely the same product (see Section 5.1).

The work carried out indicates that the reactions of phosphaalkynes on transition metal clusters is an area which is underdeveloped, and may yield interesting results. Therefore it is suggested that work be continued in the area.

5.4 Conclusions

The tripalladium cluster complex **5.7** reacts with two equivalents of *tert*-butylphosphaalkyne to give the complex $[Pd_3(\mu\text{-dppm})_3(PCBu^t)_2][PF_6]_2$, **39**. Although this complex has not been structurally characterised, the NMR data is consistent with the two phosphaalkyne ligands coordinated in an η^1 mode to the *triangulo*-palladium core.

Complex **39** has been shown to decompose slowly in solution give multiple products including the complex $[Pd_3(\mu\text{-dppm})_3(\mu_3\text{-}PCH_2Bu^t)\{(CH_3)_2CO\}][PF_6]_2$, **40**, the structure of which was determined by X-ray crystallography. This reaction represents the formal oxidative addition of one molecule of *tert*-butylphosphaalkyne into the

palladium triangle. The phosphaalkyne molecule is itself reduced to a phosphinidene ligand. It is believed that this reaction is caused by water in the solvent.

5.5 References

1 E. Sappa, A. Tiripicchio and P. Braunstein, *Chem. Rev.*, 1983, **83**, 3.

2 M.F. Meidine, J.F. Nixon and R. Mathieu, *J. Organomet. Chem.*, 1986, **314**, 307.

3 R. Bartsch, A.J. Blake, B.F.G. Johnson, P.G. Jones, C. Muller, J.F. Nixon, M. Nowotny, R. Schmutzler and D.S. Sheppard, *Phosphorus Sulfur*, 1996, **115**, 201.

4 P.E. Gaede, B.F.G. Johnson, J.F. Nixon, M. Nowotny and S. Parsons, *J. Chem. Soc., Chem. Commun.*, 1996, 1455.

5 L.T. Byrne, J.A. Johnson, G.A. Koutsantonis, B.W. Skelton and A.H. White, *J. Chem. Soc., Chem. Commun.*, 1997, 391.

6 M. Scheer, J. Krug, P. Kramkowski and J.F. Currigan, *Organometallics*, 1997, **16**, 5917.

7 W. Imhof and G. Huttner, *J. Organomet. Chem.*, 1993, **447**, 31.

8 D. Lentz and H. Michael, *Angew. Chem., Int. Ed. Engl.*, 1989, **28**, 321.

9 A.D. Burrows and D.M.P. Mingos, *Coord. Chem. Rev.*, 1996, **154**, 19.

10 R.J. Puddephatt, L. Manojlović-Muir and K.W. Muir, *Polyhedron*, 1990, **9**, 2767.

11 D.M.P. Mingos, *Acc. Chem. Res.*, 1984, **17**, 311.

12 R. Provencher, K.T. Aye, M. Brouin. J. Gagnon, N. Boudreault and P.D. Harvey, *Inorg. Chem.*, 1994, **33**, 3689.

13 R. Usón, J. Fornies, J.F. Sanz, M.A. Usón, I. Usón and S. Herrero, *Inorg. Chem.*, 1997, **36**, 1912.

14 M.C. Jennings, N.C. Payne and R.J. Puddephatt, *Inorg. Chem.*, 1987, **26**, 3776.

15 D.M. McEwan, D.P. Markham, P.G. Pringle and B.L. Shaw, *J. Chem. Soc., Dalton. Trans.*, 1986, 1809.

16 G. Ferguson, B.R. Lloyd, L. Manojlović-Muir, K.W. Muir and R.J. Puddephatt, *Inorg. Chem.*, 1986, **25**, 4190.

17 M.H. Araujo, A.G. Avent, P.B. Hitchcock, J.F. Nixon and M.D. Vargas, *Organometallics*, 1998, **17**, 5460.

6 Experimental Section

6.1 General Practical Details

All experiments were performed in an atmosphere of dry, oxygen free nitrogen using standard Schlenk line techniques. Solvents were distilled under a nitrogen atmosphere from sodium benzophenone ketyl (THF, diethyl ether, hexane), sodium metal (toluene) and CaH_2 (acetonitrile, CH_2Cl_2). They were then degassed and stored over 4Å molecular sieves.
Unless otherwise stated, all chemicals were reagent grade and used as received.
Deuterated solvents for NMR spectroscopy were degassed and dried over 4Å molecular sieves (with the exception of d_6 acetone) before use.

Characterisations

Microanalyses for C, H and N content were carried out in the analytical department of the Department of Chemistry by Mr. A. Carver.
Unless otherwise stated, IR spectra were recorded in NaCl solution cells on Nicolet Nexus, or Perkin Elmer 1600 FT-IR spectrometers.
NMR spectra were recorded using JEOL JNM-EX 270 (270MHz) or Varian Mercury400 (400MHz) spectrometers. Spectra were recorded at 20°C unless otherwise stated, and were referenced internally to the solvent [^{13}C (C_6D_6 128.0, $CDCl_3$ 77.2, d_6-acetone 29.4 and 206.3 ppm) and ^1H (C_6D_5H 7.15, $CHCl_3$ 7.27, d_6-acetone 2.05 ppm)], or externally to 85% H_3PO_4.

Starting Materials

The complexes $[MoCl(CO)_3(\eta^5\text{-}C_5H_5)]$[1], $[MoCl(CO)_3(\eta^5\text{-}C_5Me_5)]$[1], $[Mo(CH_3)(CO)_3(\eta^5\text{-}C_5H_5)]$[2], $[Pd_3(\mu_3\text{-}CO)(\mu\text{-}dppm)_3][PF_6]_2$[3], and the ligands $Ph_2PNC_4H_3C(O)Me$[4], $Ph_2PCH_2C(O)Ph$[5] and $Ph_2PCH_2C(O)NPh_2$[6] were prepared by literature methods. *tert*-Butylphosphaalkyne was donated by Dr. C. Jones of Cardiff University.

6.2 Syntheses

Reaction of *tert*-butylphosphaalkyne with [MoCl(CO)$_3$(η^5-C$_5$H$_5$)]

To a stirred solution of [MoCl(CO)$_3$(η^5-C$_5$H$_5$)] (250 mg, 0.893 mmol) in pentane (20 mL) was added *tert*-butylphosphaalkyne (300 μL, 1.79 mmol). The solution was then brought to reflux (40°C) for 78 hours. The orange solution darkened and a dark precipitate was seen. Upon cooling to room temperature, the solvent was decanted and cooled to give a dark green precipitate. This was then combined with the original precipitate. Separation of the product was carried out on a ice-cooled column (10 x 1 cm) packed with a Florisil/pentane slurry, and using CH_2Cl_2 as the elutant. A green band remained at the top of the column whilst an orange band was collected. The solvent was removed *in vacuo*, and the orange powder recrystallised by a slow diffusion of hexane into a CH_2Cl_2 solution to give the product [MoCl(CO)(η^4-1,3-P$_2$C$_2$Bu$^t_2$)(η^5-C$_5$H$_5$)], **1**, as orange crystals. (Yield = 131 mg, 35 %)

^{1}H NMR (270 MHz, CD_2Cl_2):	δ 5.56 [s, 5H, η^5-C$_5$H$_5$], 0.89 [br s, 9H, Bu^t], 0.69 [br s, 9H, Bu^t]
^{13}C{^{1}H} NMR (67 MHz, C_6D_6):	δ 227.5 [br, M-CO], 92.9 [s, η^5-C$_5$H$_5$], 36.0 [br, $\underline{C}$Me$_3$], 35.2 [br, $\underline{C}$Me$_3$], 34.4 [br s, C$\underline{Me_3}$], 32.9 [br s, C$\underline{Me_3}$]
^{31}P{^{1}H} NMR (109 MHz, CD_2Cl_2):	δ 86.9 [s, 1P], 71.1 [s, 1P]
Infrared:	ν_{CO} (Pentane) = 1988 cm^{-1}
Microanalysis; $C_{16}H_{23}MoClP_2O$	requires: C, 45.2; H, 5.41 %
	found: C, 44.9; H, 5.32 %

Reaction of *tert*-butylphosphaalkyne with [MoCl(CO)$_3$(η^5-C$_5$Me$_5$)]

The reaction was carried out as for **1** using [MoCl(CO)$_3$(η^5-C$_5$Me$_5$)] (250 mg, 0.714 mmol), *tert*-butylphosphaalkyne (290 μL, 1.78 mmol) and a reaction time of 24 hours. The orange precipitate formed was recrystallised from a slow diffusion of

hexane into a CH_2Cl_2 solution to give the product [MoCl(CO)(η^4-1,3-$P_2C_2Bu^t_2$)(η^5-C_5Me_5)], **2**, as an orange powder (Yield = 298 mg, 80 %).

^{1}H NMR (270 MHz, CD_2Cl_2)	δ 1.90 [s, 15H, C_5Me_5], 0.86 [br s, 9H, Bu^t], 0.82 [br s, 9H, Bu^t]
$^{13}C\{^1H\}$ NMR (100 MHz, CD_2Cl_2)	δ 230.5 [d, M-CO, $^2J_{PC}$ = 6.1 Hz], 107.7 [dd, η^4-1,3-$P_2\underline{C}_2Bu^t_2$, $^1J_{PC}$ = 40.2, 60.4 Hz], 107.3 [s, η^5-$\underline{C}_5Me_5$], 101.2 [dd, η^4-1,3-$P_2\underline{C}_2Bu^t_2$, $^1J_{PC}$ = 52.9, 55.1 Hz], 36.7 [app. t, $\underline{C}Me_3$, $^1J_{PC}$ + $^3J_{PC}$ = 8.0 Hz], 35.5 [app. t, $\underline{C}Me_3$, $^1J_{PC}$ + $^3J_{PC}$ = 7.3 Hz], 33.7 [app. t, C$\underline{Me}_3$, $^2J_{PC}$ + $^4J_{PC}$ = 4.4 Hz], 33.3 [app. t, C$\underline{Me}_3$, $^2J_{PC}$ + $^4J_{PC}$ = 5.0 Hz], 12.3 [d, C_5Me_5, $^3J_{PC}$ = 5.0 Hz]
$^{31}P\{^1H\}$ NMR (109 MHz, CD_2Cl_2)	δ 101.7 [d, $^2J_{PP}$ = 7 Hz, 1P,], 74.4 [br, 1P]
Infrared	ν_{CO} (CH_2Cl_2) = 1961 cm^{-1}
Microanalysis; $C_{21}H_{33}MoClP_2O$	requires: C, 51.0; H, 6.68 %
	found: C, 50.3; H, 6.66 %

Reaction of [MoCl(CO){η^4-1,3-$P_2C_2Bu^t_2$)(η^5-C_5H_5)] with H_2O

Distilled water (10 μL, 0.52 mmol) was added to a solution of **1** (22 mg, 0.052 mmol) in CH_2Cl_2 (5 mL). The solution was then left to stand for 2 days. Red crystals of [MoCl(CO){η^3,λ^3,λ^5-$PC_2Bu^t_2PH(OH)$}(η^5-C_5H_5)], **3**, precipitated out of solution (Yield = 15 mg, 65 %).

^{1}H NMR (270 MHz, $\{CD_3\}_2CO$)	δ 8.11 [dd, 1H, PH, $^1J_{PH}$= 499.0 Hz, $^3J_{PH}$= 4 Hz], 5.58 [s, 5H, η^5-C_5H_5], 1.24 [s, 9H, Bu^t], 1.03 [s, 9H, Bu^t]
$^{13}C\{^1H\}$ NMR (100 MHz, $\{CD_3\}_2CO$)	δ 244.4 [br s, M-CO], 90.0 [s, η^5-C_5H_5], 57.0 – 55.2 [m, $\underline{C}_2P$], 33.7 [d, $\underline{C}Me_3$, $^2J_{PC}$ = 7.2 Hz], 32.7 [d, $\underline{C}Me_3$, $^2J_{PC}$ = 7.9 Hz], 32.1 [dd,

	C*Me*$_3$, $^3J_{PC}$ = 5.9, 10.3 Hz], 31.0 [dd, C*Me*$_3$, $^3J_{PC}$ = 4.4, 9.3 Hz]
$^{31}P\{^1H\}$ NMR (109 MHz, $\{CD_3\}_2CO$)	δ 8.9 [d, $^1J_{HP}$= 499.0 Hz, 1P], -15.8 [s, 1P]
Infrared:	ν_{CO} (KBr) = 1921 cm^{-1}
Microanalysis; $C_{16}H_{25}MoClP_2O_2$	requires: C, 43.4; H, 5.66 %
	found: C, 43.9; H, 5.13 %

Reaction of [MoCl(CO)(η^4-1,3-$P_2C_2Bu^t_2$)(η^5-C_5H_5)] with MeOH

The reaction was carried out as for **3** using **1** (22 mg, 0.052 mmol), methanol (10 μL, 0.52 mmol) and a reaction time of 10 days. Red crystals of [MoCl(CO){η^3,λ^3,λ^5-$PC_2Bu^t_2PH(OMe)$}(η^5-C_5H_5)], **4**, precipitated out of solution (Yield = 13 mg, 56 %).

^1H NMR (270 MHz, C_6D_6)	δ 8.00 [dd, $^1J_{PH}$= 496.3 Hz, $^3J_{PH}$ = 5.0 Hz, 1H, PH], 5.41 [s, 5H, η^5-C_5H_5], 3.90 [d, $^3J_{PH}$= 12.1 Hz, 3H, POMe,], 1.00 [s, 9H, Bu^t], 0.80 [s, 9H, Bu^t]
$^{31}P\{^1H\}$ NMR (109 MHz, $\{CD_3\}_2CO$)	δ 10.6 [d, $^1J_{HP}$ = 496.3 Hz, 1P], -16.7 [s, 1P]
Infrared	ν_{CO} (KBr) = 1889 cm^{-1}

Attempted Reactions of [MoCl(CO){η^4-1,3-$P_2C_2Bu^t_2$)(η^5-C_5Me_5)] with H_2O

Slow Method:

The reaction was carried out as for **3** using **2** (40 mg, 0.081 mmol), water (16 μL, 0.082 mmol), and a reaction time of 2 weeks. After this time, no crystals formed, and there was no evidence of change in the NMR spectra.

Vigorous Method:

To a solution of **2** (40 mg, 82 mmol) in THF (20 mL) was added water (20 μL, 103 mmol). The solution was then heated at reflux for 48 hours. Analysis by ^{31}P NMR indicated that no reaction had taken place.

Reaction of [MoCl(CO){η^2-PhC≡CPh}(η^5-C_5H_5)] with $AgBF_4$, C_2H_4 and *tert*-butylphosphaalkyne

A solution of [MoCl(CO){η^2-PhC≡CPh}(η^5-C_5H_5)] (150 mg, 0.388 mmol) was stirred in CH_2Cl_2 (15 mL) whilst a stream of ethylene was bubbled through the solution for 15 minutes. Addition of $AgBF_4$ (77 mg, 0.389 mmol) resulted in the precipitation of white AgCl, and a colour change in the solution of green to red. After 15 minutes the reaction mixture was filtered through Celite under an atmosphere of ethylene to isolate a red filtrate solution of [Mo(CO)(η^2-C_2H_4){η^2(4e)-PhC≡CPh}(η^5-C_5H_5)][BF_4], **5**. To this solution was added *tert*-butylphosphaalkyne (118 μL, 0.778 mmol) with stirring for 30 minutes. The solvents were removed *in vacuo* and the residue purified by a diffusion of hexane into a CH_2Cl_2 solution to give the product [Mo(CO)(=C{Bu^t}P{η^2-C(Bu^t)=P}C{Ph}=C{Ph})(η^5-C_5H_5)][BF_4], **6**, as a red oily solid. (Yield = 155 mg, 60%)

^1H NMR (270 MHz, CD_2Cl_2)	δ 7.76-7.00 [m, 10H, Ph], 5.44 [s, 5H, η^5-C_5H_5], 1.90 [s, 9H, Bu^t], 1.14 [s, 9H, Bu^t]
$^{13}C\{^1H\}$ NMR (100 MHz, CD_2Cl_2)	δ 220.4 [M-CO], 136.1 – 126.8 [Ph], 95.6 [η^5-C_5H_5], 31.8 [Bu^t], 30.2 [Bu^t]
$^{31}P\{^1H\}$ NMR (109 MHz, CD_2Cl_2)	δ 48.7 (d, $^2J_{P,P}$ = 19.9 Hz), -87.7 (d, $^2J_{P,P}$ = 19.9 Hz)
Infrared	ν_{CO} (CH_2Cl_2) = 2053 cm^{-1}

Reaction of [MoCl(CO){η^2(4e)-PhC≡CMe}(η^5-C_5H_5)] with $AgBF_4$, C_2H_4 and *tert*-butylphosphaalkyne

A red solution of [Mo(CO)(η^2-C_2H_4){η^2-PhC≡CMe}(η^5-C_5H_5)][BF_4], **7**, was made as for **5** using [MoCl(CO){η^2(4e)-PhC≡CMe}(η^5-C_5H_5)] (205 mg, 0.602 mmol) and $AgBF_4$ (120 mg, 0.613 mmol). Addition of *tert*-butylphosphaalkyne (185 μL, 1.22 mmol) and work-up as for **6** gave as the product [Mo(CO)(=C{Bu^t}P{η^2-C(Bu^t)=P}C{R}=C{R'})(η^5-C_5H_5)][BF_4] (R ≠ R' = Ph or Me), **8**, as a red oil. (Yield = 60 mg, 37 %)

^{1}H NMR (270 MHz, CD_2Cl_2)	δ 7.59-7.27 [m, 5H, Ph], 5.65 [s, 5H, η^5-C_5H_5], 1.76 [s, 3H, Me], 1.43 [s, 9H, Bu^t], 1.08 [s, 9H, Bu^t]
^{13}C{^{1}H} NMR (100 MHz, CD_2Cl_2)	δ 223.7 [M-CO], 137.6 – 125.4 [Ph], 99.1 [η^5-C_5H_5], 32.3 [Bu^t], 30.6 [Bu^t]
^{31}P{^{1}H} NMR (109 MHz, CD_2Cl_2)	δ 38.7 [d, $^2J_{PP}$ = 20.1 Hz], -91.7 (d, $^2J_{PP}$ = 20.1 Hz)
Infrared	ν_{CO} (CH_2Cl_2) = 2051 cm^{-1}

Preparation of [$MoCl(CO)_3$(η^5-$C_5H_4Bu^t$)]

To a solution of dimethylfulvene (490 mg, 4.6 mmol) in THF (10mL) was added MeLi (2.9 mL of a 1.6M solution in hexane) with stirring at –78°C. On warming to room temperature, the yellow solution darkened in colour. The solvents were removed *in vacuo* to give an orange precipitate of [Li][$C_5H_4Bu^t$]. This was immediately redissolved in THF (10mL) and added to a solution of $Mo(CO)_6$ (1.23g, 4.55 mmol) in THF (20 mL). This was heated to reflux for 15 hours to give a dark brown solution. This was cooled to 0°C, and water (5 mL), diethyl ether (12 mL) and glacial acetic acid (1.8 mL) were added with stirring and exclusion of light to give the molybdenum hydride [$MoH(CO)_3$(η^5-$C_5H_4Bu^t$)]. After 20 minutes, CCl_4 (20 mL) was added, with an immediate colour change to a red solution. The solution was

stirred for 30 minutes, the ether phase separated and the remaining THF/water phase washed with diethyl ether (5 x 5 mL). The ether fractions were combined, and the solvent removed *in vacuo*. The red brown residue was redissolved in CH_2Cl_2, and purified on a alumina column (5 x 40 cm), using CH_2Cl_2 as the eluant. The solvent was removed *in vacuo* to give $[MoH(CO)_3(\eta^5\text{-}C_5H_4Bu^t)]$, **9**, as a dark orange powder (581 mg, 38%).

^1H NMR (270 MHz, CD_2Cl_2)	δ 5.60 [br m, 2H, η^5-$C_5\underline{H}_4Bu^t$], 5.42 [br m, 2H, η^5-$C_5\underline{H}_4Bu^t$], 1.28 [s, 9H, η^5-$C_5H_4\underline{Bu^t}$]
$^{13}C\{^1H\}$ NMR (100 MHz, CD_2Cl_2)	δ 242.8 [M-CO], 225.6 [M-CO], 96.4 [η^5-$\underline{C}_5H_4Bu^t$], 92.6 [η^5-$\underline{C}_5H_4Bu^t$], 87.9 [η^5-$\underline{C}_5H_4Bu^t$], 32.0 [η^5-$C_5H_4\underline{C}Me_3$], 31.4 [η^5-$C_5H_4C\underline{Me_3}$]
Infrared	ν_{CO} (CH_2Cl_2) = 2050, 1975, 1951 cm^{-1}

Reaction of $[MoCl(CO)_3(\eta^5\text{-}C_5H_4Bu^t)]$ with diphenylacetylene

To a solution of $[MoCl(CO)_3(\eta^5\text{-}C_5H_4Bu^t)]$ (580 mg, 1.73 mmol) in pentane (20 mL) was added diphenylacetylene (320 mg, 1.79 mmol). The mixture was heated at reflux for 24 hours, whereupon the orange solution faded, and a green precipitate formed. On cooling to room temperature, the solvent was decanted and the precipitate washed with diethyl ether (5 x 10 mL). Removal of the solvents *in vacuo*, followed by recrystallisation by a diffusion of hexane into a CH_2Cl_2 solution gave the product $[MoCl(CO)\{\eta^2(4e)\text{-}PhC{\equiv}CPh\}(\eta^5\text{-}C_5H_4Bu^t)]$, **10**, as a bright green powder. (Yield = 710 mg, 88 %)

^1H NMR (270 MHz, CD_2Cl_2)	δ 7.48 – 7.10 [m, 10H, Ph], 5.51 [br m, 2H, η^5-$C_5\underline{H}_4Bu^t$], 5.43 [br m, 2H, η^5-$C_5\underline{H}_4Bu^t$], 1.15 [s, 9H, η^5-$C_5H_4\underline{Bu^t}$]
$^{13}C\{1H\}$ NMR (100 MHz, CD_2Cl_2)	δ 263.9 [M-CO], 130.7 – 126.8 [Ph], 97.6 [η^5-$\underline{C}_5H_4Bu^t$], 92.5 [η^5-$\underline{C}_5H_4Bu^t$], 88.5 [η

	^{5}-$\underline{C}_5H_4Bu^t$], 29.8 [η^5-$C_5H_4\underline{C}Me_3$], 13.2 [η^5-$C_5H_4C\underline{Me_3}$]
Infrared	ν_{CO} (CH_2Cl_2) = 1938 cm^{-1}

Reaction of [MoCl(CO)(η^2-PhC≡CPh)(η^5-$C_5H_4Bu^t$)] with $AgBF_4$, C_2H_4 and *tert*-butylphosphaalkyne

A red solution of [Mo(CO)(η^2-C_2H_4){η^2-PhC≡CPh}(η^5-$C_5H_4Bu^t$)][BF_4], **11**, was made as for **5** using **10** (100 mg, 0.218 mmol) and $AgBF_4$ (43 mg, 0.218 mmol). Addition of *tert*-butylphosphaalkyne (130 μL, 0.86 mmol) and work-up as for **6** gave the product [Mo(CO)(=C{Bu^t}P{η^2-C(Bu^t)=P}C{Ph}=C{Ph})(η^5-$C_5H_4Bu^t$)][BF_4], **12**, as a green oil. (Yield = 74 mg, 50 %)

^{1}H NMR (270 MHz, CD_2Cl_2)	δ 7.60-6.90 [m, 10H, Ph], 5.60 [br m, 2H, η^5-$C_5\underline{H_4}Bu^t$], 5.42 [br m, 2H, η^5-$C_5\underline{H_4}CBu^t$], 1.95 [s, 9H, Bu^t], 1.28 [s, 9H, Bu^t], 1.12 [s, 9H, Bu^t]
^{13}C{^{1}H} NMR (100 MHz, CD_2Cl_2)	δ 226.1 [M-CO], 135.4 – 126.0 [Ph], 106.8 [η^5-$\underline{C}_5H_4Bu^t$], 103.8 [η^5-$\underline{C}_5H_4Bu^t$]. 100.4 [η^5-$\underline{C}_5H_4Bu^t$], 96.9 [η^5-$\underline{C}_5H_4Bu^t$], 32.2 [$\underline{C}Me_3$], 32.0 [Bu^t], 31.4 [Bu^t], 30.0 [Bu^t]
^{31}P{^{1}H} NMR (109 MHz, CD_2Cl_2)	δ 51.3 [d, $^2J_{PP}$ = 19.5 Hz], -93.4 [d, $^2J_{PP}$ = 19.5 Hz]
Infrared	ν_{CO} (CH_2Cl_2) = 2044 cm^{-1}

Reaction of 6 with DIBAL-H

To a cooled (-78°C), stirred solution of **6** (130 mg, 0.188 mmol) in THF (15 mL) was added $(Bu^i)_3AlH$ (110 μL of a 1.8M solution in THF). The solution was allowed to warm to room temperature, and the solvents were removed *in vacuo* to give a red oily residue. This was extracted with diethyl ether to separate the product from the aluminium salts, and the solvents removed *in vacuo* to give a second red oily residue.

The product $[Mo(CO)(-CH\{Bu^t\}\overline{P\{\eta^2\text{-}C(Bu^t)=P\}\{\eta^2\text{-}C(Ph)=C(Ph)\}})(\eta^5\text{-}C_5H_5)]$ **,13,** was isolated as a red oil by diffusion of hexane into a CH_2Cl_2 solution. (Yield = 90 mg, 80 %)

^1H NMR (270 MHz, C_6D_6)	δ 8.58 [d, $^2J_{HP}$ = 8.6 Hz, 1H, Mo-C*H*(Bu^t)-P], 7.50 - 6.80 [m, 10H, Ph], 5.13 [s, 5H, η^5-C_5H_5], 1.56 [s, 9H, Bu^t], 1.22 [s, 9H, Bu^t]
$^{13}C\{1H\}$ NMR (67 MHz, C_6D_6)	δ 226.1 [M-CO], 135.4 – 126.0 [Ph], 91.5 [η^5-C_5H_5], 32.9 [Bu^t], 24.0 [d, $^1J_{CP}$ = 29.6 Hz, Mo-CH(Bu^t)-P], 23.4 [Bu^t]
$^{31}P\{^1H\}$ NMR (109 MHz, C_6D_6)	δ 21.8 [d, $^2J_{PP}$ = 23.1 Hz], -70.8 [d, $^2J_{PP}$ = 23.1 Hz]
Infrared	ν_{CO} (CH_2Cl_2) = 1882 cm^{-1}

Reaction of $[MoCl(CO)_3(\eta^5\text{-}C_5H_5)]$ with $Ph_2PNC_4H_3C(O)Me$

$[Mo(\eta^5\text{-}C_5H_5)(CO)_3Cl]$ (150 mg, 0.53 mmol) and $Ph_2PNC_4H_3C(O)Me$ (149 mg, 0.53 mmol) were dissolved in hexane (20 mL). The solution was brought to reflux for 6 hours, during which there was a colour change from orange to dark red. The volatiles were removed *in vacuo* and the residue recrystallised by addition of toluene to a CH_2Cl_2 solution, to give the product $[MoCl(CO)_2\{Ph_2PNC_4H_3C(O)Me\text{-}P\}(\eta^5\text{-}C_5H_5)]$, **14**, as a dark red powder. Crystals suitable for X-ray crystallography were obtained by a layer diffusion of toluene into a CH_2Cl_2 solution at room temperature, and the molecular structure determined. (Yield = 281 mg, 89 %).

^{1}H NMR (270 MHz, $CDCl_3$)	δ 7.72-7.38 [m, 10H, Ph], 7.20 [m, 1H, Pyrrole], 6.46 [m, 1H, Pyrrole], 6.21 [m, 1H, Pyrrole], 5.61 [s, 5H, η^5-C_5H_5], 2.31 [s, 3H, Me]
$^{13}C\{^1H\}$ NMR (100 MHz, $CDCl_3$)	δ 254.2 [d, M-CO, $^2J_{PC}$ = 31.4 Hz], 242.9 [d, M-CO, $^2J_{PC}$ < 1 Hz], 185.5 [>C=O], 135.2 - 128.0 [Ph and pyrrole], 96.1 [η^5-C_5H_5], 26.0 [Me],
$^{31}P\{^1H\}$ NMR (109 MHz, $CDCl_3$)	δ 112.2 [$Ph_2PNC_4H_3C(O)Me$]
Infrared	ν_{CO} (CH_2Cl_2) = 1970, 1888 cm^{-1} (M-CO) 1654 cm^{-1} (>C=O)
Microanalysis: $C_{25}H_{21}ClMoNO_3P$	requires: C, 55.0; H, 3.88; N, 2.57 % found: C, 54.9; H, 3.94; N, 2.64 %

Reaction of $[MoCl(CO)_3(\eta^5\text{-}C_5Me_5)]$ with $Ph_2PNC_4H_3C(O)Me$

The reaction was carried out as for **14** using $[MoCl(CO)_3(\eta^5\text{-}C_5Me_5)]$ (228 mg, 0.65 mmol) and $Ph_2PNC_4H_3C(O)Me$ (191 mg, 0.651 mmol. The product $[MoCl(CO)_2\{Ph_2PNC_4H_3C(O)Me\text{-}P\}(\eta^5\text{-}C_5Me_5)]$, **15**, was recrystallised as a dark red powder from a diffusion of toluene into a CH_2Cl_2 solution. (Yield = 315 mg, 79 %)

^{1}H NMR (270 MHz, $CDCl_3$)	δ 7.39 – 7.22 [m, 10H, Ph], 7.12 [m, 1H, pyrrole], 6.39 [m, 1H, pyrrole], 6.22 [m, 1H, pyrrole], 2.41 [s, 3H, Me], 1.94 [s, 15H, η^5-$C_5\underline{Me_5}$]
$^{13}C\{^1H\}$ NMR (100 MHz, $CDCl_3$)	δ 246.3 [d, $^2J_{PC}$ < 5 Hz, M-CO], 227.4 [d, $^2J_{PC}$ < 5 Hz, M-CO], 188.1 [s, >C=O], 132.8 – 124.8 [m, Ph and pyrrole], 108.8 [s, η^5-$\underline{C_5}Me_5$], 25.7 [s, Me], 10.7 [s, η^5-$C_5\underline{Me_5}$]

$^{31}P\{^{1}H\}$ NMR (109 MHz, $CDCl_3$)	δ 58.6 [s, $Ph_2PNC_4H_3C(O)Me$]
Infrared	ν_{CO} (CH_2Cl_2) = 1964, 1880 cm^{-1} (M-CO)
	1658 cm^{-1} (>C=O)

Reaction of $[MoCl(CO)_3(\eta^5\text{-}C_5H_5)]$ with $Ph_2PCH_2C(O)Ph$

The reaction was carried out as for **14** using $[MoCl(CO)_3(\eta^5\text{-}C_5H_5)]$ (246 mg, 0.88 mmol), and Ph_2PCH_2COPh (267 mg, 0.88 mmol). The product $[MoCl(CO)_2\{Ph_2PCH_2C(O)Ph\text{-}P\}(\eta^5\text{-}C_5H_5)]$, **16**, was recrystallised from a layer diffusion of toluene into a CH_2Cl_2 solution as a dark red powder. (Yield = 446 mg, 91 %)

^{1}H NMR (270 MHz, $CDCl_3$)	δ 7.78-7.28 [m, 15H, Ph], 5.37 [s, 5H, η^5-C_5H_5], 4.41 [dd, 1H, -CH_2-, $^{2}J_{HH}$=15.6 Hz, $^{2}J_{HP}$=9.9 Hz], 4.14 [dd, 1H, -CH_2-, $^{2}J_{HH}$=15.6 Hz, $^{2}J_{HP}$=7.9 Hz]
$^{13}C\{^{1}H\}$ NMR (100 MHz, $CDCl_3$)	δ 256.8 [d, M-CO, $^{2}J_{PC}$= 29.5 Hz], 243.6 [d, M-CO, $^{2}J_{PC}$= 8.2 Hz], 195.2 [d, >C=O, $^{1}J_{PC}$= 9.7 Hz], 137.1 - 128.2 [Ph], 95.2 [η^5-C_5H_5], 36.4 [d, -CH_2-, $^{1}J_{PC}$= 20.4 Hz],
$^{31}P\{^{1}H\}$ NMR (109 MHz, $CDCl_3$)	δ 48.2 [$Ph_2PCH_2C(O)Ph$]
Infrared	ν_{CO} (CH_2Cl_2) = 1970, 1888 cm^{-1} (M-CO)
	1656 cm^{-1} (>C=O)
Microanalysis; $C_{27}H_{22}ClMoO_3P$	requires: C, 58.2; H, 3.98 %
	found: C, 57.8, H, 4.01 %

Reaction of $[Mo(\eta^5\text{-}C_5Me_5)(CO)_3Cl]$ with $Ph_2PCH_2C(O)Ph$

The reaction was carried out as for **14** using $[MoCl(CO)_3(\eta^5\text{-}C_5Me_5)]$ (36 mg, 0.103 mmol) and $Ph_2PCH_2C(O)Ph$ (32 mg, 0.105 mmol). The product

$[MoCl(CO)_2\{Ph_2PCH_2C(O)Ph\text{-}P\}(\eta^5\text{-}C_5Me_5)]$, **17**, was recrystallised as a dark red powder by slow diffusion of toluene into a CH_2Cl_2 solution. (Yield = 55 mg, 85 %)

^1H NMR (270 MHz, $CDCl_3$)	δ 7.67-7.18 [m, 15H, Ph], 4.64 [dd, 1H, -CH_2-, $^2J_{HH}$=14.9 Hz, $^2J_{HP}$=8.1 Hz], 3.73 [dd, 1H, -CH_2-, $^2J_{HH}$=14.9 Hz, $^2J_{HP}$=7.0 Hz], 1.70 [s, 15H, η^5-C_5Me_5]
$^{13}C\{^1H\}$ NMR (100 MHz, $CDCl_3$)	δ 259.0 [d, M-CO, $^2J_{PC}$= 27.1 Hz], 246.2 [d, M-CO, $^2J_{PC}$= 5.4 Hz], 195.2 [d, >C=O, $^2J_{PC}$= 8.1 Hz], 137.0 - 127.6 [Ph], 106.3 [$\underline{C}_5Me_5$], 34.1 [d, -CH_2-, $^1J_{PC}$= 13.6Hz], 10.0 [$C_5\underline{Me}_5$]
$^{31}P\{^1H\}$ NMR (109 MHz, $CDCl_3$)	δ 45.4 [$Ph_2PCH_2C(O)Ph$]
Infrared	ν_{CO} (CH_2Cl_2) = 1960, 1879 cm^{-1} (M-CO) 1656 cm^{-1} (>C=O)

Reaction of $[MoCl(CO)_3(\eta^5\text{-}C_5H_5)]$ with $Ph_2PCH_2C(O)NPh_2$

The reaction was carried out as for **14** using $[MoCl(CO)_3(\eta^5\text{-}C_5H_5)]$ (189 mg, 0.67 mmol) and $Ph_2PCH_2C(O)NPh_2$ (266 mg, 0.67 mmol). The product $[MoCl(CO)_2\{Ph_2PCH_2C(O)NPh_2\text{-}P\}(\eta^5\text{-}C_5H_5)]$, **18**, was recrystallised as a dark orange powder from a slow diffusion of toluene into a CH_2Cl_2 solution. (Yield = 414 mg, 93 %)

^1H NMR (270 MHz, $CDCl_3$)	δ 7.74-7.18 [m, 20H, Ph], 5.37 [s, 5H, η^5-C_5H_5], 3.51 [dd, 1H, -CH_2-, $^2J_{HH}$ = 16.0 Hz, $^2J_{HP}$ = 11.7 Hz], 3.33 [dd, 1H, -CH_2-, $^2J_{HH}$ = 16.0 Hz, $^2J_{HP}$ = 6.9 Hz]
$^{13}C\{^1H\}$ NMR (100 MHz, $CDCl_3$)	δ 257.5 [d, M-CO, $^2J_{PC}$ = 19.5 Hz], 243.7 [d, M-CO, $^2J_{PC}$ = 6.7 Hz], 167.3 [s, >C=O], 142.4 - 126.5 [Ph], 95.6 [η^5-C_5H_5], 35.7 [d, -CH_2-, $^1J_{PC}$ = 25.7 Hz],

$^{31}P\{^1H\}$ NMR (109 MHz, $CDCl_3$) δ 52.1 [$Ph_2PCH_2C(O)Ph$]

Infrared ν_{CO} (CH_2Cl_2) = 1964, 1872 cm^{-1} (M-CO)
1666 cm^{-1} (>C=O)

Microanalysis; $C_{33}H_{27}ClMoO_3PN.^1/_3CH_2Cl_2$ requires: C, 59.2; H, 4.12; N, 2.07 %
found: C, 59.1; H, 4.07; N, 2.02 %

Reaction of [MoCl(CO)$_3$(η^5-C_5Me_5)] with $Ph_2PCH_2C(O)NPh_2$

The reaction was carried out as for **14** using [MoCl(CO)$_3$(η^5-C_5Me_5)] (173 mg, 0.49 mmol) and $Ph_2PCH_2C(O)NPh_2$ (195 mg, 0.49 mmol). The product [MoCl(CO)$_2${$Ph_2PCH_2C(O)NPh_2$-*P*}(η^5-C_5Me_5)], **19**, was recrystallised as a dark red powder by slow diffusion of toluene into a CH_2Cl_2 solution. (Yield = 280 mg, 79 %)

^1H NMR (270 MHz, $CDCl_3$) δ 7.73-7.09 [m, 20H, Ph], 3.84 [dd, 1H, -CH_2-, $^2J_{HH}$ = 16.0 Hz, $^2J_{HP}$ = 8.0 Hz], 3.29 [dd, 1H, -CH_2-, $^2J_{HH}$ = 16.0 Hz, $^2J_{HP}$ = 6.5 Hz], 1.77 [s, 15H, η^5-C_5Me_5],

$^{13}C\{^1H\}$ NMR (100 MHz, $CDCl_3$) δ 258.6 [d, M-CO, $^2J_{PC}$ = 18.2 Hz], 245.8 [d, M-CO, $^2J_{PC}$ = 4.8 Hz], 167.4 [>C=O], 121.3 - 110.6 [Ph], 96.9 [s, $\underline{C_5}Me_5$] 31.9 [d, -CH_2-, $^1J_{PC}$ = 26.0 Hz], 9.8 [Me]

$^{31}P\{^1H\}$ NMR (109 MHz, $CDCl_3$) δ 52.1 [$Ph_2PCH_2C(O)NPh_2$]

Infrared ν_{CO} (CH_2Cl_2) = 1944, 1860cm^{-1} (M-CO)
1669cm^{-1} (>C=O)

Microanalysis: $C_{38}H_{37}ClMoO_3PN.¼CH_2Cl_2$ requires: C, 62.1; H, 5.11; N, 1.89 %
found: C, 62.2; H, 5.23; N, 1.90 %

Reaction of [MoCl(CO)$_2${$Ph_2PNC_4H_3C(O)Me$-*P*}(η^5-C_5H_5)] with $AgBF_4$

$AgBF_4$ (148 mg, 0.76 mmol) was added to a solution of **14** (413 mg, 0.76 mmol) in CH_2Cl_2 (20 mL), and the mixture stirred with the exclusion of light for 20 minutes.

The solution was seen to darken, and a white preciptate of AgCl form. The solution was filtered through Celite, and the volatiles removed from the filtrate *in vacuo*. The residue was recrystallised by diffusion of toluene into a CH_2Cl_2 solution to give the product $[Mo(CO)_2\{Ph_2PNC_4H_3C(O)Me\text{-}P,O\}(\eta^5\text{-}C_5H_5)][BF_4]$, **20**, as a dark red powder. Crystals suitable for X-ray crystallography were obtained by a layer diffusion of toluene into a CH_2Cl_2 solution at room temperature, and the molecular structure determined. (Yield = 440 mg, 97 %).

^1H NMR (270 MHz, $CDCl_3$)	δ 7.67-7.45 [m, 11H, Ph and pyrrole], 7.29 [m, 1H, Pyrrole], 6.56 [m, 1H, Pyrrole], 5.55 [s, 5H, η^5-C_5H_5], 2.59 [s, 3H, Me]
$^{13}C\{^1H\}$ NMR (100 MHz, $CDCl_3$)	δ 248.0 [d, M-CO, $^2J_{PC}$ = 30.0 Hz], 240.0 [d, M-CO, $^2J_{PC}$ = 3.2 Hz], 199.3 [d, >C=O, $^3J_{PC}$ =6.8 Hz], 135.9 - 129.7 [Ph and pyrrole], 116.3, [pyrrole], 97.7 [η^5-C_5H_5], 27.8 [Me],
$^{31}P\{^1H\}$ NMR (109 MHz, $CDCl_3$)	δ 114.6 [$Ph_2PNC_4H_3C(O)Me$]
Infrared	ν_{CO} (CH_2Cl_2) = 1997, 1928 cm^{-1} (M-CO) 1553 cm^{-1} (>C=O)

Microanalysis; $C_{25}H_{21}BF_4MoNO_3P.¼CH_2Cl_2$ requires: C, 49.0; H, 3.50; N, 2.27 %
found: C, 49.2; H, 3.73; N, 2.17%

Reaction of $[MoCl(CO)_2\{Ph_2PNC_4H_3C(O)Me\text{-}P\}(\eta^5\text{-}C_5Me_5)]$ with $AgBF_4$

The reaction was carried out as for **20**, using **15** (315 mg, 0.511 mmol), $AgBF_4$ (100 mg, 0.52 mmol) and a reaction time of 1 hour. The red product $[Mo(CO)_2\{Ph_2PNC_4H_3C(O)Me\text{-}P,O\}(\eta^5\text{-}C_5Me_5)][BF_4]$, **21**, was recrystallised by diffusion of toluene into a CH_2Cl_2 solution. (Yield = 284 mg, 83 %).

^1H NMR (270 MHz, $CDCl_3$)	δ 7.85-7.56 [m, 10H, Ph], 7.20 [m, 1H, Pyrrole], 7.16 [m, 1H, Pyrrole] 6.59 [m,

	1H, Pyrrole], 2.79 [s, 3H, Me], 1.66 [s, 15H, η^5-C_5Me_5]
$^{13}C\{^1H\}$ NMR (100 MHz, $CDCl_3$)	δ 244.4 [d, $^2J_{PC}$ = 28.0 Hz, M-CO], 225.9 [d, $^2J_{PC}$ < 2 Hz, M-CO], 202.7 [d, $^2J_{PC}$ = 8.1 Hz, >C=O], 135.1 – 123.8 [m, Ph and pyrrole], 109.4 [s, η^5-$\underline{C_5}Me_5$], 27.3 [s, Me], 10.6 [s, η^5-$C_5\underline{Me_5}$]
$^{31}P\{^1H\}$ NMR (109 MHz, $CDCl_3$)	δ 108.9 [$Ph_2PNC_4H_3C(O)Me$]
Infrared	ν_{CO} (CH_2Cl_2) = 1990, 1916 cm^{-1} (M-CO) 1558 cm^{-1} (>C=O)

Reaction of [$MoCl(CO)_2\{Ph_2PCH_2C(O)Ph$-*P*}($\eta^5$-$C_5H_5$)] with $AgBF_4$

The reaction was carried out as for **20**, using **16** (63 mg, 0.101 mmol), $AgBF_4$ (20 mg, 0.102 mmol) and a reaction time of 30 minutes. The red product [$Mo(CO)_2\{Ph_2PCH_2C(O)Ph$-*P,O*}($\eta^5$-$C_5H_5$)][$BF_4$], **22**, was recrystallised from a diffusion of toluene into a CH_2Cl_2 solution. (Yield = 54 mg, 83 %).

^1H NMR (270 MHz, $CDCl_3$)	δ 7.98-7.33 [m, 15H, Ph], 5.53 [s, 5H, η^5-C_5H_5] 5.00 [dd, 1H, -CH_2-, $^2J_{HH}$ = 18.3Hz, $^2J_{HP}$ = 9.0 Hz], 3.73 [dd, 1H, -CH_2-, $^2J_{HH}$ = 18.3 Hz, $^2J_{HP}$ = 12.3 Hz]
$^{13}C\{^1H\}$ NMR (100 MHz, $CDCl_3$)	δ 247.0 [d, M-CO, $^2J_{PC}$=29.7 Hz], 241.9 [d, M-CO, $^2J_{PC}$ < 2 Hz], 216.1 [d, >C=O, $^2J_{PC}$ = 10.4 Hz], 137.2 - 128.9 [Ph], 96.1 [d, η^5-C_5H_5, $^2J_{PC}$ = 8.3 Hz], 44.7 [d, -CH_2-, $^1J_{PC}$ = 28.3 Hz],
$^{31}P\{^1H\}$ NMR (109 MHz, $CDCl_3$)	δ 72.5 [$Ph_2PCH_2C(O)Ph$]
Infrared	ν_{CO} (CH_2Cl_2) = 1987, 1912 cm^{-1} (M-CO) 1556 cm^{-1} (>C=O)

Reaction of $[MoCl(CO)_2\{Ph_2PCH_2C(O)Ph\text{-}P\}(\eta^5\text{-}C_5Me_5)]$ with $AgBF_4$

The reaction was carried out as before, using **17** (57 mg, 0.102 mmol), $AgBF_4$ (20 mg, 0.102 mmol) and a reaction time of 40 minutes. The red product $[Mo(CO)_2\{Ph_2PCH_2C(O)Ph\text{-}P,O\}(\eta^5\text{-}C_5Me_5)][BF_4]$, **23**, was recrystallised from a diffusion of toluene into a CH_2Cl_2 solution. (Yield = 59 mg, 95 %)

^1H NMR (270 MHz, $CDCl_3$)	δ 8.15-7.41 [m, 15H, Ph], 5.00 [dd, 1H, -CH_2-, $^2J_{HH}$ = 19.0 Hz, $^2J_{HP}$ = 8.2 Hz], 4.29 [dd, 1H, -CH_2-, $^2J_{HH}$ = 19.0 Hz, $^2J_{HP}$ = 11.2 Hz], 1.70 [s, 15H, η^5-C_5Me_5]
$^{13}C\{^1H\}$ NMR (100 MHz, $CDCl_3$)	δ 251.3 [d, M-CO, $^2J_{PC}$ = 27.2 Hz], 245.8 [d, M-CO, $^2J_{PC}$ < 2 Hz], 214.8 [d, >C=O, $^2J_{PC}$ = 12.5 Hz], 133.6 - 128.0 [Ph], 108.9 [s, η^5-$\underline{C_5}Me_5$], 44.5 [d, -CH_2-, $^1J_{PC}$ = 26.5 Hz], 10.2 [s, η^5-$C_5\underline{Me_5}$]
$^{31}P\{^1H\}$ NMR (109 MHz, $CDCl_3$)	δ 65.6 [$Ph_2PCH_2C(O)Ph$]
Infrared	ν_{CO} (CH_2Cl_2) = 1980, 1905 cm^{-1} (M-CO) 1559 cm^{-1} (>C=O)

Reaction of $[MoCl(CO)_2\{Ph_2PCH_2C(O)NPh_2\text{-}P\}(\eta^5\text{-}C_5H_5)]$ with $AgBF_4$

The reaction was carried out for **20**, using **18** (204 mg, 0.307 mmol), $AgBF_4$ (60 mg, 0.307 mmol) and a reaction time of 1 hour. The red product $[Mo(CO)_2\{Ph_2PCH_2C(O)NPh_2\text{-}P,O\}(\eta^5\text{-}C_5H_5)][BF_4]$, **24**, was recrystallised by diffusion of toluene into a CH_2Cl_2 solution. (Yield = 192 mg, 88 %)

^1H NMR (270 MHz, $CDCl_3$)	δ 7.61-7.7.10 [m, 20H, Ph], 5.51 [s, 5H, η^5-C_5H_5], 4.42 [dd, 1H, -CH_2-, $^2J_{HH}$ = 16.0 Hz, $^2J_{HP}$ = 8.6 Hz], 3.04 [dd, 1H, -CH_2-, $^2J_{HH}$ = 16.0 Hz, $^2J_{HP}$ = 12.5 Hz]

$^{13}C\{^1H\}$ NMR (67 MHz, $CDCl_3$)	δ 250.2 [d, $^2J_{CP}$ = 19.8 Hz, M-CO], 242.4 [d, $^2J_{CP}$ < 2 Hz, M-CO], 179.6 [d, $^2J_{CP}$ = 8.8 Hz, >C=O], 141.8 - 125.4 [m, Ph], 95.8 [Cp], 31.7 [d, $^2J_{CP}$ = 16.2 Hz, -CH_2-]
$^{31}P\{^1H\}$ NMR (109 MHz, $CDCl_3$)	δ 65.7 [$Ph_2PCH_2C(O)NPh_2$]
Infrared	ν_{CO} (CH_2Cl_2) = 1980, 1902 cm^{-1} (M-CO) 1542 cm^{-1} (>C=O)

Reaction of [MoCl(CO)$_2${Ph$_2$PCH$_2$C(O)NPh$_2$-*P*}(η^5-C$_5$Me$_5$)] with AgBF$_4$

The reaction was carried out as before, using **19** (186 mg, 0.259 mmol), $AgBF_4$ (51 mg, 0.259 mmol) and a reaction time of 2 hours. The purple product [Mo(CO)$_2${Ph$_2$PCH$_2$C(O)NPh$_2$-*P,O*}(η^5-C$_5$Me$_5$)][BF$_4$], **25**, was recrystallised by diffusion of toluene into a CH_2Cl_2 solution. (Yield = 185 mg, 93 %)

^1H NMR (270 MHz, $CDCl_3$)	δ 7.59-7.23 [m, 20H, Ph], 4.23 [dd, 1H, -CH_2-, $^2J_{HH}$ = 15.1 Hz, $^2J_{HP}$ = 8.6 Hz], 2.94 [dd, 1H, -CH_2-, $^2J_{HH}$ = 15.1 Hz, $^2J_{HP}$ = 12.3 Hz], 1.60 [s, 15H, η^5-C$_5$Me$_5$]
$^{13}C\{^1H\}$ NMR (67 MHz, $CDCl_3$)	δ 251.1 [d, M-CO, $^2J_{PC}$ = 18.6 Hz], 244.3 [d, M-CO, $^2J_{PC}$ < 2Hz], 178.8 [d, >C=O, $^2J_{PC}$ = 10.6 Hz], 120.4 – 109.9 [Ph], 98.2 [s, η^5-*C*$_5$Me$_5$], 31.5 [d, -CH_2-, $^1J_{PC}$ = 15.9 Hz], 10.5 [s, η^5-C$_5$*Me*$_5$]
$^{31}P\{^1H\}$ NMR (109 MHz, $CDCl_3$)	δ 57.1 [$Ph_2PCH_2C(O)NPh_2$]
Infrared	ν_{CO} (CH_2Cl_2) = 1963, 1888 cm^{-1} (M-CO) 1547 cm^{-1} (>C=O)

Reaction of $[Mo(CH_3)(CO)_3(\eta^5\text{-}C_5H_5)]$ with $HBF_4.Et_2O$ and $Ph_2PNC_4H_3C(O)Me$

$[Mo(CH_3)(CO)_3(\eta^5\text{-}C_5H_5)]$ (120 mg, 0.45 mmol) was dissolved in CH_2Cl_2 (20mL) and cooled to -78°C. $HBF_4.Et_2O$ (73μL of a 54 % solution in diethylether) was added dropwise with stirring. The solution was allowed to warm to room temperature, producing a colour change from orange to dark purple. The solution was cooled back to -78°C, and $Ph_2PNC_4H_3C(O)Me$ (133 mg, 0.46 mmol) was added. The solution was then allowed to warm back to room temperature and was stirred at ambient temperature for 16 hours, causing a colour change to dark red. The volatiles were *removed in vacuo*, to give the red product $[Mo(CO)_2\{Ph_2PNC_4H_3C(O)Me\text{-}P,O\}(\eta^5\text{-}C_5H_5)][BF_4]$, **20**. The complex was characterised by comparison of the $^{31}P\{^1H\}$ NMR and infrared spectra with a sample of the product previously prepared by another route. (Yield = 228 mg, 86 %).

$^{31}P\{^1H\}$ NMR (109 MHz, $CDCl_3$)	δ 114.6 $[Ph_2PNC_4H_3C(O)Me]$
Infrared	ν_{CO} (CH_2Cl_2) = 1997, 1928 cm^{-1} (M-CO)
	1553 cm^{-1} (>C=O)

Reaction of $[Mo(CH_3)(CO)_3(\eta^5\text{-}C_5H_5)]$ with $HBF_4.Et_2O$ and $Ph_2PCH_2C(O)Ph$

The reaction was carried out as for **20**, $[Mo(CH_3)(CO)_3(\eta^5\text{-}C_5H_5)]$ (137 mg, 0.51 mmol), $HBF_4.Et_2O$ (83 μL of a 54 % solution in diethylether), and $Ph_2PCH_2C(O)Ph$ (117 mg, 0.51 mmol). The red product $[Mo(CO)_2\{Ph_2PCH_2C(O)Ph\text{-}P,O\}(\eta^5\text{-}C_5H_5)][BF_4]$, **22**, was characterised by comparison of the $^{31}P\{^1H\}$ NMR and infrared spectra with a with a sample of the product previously prepared by another route. (Yield = 265 mg, 85 %).

$^{31}P\{^1H\}$ NMR (109 MHz, $CDCl_3$)	δ 72.5 $[Ph_2PCH_2C(O)Ph]$
Infrared	ν_{CO} (CH_2Cl_2) = 1987, 1912 cm^{-1} (M-CO)
	1556 cm^{-1} (>C=O)

Reaction of [MoCl(CO)$_2${Ph$_2$PCH$_2$C(O)Ph-*P*}(η^5-C$_5$H$_5$)] with BuLi

To a cooled (-78°C), stirred, solution of **16** (72mg, 0.129mmol) in THF (15mL) was added BuLi (81μL of a 1.6M solution in diethyl ether) in a dropwise fashion. The solution was allowed to warm to room temperature and stirred for a further hour. The solution was seen to lighten in colour, and a white precipitate of LiCl form. The solution was filtered through Celite, and the solvents removed from the filtrate *in vacuo* to give an orange residue. This was recrystallised by a hexane diffusion into a CH_2Cl_2 solution to give the product [Mo(CO)$_2${Ph$_2$PCH=C(O)Ph-*P,O*}(η^5-C$_5$H$_5$)], **26**, as an orange precipitate. Crystals suitable for X-ray crystallography were obtained by slow evaporation of a $CDCl_3$ solution at room temperature, and the molecular structure determined. (Yield = 62 mg, 93 %).

^{1}H NMR (400 MHz, $CDCl_3$)	δ 7.74-7.20 [m, 15H, Ph], 5.19 [d, $^1J_{HP}$ = 1.2 Hz, 1H, PCH=C], 5.04 [s, 5H, η^5-C$_5$H$_5$]
^{13}C{^{1}H} NMR (100 MHz, $CDCl_3$)	δ 132.2 – 125.7 [Ph], 94.0 [η^5-C$_5$H$_5$], 45.6 [d, $^1J_{CP}$ = 70.8 Hz, P<u>C</u>H=C]
^{31}P{^{1}H} NMR (109 MHz, $CDCl_3$)	δ 68.4 [Ph$_2$PCH=CPhO$^-$]
Infrared	ν_{CO} (CH_2Cl_2) = 1990, 1913 cm^{-1} (M-CO) 1460 cm^{-1} (>C=O)
Microanalysis; C$_{27}$H$_{21}$MoO$_3$P.¼CH$_2$Cl$_2$	requires: C, 60.4; H, 4.00 % found: C, 60.6; H, 4.21 %

Reaction of [MoCl(CO)$_2${Ph$_2$PNC$_4$H$_3$C(O)Me-*P*}(η^5-C$_5$H$_5$)] with BuLi

The reaction was repeated as for **26** using **14** (65 mg, 0.119 mmol) and BuLi (75 μL of a 1.6M solution in diethyl ether). Analysis by ^{31}P{^{1}H} NMR indicated the formation of multiple products which proved intractable.

Reaction of [MoCl(CO)$_2${Ph$_2$PNC$_4$H$_3$C(O)Me-*P*}(η^5-C$_5$Me$_5$)] with BuLi

The reaction was repeated as for **26** using **15** (67 mg, 0.103 mmol) and BuLi (68 μL of a 1.6M solution in diethyl ether). Analysis by $^{31}P\{^1H\}$ NMR indicated the formation of multiple products which proved intractable.

Reaction of [MoCl(CO)$_2${Ph$_2$PCH$_2$C(O)Ph-*P*}(η^5-C$_5$Me$_5$)] with BuLi

The reaction was repeated as for **26** using **17** (65 mg, 0.104 mmol) and BuLi (64 μL of a 1.6M solution in diethyl ether). Analysis by $^{31}P\{^1H\}$ NMR indicated the formation of multiple products which proved intractable.

Reaction of [MoCl(CO)$_2${Ph$_2$PCH$_2$C(O)NPh$_2$-*P*}(η^5-C$_5$H$_5$)] with BuLi

The reaction was repeated as for **26** using **18** (70 mg, 0.105 mmol) and BuLi (66 μL of a 1.6M solution in diethyl ether). Analysis by $^{31}P\{^1H\}$ NMR indicated the formation of multiple products which proved intractable.

Reaction of [MoCl(CO)$_2${Ph$_2$PCH$_2$C(O)NPh$_2$-*P*}(η^5-C$_5$Me$_5$)] with BuLi

The reaction was repeated as for **26** using **18** (80 mg, 0.104 mmol) and BuLi (66 μL of a 1.6M solution in diethyl ether). Analysis by $^{31}P\{^1H\}$ NMR indicated the formation of multiple products which proved intractable.

Reaction of [Mo(CO)$_2${Ph$_2$PCH$_2$C(O)Ph-*P,O*}(η^5-C$_5$H$_5$)][BF$_4$] with Et$_3$N

To a solution of **22** (74 mg, 0.133 mmol) in CH_2Cl_2 (10 mL) was added Et_3N (19 μL, 0.135 mmol). The solution was stirred for 2 hours, after which an IR spectrum showed no trace of starting material. The solvents were removed *in vacuo* to give an

orange residue. This was recrystallised by diffusion of hexane into a CH_2Cl_2 solution to give orange crystals of **26**. The compound was characterised by comparison of IR and $^{31}P\{^1H\}$ NMR data with a sample of the product previously prepared by another route. (Yield = 65 mg, 94 %)

$^{31}P\{^1H\}$ NMR (109 MHz, $CDCl_3$)	δ 68.4 [$Ph_2PCH{=}CPhO^-$]
Infrared	ν_{CO} (CH_2Cl_2) = 1990, 1913 cm^{-1} (M-CO)
	1460 cm^{-1} (>C=O)

Reaction of [Mo(CO)$_2${Ph$_2$PNC$_4$H$_3$C(O)Me-*P,O*}(η^5-C$_5$H$_5$)][BF$_4$] with Et$_3$N

The reaction was carried out as before using **20** (80 mg, 0.133 mmol) and Et_3N (19 μL, 0.135 mmol). Analysis by $^{31}P\{^1H\}$ NMR indicated the formation of multiple products which proved intractable.

Reaction of [Mo(CO)$_2${Ph$_2$PCH$_2$C(O)NPH$_2$-*P,O*}(η^5-C$_5$H$_5$)][BF$_4$] with Et$_3$N

The reaction was repeated as above using **24** (85 mg, 0.121 mmol) and Et_3N (17 μL, 125 mmol). Analysis by $^{31}P\{^1H\}$ NMR indicated the formation of multiple products which proved intractable.

Reaction of [Mo(CO)$_2${Ph$_2$PCH=C(O)Ph-*P,O*}(η^5-C$_5$H$_5$)] with HBF$_4$.Et$_2$O

To a cooled (-78°C), stirred, solution of **26** (69 mg, 130 mmol) in CH_2Cl_2 (10 mL) was added $HBF_4.Et_2O$ (40μL of a 53 % solution in diethyl ether) in a dropwise fashion. The solution was allowed to warm to room temperature and stirred for a further hour. A colour change by the solution from orange to red was observed. The solvents were removed *in vacuo* to give a red residue which was recrystallised by diffusion of toluene into a CH_2Cl_2 solution, to give a red oily precipitate of **22**. The

compound was characterised by comparison of IR and $^{31}P\{^1H\}$ NMR data with a sample of the product previously prepared by another route. (Yield = 75 mg, 95 %)

$^{31}P\{^1H\}$ NMR (109 MHz, $CDCl_3$)	δ 72.5 [$Ph_2PCH_2C(O)Ph$]
Infrared	ν_{CO} (CH_2Cl_2) = 1987, 1912 cm^{-1} (M-CO)
	1556 cm^{-1} (>C=O)

Reaction of [$Mo(CO)_2\{Ph_2PNC_4H_3C(O)Me$-*P,O*}($\eta^5$-$C_5H_5$)][$BF_4$] with [$PhCH_2NEt_3$][Cl]

To a solution of **20** (40 mg, 0.060 mmol) in CH_2Cl_2 (10mL) was added [$PhCH_2NEt_3$][Cl] (15 mg, 0.061 mmol). The solution was stirred for 2 hours, and then Et_2O (20mL) was added to precipitate the [$PhCH_2NEt_3$][BF_4] generated. The solution was filtered to remove the salt, and the organic removed *in vacuo* to give a red residue. The residue was recrystallised by diffusion of toluene into a CH_2Cl_2 solution to give **14** as an oily red precipitate. The product was characterised by comparison of the $^{31}P\{^1H\}$ NMR and IR spectra of the complex with a sample of the product previously prepared by another route. (Yield = 30 mg, 90 %)

$^{31}P\{^1H\}$ NMR (109 MHz, $CDCl_3$)	δ 112.2 [$Ph_2PNC_4H_3C(O)Me$]
Infrared	ν_{CO} (CH_2Cl_2) = 1970, 1888 cm^{-1} (M-CO)
	1654 cm^{-1} (>C=O)

Reaction of [$Mo(CO)_2\{Ph_2PNC_4H_3C(O)Me$-*P,O*}($\eta^5$-$C_5Me_5$)][$BF_4$] with [$PhCH_2NEt_3$][Cl]

The reaction was carried out as before using **21** (40 mg, 0.60 mmol) and [$PhCH_2NEt_3$][Cl] (15 mg, 0.061 mmol). The red product **15** was characterised by comparison of the IR and $^{31}P\{^1H\}$ NMR data of the complex, with a sample of the product previously prepared by another route (Yield = 30 mg, 81 %)

$^{31}P\{^{1}H\}$ NMR (109 MHz, $CDCl_3$)	δ 58.6 [$Ph_2PNC_4H_3C(O)Me$]
Infrared	ν_{CO} (CH_2Cl_2) = 1964, 1880 cm^{-1} (M-CO)
	1658 cm^{-1} (>C=O)

Reaction of [$Mo(CO)_2\{Ph_2PCH_2C(O)Ph$-*P,O*}($\eta^5$-$C_5H_5$)][$BF_4$] with [$PhCH_2NEt_3$][Cl]

The reaction was carried out as before using **22** (40 mg, 0.066 mmol) and [$PhCH_2NEt_3$][Cl] (16 mg, 0.066 mmol). The red product **16** was characterised by comparison of the IR and $^{31}P\{^{1}H\}$ NMR data of the complex, with a sample of the product previously prepared by another route. (Yield = 31 mg, 84 %)

$^{31}P\{^{1}H\}$ NMR (109 MHz, $CDCl_3$)	δ 48.2 [$Ph_2PCH_2C(O)Ph$]
Infrared	ν_{CO} (CH_2Cl_2) = 1970, 1888 cm^{-1} (M-CO)
	1656 cm^{-1} (>C=O)

Reaction of [$Mo(CO)_2\{Ph_2PCH_2C(O)Ph$-*P,O*}($\eta^5$-$C_5Me_5$)][$BF_4$] with [$PhCH_2NEt_3$][Cl[

The reaction was carried out as before using **23** (40 mg, 0.059 mmol) and [$PhCH_2NEt_3$][Cl] (14 mg, 0.60 mmol). The red product **17** was characterised by comparison of the IR and $^{31}P\{^{1}H\}$ NMR data of the complex with a sample of the product previously prepared by another route. (Yield = 29 mg, 78 %)

$^{31}P\{^{1}H\}$ NMR (109 MHz, $CDCl_3$)	δ 45.4 [$Ph_2PCH_2C(O)Ph$]
Infrared	ν_{CO} (CH_2Cl_2) = 1960, 1878 cm^{-1} (M-CO)
	1656 cm^{-1} (>C=O)

Reaction of $[Mo(CO)_2\{Ph_2PCH_2C(O)NPh_2\text{-}P,O\}(\eta^5\text{-}C_5H_5)][BF_4]$ with $[PhCH_2NEt_3][Cl]$

The reaction was carried out as before using **24** (40 mg, 0.060 mmol) and $[PhCH_2NEt_3][Cl]$ (14 mg, 0.60 mmol). The red product **18** was characterised by comparison of the IR and $^{31}P\{^1H\}$ NMR data of the complex with a sample of the product previously prepared by another route. (Yield = 32 mg, 76 %)

$^{31}P\{^1H\}$ NMR (109 MHz, $CDCl_3$)	δ 52.1 $[Ph_2PCH_2C(O)Ph]$
Infrared	ν_{CO} (CH_2Cl_2) = 1964, 1872 cm^{-1} (M-CO)
	1666 cm^{-1} (>C=O)

Reaction of $[Mo(CO)_2\{Ph_2PCH_2C(O)NPh_2\text{-}P,O\}(\eta^5\text{-}C_5Me_5)][BF_4]$ with $[PhCH_2NEt_3][Cl]$

The reaction was carried out as before using **25** (40 mg, 0.052 mmol) and $[Et_3NBenz]Cl$ (13 mg, 0.054 mmol). The red product **19** was characterised by comparison of the IR and $^{31}P\{^1H\}$ NMR data of the complex with a sample of the product previously prepared by another route. (Yield = 33 mg, 88 %)

$^{31}P\{^1H\}$ NMR (109 MHz, $CDCl_3$)	δ 52.1 $[Ph_2PCH_2C(O)NPh_2]$
Infrared	ν_{CO} (CH_2Cl_2) = 1944, 1860cm^{-1} (M-CO)
	1669cm^{-1} (>C=O)

Reaction of $[Mo(CO)_2\{Ph_2PNC_4H_3C(O)Me\text{-}P,O\}(\eta^5\text{-}C_5H_5)][BF_4]$ with PPh_2Me

To a solution of **20** (61 mg, 0.102 mmol) in CH_2Cl_2 (15mL) was added PPh_2Me (21 μL, 0.110 mmol) and the solution stirred for 48 hours. The product $[Mo(CO)_2\{Ph_2PNC_4H_3C(O)Me\text{-}P\}(PPh_2Me)(\eta^5\text{-}C_5H_5)][BF_4]$, **27**, was isolated by diffusion of hexane into a CH_2Cl_2 solution as an orange oil. (Yield = 73 mg, 90 %)

^{1}H NMR (400 MHz, $CDCl_3$)	δ 7.75 – 7.22 [m, 20H, Ph], 6.60 [m, 1H, pyrrole], 5.21 [s, 5H, η^5-C_5H_5], 2.21 [d, $^2J_{HP}$ = 9.4 Hz, 3H, $Ph_2P\underline{CH_3}$], 2.05 [s, 3H, CH_3]
$^{13}C\{^1H\}$ NMR (100 MHz, $CDCl_3$)	δ 230.8 [t, $^2J_{CP}$ = 29.2 Hz] 185.1 [>C=O], 137.9 [d, J_{CP} = 12.4 Hz, pyrrole], 133.9 – 128.2 [Ph and pyrrole], 126.6 [pyrrole], 112.6 [d, J_{CP} = 9.5 Hz, pyrrole], 96.1 [η^5-C_5H_5], 25.7 [Me], 19.8 [d, $^1J_{CP}$ = 34.8 Hz, Me]
$^{31}P\{^1H\}$ NMR (109 MHz, $CDCl_3$)	δ 122.5 [d, $Ph_2PNC_4H_3C(O)Me$, $^2J_{PP}$ = 20.9 Hz], 40.6 [d, PPh_2Me, $^2J_{PP}$ = 20.9 Hz]
Infrared	ν_{CO} (CH_2Cl_2) = 1978, 1900 cm^{-1} (M-CO) 1669 cm^{-1} (>C=O)

Reaction of $[Mo(CO)_2\{Ph_2PNC_4H_3C(O)Me\text{-}P,O\}(\eta^5\text{-}C_5H_5)][BF_4]$ with PMe_2Ph

The reaction was carried out as for **27** using **20** (61 mg, 0.102 mmol), PMe_2Ph (21 μL, 0.110 mmol) and a reaction time of 48 hours. The product $[Mo(CO)_2\{Ph_2PNC_4H_3C(O)Ph\text{-}P\}\{PPhMe_2\}(\eta^5\text{-}C_5H_5)][BF_4]$, **28**, was isolated by diffusion of hexane into a CH_2Cl_2 solution as an orange oil. (Yield = 64 mg, 86 %)

^{1}H NMR (400 MHz, $CDCl_3$)	δ 7.68 – 7.28 [m, 25H, Ph], 7.15 [m, 1H, pyrrole], 6.96 [m, 1H, pyrrole], 6.42 [m, 1H, pyrrole], 5.14 [s, 5H, η^5-C_5H_5], 2.16 [s, 3H, Me], 1.96 [d $^2J_{HP}$ = 9.9Hz, 6H, PMe_2Ph]
$^{13}C\{^1H\}$ NMR (100 MHz, $CDCl_3$)	δ 231.2 [t, $^2J_{CP}$ = 29.2 Hz], 184.7 [>C=O], 136.5 – 125.9 [Ph and pyrrole], 112.3 [d, J_{CP} = 9.6 Hz, pyrrole], 96.3 [η^5-C_5H_5], 25.8 [Me], 18.8 [d, $^1J_{CP}$ = 34.3 Hz, Me]

$^{31}P\{^{1}H\}$ NMR (109MHz, $CDCl_3$)	δ 127.7 [d, $Ph_2PNC_4H_3C(O)Me$, $^{2}J_{PP}$ = 21.1 Hz], 26.2 [d, PMe_2Ph, $^{2}J_{PP}$ = 20.9 Hz
Infrared	ν_{CO} (CH_2Cl_2) = 1974, 1898 cm^{-1} (M-CO) 1669 cm^{-1} (>C=O)

Reaction of $[Mo(CO)_2\{Ph_2PNC_4H_3C(O)Me\text{-}P,O\}(\eta^5\text{-}C_5H_5)][BF_4]$ with PMe_3

The reaction was carried out as for **27** using **20** (74 mg, 0.124 mmol), PMe_3 (124 mL of a 1M THF solution) and a reaction time of 48 hours. The product $[Mo(\eta^5\text{-}C_5H_5)(CO)_2\{Ph_2PNC_4H_3C(O)Ph\text{-}P\}\{PMe_3\}][BF_4]$, **29**, was isolated by diffusion of hexane into a CH_2Cl_2 solution as an orange oil. (Yield = 71 mg, 85 %)

^{1}H NMR (400 MHz, $CDCl_3$)	δ 7.65 – 7.20 [m, 20H, Ph], 7.30 [m, 1H, pyrrole], 7.04 [m, 1H, pyrrole], 6.44 [m, 1H, pyrrole], 5.22 [s, 5H, η^5-C_5H_5], 2.16 [s, 3H, Me], 1.66 [d, $^{2}J_{HP}$ = 10.3 Hz, 9H, PMe_3]
$^{13}C\{^{1}H\}$ NMR (100 MHz, $CDCl_3$)	231.1 [t, $^{2}J_{CP}$ = 29.6 Hz, M-CO], 184.4 [>C=O], 135.7 – 127.3 [Ph and pyrrole], 124.8 [pyrrole], 111.0 [d, J_{CP} = 7.6 Hz, pyrrole], 93.5 [η^5-C_5H_5], 25.5 [Me], 18.1 [d, $^{1}J_{CP}$=35.2 Hz, PMe_3]
$^{31}P\{^{1}H\}$ NMR (161 MHz, $CDCl_3$)	δ 125.1 [d, $Ph_2PNC_4H_3C(O)Me$, $^{2}J_{PP}$ = 23.5 Hz], 20.3 [d, PMe_3, $^{2}J_{PP}$ = 23.5 Hz]
Infrared	ν_{CO} (CH_2Cl_2) = 1972, 1896 cm^{-1} (M-CO) 1664 cm^{-1} (>C=O)

Reaction of $[Mo(CO)_2\{Ph_2PNC_4H_3C(O)Me\}(\eta^5\text{-}C_5H_5)][BF_4]$ with $P(OMe)_3$

The reaction was carried out as for **27** using **20** (47 mg, 0.079 mmol), $P(OMe)_3$ (10 μL, 0.080 mmol) and a reaction time of 24 hours. The product

$[Mo(CO)_2\{Ph_2PNC_4H_3C(O)Ph\text{-}P\}\{P(OMe)_3\}(\eta^5\text{-}C_5H_5)][BF_4]$, **30**, was isolated by diffusion of hexane into a CH_2Cl_2 solution as an orange oil. (Yield = 52 mg, 91 %)

^1H NMR (270 MHz, $CDCl_3$)	δ 7.99 – 6.60 (m, 10H, Ph), 6.80 (m, 1H, pyrrole), 6.23 (m, 1H, pyrrole), 5.94 (m, 1H, pyrrole), 5.33 (5H, s, η^5-C_5H_5), 3.42 (d $^3J_{HP}$ = 13.3 Hz, 9H, P{OMe}$_3$), 2.10 (s, 3H, Me)
$^{13}C\{^1H\}$ NMR (100 MHz, $CDCl_3$)	δ 223.6 [t, $^2J_{CP}$ = 29.7 Hz, M-CO], 185.5 [>C=O], 137.0 – 124.9 [Ph and pyrrole], 112.3 [d, J_{CP} = 8.6 Hz, pyrrole], 94.8 [η^5-C_5H_5], 55.0 [d, $^2J_{CP}$ = 8.6 Hz, MeO], 26.5 [Me]
$^{31}P\{^1H\}$ NMR (109 MHz, $CDCl_3$)	δ 168.7 [d, P(OMe)$_3$, $^2J_{PP}$ = 23.5 Hz], 121.2 [d, $Ph_2PNC_4H_3C(O)Me$, $^2J_{PP}$ = 23.5 Hz]
Infrared	ν_{CO} (CH_2Cl_2) = 1966, 1889 cm^{-1} (M-CO) 1665 cm^{-1} (>C=O)

Reactions of $[Mo(CO)_2\{Ph_2PNC_4H_3C(O)Me\text{-}P,O\}(\eta^5\text{-}C_5H_5)][BF_4]$ with PPh_3, dpph, PCy_3, but-2-yne, *tert*-butylphosphaalkyne and triphenylphosphine oxide

The reactions were carried out as for **27**, using **20**, 1 equivalent of the added reagent (0.5 equivalents for dpph) and $CDCl_3$ (0.5mL). The reactions were monitored by NMR spectroscopy but, in all cases, even after 14 days there was no evidence for the formation of any products.

Reactions of $[Mo(CO)_2\{Ph_2PNC_4H_3C(O)Me\text{-}P,O\}(\eta^5\text{-}C_5Me_5)][BF_4]$ with PPh_3, PPh_2Me, PMe_2Ph, PMe_3, $P(OMe)_3$, dpph, PCy_3, but-2-yne, *tert*-butylphosphaalkyne and triphenylphosphine oxide

The reactions were carried out as for **27**, using **21** (60 mg, 0.088 mmol, $CDCl_3$ (0.5 mL) and one equivalent (0.5 equivalents for dpph) of the added reagent. The reactions were monitored by NMR spectroscopy but, in all cases, even after 14 days there was no evidence for the formation of any products.

Reaction of $[Mo(CO)_2\{Ph_2PCH_2C(O)Ph\text{-}P,O\}(\eta^5\text{-}C_5H_5)][BF_4]$ with PPh_3

The reaction was repeated as for **27** using **22** (62 mg, 0.102 mmol) and PPh_3 (27 mg, 0.103 mmol) and a reaction time of 7 days. The solvents were removed *in vacuo* to give a red residue which was isolated by diffusion of toluene into a CH_2Cl_2 solution to give a red oily precipitate of $[Mo(CO)_2\{Ph_2PCH_2C(O)Ph\text{-}P\}(PPh_3)(\eta^5\text{-}C_5H_5)][BF_4]$, **31**. (Yield = 83 mg, 94 %).

^1H NMR (270 MHz, $CDCl_3$)	δ 7.81-7.33 [m, 30H, Ph], 5.17 [s, 5H, η^5-C_5H_5] 4.62 [d, 2H, -CH_2-, $^2J_{HP}$ = 8.3 Hz]
$^{13}C\{^1H\}$ NMR (100 MHz, $CDCl_3$)	δ 233.9 [t, M-CO, $^2J_{PC}$ = 27.1 Hz], 193.3 [d, >C=O, $^2J_{PC}$ = 5.7 Hz], 136.3 - 128.0 [Ph], 95.4 [η^5-C_5H_5], 40.9 [d, -CH_2-, $^1J_{PC}$= 28.5 Hz]
$^{31}P\{^1H\}$ NMR (161 MHz, $CDCl_3$)	δ 57.7 [d, PPh_3, $^2J_{PP}$ = 18.8 Hz], 47.3 [d, $Ph_2PCH_2C(O)Ph$, $^2J_{PP}$ = 18.8 Hz]
Infrared	ν_{CO} (CH_2Cl_2) = 1974, 1895 cm^{-1} (M-CO) 1684 cm^{-1} (>C=O)

Reaction $[Mo(CO)_2\{Ph_2PCH_2C(O)Ph\text{-}P,O\}(\eta^5\text{-}C_5H_5)][BF_4]$ with PPh_2Me

The reaction was carried out as for **27** using **22** (68 mg, 0.112 mmol), PPh_2Me (23 μL, 0.114 mmol) and a reaction time of 18 hours. The product $[Mo(CO)_2\{Ph_2PCH_2C(O)Ph\text{-}P\}(PPh_2Me)(\eta^5\text{-}C_5H_5)][BF_4]$, **32**, was isolated by diffusion of toluene into a CH_2Cl_2 solution to give a red oily precipitate. (Yield = 81 mg, 90 %)

^1H NMR (400 MHz, $CDCl_3$)	δ 7.73-7.27 [m, 30H, Ph], 5.21 [s, 5H, η^5-C_5H_5] 4.42 [d, 2H, -CH_2-, $^2J_{HP}$ = 8.6 Hz], 2.23 [d, 3H, Me, $^2J_{HP}$ = 9.0 Hz]
$^{13}C\{^1H\}$ NMR (100 MHz, $CDCl_3$)	δ 234.1 [t, $^2J_{CP}$ = 27.1 Hz, M-CO], 193.3 [d, $^1J_{CP}$ = 4.7 Hz, >C=O], 134.3 – 128.3 [Ph], 95.1 [η^5-C_5H_5], 40.6 [d, $^1J_{CP}$ = 27.1 Hz, -CH_2-], 19.9 [d, $^1J_{CP}$ = 35.6 Hz, PPh_2Me]
$^{31}P\{^1H\}$ NMR (161 MHz, $CDCl_3$)	δ 48.8 [d, $Ph_2PCH_2C(O)Ph$, $^2J_{PP}$ = 19.8 Hz], 41.2 [d, PPh_2Me, $^2J_{PP}$ = 19.8 Hz]
Infrared	ν_{CO} (CH_2Cl_2) = 1973, 1892 cm^{-1} (M-CO) 1665 cm^{-1} (>C=O)

Reaction of $[Mo(CO)_2\{Ph_2PCH_2C(O)Ph\text{-}P,O\}(\eta^5\text{-}C_5H_5)][BF_4]$ with PMe_2Ph

The reaction was carried out as for **27** using **22** (72 mg, 0.130 mmol), PMe_2Ph (20 μL, 0.133 mmol) and a reaction time of 18 hours. The product $[Mo(CO)_2\{Ph_2PCH_2C(O)Ph\text{-}P,O\}(PMe_2Ph)(\eta^5\text{-}C_5H_5)][BF_4]$, **33**, was isolated by diffusion of toluene into a CH_2Cl_2 solution to give a red oily precipitate. (Yield = 85 mg, 88 %)

^1H NMR (400 MHz, $CDCl_3$)	δ 7.79-7.35 [m, 25H, Ph], 5.28 [s, 5H, η^5-C_5H_5] 4.33 [d, 2H, -CH_2-, $^2J_{HP}$ = 8.6 Hz], 2.06 [d, 6H, Me, $^2J_{HP}$ = 9.0 Hz]

$^{13}C\{^1H\}$ NMR (100 MHz, $CDCl_3$)	δ 234.3 [t, $^2J_{CP}$ = 27.6 Hz, M-CO], 193.0 [d, $^1J_{CP}$ = 3.7 Hz, >C=O], 144.8 – 128.0 [Ph], 94.7 [η^5-C_5H_5], 40.7 [d, $^1J_{CP}$ = 28.5 Hz, -CH_2-], 18.8 [d, $^1J_{CP}$ = 34.2 Hz, P*Me*$_2$Ph]
$^{31}P\{^1H\}$ NMR (161 MHz, $CDCl_3$)	δ 52.1 [d, $Ph_2PCH_2C(O)Ph$, $^2J_{PP}$ = 21.0 Hz], 25.6 [d, PMe_2Ph, $^2J_{PP}$ = 21.0 Hz]
Infrared	ν_{CO} (CH_2Cl_2) = 1972, 1890 cm^{-1} (M-CO) 1663 cm^{-1} (>C=O)

Reaction of $[Mo(CO)_2\{Ph_2PCH_2C(O)Ph\text{-}P,O\}(\eta^5\text{-}C_5H_5)][BF_4]$ with PMe_3

The reaction was carried out as for **27** using **22** (84 mg, 0.138 mmol), PMe_3 (138 μL of 1M solution in THF) and a reaction time of 18 hours. The product **26**, was recrystallised from a diffusion of hexane into a CH_2Cl_2 solution as orange crystals. The compound was characterised by comparison of IR and $^{31}P\{^1H\}$ NMR data with the previously synthesised compound. (Yield = 69 mg, 96 %)

$^{31}P\{^1H\}$ NMR (109 MHz, $CDCl_3$)	δ 68.4 [$Ph_2PCH{=}CPhO^-$]
Infrared	ν_{CO} (CH_2Cl_2) = 1990, 1913 cm^{-1} (M-CO) 1460 cm^{-1} (>C=O)

Reaction of $[Mo(CO)_2\{Ph_2PCH_2C(O)Ph\text{-}P,O\}(\eta^5\text{-}C_5H_5)][BF_4]$ with dpph

The reaction was carried out as for **27** using **22** (79 mg, 0.130 mmol), dpph (30 mg, 0.075 mmol) and a reaction time of 18 hours. The product $[\{Mo(CO)_2\{Ph_2PCH_2C(O)Ph\text{-}P\}(\eta^5\text{-}C_5H_5)\}_2(dpph)][BF_4]_2$, **34**, was isolated by diffusion of toluene into a CH_2Cl_2 solution to give a red oily precipitate. (Yield = 90 mg, 83 %)

^{1}H NMR (400 MHz, $CDCl_3$)	δ 7.95 – 7.16 [m, 50H, Ph], 5.21 [s, 10H, η^5-C_5H_5], 4.50 [d, $^1J_{HP}$ = 8.2 Hz, 4H, PCH_2C(O)-], 3.66 [m, 4H, P$CH_2CH_2CH_2$-], 2.55 [m, 4H, $PCH_2CH_2CH_2$-], 1.18 [m, 4H, $PCH_2CH_2CH_2$-]
^{13}C{^{1}H} NMR (100 MHz, $CDCl_3$)	δ 234.1 [t, $^2J_{CP}$ = 27.1 Hz, M-CO], 193.3 [t, $^2J_{CP}$ = 5.3 Hz, M-CO], 139.8 – 127.2 [Ph], 95.3 [η^5-C_5H_5], 40.3 [d, $^1J_{CP}$ = 28.1 Hz, -$\underline{C}H_2C(O)$-], 35.8 [d, $^1J_{CP}$ = 28.1 Hz, P$\underline{C}H_2CH_2CH_2$-], 34.9 [d, $^2J_{CP}$ = 8.2Hz, $PCH_2\underline{C}H_2CH_2$-], 33.4 [d, $^2J_{CP}$ < 2 Hz, $PCH_2CH_2\underline{C}H_2$-]
^{31}P{^{1}H} NMR (161 MHz, $CDCl_3$)	δ 48.6 [d, $^2J_{PP}$ = 18.5 Hz, $Ph_2PCH_2C(O)Ph$], 47.3 [d, $^2J_{PP}$ = 18.5 Hz, dpph]
Infrared	ν_{CO} (CH_2Cl_2) = 1969, 1889 cm^{-1} (M-CO) 1679 cm^{-1} (>C=O)

Reaction of [Mo(CO)$_2$(Ph$_2$PCH$_2$C(O)Ph-*P,O*}(η^5-C$_5$H$_5$)][BF$_4$] with P(OMe)$_3$

The reaction was carried out as for **27**, using **22** (24 mg, 0.039 mmol), trimethylphosphite (6 μL, 0.041 mmol) and a reaction time of 18 hours. Analysis by ^{31}P{^{1}H} NMR indicated the formation of multiple products which proved intractable.

Reactions of [Mo(CO)$_2$(Ph$_2$PCH$_2$C(O)Ph-*P,O*}(η^5-C$_5$H$_5$)][BF$_4$] with PCy$_3$, but-2-yne, *tert*-butylphosphaalkyne and triphenylphosphine oxide

The reactions were carried out as for **27**, using **22**, 1 equivalent of the added reagents and $CDCl_3$ (0.5mL). The reactions were monitored by NMR spectroscopy but, in all cases, even after 14 days there was no evidence for the formation of any products.

Reactions of $[Mo(CO)_2\{Ph_2PCH_2C(O)Ph\text{-}P,O\}(\eta^5\text{-}C_5Me_5)][BF_4]$ with PPh_3, PPh_2Me, PMe_2Ph, PMe_3, $P(OMe)_3$, dpph, but-2-yne, with *tert*-butylphosphaalkyne and triphenylphosphine oxide

The reactions were carried out as for **27**, using **23** (60mg, 0.088mmol), 1 equivalent of the added reagent (0.5 equivalents for dpph) and $CDCl_3$ (0.5mL). The reactions were monitored by NMR spectroscopy but, in all cases, even after 14 days there was no evidence for the formation of any products.

Reaction of $[Mo(CO)_2\{Ph_2PCH_2C(O)NPh_2\text{-}P,O\}(\eta^5\text{-}C_5H_5)][BF_4]$ with PPh_3

The reaction was carried out as for **27**, using **24** (44 mg, 0.063 mmol), PPh_3 (17 mg, 0.063 mmol) and a reaction time of 14 days. The product $[Mo(CO)_2\{Ph_2PCH_2C(O)NPh_2\text{-}P\}(PPh_3)(\eta^5\text{-}C_5H_5)][BF_4]$, **35**, was isolated by diffusion of toluene into a CH_2Cl_2 solution to give a red oily precipitate. (Yield = 55 mg, 90 %)

^1H NMR (270 MHz, $CDCl_3$)	δ 7.79 – 7.27 [m, 35H, Ph], 5.20 [s, 5H, η^5-C_5H_5], 3.65 [d, $^2J_{HP}$ = 7.8 Hz, 2H, -CH_2-]
$^{13}C\{^1H\}$ NMR (100 MHz, $CDCl_3$)	δ 234.8 [t, $^2J_{CP}$ = 17.4 Hz, M-CO], 165.0 [>C=O], 136.7 – 126.8 [Ph], 95.2 [η^5-C_5H_5], 27.8 [d, $^1J_{CP}$ = 16.8 Hz, -CH_2-]
$^{31}P\{^1H\}$ NMR (161 MHz, $CDCl_3$)	δ 60.1 [d, PPh_3, $^2J_{PP}$=17.6 Hz], 54.6 [d, $Ph_2PCH_2C(O)NPh_2$, $^2J_{PP}$=17.6 Hz],
Infrared	ν_{CO} (CH_2Cl_2) = 1974, 1896 cm^{-1} (M-CO) 1663 cm^{-1} (>C=O)

Reaction of $[Mo(CO)_2\{Ph_2PCH_2C(O)NPh_2\text{-}P,O\}(\eta^5\text{-}C_5H_5)][BF_4]$ with PPh_2Me

The reaction was carried out as for **27**, using **34** (44 mg, 0.063 mmol), PPh_2Me (12 μL, 0.063 mmol) and a reaction time of 7 days. The product $[Mo(CO)_2\{Ph_2PCH_2C(O)NPh_2\text{-}P\}(PMePh_2)(\eta^5\text{-}C_5H_5)][BF_4]$, **23**, was isolated by diffusion of toluene into a CH_2Cl_2 solution to give a red oily precipitate. (Yield = 49 mg, 86 %)

^1H NMR (270 MHz, $CDCl_3$)	δ 7.73 – 6.86 [m, 30H, Ph], 5.20 [s, 5H, η^5-C_5H_5], 3.72 [d $^2J_{HP}$ = 7.81 Hz, 2H, CH_2], 2.16 [d $^2J_{HP}$ = 9.4 Hz, 3H, Me]
$^{13}C\{^1H\}$ NMR (100 MHz, $CDCl_3$)	δ 235.2 [d, $^2J_{CP}$ = 17.5 Hz, M-CO], 165.1 [>C=O], 134.1 – 126.1 [Ph], 94.9 [η^5-C_5H_5], 27.6 [d, $^1J_{CP}$ = 16.9 Hz, -CH_2-], 20.1 [d $^1J_{CP}$ = 33.3 Hz, Me]
$^{31}P\{^1H\}$ NMR (161 MHz, $CDCl_3$)	δ 55.6 [d, $^2J_{PP}$ = 17.6 Hz, $Ph_2PCH_2C(O)NPh_2$], 41.3 [d, $^2J_{PP}$=17.6Hz, PPh_2Me]
Infrared	ν_{CO} (CH_2Cl_2) = 1972, 1892 cm^{-1} (M-CO) 1663 cm^{-1} (>C=O)

Reaction of $[Mo(CO)_2\{Ph_2PCH_2C(O)NPh_2\text{-}P,O\}(\eta^5\text{-}C_5H_5)][BF_4]$ with PMe_2Ph

The reaction was carried out as for **27**, using **24** (44 mg, 0.063 mmol), PMe_2Ph (8 μL, 0.063 mmol) and a reaction time of 7 days. The product $[Mo(CO)_2\{Ph_2PCH_2C(O)NPh_2\}(PMe_2Ph)(\eta^5\text{-}C_5H_5)][BF_4]$, **37**, was isolated by diffusion of toluene into a CH_2Cl_2 solution to give a orange oily precipitate. (Yield = 45 mg, 85 %)

^1H NMR (270 MHz, $CDCl_3$)	δ 7.61-6.86 [m, 25H, Ph], 5.07 [s, 5H, η^5-C_5H_5], 3.67 [d, $^2J_{HP}$ = 8.2 Hz, 2H, CH_2], 2.04 [d, $^2J_{HP}$ = 9.9 Hz, 6H, Me]

$^{13}C\{1H\}$ NMR (100 MHz, $CDCl_3$)	δ 235.3 [t, $^2J_{CP}$ = 17.6 Hz, M-CO], 164.9 [>C=O], 134.6 – 126.5 [Ph], 94.7 [η^5-C_5H_5], 27.5 [d, $^1J_{CP}$ = 17.1 Hz, -CH_2-], 18.7 [d, $^1J_{CP}$ = 33.9 Hz, P*Me*$_2$Ph]
$^{31}P\{^1H\}$ NMR (161 MHz, $CDCl_3$)	δ 55.8 [d, $^2J_{PP}$ = 21.0 Hz, $Ph_2PCH_2C(O)NPh_2$], 26.5 [d, $^2J_{PP}$ = 21.0 Hz, PMe_2Ph]
Infrared	ν_{CO} (CH_2Cl_2) = 1968, 1888 cm^{-1} (M-CO) 1663 cm^{-1} (>C=O)

Reaction of $[Mo(CO)_2\{Ph_2PCH_2C(O)NPh_2$-*P,O*$\}(\eta^5$-$C_5H_5)][BF_4]$ with PMe_3

The reaction was carried out as for **27**, using **24** (44 mg, 0.063 mmol), PMe_3 (63 μL of 1M solution in THF) and a reaction time of 7 days. The product $[Mo(CO)_2\{Ph_2PCH_2C(O)NPh_2$-*P*$\}(PMe_3)(\eta^5$-$C_5H_5)][BF_4]$, **38**, was isolated by diffusion of toluene into a CH_2Cl_2 solution to give a orange oily precipitate. (Yield = 43 mg, 88 %)

^1H NMR (270 MHz, $CDCl_3$)	δ 7.88 - 6.97 [m, 10H, Ph], 5.36 [s, 5H, η^5-C_5H_5], 3.85 [d, $^2J_{HP}$ = 8.2 Hz, 2H, -CH_2-], 1.70 [d, $^2J_{HP}$ = 10.2 Hz, 9H, Me]
$^{13}C\{^1H\}$ NMR (100 MHz, $CDCl_3$)	δ 235.7 [d, $^2J_{CP}$ = 17.6 Hz, M-CO], 165.1 [>C=O], 134.0 – 127.1 [Ph], 94.8 [η^5-C_5H_5], 27.4 [d, $^1J_{CP}$ = 16.9 Hz, -CH_2-], 18.2 [d, $^1J_{CP}$ = 34.9 Hz, P*Me*$_3$]
$^{31}P\{^1H\}$ NMR (161 MHz, $CDCl_3$)	δ 55.6 [d, $^2J_{PP}$ = 21.1 Hz, $Ph_2PCH_2C(O)NPh_2$], 22.5 [d, $^2J_{PP}$ = 21.1 Hz, PMe_3]
Infrared	ν_{CO} (CH_2Cl_2) = 1968, 1888 cm^{-1} (M-CO) 1663 cm^{-1} (>C=O)

Reaction of $[Mo(CO)_2\{Ph_2PCH_2C(O)NPh_2\text{-}P,O\}(\eta^5\text{-}C_5H_5)][BF_4]$ with $P(OMe)_3$, dpph and PCy_3

The reactions were carried out as for **27**, using **24** , one equivalent of the added reagent (0.5 equivalents for dpph) and a reaction time of 7 days. In all reactions, analysis by $^{31}P\{^1H\}$ NMR indicated the formation of multiple products which proved intractable.

Reactions of $[Mo(CO)_2\{Ph_2PCH_2C(O)NPh_2\text{-}P,O\}(\eta^5\text{-}C_5H_5)][BF_4]$ with but-2-yne, *tert*-butylphosphaalkyne and triphenylphosphine oxide

The reactions were carried out as for **27** using **24,** 1 equivalent of the added reagent and $CDCl_3$ (0.5mL). The reactions were monitored by NMR spectroscopy but, in all cases, even after 14 days there was no evidence for the formation of any products.

Reaction of $[Mo(\eta^5\text{-}C_5Me_5)(CO)_2(Ph_2PCH_2CONPh_2)][BF_4]$ with PPh_3, PPh_2Me, PMe_2Ph, PMe_3, $P(OMe)_3$, dpph, PCy_3, but-2-yne, *tert*-butylphosphaalkyne and triphenylphosphine oxide

The reactions were carried out as for **27** using **26,** 1 equivalent of the added reagent (0.5 equivalents for dpph) and $CDCl_3$ (0.5mL). The reactions were monitored by NMR spectroscopy but, in all cases, even after 14 days there was no evidence for the formation of any products.

Reaction of $[Pd_3(\mu_3\text{-}CO)(\mu\text{-}dppm)_3][PF_6]_2$ with *tert*-butylphosphaalkyne

To a solution of $[Pd_3(\mu_3\text{-}CO)(\mu\text{-}dppm)_3][PF_6]_2$ (100 mg, 0.056 mmol) in acetone (15 mL) was added *tert*-butylphosphaalkyne (20 μL, 0.132 mmol). The mixture was stirred at room temperature for 36 hours, after which no evidence of starting material was seen in the IR spectra. The solvents were removed *in vacou* to give a brown oil.

This was recrystallised by diffusion of toluene into an acetone solution to give the product $[Pd_3(P{\equiv}CBu^t)_2(\mu\text{-dppm})_3][PF_6]_2$, **39**, as green crystals. (Yield = 105 mg, 95 %)

^1H NMR (400 MHz, d_6-acetone)	δ 7.49-6.91 [m, 60H, Ph], 4.62 [br m, 6H, $-CH_2-$], 1.77 [s, 18H, Bu^t]
$^{13}C\{^1H\}$ NMR (100 MHz, d_6-acetone)	δ 214.77 [at, $^1J_{CP} + {}^3J_{CP}$ = 59.9 Hz, $P{\equiv}\underline{C}Bu^t$], 133.33 – 128.97 [Ph], 32.50 [s, $C\underline{Me_3}$], 31.41 [t, $^1J_{CP}$ = 117.0 Hz, $P\underline{CH_2}P$]
$^{31}P\{^1H\}$ NMR (109 MHz, d_6-acetone)	δ -6.3 [t, $^2J_{PP}$ = 21.7 Hz, 6P, dppm], -121.4 [sept, $^2J_{PP}$ = 21.7, Hz 2P, $P{\equiv}CBu^t$], -142.8 [sept, $^1J_{PF}$ = 710.7 Hz, 2P, PF_6^-]

6.3 References

1 W.A. Herrmann (Ed.), *Synthetic Methods of Organometallic and Inorganic Chemistry*, Thieme, **8**, 103.

2 T.S. Piper and G. Wilkinson, *J. Inorg. Nucl. Chem.*, 1956, **3**, 104.

3 L. Manojlović-Muir, K,W. Muir, B.R. Lloyd and R.J. Puddephatt, *J. Chem. Soc., Chem. Commun.*, 1983, 1336.

4 M. Palmer, *PhD thesis*, University of Bath, 2000.

5 S.-E. Bouaoud, P. Braunstein, D. Grandjean, D. Matt and D. Nobel, *Inorg. Chem.*, 1986, **25**, 3765.

6 J. Andrieu, P. Braunstein and A.D. Burrows, *J. Chem. Res.(S)*, 1993, 380.

7 Single Crystal X-Ray Diffraction Data

7.1 Crystallography

Data for complexes **2, 3** and $\mathbf{L}^1$ were collected on a Enraf-Nonius CAD4 automatic four-circle diffractometer, data for **14, 26** and **40** were collected on a Kappa-CCD area detector diffractometer, whilst data for **20** was collected on a Siemens SMART CCD area detector diffractometer. The crystal structures were solved by Dr. Mary Mahon, with the exception of **20** which was solved by Dr. John Jeffrey. The solution of the structures and their refinement was carried out using SHELX86[1] and SHELX93[2] respectively. The figures of the asymmetric units along with their labelling were produced using ORTEX.[3]

Hydrogen atoms were included in calculated positions on carbon centres for all structures.

7.2 Structure of $[MoCl(CO)(\eta^4\text{-}P_2C_2Bu^t_2)(\eta^5\text{-}C_5Me_5)]$, 2

Table 7.1 Summary of crystallographic data for $[MoCl(CO)(\eta^4\text{-}P_2C_2Bu^t_2)(\eta^5\text{-}C_5Me_5)]$, **2**

Empirical Formula	$C_{21}H_{33}ClMoOP_2$
Formula Weight	494.80
Temperature	170(2) K
Wavelength	0.71069 Å
Crystal system	Orthorhombic
Space group	$Pna2_1$
Unit cell dimensions	a = 8.4220(10) Å $\alpha = 90°$
	b = 17.5960(10) Å $\beta = 90°$
	c = 15.0730(10) Å $\gamma = 90°$
Volume	2233.7(3) $Å^3$
Z	4
Density (calculated)	1.471 Mg/m^3
Absorption coefficient	0.858 mm^{-1}
F(000)	1024
Crystal size	0.3 x 0.3 x 0.3 mm
Theta range for data collection	2.70 to 24.99°
Index ranges	$0 \leq h \leq 10$; $0 \leq k \leq 20$; $-17 \leq l \leq 0$
Reflections collected	2075
Independent reflections	2018 [R(int) = 0.0094]
Refinement method	Full-matrix least squares on F^2
Data / restraints / parameters	2018 / 2 / 150
Goodness-of-fit on F^2	0.810
Final R indices [$I>2\sigma(I)$]	$R_1 = 0.0212$ $wR_2 = 0.0868$
R indices (all data)	$R_1 = 0.0237$ $wR_2 = 0.0896$
Largest diff. peak and hole	0.447 and –0.377 $eÅ^{-3}$

Table 7.2 Atomic coordinates (x 10^4) and equivalent isotropic displacement parameters ($Å^2$ x 10^3) for **2**.

Atom	x	y	z	U(eq)
Mo(1)	2021(1)	2500	295(1)	11(1)
P(1)	2971(1)	2500	-1278(1)	15(1)
P(2)	-114(1)	2500	-863(1)	14(1)
Cl(1)	210(2)	3470(1)	997(1)	17(1)
O(1)	-324(6)	1377(4)	1133(4)	19(1)
C(1)	1300(2)	4003(1)	-1267(1)	18(1)
C(2)	-306(3)	4329(1)	-966(2)	25(1)
C(3)	1334(3)	4017(1)	-2290(2)	29(1)
C(4)	2639(3)	4498(1)	-911(2)	32(1)
C(5)	3123(3)	2500	1688(2)	15(1)
C(6)	3772(2)	3160(1)	1260(1)	16(1)
C(7)	4724(2)	2909(1)	550(1)	16(1)
C(8)	2213(4)	2500	2545(2)	20(1)
C(9)	3660(3)	3957(1)	1605(2)	24(1)
C(10)	5840(2)	3388(1)	11(2)	23(1)
C(11)	499(9)	1798(4)	770(4)	17(2)
C(12)	1465(2)	3174(1)	-1006(1)	14(1)

Table 7.3 Bond lengths [Å] and angles [°] for **2**

Mo(1)-C(11)#1	1.919(7)	Mo(1)-C(11)	1.919(7)
Mo(1)-C(5)	2.295(3)	Mo(1)-C(12)#1	2.339(2)
Mo(1)-C(12)	2.339(2)	Mo(1)-C(6)	2.374(2)
Mo(1)-C(6)#1	2.374(2)	Mo(1)-C(7)	2.418(2)
Mo(1)-C(7)#1	2.418(2)	Mo(1)-P(1)	2.5015(9)
Mo(1)-P(2)	2.5057(7)	Mo(1)-Cl(1)#1	2.521(2)
P(1)-C(12)#1	1.784(2)	P(1)-C(12)	1.784(2)

P(1)-P(2)	2.6719(10)	P(2)-C(12)	1.795(2)
P(2)-C(12)#1	1.795(2)	Cl(1)-O(1)#1	0.563(4)
Cl(1)-C(11)#1	0.630(5)	O(1)-Cl(1)#1	0.563(4)
O(1)-C(11)	1.152(8)	C(1)-C(12)	1.517(3)
C(1)-C(4)	1.522(3)	C(1)-C(2)	1.538(3)
C(1)-C(3)	1.542(3)	C(5)-C(6)	1.437(3)
C(5)-C(6)#1	1.437(3)	C(5)-C(8)	1.502(4)
C(6)-C(7)	1.407(3)	C(6)-C(9)	1.499(3)
C(7)-C(7)#1	1.440(4)	C(7)-C(10)	1.501(3)
C(11)-Cl(1)#1	0.630(5)		
C(11)#1-Mo(1)-C(11)	80.2(4)	C(11)#1-Mo(1)-C(5)	85.9(2)
C(11)-Mo(1)-C(5)	85.9(2)	C(11)#1-Mo(1)-C(12)#1	120.4(2)
C(11)-Mo(1)-C(12)#1	81.5(2)	C(5)-Mo(1)-C(12)#1	147.97(5)
C(11)#1-Mo(1)-C(12)	81.5(2)	C(11)-Mo(1)-C(12)	120.4(2)
C(5)-Mo(1)-C(12)	147.97(5)	C(12)#1-Mo(1)-C(12)	60.94(10)
C(11)#1-Mo(1)-C(6)	82.6(2)	C(11)-Mo(1)-C(6)	120.1(2)
C(5)-Mo(1)-C(6)	35.78(6)	C(12)#1-Mo(1)-C(6)	152.34(7)
C(12)-Mo(1)-C(6)	112.95(7)	C(11)#1-Mo(1)-C(6)#1	120.1(2)
C(11)#1-Mo(1)-C(6)#1	82.6(2)	C(5)-Mo(1)-C(6)#1	35.78(6)
C(12)#1-Mo(1)-C(6)#1	112.95(7)	C(12)-Mo(1)-C(6)#1	152.34(7)
C(6)-Mo(1)-C(6)#1	58.53(10)	C(11)#1-Mo(1)-C(7)	112.2(2)
C(11)-Mo(1)-C(7)	139.6(2)	C(5)-Mo(1)-C(7)	58.27(8)
C(12)#1-Mo(1)-C(7)	118.22(7)	C(12)-Mo(1)-C(7)	99.84(7)
C(6)-Mo(1)-C(7)	34.13(7)	C(6)#1-Mo(1)-C(7)	57.54(7)
C(11)#1-Mo(1)-C(7)#1	139.6(2)	C(11)-Mo(1)-C(7)#1	112.2(2)
C(5)-Mo(1)-C(7)#1	58.27(8)	C(12)#1-Mo(1)-C(7)#1	99.84(7)
C(12)-Mo(1)-C(7)#1	118.22(7)	C(6)-Mo(1)-C(7)#1	57.54(7)
C(6)#1-Mo(1)-C(7)#1	34.13(7)	C(7)-Mo(1)-C(7)#1	34.65(10)
C(11)#1-Mo(1)-P(1)	124.5(2)	C(11)1-Mo(1)-P(1)	124.5(2)
C(5)-Mo(1)-P(1)	137.52(7)	C(12)#1-Mo(1)-P(1)	43.09(5)
C(12)-Mo(1)-P(1)	43.09(5)	C(6)-Mo(1)-P(1)	112.44(5)
C(6)#1-Mo(1)-P(1)	112.44(5)	C(7)-Mo(1)-P(1)	81.37(5)

C(7)#1-Mo(1)-P(1)	81.37(5)	C(11)#1-Mo(1)-P(2)	77.3(2)
C(11)-Mo(1)-P(2)	77.3(2)	C(5)-Mo(1)-P(2)	157.98(7)
C(12)#1-Mo(1)-P(2)	43.32(5)	C(12)-Mo(1)-P(2)	43.32(5)
C(6)-Mo(1)-P(2)	150.73(5)	C(6)#1-Mo(1)-P(2)	150.73(5)
C(7)-Mo(1)-P(2)	141.84(5)	C(7)#1-Mo(1)-P(2)	141.84(5)
P(1)-Mo(1)-P(2)	64.50(2)	C(11)#1-Mo(1)-Cl(1)#1	82.8(2)
C(11)-Mo(1)-Cl(1)#1	4.9(2)	C(5)-Mo(1)-Cl(1)#1	81.99(7)
C(12)#1-Mo(1)-Cl(1)#1	83.54(6)	C(12)-Mo(1)-Cl(1)#1	125.02(7)
C(6)-Mo(1)-Cl(1)#1	116.72(7)	C(6)#1-Mo(1)-Cl(1)#1	77.76(7)
C(7)-Mo(1)-Cl(1)#1	134.76(7)	C(7)#1-Mo(1)-Cl(1)#1	107.53(7)
P(1)-Mo(1)-Cl(1)#1	126.23(4)	P(2)-Mo(1)-Cl(1)#1	81.85(5)
C(12)#1-P(1)-C(12)	83.35(13)	C(12)#1-P(1)-Mo(1)	63.60(7)
C(12)-P(1)-Mo(1)	63.60(7)	C(12)#1-P(1)-P(2)	41.86(6)
C(12)-P(1)-P(2)	41.86(6)	Mo(1)-P(1)-P(2)	57.83(2)
C(12)-P(2)-C(12)#1	82.73(13)	C(12)-P(2)-Mo(1)	63.40(6)
C(12)#1-P(2)-Mo(1)	63.40(6)	C(12)-P(2)-P(1)	41.55(6)
C(12)#1-P(2)-P(1)	41.55(6)	Mo(1)-P(2)-P(1)	57.68(2)
O(1)#1-Cl(1)-C(11)#1	149.7(12)	O(1)#1-Cl(1)-Mo(1)	163.8(9)
C(11)#1-Cl(1)-Mo(1)	15.0(7)	Cl(1)#1-O(1)-C(11)	16.0(7)
C(12)-C(1)-C(4)	113.0(2)	C(12)-C(1)-C(2)	111.3(2)
C(4)-C(1)-C(2)	109.5(2)	C(12)-C(1)-C(3)	105.9(2)
C(4)-C(1)-C(3)	109.2(2)	C(2)-C(1)-C(3)	107.7(2)
C(6)-C(5)-C(6)#1	107.8(3)	C(6)-C(5)-C(8)	125.52(13)
C(6)#1-C(5)-C(8)	125.52(13)	C(6)-C(5)-Mo(1)	75.10(14)
C(6)#1-C(5)-Mo(1)	75.10(14)	C(8)-C(5)-Mo(1)	125.5(2)
C(7)-C(6)-C(5)	107.8(2)	C(7)-C(6)-C(9)	126.4(2)
C(5)-C(6)-C(9)	125.1(2)	C(7)-C(6)-Mo(1)	74.65(11)
C(5)-C(6)-Mo(1)	69.12(14)	C(9)-C(6)-Mo(1)	129.11(14)
C(6)-C(7)-C(7)#1	108.25(12)	C(6)-C(7)-C(10)	126.3(2)
C(7)#1-C(7)-C(10)	124.12(12)	C(6)-C(7)-Mo(1)	71.23(11)
C(7)#1-C(7)-Mo(1)	72.68(5)	C(10)-C(7)-Mo(1)	132.10(14)
Cl(1)#1-C(11)-O(1)	14.3(6)	Cl(1)#1-C(11)-Mo(1)	160.2(9)
O(1)-C(11)-Mo(1)	173.1(7)	C(1)-C(12)-P(1)	130.2(2)

C(1)-C(12)-P(2)	126.8(2)	P(1)-C(12)-P(2)	96.59(10)
C(1)-C(12)-Mo(1)	136.32(14)	P(1)-C(12)-Mo(1)	73.31(7)
P(2)-C(12)-Mo(1)	73.28(7)		

Symmetry transformations used to generate equivalent atoms:

#1 x, -y+½, z

7.3 Structure of [MoCl(CO){η^3,λ^3,λ^5-$PC_2Bu^t_2PH(OH)$}(η^5-C_5H_5)], 3

Table 7.4 Summary of crystallographic data for [MoCl(CO){η^3,λ^3,λ^5-$PC_2Bu^t_2PH(OH)$}(η^5-C_5H_5)], **3**

Empirical Formula	$C_{16}H_{23}ClMoO_2P.\ 0.5\ CH_2Cl_2$
Formula Weight	461.91
Temperature	293(2) K
Wavelength	0.71069 Å
Crystal system	Triclinic
Space group	P-1
Unit cell dimensions	a = 10.067(2) Å α = 67.90(2)°
	b = 13.036(4) Å β = 87.66(2)°
	c = 17.169(4) Å γ = 72.600(10)°
Volume	1985.5(9) $Å^3$
Z	4
Density (calculated)	1.545 Mg/m^3
Absorption coefficient	1.028 mm^{-1}
F(000)	938
Crystal size	0.2 x 0.2 x 0.16 mm
Theta range for data collection	2.13 to 24.98°
Index ranges	$0 \le h \le 11$; $-14 \le k \le 15$; $-20 \le l \le 20$
Reflections collected	7673
Independent reflections	6974 [R(int) = 0.0097]
Refinement method	Full-matrix least squares on F^2
Data / restraints / parameters	6971 / 0 / 428
Goodness-of-fit on F^2	0.612
Final R indices [$I>2\sigma(I)$]	R_1 = 0.0318 wR_2 = 0.0890
R indices (all data)	R_1 = 0.0418 wR_2 = 0.0966
Largest diff. peak and hole	0.744 and –0.662 $eÅ^{-3}$

Table 7.5 Atomic coordinates (x 10^4) and equivalent isotropic displacement parameters ($Å^2$ x 10^3) for **3**.

Atom	x	y	z	U(eq)
Mo(1)	1394(1)	1449(1)	1256(1)	35(1)
P(1)	2819(1)	-724(1)	2586(1)	39(1)
P(2)	2338(1)	1311(1)	2577(1)	40(1)
Cl(1)	2475(1)	3073(1)	544(1)	57(1)
O(1)	-928(4)	3546(3)	1370(3)	89(1)
O(2)	3588(3)	-1671(2)	3462(2)	61(1)
C(1)	-117(4)	2809(4)	1377(3)	54(1)
C(2)	1834(5)	224(4)	472(3)	55(1)
C(3)	655(5)	115(3)	912(3)	57(1)
C(4)	-389(4)	1212(4)	628(3)	57(1)
C(5)	178(5)	2002(4)	6(3)	57(1)
C(6)	1557(5)	1381(4)	-84(2)	58(1)
C(7)	3489(3)	420(3)	2056(2)	38(1)
C(8)	5013(4)	335(3)	1850(3)	51(1)
C(9)	5989(4)	-840(4)	2441(4)	78(2)
C(10)	5421(5)	1313(4)	1962(4)	71(1)
C(11)	5208(5)	414(5)	942(3)	75(1)
C(12)	1305(4)	332(3)	2633(2)	41(1)
C(13)	131(4)	124(4)	3202(3)	59(1)
C(14)	718(7)	-481(6)	4122(3)	96(2)
C(15)	-509(6)	-690(5)	3004(4)	81(2)
C(16)	-1019(6)	1252(5)	3069(5)	109(2)
Mo(2)	-3331(1)	5081(1)	-3421(1)	44(1)
P(3)	-2141(1)	5228(1)	-1992(1)	42(1)
P(4)	-1873(1)	3397(1)	-2276(1)	38(1)
Cl(3)	-5054(1)	3975(1)	-3333(1)	62(1)
O(3)	-1906(4)	3695(3)	-4501(2)	83(1)

O(4)	-1257(3)	4927(2)	-1148(2)	53(1)
C(17)	-2352(5)	4136(4)	-4101(2)	57(1)
C(18)	-3402(7)	7020(3)	-3891(3)	74(2)
C(19)	-4724(7)	7008(4)	-3610(3)	80(2)
C(20)	-5361(7)	6609(4)	-4095(4)	88(2)
C(21)	-4430(8)	6381(4)	-4687(3)	95(2)
C(22)	-3222(7)	6654(4)	-4571(3)	85(2)
C(23)	-3251(4)	4417(3)	-1963(2)	39(1)
C(24)	-4348(4)	4147(3)	-1331(2)	49(1)
C(25)	-3816(5)	4047(5)	-468(3)	71(1)
C(26)	-4558(6)	2985(4)	-1203(3)	72(1)
C(27)	-5742(5)	5111(4)	-1622(4)	76(1)
C(28)	-1253(4)	4686(3)	-2719(2)	42(1)
C(29)	225(5)	4672(4)	-2973(3)	59(1)
C(30)	1271(5)	3948(5)	-2199(3)	81(2)
C(31)	325(7)	5925(5)	-3319(4)	97(2)
C(32)	649(6)	4151(5)	-3637(4)	84(2)
C(33)	4626(15)	-194(8)	4661(6)	91(4)
Cl(5)	6337(2)	-129(2)	4640(2)	142(1)

Table 7.6 Bond lengths [Å] and angles [°] for **3**.

Mo(1)-C(1)	2.035(4)	Mo(1)-C(5)	2.268(4)
Mo(1)-C(12)	2.279(4)	Mo(1)-C(4)	2.284(4)
Mo(1)-C(7)	2.300(3)	Mo(1)-C(6)	2.332(4)
Mo(1)-C(3)	2.347(4)	Mo(1)-C(2)	2.388(4)
Mo(1)-P(2)	2.4178(11)	Mo(1)-Cl(1)	2.5463(12)
Mo(1)-P(1)	2.8571(14)	P(1)-O(2)	1.584(3)
P(1)-C(7)	1.743(3)	P(1)-C(12)	1.744(4)
P(1)-P(2)	2.5431(14)	P(2)-C(7)	1.839(3)
P(2)-C(12)	1.847(3)	O(1)-C(1)	1.055(5)
C(2)-C(3)	1.395(6)	C(2)-C(6)	1.397(6)

C(3)-C(4)	1.416(6)	C(4)-C(5)	1.415(6)
C(5)-C(6)	1.418(6)	C(7)-C(8)	1.542(5)
C(8)-C(10)	1.529(6)	C(8)-C(11)	1.531(6)
C(8)-C(9)	1.534(6)	C(12)-C(13)	1.524(5)
C(13)-C(16)	1.518(7)	C(13)-C(14)	1.526(7)
C(13)-C(15)	1.535(6)	Mo(2)-C(17)	2.029(5)
Mo(2)-C(21)	2.264(4)	Mo(2)-C(22)	2.278(4)
Mo(2)-C(28)	2.278(4)	Mo(2)-C(23)	2.317(3)
Mo(2)-C(18)	2.324(4)	Mo(2)-C(20)	2.346(5)
Mo(2)-C(19)	2.387(4)	Mo(2)-P(4)	2.4290(12)
Mo(2)-Cl(3)	2.5339(12)	Mo(2)-P(3)	2.8664(11)
P(3)-O(4)	1.587(3)	P(3)-C(23)	1.740(4)
P(3)-C(28)	1.747(4)	P(3)-P(4)	2.5467(14)
P(4)-C(23)	1.832(3)	P(4)-C(28)	1.849(3)
O(3)-C(17)	1.059(5)	C(18)-C(19)	1.399(8)
C(18)-C(22)	1.405(7)	C(19)-C(20)	1.394(7)
C(20)-C(21)	1.409(9)	C(21)-C(22)	1.406(9)
C(23)-C(24)	1.539(5)	C(24)-C(26)	1.524(6)
C(24)-C(27)	1.526(6)	C(24)-C(25)	1.541(6)
C(28)-C(29)	1.530(5)	C(29)-C(32)	1.522(6)
C(29)-C(30)	1.530(7)	C(29)-C(31)	1.548(6)
C(33)-Cl(5)#1	1.613(14)	C(33)-C(33)#1	1.71(2)
C(33)-Cl(5)	1.748(14)	Cl(5)-C(33)#1	1.613(14)
C(1)-Mo(1)-C(5)	84.2(2)	C(1)-Mo(1)-C(12)	90.2(2)
C(5)-Mo(1)-C(12)	137.2(2)	C(1)-Mo(1)-C(4)	84.4(2)
C(5)-Mo(1)-C(4)	36.2(2)	C(12)-Mo(1)-C(4)	101.1(2)
C(1)-Mo(1)-C(7)	127.14(14)	C(5)-Mo(1)-C(7)	146.49(14)
C(12)-Mo(1)-C(7)	62.97(12)	C(4)-Mo(1)-C(7)	141.94(14)
C(1)-Mo(1)-C(6)	117.0(2)	C(5)-Mo(1)-C(6)	35.9(2)
C(12)-Mo(1)-C(6)	142.05(14)	C(4)-Mo(1)-C(6)	59.5(2)
C(7)-Mo(1)-C(6)	110.66(14)	C(1)-Mo(1)-C(3)	117.1(2)
C(5)-Mo(1)-C(3)	59.1(2)	C(12)-Mo(1)-C(3)	87.00(14)

C(4)-Mo(1)-C(3)	35.58(14)	C(7)-Mo(1)-C(3)	106.60(13)
C(6)-Mo(1)-C(3)	57.8(2)	C(1)-Mo(1)-C(2)	140.7(2)
C(5)-Mo(1)-C(2)	58.56(14)	C(12)-Mo(1)-C(2)	108.03(14)
C(4)-Mo(1)-C(2)	58.5(2)	C(7)-Mo(1)-C(2)	92.06(13)
C(6)-Mo(1)-C(2)	34.41(14)	C(3)-Mo(1)-C(2)	34.3(2)
C(1)-Mo(1)-P(2)	82.28(12)	C(5)-Mo(1)-P(2)	166.12(11)
C(12)-Mo(1)-P(2)	46.21(9)	C(4)-Mo(1)-P(2)	144.26(12)
C(7)-Mo(1)-P(2)	45.79(8)	C(6)-Mo(1)-P(2)	154.11(12)
C(3)-Mo(1)-P(2)	131.00(11)	C(2)-Mo(1)-P(2)	135.32(10)
C(1)-Mo(1)-Cl(1)	80.06(12)	C(5)-Mo(1)-Cl(1)	88.00(12)
C(12)-Mo(1)-Cl(1)	132.75(9)	C(4)-Mo(1)-Cl(1)	123.41(12)
C(7)-Mo(1)-Cl(1)	86.65(9)	C(6)-Mo(1)-Cl(1)	80.55(12)
C(3)-Mo(1)-Cl(1)	138.40(12)	C(2)-Mo(1)-Cl(1)	108.36(12)
P(2)-Mo(1)-Cl(1)	86.57(4)	C(1)-Mo(1)-P(1)	126.80(12)
C(5)-Mo(1)-P(1)	135.98(11)	C(12)-Mo(1)-P(1)	37.36(9)
C(4)-Mo(1)-P(1)	108.86(11)	C(7)-Mo(1)-P(1)	37.31(9)
C(6)-Mo(1)-P(1)	113.67(11)	C(3)-Mo(1)-P(1)	77.84(10)
C(2)-Mo(1)-P(1)	81.24(11)	P(2)-Mo(1)-P(1)	56.64(3)
Cl(1)-Mo(1)-P(1)	123.95(4)	O(2)-P(1)-C(7)	118.4(2)
O(2)-P(1)-C(12)	116.3(2)	C(7)-P(2)-C(12)	86.6(2)
O(2)-P(1)-P(2)	110.40(12)	C(7)-P(1)-P(2)	46.30(11)
C(12)-P(1)-P(2)	46.59(11)	O(2)-P(1)-Mo(1)	162.88(12)
C(7)-P(1)-Mo(1)	53.12(11)	C(12)-P(1)-Mo(1)	52.43(12)
P(2)-P(1)-Mo(1)	52.57(3)	C(7)-P(2)-C(12)	80.9(2)
C(7)-P(2)-Mo(1)	63.72(11)	C(12)-P(2)-Mo(1)	62.93(12)
C(7)-P(2)-P(1)	43.25(11)	C(12)-P(2)-P(1)	43.31(11)
Mo(1)-P(2)-P(1)	70.79(4)	O(1)-C(1)-Mo(1)	173.9(4)
C(3)-C(2)-C(6)	108.3(4)	C(3)-C(2)-Mo(1)	71.3(2)
C(6)-C(2)-Mo(1)	70.6(2)	C(2)-C(3)-C(4)	108.8(4)
C(2)-C(3)-Mo(1)	74.5(2)	C(4)-C(3)-Mo(1)	69.8(2)
C(3)-C(4)-C(5)	107.0(4)	C(3)-C(4)-Mo(1)	74.6(2)
C(5)-C(4)-Mo(1)	71.3(2)	C(4)-C(5)-C(6)	107.8
C(4)-C(5)-Mo(1)	72.5(2)	C(6)-C(5)-Mo(1)	74.5(2)

C(2)-C(6)-C(5)	108.1(4)	C(2)-C(6)-Mo(1)	75.0(2)
C(5)-C(6)-Mo(1)	69.6(2)	C(8)-C(7)-P(1)	127.2(3)
C(8)-C97)-P(2)	128.7(3)	P(1)-C(7)-P(2)	90.5(2)
C(8)-C(7)-Mo(1)	132.4(2)	P(1)-C(7)-Mo(1)	89.57(14)
P(2)-C(7)-Mo(1)	70.49	C(10)-C(8)-C(11)	109.1(4)
C(10)-C(8)-C(9)	109.1(4)	C(11)-C(8)-C(9)	107.9(4)
C(10)-C(8)-C(7)	110.3(3)	C(11)-C(8)-C(7)	110.7(3)
C(9)-C(8)-C(7)	109.6(3)	C(13)-C(12)-P(1)	126.4(3)
C(13)-C(12)-P(2)	126.7(3)	P(1)-C(12)-P(2)	90.1(2)
C(13)-C(12)-Mo(1)	134.6(3)	P(1)-C(12)-Mo(1)	90.2(2)
P(2)-C(12)-Mo(1)	70.86(12)	C(16)-C(13)-C(12)	115.4(4)
C(16)-C(13)-C(14)	110.5(5)	C(12)-C(13)-C(14)	109.7(4)
C(16)-C(13)-C(15)	108.2(4)	C(12)-C(13)-C(15)	109.4(3)
C(14)-C(13)-C(15)	107.3(4)	C(17)-Mo(2)-C(21)	83.8(2)
C(17)-Mo(2)-C(22)	85.2(2)	C(21)-Mo(2)-C(22)	36.1(2)
C(17)-Mo(2)-C(28)	90.2(2)	C(21)-Mo(2)-C(28)	134.7(2)
C(22)-Mo(2)-C(28)	98.8(2)	C(17)-Mo(2)-C(23)	125.72(14)
C(21)-Mo(2)-C(23)	148.9(2)	C(22)-Mo(2)-C(23)	141.2(2)
C(28)-Mo(1)-C(23)	62.74(13)	C(17)-Mo(2)-C(18)	118.3(2)
C(21)-Mo(2)-C(18)	59.1(2)	C(22)-Mo(2)-C(18)	35.5(2)
C(28)-Mo(2)-C(18)	85.7(2)	C(23)-Mo(2)-C(18)	106.22(14)
C(17)-Mo(2)-C(20)	115.7(2)	C(21)-Mo(2)-C(20)	35.5(2)
C(22)-Mo(2)-C(20)	59.1(2)	C(28)-Mo(2)-C(20)	141.9(2)
C(23)-Mo(2)-C(20)	113.5(2)	C(18)-Mo(2)-C(20)	58.0(2)
C(17)-Mo(2)-C(19)	140.6(2)	C(21)-Mo(2)-C(19)	58.2(2)
C(22)-Mo(2)-C(19)	58.3(2)	C(28)-Mo(2)-C(19)	108.5(2)
C(23)-Mo(2)-C(19)	93.7(2)	C(18)-Mo(2)-C(19)	34.5(2)
C(20)-Mo(2)-C(19)	34.2(2)	C(17)-Mo(2)-P(4)	81.44(12)
C(21)-Mo(2)-P(4)	165.2(2)	C(22)-Mo(2)-P(4)	165.2(2)
C(28)-Mo(2)-P(4)	46.12(9)	C(23)-Mo(2)-P(4)	45.35(8)
C(18)-Mo(2)-P(4)	129.65(13)	C(20)-Mo(2)-P(4)	156.7(2)
C(19)-Mo(2)-P(4)	136.37(13)	C(17)-Mo(2)-Cl(3)	81.53(13)
C(21)-Mo(2)-Cl(3)	88.3(2)	C(22)-Mo(2)-Cl(3)	124.0(2)

C(28)-Mo(2)-Cl(3)	135.18(9)	C(23)-Mo(2)-Cl(3)	86.91(9)
C(18)-Mo(2)-Cl(3)	136.7(2)	C(20)-Mo(2)-Cl(3)	78.8(2)
C(19)-Mo(2)-Cl(3)	105.4(2)	P(4)-Mo(2)-Cl(3)	89.06(4)
C(17)-Mo(2)-P(3)	126.79(13)	C(21)-Mo(2)-P(3)	135.14(14)
C(22)-Mo(2)-P(3)	107.1(2)	C(28)-Mo(2)-P(3)	37.54(9)
C(23)-Mo(2)-P(3)	37.37(9)	C(18)-Mo(2)-P(3)	76.61(11)
C(20)-Mo(2)-P(3)	114.8(2)	C(19)-Mo(2)-P(3)	81.93(13)
P(4)-Mo(2)-P(3)	56.77(3)	Cl(3)-Mo(2)-P(3)	124.21(4)
O(4)-P(3)-C(23)	118.2(2)	O(4)-P(3)-C(28)	116.2(2)
C(23)-P(3)-C(28)	86.6(2)	O(4)-P(3)-P(4)	110.69(11)
C(23)-P(3)-P(4)	46.00(11)	C(28)-P(3)-P(4)	46.55(11)
O(4)-P(3)-Mo(2)	163.48(11)	C(23)-P(3)-Mo(2)	53.90(11)
C(28)-P(3)-Mo(2)	52.62(12)	P(4)-P(3)-Mo(2)	52.92(3)
C(23)-P(4)-C(28)	81.0(2)	C(23)-P(4)-Mo(2)	64.08(11)
C(28)-P(4)-Mo(2)	62.62(12)	C(23)-P(4)-P(3)	43.09(11)
C(28)-P(4)-P(3)	43.30(11)	Mo(2)-P(4)-P(3)	70.30(4)
O(3)-C(17)-Mo(2)	175.0(4)	C(19)-C918)-C(22)	108.5(5)
C(19)-C(18)-Mo(2)	75.2(3)	C(22)-C(18)-Mo(2)	70.4(2)
C(20)-C(19)-C(18)	108.3(5)	C(20)-C(19)-Mo(2)	71.3(3)
C(18)-C(19)-Mo(2)	70.3(3)	C(19)-C(20)-C(21)	107.7(6)
C(19)-C(20)-Mo(2)	74.5(3)	C(21)-C(20)-Mo(2)	69.1(3)
C(20)-C(21)-C(22)	108.3(5)	C(20)-C(21)-Mo(2)	74.5(3)
C(22)-C(21)-Mo(2)	72.5(3)	C(18)-C(22)-C(21)	107.2(6)
C(18)-C(22)-Mo(2)	74.0(3)	C(21)-C(22)-Mo(2)	71.4(3)
C(24)-C(23)-P(3)	127.7(2)	C(24)-C(23)-P(4)	128.1(2)
P(3)-C(23)-P(4)	90.9(2)	C(24)-C(23)-Mo(2)	132.6(2)
P(3)-C(23)-Mo(2)	88.73(14)	P(4)-C(23)-Mo(2)	70.57(11)
C(26)-C(24)-C(27)	109.6(4)	C(26)-C(24)-C(23)	111.5(3)
C(27)-C(24)-C(23)	110.9(3)	C(26)-C(24)-C(25)	107.0(4)
C(27)-C(24)-C(25)	109.1(4)	C(23)-C(24)-C(25)	108.6(3)
C(29)-C(28)-P(3)	126.8(3)	C(29)-C(28)-P(4)	125.5(3)
P(3)-C(28)-P(4)	90.1(2)	C(29)-C(28)-Mo(2)	135.1(3)
P(3)-C(28)-Mo(2)	89.9(2)	P(4)-C(28)-Mo(2)	71.26(12)

C(32)-C(29)-C(30)	108.1(4)	C(32)-C(29)-C(28)	112.3(4)
C(30)-C(29)-C(28)	109.7(3)	C(32)-C(29)-C(31)	108.9(4)
C(30)-C(29)-C(31)	108.0(4)	C(28)-C(29)-C(31)	109.8(4)
Cl(5)#1-C(33)-C(33)#1	63.4(8)	Cl(5)#1-C(33)-Cl(5)	119.0(5)
C(33)#1-C(33)-Cl(5)	55.6(8)	C(33)#1-Cl(5)-C(33)	61.0(5)

Symmetry transformations used to generate equivalent atoms:

#1 -x+1,-y,-z+1

7.4 Structure of $Ph_2PNC_4H_3C(O)CH_3$, L^1

Table 7.4 Summary of crystallographic data for $Ph_2PNC_4H_3C(O)CH_3$, L^1

Empirical Formula	$C_{18}H_{16}NOP$
Formula Weight	293.29
Temperature	293(2) K
Wavelength	0.71069 Å
Crystal system	Monoclinic
Space group	$P2_1/a$
Unit cell dimensions	a = 9.501(3) Å $\alpha = 90°$
	b = 16.156(3) Å $\beta = 112.91(2)°$
	c = 11.009(3) Å $\gamma = 90°$
Volume	1556.6(7) $Å^3$
Z	4
Density (calculated)	1.252 Mg/m^3
Absorption coefficient	0.175 mm^{-1}
F(000)	616
Crystal size	0.50 x 0.50 x 0.50 mm
Theta range for data collection	2.01 to 25.96°
Index ranges	$0 \leq h \leq 11; 0 \leq k \leq 19; -13 \leq l \leq 12$
Reflections collected	3326
Independent reflections	3036 [R(int) = 0.0085]
Refinement method	Full-matrix least squares on F^2
Data / restraints / parameters	3036 / 0 / 192
Goodness-of-fit on F^2	1.046
Final R indices [$I>2\sigma(I)$]	$R_1 = 0.0348$ $wR_2 = 0.0998$
R indices (all data)	$R_1 = 0.0564$ $wR_2 = 0.1065$
Largest diff. peak and hole	0.234 and –0.178 $eÅ^{-3}$

Table 7.8 Atomic coordinates (x 10^4) and equivalent isotropic displacement parameters ($Å^2$ x 10^3) for $\mathbf{L^1}$.

Atom	x	y	z	U(eq)
P(1)	1452(1)	123(1)	8545(1)	44(1)
N(1)	155(2)	878(1)	7584(1)	47(1)
O(1)	2717(2)	1680(1)	9441(2)	75(1)
C(1)	35921)	-806(1)	7792(2)	43(1)
C(2)	-615(2)	-1114(1)	8357(2)	58(1)
C(3)	-443(3)	-1824(1)	7887(2)	72(1)
C(4)	-1286(3)	-2252(1)	6875(2)	71(1)
C(5)	-331(2)	-1958(1)	6297(2)	65(1)
C(6)	480(2)	-1238(1)	6753(2)	53(1)
C(7)	2846(2)	128(1)	7787(2)	43(1)
C(8)	4131(2)	-361(1)	8375(2)	60(1)
C(9)	5236(2)	-400(2)	7863(2)	75(1)
C(10)	5081(3)	57(2)	6772(3)	79(1)
C(11)	3822(3)	550(1)	6182(2)	67(1)
C(12)	2700(2)	586(1)	6685(2)	53(1)
C(13)	-1199(2)	739(1)	6549(2)	57(1)
C(14)	-1956(3)	1465(1)	6147(2)	71(1)
C(15)	-1054(3)	2078(1)	6951(2)	72(1)
C(16)	257(2)	1722(1)	7840(2)	54(1)
C(17)	1590(3)	2091(1)	8833(2)	63(1)
C(18)	1548(3)	3002(1)	9095(3)	96(1)

Table 7.9 Bond lengths [Å] and angles [°] for $\mathbf{L^1}$.

P(1)-N(1)	1.7637(14)	P(1)-C(7)	1.8190(18)
P(1)-C(1)	1.8293(17)	N(1)-C(13)	1.365(2)
N(1)-C(16)	1.388(2)	O(1)-C(17)	1.216(2)
C(1)-C(6)	1.382(2)	C(1)-C(2)	1.393(2)
C(2)-C(3)	1.373(3)	C(3)-C(4)	1.369(3)
C(4)-C(5)	1.380(3)	C(5)-C(6)	1.378(3)
C(7)-C(12)	1.382(2)	C(7)-C(8)	1.385(2)
C(8)-C(9)	1.373(3)	C(9)-C(10)	1.369(4)
C(10)-C(11)	1.372(3)	C(11)-C(12)	1.379(3)
C(13)-C(14)	1.358(3)	C(14)-C(15)	1.380(3)
C(15)-C(16)	1.375(3)	C(16)-C(17)	1.441(3)
C(17)-C(18)	1.504(3)		
N(1)-P(1)-C(7)	100.66(7)	N(1)-P(1)-C(1)	98.87(7)
C(7)-P(1)-C(1)	100.48(7)	C(13)-N(1)-C(16)	107.45(15)
C(13)-N(1)-P(1)	126.74(12)	C(16)-N(1)-P(1)	125.48(12)
C(6)-C(1)-C(2)	118.21(16)	C(6)-C(1)-P(1)	125.03(13)
C(2)-C(1)-P(1)	116.69(13)	C(3)-C(2)-C(1)	120.88(17)
C(4)-C(3)-C(2)	120.07(18)	C(3)-C(4)-C(5)	120.09(19)
C(6)-C(5)-C(4)	119.83(19)	C(5)-C(6)-C(1)	120.90(17)
C(12)-C(7)-C(8)	118.96(17)	C(12)-C(7)-P(1)	124.31(13)
C(8)-C(7)-P(1)	116.74(14)	C(9)-C(8)-C(7)	120.7(2)
C(10)-C(9)-C(8)	119.8(2)	C(9)-C(10)-C(11)	120.3(2)
C(10)-C(11)-C(12)	120.2(2)	C(11)-C(12)-C(7)	120.07(18)
C(14)-C(13)-N(1)	109.71(19)	C(13)-C(14)-C(15)	107.01(19)
C(16)-C(15)-C(14)	108.74(18)	C(15)-C(16)-N(1)	107.09(17)
C(15)-C(16)-C(17)	130.68(19)	N(1)-C(16)-C(17)	122.14(17)
O(1)-C(17)-C(16)	121.11(18)	O(1)-C(17)-C(18)	120.8(2)
C(16)-C(17)-C(18)	118.0(2)		

7.5 Structure of [MoCl(CO){$Ph_2PNC_4H_3C(O)CH_3$-*P*}(η^5-C_5H_5)], 14

Table 7.10 Summary of crystallographic data for [MoCl(CO){$Ph_2PNC_4H_3C(O)CH_3$-*P*}(η^5-C_5H_5)], **14**

Empirical Formula	$C_{25}H_{21}ClMoNO_3P$. 0.5 CH_2Cl_2
Formula Weight	588.25
Temperature	170(2) K
Wavelength	0.71069 Å
Crystal system	Triclinic
Space group	P-1
Unit cell dimensions	a = 9.762(3) Å α = 110.50(3)°
	b = 10.383(4) Å β = 93.69(3)°
	c = 14.411(5) Å γ = 100.85(3)°
Volume	1330.2(8) $Å^3$
Z	2
Density (calculated)	1.469 Mg/m^3
Absorption coefficient	0.780 mm^{-1}
F(000)	594
Crystal size	0.2 x 0.2 x 0.2 mm
Theta range for data collection	2.13 to 25.02°
Index ranges	$0 \leq h \leq 11$; $-12 \leq k \leq 12$; $-17 \leq l \leq 17$
Reflections collected	5137
Independent reflections	4686 [R(int) = 0.0242]
Reflections observed (>2σ)	3577
Refinement method	Full-matrix least squares on F^2
Data / restraints / parameters	4686 / 0 / 300
Goodness-of-fit on F^2	0.931
Final R indices [I>2σ(I)]	R_1 = 0.0492 wR_2 = 0.1225
R indices (all data)	R_1 = 0.0715 wR_2 = 0.1327
Largest diff. peak and hole	1.406 and –0.631 $eÅ^{-3}$

Table 7.11 Atomic coordinates (x 10^4) and equivalent isotropic displacement parameters ($Å^2$ x10^3) for **14**.

Atom	x	y	z	U(eq)
Mo(1)	2012(1)	8540(1)	3150(1)	17(1)
Cl(1)	115(1)	8213(1)	1784(1)	24(1)
P(1)	3350(1)	9060(1)	1838(1)	17(1)
O(1)	566(4)	10944(4)	4274(3)	33(1)
O(2)	4478(4)	11006(4)	4455(3)	34(1)
O(3)	5096(4)	7452(4)	2457(3)	25(1)
N(1)	5099(4)	10018(4)	2164(3)	20(1)
C(1)	671(3)	6993(4)	3761(3)	29(1)
C(2)	2019(4)	7586(4)	4350(2)	25(1)
C(3)	3040(3)	7093(4)	3741(2)	22(1)
C(4)	2323(4)	6194(4)	2775(2)	25(1)
C(5)	859(3)	6133(4)	2787(2)	28(1)
C(6)	1106(3)	10073(6)	3845(4)	22(1)
C(7)	3595(6)	10095(6)	3968(4)	24(1)
C(8)	5617(6)	11255(6)	2015(4)	28(1)
C(9)	7018(6)	11701(6)	234694)	32(1)
C(10)	7421(6)	10742(6)	2726(4)	27(1)
C(11)	6256(5)	9707(6)	2607(4)	23(1)
C(12)	6151(5)	8407(6)	2792(4)	22(1)
C(13)	7376(6)	8257(6)	3392(4)	29(1)
C(14)	3483(6)	7594(5)	714(4)	21(1)
C(15)	2379(6)	6387(6)	357(4)	26(1)
C(16)	2467(7)	5251(6)	-476(4)	33(1)
C(17)	3652(7)	5293(6)	-962(4)	37(2)
C(18)	4744(6)	6488(6)	-603(4)	31(1)
C(19)	4656(6)	7624(6)	228(4)	25(1)
C(20)	2598(5)	10228(5)	1367(4)	20(1)

C(21)	2322(6)	9960(5)	348(4)	23(1)
C(22)	1712(6)	10862(6)	23(4)	28(1)
C(23)	1368(6)	12028(6)	701(5)	33(1)
C(24)	1649(6)	12309(6)	1716(4)	31(1)
C(25)	2257(6)	11409(6)	2051(4)	29(1)
C(26)	3646(16)	5637(16)	5561(11)	52(4)
Cl(2)	2388(5)	4253(6)	4815(4)	55(1)
Cl(3)	4522(4)	5320(4)	6523(3)	43(1)
Cl(2A)	5000	5000	5000	89(10)
Cl(3A)	1972(18)	4715(18)	5112(13)	72(4)

Table 6.? Bond lengths [Å] and angles [°] for **14**

Mo(1)-C(6)	1.961(5)	Mo(1)-C(7)	1.969(6)
Mo(1)-C(2)	2.274(4)	Mo(1)-C(3)	2.312(3)
Mo(1)-C(1)	2.327(4)	Mo(1)-C(4)	2.386(3)
Mo(1)-C(5)	2.396(4)	Mo(1)-Cl(1)	2.4991(16)
Mo(1)-P(1)	2.5176(16)	P(1)-N(1)	1.748(4)
P(1)-C(20)	1.821(5)	P(1)-C(14)	1.825(5)
O(1)-C(6)	1.145(6)	O(2)-C(7)	1.131(7)
O(3)-C(12)	1.222(6)	N(1)-C(8)	1.383(7)
N(1)-C(11)	1.407(6)	C(1)-C(5)	1.4200
C(1)-C(2)	1.4200	C(2)-C(3)	1.4200
C(3)-C(4)	1.4200	C(4)-C(5)	1.4200
C(8)-C(9)	1.355(8)	C(9)-C(10)	1.395(8)
C(10)-C(11)	1.366(8)	C(11)-C(12)	1.451(7)
C(12)-C(13)	1.495(7)	C(14)-C(19)	1.381(7)
C(14)-C(15)	1.403(7)	C(15)-C(16)	1.378(8)
C(16)-C(17)	1.392(9)	C(17)-C(18)	1.387(9)
C(18)-C(19)	1.377(8)	C(20)-C(25)	1.393(7)
C(20)-C(21)	1.393(7)	C(21)-C(22)	1.389(7)
C(22)-C(23)	1.379(8)	C(24)-C(25)	1.396(8)

C(26)-Cl(2)	1.677(16)	C(26)-Cl(3A)	1.69(2)
C(26)-Cl(2A)	1.1712(15)	C(26)-Cl(3)	1.742(16)
Cl(2)-Cl(3A)	0. 728(16)	Cl(2A)-C(26)#1	1.712(15)
Cl(2A)-Cl(3)#1	2.196(4)		
C(6)-Mo(1)-C(7)	76.0(2)	C(6)-Mo(1)-C(2)	96.88(17)
C(7)-Mo(1)-C(2)	90.09(17)	C(6)-Mo(1)-C(3)	130.43(17)
C(7)-Mo(1)-C(3)	87.02(17)	C(2)-Mo(1)-C(3)	36.1
C(6)-Mo(1)-C(1)	92.32(17)	C(7)-Mo(1)-C(1)	123.63(18)
C(2)-Mo(1)-C(1)	35.93(5)	C(3)-Mo(1)-C(1)	59.37(6)
C(6)-Mo(1)-C(4)	150.59(17)	C(7)-Mo(1)-C(4)	117.14(17)
C(2)-Mo(1)-C(4)	59.02(6)	C(3)-Mo(1)-C(4)	35.1
C(1)-Mo(1)-C(4)	58.33(6)	C(6)-Mo(1)-C(5)	120.35(18)
C(7)-Mo(1)-C(5)	144.87(17)	C(2)-Mo(1)-C(5)	58.87(7)
C(3)-Mo(1)-C(5)	58.40(6)	C(1)-Mo(1)-C(5)	35.0
C(4)-Mo(1)-C(5)	34.5	C(6)-Mo(1)-Cl(1)	80.03(15)
C(7)-Mo(1)-Cl(1)	134.99(15)	C(2)-Mo(1)-Cl(1)	130.53(10)
C(3)-Mo(1)-Cl(1)	136.48(9)	C(1)-Mo(1)-Cl(1)	94.61(10)
C(4)-Mo(1)-Cl(1)	102.30(9)	C(5)-Mo(1)-Cl(1)	80.10(9)
C(6)-Mo(1)-P(1)	111.62(16)	C(7)-Mo(1)-P(1)	77.86(16)
C(2)-Mo(1)-P(1)	144.83(9)	C(3)-Mo(1)-P(1)	109.57(9)
C(1)-Mo(1)-P(1)	152.05(9)	C(1)-Mo(1)-P(1)	152.05(9)
C(4)-Mo(1)-P(1)	97.25(8)	C(5)-Mo(1)-P(1)	117.14(10)
Cl(1)-Mo(1)-P(1)	76.42(5)	N(1)-P(1)-C(20)	98.7(2)
N(1)-P(1)-C(14)	100.8(2)	C(20)-P(1)-C(14)	104.4(2)
N(1)-P(1)-Mo(1)	119.98(15)	C(20)-P(1)-Mo(1)	111.17(17)
C(14)-P(1)-Mo(1)	118.93(17)	C(8)-N(1)-C(11)	106.1(4)
C(8)-N(1)-P(1)	125.5(4)	C(11)-N(1)-P(1)	128.3(3)
C(5)-C(1)-C(2)	108.0	C(1)-C(2)-Mo(1)	74.08(14)
C(3)-C(2)-Mo(1)	73.41(14)	C(4)-C(3)-C(2)	108.0
C(4)-C(3)-Mo(1)	75.31(14)	C(2)-C(3)-Mo(1)	70.53(14)
C(3)-C(4)-C(5)	108.0	C(3)-C(4)-Mo(1)	69.55(13)
C(5)-C(4)-Mo(1)	73.09(13)	C(1)-C(5)-C(4)	108.0

C(1)-C(5)-Mo(1)	69.89(13)	C(4)-C(5)-Mo(1)	72.37(13)
O(1)-C(6)-Mo(1)	177.6(5)	O(2)-C(7)-Mo(1)	178.0(5)
C(9)-C(8)-N(1)	109.7(5)	C(8)-C(9)-C(10)	107.8(5)
C(11)-C(10)-C(9)	107.9(5)	C(10)-C(11)-N(1)	108.4(5)
C(10)-C(11)-C(12)	129.1(5)	N(1)-C(11)-C(12)	122.2(5)
O(3)-C(12)-C(11)	121.0(5)	O(3)-C(12)-C(13)	120.7(5)
C(11)-C(12)-C(13)	118.2(5)	C(19)-C(14)-C(15)	119.4(5)
C(19)-C(14)-P(1)	121.9(4)	C(15)-C(14)-P(1)	118.7(4)
C(16)-C(15)-C(14)	119.9(5)	C(16)-C(15)-C(14)	119.9(5)
C(15)-C(16)-C(17)	120.3(6)	C(18)-C(17)-C(16)	119.5(5)
C(19)-C(18)-C(17)	120.3(5)	C(18)-C(19)-C(14)	120.6(5)
C(25)-C(20)-C(21)	119.0(5)	C(25)-C(20)-P(1)	118.6(4)
C(21)-C(20)-P(1)	122.4(4)	C(22)-C(21)-C(20)	120.3(5)
C(23)-C(22)-C(21)	120.6(5)	C(22)-C(23)-C(24)	119.6(5)
C(23)-C(24)-C(25)	120.4(5)	C(20)-C(25)-C(24)	120.1(5)
Cl(2)-C(26)-Cl(3A)	25.0(6)	Cl(2)-C(26)-Cl(2A)	94.5(8)
Cl(3A)-C(26)-C(2A)	119.4(11)	Cl(2)-C(26)-Cl(3)	113.6(9)
Cl(3A)-C(26)-Cl(3)	117.4(10)	Cl(2A)-C(26)-Cl(3)	78.9(7)
Cl(3A)-Cl(2)-C(26)	78.3(15)	C(26)-Cl(3)-Cl(2A)	49.9(5)
C(26)-Cl(2A)-C(26)#1	180.0(10)	C(26)-Cl(2A)-Cl(3)	51.1(5)
C(26)#1-Cl(2A)-Cl(3)	128.9(5)	C(26)-Cl(2A)-Cl(3)#1	128.9(5)
C(26)#1-Cl(2A)-Cl(3)#1	51.1(5)	Cl(3)-Cl(2A)-Cl(3)#1	180.000(1)
Cl(2)-Cl(3A)-C(26)	76.7(15)		

Symmetry transformations used to generate equivalent atoms:

#1 -x+1, -y+1, -z+1

7.6 Crystal Structure of $[Mo(CO)_2\{Ph_2PNC_4H_3C(O)CH_3\text{-}P,O\}(\eta^5\text{-}C_5H_5)][BF_4]$, 20

Table 7.13 Summary of crystallographic data for $[MoCl(CO)\{Ph_2PNC_4H_3C(O)CH_3\text{-}P\}(\eta^5\text{-}C_5H_5)]$, **20**

Empirical Formula	$C_{25}H_{21}BF_4MoNO_3P$
Formula Weight	597.15
Temperature	173(2) K
Wavelength	0.71073 Å
Crystal system	Triclinic
Space group	P-1
Unit cell dimensions	a = 10.2215(7) Å α = 89.0780(10)°
	b = 10.9379(7) Å β = 84.0120(10)°
	c = 11.0922(8) Å γ = 79.2000(10)°
Volume	1211.51(14) $Å^3$
Z	2
Density (calculated)	1.637 Mg/m^3
Absorption coefficient	0.667 mm^{-1}
F(000)	600
Crystal size	2.00 x 0.2 x 0.2 mm
Theta range for data collection	1.85 to 27.51°
Index ranges	$-12 \leq h \leq 13$; $-14 \leq k \leq 14$; $-14 \leq l \leq 14$
Reflections collected	12695
Independent reflections	5507 [R(int) = 0.0271]
Reflections observed (>2σ)	4310
Refinement method	Full-matrix least squares on F^2
Data / restraints / parameters	5507 / 0 / 326
Goodness-of-fit on F^2	0.921
Final R indices [I>2σ(I)]	$R_1 = 0.0313$ $wR_2 = 0.0702$
R indices (all data)	$R_1 = 0.0453$ $wR_2 = 0.0733$
Largest diff. peak and hole	1.063 and –0.409 $eÅ^{-3}$

Table 7.14 Atomic coordinates (x 10^4) and equivalent isotropic displacement parameters ($Å^2$ x 10^3) for **20**.

Atom	x	y	z	U(eq)
Mo	2086(1)	2609(1)	1786(1)	28(1)
C(1)	1127(3)	3350(3)	395(3)	47(1)
O(1)	550(3)	3698(2)	-414(2)	80(1)
C(2)	478(3)	3686(2)	2606(2)	36(1)
O(2)	-465(2)	4312(2)	3060(2)	49(1)
C(11)	969(3)	1047(3)	2423(3)	43(1)
C(12)	1903(3)	1131(3)	3245(2)	43(1)
C(13)	3191(3)	803(2)	2630(3)	45(1)
C(14)	3027(3)	496(2)	1438(3)	52(1)
C(15)	1664(3)	644(3)	1310(3)	48(1)
P	3071(1)	3994(1)	2971(1)	25(1)
C(21)	2213(2)	5574(2)	3360(2)	28(1)
C(22)	1503(2)	6263(2)	2493(2)	32(1)
C(23)	897(3)	7493(2)	2711(3)	40(1)
C(24)	978(3)	8035(3)	3804(3)	44(1)
C(25)	1679(3)	7374(2)	4676(2)	42(1)
C(26)	2300(2)	6143(2)	4462(2)	33(1)
C(31)	3488(2)	3252(2)	4399(2)	27(1)
C(32)	2471(3)	3215(2)	5325(2)	32(1)
C(33)	2713(3)	2476(3)	6334(2)	38(1)
C(34)	3978(3)	1776(3)	6419(2)	41(1)
C(35)	4994(3)	1816(3)	5509(2)	41(1)
C(36)	4755(3)	2552(2)	4491(2)	34(1)
N(51)	4602(2)	4273(2)	2318(2)	28(1)
C(52)	5373(3)	4983(2)	2850(2)	34(1)
C(53)	6558(3)	4956(3)	2140(2)	38(1)
C(54)	6546(3)	4210(2)	1135(2)	38(1)
C(55)	5339(2)	3792(2)	1233(2)	30(1)

C(56)	4886(3)	3056(2)	370(2)	31(1)
O(57)	3764(2)	2742(2)	465(1)	36(1)
C(58)	5809(3)	2656(2)	-758(2)	38(1)
B	7605(3)	662(3)	1799(3)	43(1)
F(1)	8289(2)	-540(2)	1686(2)	67(1)
F(2)	8234(2)	1388(2)	966(2)	61(1)
F(3)	7609(2)	1076(3)	2949(2)	96(1)
F(4)	6293(2)	725(2)	1546(2)	58(1)

Table 7.15 Bond lengths [Å] and angles [°] for **20**.

Mo-C(2)	1.978(3)	Mo-C(1)	1.993(3)
Mo-O(57)	2.1619(17)	Mo-C(12)	2.288(3)
Mo-C(11)	2.291(3)	Mo-C(13)	2.320(3)
Mo-C(15)	2.348(3)	Mo-C(14)	2.352(3)
Mo-P	2.4399(6)	C(1)-O(1)	1.146(3)
C(2)-O(2)	1.146(3)	C(11)-C(15)	1.394(4)
C(11)-C(12)	1.403(4)	C(12)-C(13)	1.404(4)
C(13)-C(14)	1.403(4)	C(14)-C(15)	1.394(4)
P-N(51)	1.733(2)	P-C(31)	1.822(2)
P-C(21)	1.821(2)	C(21)-C(22)	1.392(3)
C(21)-C(26)	1.399(3)	C(22)-C(23)	1.385(3)
C(23)-C(24)	1.374(4)	C(24)-C(25)	1.378(4)
C(25)-C(26)	1.390(3)	C(31)-C(32)	1.389(3)
C(31)-C(36)	1.388(3)	C(32)-C(33)	1.385(3)
C(33)-C(34)	1.386(4)	C(34)-C(35)	1.377(4)
C(35)-C(36)	1.392(3)	N(51)-C(52)	1.383(3)
N(51)-C(55)	1.406(3)	C(52)-C(53)	1.369(4)
C(53)-C(54)	1.395(4)	C(54)-C(55)	1.387(4)
C(55)-C(56)	1.427(3)	C(56)-O(57)	1.251(3)
C(56)-C(58)	1.505(3)	B-F(3)	1.361(4)
B-F(1)	1.370(4)	B-F(4)	1.388(4)

B-F(2)	1.393(4)		
C(2)-Mo-C(1)	77.55(11)	C(2)-Mo-O(57)	139.64(9)
C(1)-Mo-O(57)	79.57(10)	C(2)-Mo-C(12)	89.45(11)
C(1)-Mo-C(12)	138.77(12)	O(57)-Mo-C(12)	128.69(9)
C(2)-Mo-C(11)	83.16(10)	C(1)-Mo-C(11)	103.35(12)
O(57)-Mo-C(11)	134.67(9)	C(12)-Mo-C(11)	35.69(10)
C(2)-Mo-C(13)	123.58(11)	C(1)-Mo-C(13)	146.03(12)
O(57)-Mo-C(13)	93.22(9)	C(12)-Mo-C(13)	35.46(10)
C(11)-Mo-C(13)	59.04(10)	C(2)-Mo-C(15)	111.86(11)
C(1)-Mo-C(15)	90.09(11)	O(57)-Mo-C(15)	100.91(9)
C(12)-Mo-C(15)	58.57(10)	C(11)-Mo-C(15)	34.94(10)
C(13)-Mo-C(15)	58.45(10)	C(2)-Mo-C(14)	140.96(11)
C(1)-Mo-C(14)	111.46(12)	O(57)-Mo-C(14)	78.66(9)
C(12)-Mo-C(14)	58.13(10)	C(11)-Mo-C(14)	57.88(10)
C(13)-Mo-C(14)	34.95(10)	C(15)-Mo-C(14)	34.51(11)
C(2)-Mo-P	78.06(7)	C(1)-Mo-P	117.29(9)
O(57)-Mo-P	83.61(5)	C(12)-Mo-P	97.38(7)
C(11)-Mo-P	129.52(7)	C(13)-Mo-P	94.47(7)
C(15)-Mo-P	152.57(8)	C(14)-Mo-P	123.50(9)
O(1)-C(1)-Mo	175.3(3)	O(2)-C(2)-Mo	178.6(2)
C(15)-C(11)-C(12)	108.4(3)	C(15)-C(11)-Mo	74.78(16)
C(12)-C(11)-Mo	72.05(15)	C(13)-C(12)-C(11)	108.1(3)
C(13)-C(12)-Mo	73.50(15)	C(11)-C(12)-Mo	72.26(16)
C(14)-C(13)-C(12)	106.9(3)	C(14)-C(13)-Mo	73.79(16)
C(12)-C(13)-Mo	71.04(15)	C(13)-C(14)-C(15)	109.1(3)
C(13)-C(14)-Mo	71.27(15)	C(15)-C(14)-Mo	72.59(16)
C(11)-C(15)-C(14)	107.4(3)	C(11)-C(15)-Mo	70.28(16)
C(14)-C(15)-Mo	72.90(16)	N(51)-P-C(31)	102.77(10)
N(51)-P-C(21)	100.65(10)	C(31)-P-C(21)	105.91(11)
N(51)-P-Mo	113.94(7)	C(31)-P-Mo	109.68(8)
C(21)-P-Mo	121.93(8)	C(22)-C(21)-C(26)	118.8(2)
C(22)-C(21)-P	118.21(18)	C(26)-C(21)-P	122.85(18)

C(23)-C(22)-C(21)	120.7(2)	C(24)-C(23)-C(22)	119.7(2)
C(23)-C(24)-C(25)	120.7(2)	C(24)-C(25)-C(26)	120.0(2)
C(25)-C(26)-C(21)	120.0(2)	C(32)-C(31)-C(36)	119.7(2)
C(32)-C(31)-P	119.11(17)	C(36)-C(31)-P	120.28(18)
C(33)-C(32)-C(31)	120.3(2)	C(34)-C(33)-C(32)	119.8(2)
C(35)-C(34)-C(33)	120.2(2)	C(34)-C(35)-C(36)	120.3(2)
C(35)-C (36)-C(31)	119.7(2)	C(52)-N(51)-C(55)	106.9(2)
C(52)-N(51)-P	124.18(16)	C(55)-N(51)-P	128.77(17)
C(53)-C(52)-N(51)	109.7(2)	C(52)-C(53)-C(54)	107.5(2)
C(55)-C(54)-C(53)	108.3(2)	C(54)-C(55)-N(51)	107.6(2)
C(54)-C(55)-C(56)	126.8(2)	N(51)-C(55)-C(56)	125.6(2)
O(57)-C(56)-C(55)	124.9(2)	O(57)-C(56)-C(58)	117.4(2)
C(55)-C(56)-C(58)	117.7(2)	C(56)-O(57)-Mo	141.33(15)
F(3)-B-F(1)	109.7(3)	F(3)-B-F(4)	109.3(3)
F(1)-B-F(4)	110.0(3)	F(3)-B-F(2)	110.6(3)
F(1)-B-F(2)	108.0(2)	F(4)-B-F(2)	109.2(2)

7.7 Structure of $[Mo(CO)_2(Ph_2PCH=C(O)Ph\text{-}P,O)(\eta^5\text{-}C_5H_5)]$, 26

Table 7.16 Summary of crystallographic data for $[Mo(CO)_2(Ph_2PCH=C(O)Ph\text{-}P,O)(\eta^5\text{-}C_5H_5)]$, **26**

Empirical Formula	$C_{27}H_{21}MoO_3P$
Formula Weight	520.35
Temperature	170(2) K
Wavelength	0.71073 Å
Crystal system	Orthorhombic
Space group	$P2_12_12_1$
Unit cell dimensions	a = 8.25200(10) Å $\alpha = 90°$
	b = 14.3430(3) Å $\beta = 90°$
	c = 19.0700(2) Å $\gamma = 90°$
Volume	2257.10(6) $Å^3$
Z	4
Density (calculated)	1.531 Mg/m^3
Absorption coefficient	0.679 mm^{-1}
F(000)	1056
Crystal size	0.15 x 0.15 x 0.15 mm
Theta range for data collection	1.78 to 27.48°
Index ranges	$-9 \leq h \leq 10$; $-18 \leq k \leq 18$; $-24 \leq l \leq 24$
Reflections collected	34621
Independent reflections	5171 [R(int) = 0.0436]
Reflections observed (>2σ)	4913
Refinement method	Full-matrix least squares on F^2
Data / restraints / parameters	5171 / 0 / 294
Goodness-of-fit on F^2	0.830
Final R indices [I>2σ(I)]	$R_1 = 0.0340$ $wR_2 = 0.0868$
R indices (all data)	$R_1 = 0.0436$ $wR_2 = 0.1162$
Largest diff. peak and hole	1.230 and –1.535 $eÅ^{-3}$

Table 7.17 Atomic coordinates (x 10^4) and equivalent isotropic displacement parameters ($Å^2$ x 10^3) for **13**.

Atom	x	y	z	U(eq)
Mo(1)	1785(1)	2171(1)	2268(1)	22(1)
P(1)	4027(1)	1478(1)	2927(1)	21(1)
O(1)	2149(4)	4292(2)	1908(2)	42(1)
O(2)	1493(4)	3211(3)	3701(2)	44(1)
O(3)	3613(3)	1950(2)	1482(1)	25(1)
C(1)	2077(5)	3503(3)	2033(2)	29(1)
C(2)	1591(5)	2826(3)	3175(2)	30(1)
C(3)	-456(5)	1934(3)	1541(3)	38(1)
C(4)	-961(5)	2057(3)	2247(3)	39(1)
C(5)	-365(5)	1290(3)	2635(2)	38(1)
C(6)	500(6)	706(3)	2171(3)	38(1)
C(7)	433(5)	1107(3)	1502(2)	37(1)
C(8)	4832(4)	1373(2)	1592(2)	21(1)
C(9)	5247(5)	1040(2)	2242(2)	23(1)
C(10)	3420(5)	512(3)	3490(2)	25(1)
C(11)	2487(6)	679(3)	4089(2)	36(1)
C(12)	1987(7)	-59(3)	4507(2)	41(1)
C(13)	2409(6)	-961(3)	4335(3)	37(1)
C(14)	3308(6)	-1137(3)	3733(2)	33(1)
C(15)	3809(5)	-400(3)	3311(2)	27(1)
C(16)	5396(4)	2149(3)	3494(2)	25(1)
C(17)	6398(6)	1724(3)	3986(2)	37(1)
C(18)	7548(6)	2232(4)	4349(2)	45(1)
C(19)	7705(6)	3180(4)	4220(3)	45(1)
C(20)	6718(6)	3617(3)	3740(3)	41(1)
C(21)	5566(5)	3107(3)	3382(2)	32(1)
C(22)	5818(4)	1142(3)	961(2)	21(1)

C(23)	6740(5)	319(3)	931(2)	27(1)
C(24)	7732(5)	138(3)	359(2)	31(1)
C(25)	7849(5)	777(3)	-187(2)	34(1)
C(26)	6924(5)	1588(3)	-163(2)	31(1)
C(27)	5905(5)	1761(3)	400(2)	26(1)

Table 7.18 Bond lengths [Å] and angles [°] for **13**

Mo(1)-C(2)	1.974(4)	Mo(1)-C(1)	1.977(4)
Mo(1)-O(3)	2.151(2)	Mo(1)-C(4)	2.272(4)
Mo(1)-C(5)	2.288(4)	Mo(1)-C(3)	2.337(4)
Mo(1)-C(6)	2.362(4)	Mo(1)-C(7)	2.389(4)
Mo(1)-P(1)	2.4475(10)	P(1)-C(9)	1.765(4)
P(1)-C(10)	1.823(4)	P(1)-C(16)	1.835(4)
O(1)-C(1)	1.158(5)	O(2)-C(2)	1.149(5)
O(3)-C(8)	1.319(5)	C(3)-C(7)	1.397(7)
C(3)-C(4)	1.422(7)	C(4)-C(5)	1.414(7)
C(5)-C(6)	1.412(7)	C(6)-C(7)	1.401(7)
C(8)-C(9)	1.372(5)	C(8)-C(22)	1.491(5)
C(10)-C(15)	1.390(5)	C(10)-C(11)	1.397(5)
C(11)-C(12)	1.389(6)	C(12)-C(13)	1.379(7)
C(13)-C(14)	1.390(7)	C(14)-C(15)	1.390(6)
C(16)-C(17)	1.391(6)	C(16)-C(21)	1.397(6)
C(17)-C(18)	1.383(7)	C(18)-C(19)	1.387(8)
C(19)-C(20)	1.376(8)	C(20)-C(21)	1.381(6)
C(22)-C(27)	1.393(5)	C(22)-C(23)	1.405(5)
C(23)-C(24)	1.387(6)	C(24)-C(25)	1.390(6)
C(25)-C(26)	1.393(6)	C(26)-C(27)	1.386(6)
C(2)-Mo(1)-C(1)	75.43(17)	C(2)-Mo(1)-O(3)	137.53(14)
C(1)-Mo(1)-O(3)	84.22(13)	C(2)-Mo(1)-C(4)	88.21(16)
C(1)-Mo(1)-C(4)	100.79(17)	O(3)-Mo(1)-C(4)	132.59(14)

C(2)-Mo(1)-C(5)	86.14(17)	C(1)-Mo(1)-C(5)	134.25(17)
O(3)-Mo(1)-C(5)	132.48(14)	C(4)-Mo(1)-C(5)	36.13(17)
C(2)-Mo(1)-C(3)	121.68(16)	C(1)-Mo(1)-C(3)	95.87(17)
O(3)-Mo(1)-C(3)	96.86(13)	C(4)-Mo(1)-C(3)	35.91(16)
C(5)-Mo(1)-C(3)	59.17(17)	C(2)-Mo(1)-C(6)	117.14(17)
C(1)-Mo(1)-C(6)	153.78(16)	O(3)-Mo(1)-C(6)	97.38(14)
C(4)-Mo(1)-C(6)	59.13(17)	C(5)-Mo(1)-C(6)	35.32(17)
C(3)-Mo(1)-C(6)	57.91(17)	C(2)-Mo(1)-C(7)	143.29(16)
C(1)-Mo(1)-C(7)	122.38(17)	O(3)-Mo(1)-C(7)	78.87(13)
C(4)-Mo(1)-C(7)	58.51(16)	C(5)-Mo(1)-C(7)	58.11(16)
C(3)-Mo(1)-C(7)	34.35(17)	C(6)-Mo(1)-C(7)	34.29(17)
C(2)-Mo(1)-P(1)	78.77(12)	C(1)-Mo(1)-P(1)	114.62(12)
O(3)-Mo(1)-P(1)	76.54(7)	C(4)-Mo(1)-P(1)	137.20(13)
C(5)-Mo(1)-P(1)	101.83(12)	C(3)-Mo(1)-P(1)	147.56(12)
C(6)-Mo(1)-P(1)	91.04(12)	C(7)-Mo(1)-P(1)	114.04(12)
C(9)-P(1)-C(10)	108.81(17)	C(9)-P(1)-C(16)	105.74(17)
C(10)-P(1)-C(16)	102.76(17)	C(9)-P(1)-Mo(1)	101.28(13)
C(10)-P(1)-Mo(1)	113.78(13)	C(16)-P(1)-Mo(1)	123.68(13)
C(8)-O(3)-Mo(1)	121.1(2)	O(1)-C(1)-Mo(1)	175.7(4)
O(2)-C(2)-Mo(1)	179.3(4)	C(7)-C(3)-C(4)	108.0(4)
C(7)-C(3)-Mo(1)	74.9(2)	C(4)-C(3)-Mo(1)	69.6(2)
C(5)-C(4)-C(3)	107.3(4)	C(5)-C(4)-Mo(1)	72.6(2)
C(3)-C(4)-Mo(1)	74.5(2)	C(6)-C(5)-C(4)	108.1(4)
C(6)-C(5)-Mo(1)	75.2(2)	C(4)-C(5)-Mo(1)	71.3(2)
C(7)-C(6)-C(5)	107.8(4)	C(7)-C(6)-Mo(1)	73.9(2)
C(5)-C(6)-Mo(1)	69.5(2)	C(3)-C(7)-C(6)	108.8(4)
C(3)-C(7)-Mo(1)	70.8(2)	C(6)-C(7)-Mo(1)	71.8(2)
O(3)-C(8)-C(9)	123.5(3)	O(3)-C(8)-C(22)	115.3(3)
C(9)-C(8)-C(22)	121.1(3)	C(8)-C(9)-P(1)	113.7(3)
C(15)-C(10)-C(11)	119.2(3)	C(15)-C(10)-P(1)	120.5(3)
C(11)-C(10)-P(1)	120.2(3)	C(12)-C(11)-C(10)	120.2(4)
C(13)-C(12)-C(11)	120.2(4)	C(12)-C(13)-C(14)	120.1(4)
C(15)-C(14)-C(13)	119.9(4)	C(14)-C(15)-C(10)	120.3(4)

C(17)-C(16)-C(21)	118.3(4)	C(17)-C(16)-P(1)	122.2(3)
C(21)-C(16)-P(1)	119.2(3)	C(18)-C(17)-C(16)	121.0(5)
C(17)-C(18)-C(19)	119.5(5)	C(20)-C(19)-C(18)	120.6(5)
C(19)-C(20)-C(21)	119.7(5)	C(20)-C(21)-C(16)	121.0(4)
C(27)-C(22)-C(23)	118.5(3)	C(27)-C(22)-C(8)	120.4(3)
C(23)-C(22)-C(8)	121.1(3)	C(24)-C(23)-C(22)	120.6(4)
C(23)-C(24)-C(25)	120.4(4)	C(24)-C(25)-C(26)	119.2(4)
C(27)-C(26)-C(25)	120.5(4)	C(26)-C(27)-C(22)	120.8(4)

7.8 Structure of $[Pd_3(\mu\text{-dppm})_3(\mu^3\text{-}PCH_2Bu^t)\{(CH_3)_2CO\}][PF_6]_2$, 40

Table 7.19 Summary of crystallographic data for $[Pd_3(\mu\text{-dppm})_3(\mu^3\text{-}PCH_2Bu^t)\{(CH_3)_2CO\}][PF_6]_2$, **40**

Empirical Formula	$C_{94.5}H_{100}F_{12}O_{2.5}P_9Pd_3$
Formula Weight	2101.68
Temperature	150(2) K
Wavelength	0.71070 Å
Crystal system	Monoclinic
Space group	Cc
Unit cell dimensions	a = 23.49700(10)Å α = 90°
	b = 14.44600(10)Å β = 99.7450(3)°
	c = 28.0660(2)Å γ = 90°
Volume	9389.19(10) $Å^3$
Z	4
Density (calculated)	1.487 Mg/m^3
Absorption coefficient	0.793 mm^{-1}
F(000)	4272
Crystal size	0.225 x 0.2 x 0.175 mm
Theta range for data collection	3.51 to 27.49°
Index ranges	$-30 \leq h \leq 30$; $-18 \leq k \leq 18$; $-36 \leq l \leq 36$
Reflections collected	61533
Independent reflections	20114 [R(int) = 0.0322]
Refinement method	Full-matrix least squares on F^2
Data / restraints / parameters	20114 / 0 / 1145
Goodness-of-fit on F^2	0.971
Final R indices [$I>2\sigma(I)$]	$R_1 = 0.0281$ $wR_2 = 0.0651$
R indices (all data)	$R_1 = 0.0309$ $wR_2 = 0.0667$
Absolute structure parameter	0.000(10)
Largest diff. peak and hole	1.084 and -0.999 $eÅ^{-3}$

Table 7.19 Atomic coordinates (x 10^4) and equivalent isotropic displacement parameters ($Å^2$ x 10^3) for **40**.

Atom	x	y	z	U(eq)
Pd(1)	-6460	-2170(1)	-7530	18(1)
Pd(2)	-7530	-4136(1)	-8120	16(1)
Pd(3)	-8096(1)	-2511(1)	-8125(1)	17(1)
P(1)	-5927(1)	-3547(1)	-7567(1)	18(1)
P(2)	-6808(1)	-5178(1)	-7861(1)	18(1)
P(3)	-6934(1)	-720(1)	-7560(1)	19(1)
P(4)	-8264(1)	-1053(1)	-7844(1)	22(1)
P(5)	-8147(1)	-4745(1)	-8797(1)	18(1)
P(6)	-8775(1)	-2911(1)	-8803(1)	18(1)
P(7)	-11012(1)	-397(1)	-5728(1)	60(1)
P(8)	-7702(1)	-318(1)	-5699(1)	42(1)
P(9)	-7308(1)	-2958(1)	-7601(1)	18(1)
F(1)	-11294(1)	161(2)	-6209(1)	70(1)
F(2)	-11656(3)	-757(5)	-5729(3)	84(2)
F(3)	-10925(3)	-1267(7)	-6032(3)	99(4)
F(4)	-10437(3)	81(8)	-5735(3)	131(4)
F(5)	-11226(4)	499(4)	-5421(2)	99(2)
F(2')	-10439(11)	-529(14)	-6009(8)	143(9)
F(3')	-10811(8)	436(9)	-5481(6)	96(5)
F(4')	-11490(9)	-521(19)	-5479(9)	150(10)
F(5')	-11180(20)	-1390(20)	-5914(13)	230(20)
F(6)	-10732(2)	-916(3)	-5253(1)	121(2)
F(7)	-8390(1)	-317(2)	-5789(1)	70(1)
F(8)	-7731(1)	522(2)	-6078(1)	67(1)
F(9)	-7018(1)	-264(2)	-5623(1)	63(1)
F(10)	-7672(2)	-1139(2)	-5330(1)	81(1)

F(11)	-7697(1)	-1022(2)	-6137(1)	64(1)
F(12)	-7698(1)	403(2)	-5269(1)	68(1)
O(1)	-5626(1)	-1391(2)	-7407(1)	29(1)
O(2)	-7303(1)	2654(2)	-4680(1)	56(1)
O(3)	-4456(4)	1766(5)	-5106(3)	95(3)
C(1)	-5717(1)	-3647(2)	-8156(1)	23(1)
C(2)	-5281(1)	-4260(2)	-8236(1)	26(1)
C(3)	-5128(2)	-4322(3)	-8687(1)	35(1)
C(4)	-5413(2)	-3791(3)	-9070(1)	41(1)
C(5)	-5846(2)	-3199(3)	-8996(1)	45(1)
C(6)	-5999(2)	-3120(2)	-8541(1)	33(1)
C(7)	-5239(1)	-3493(2)	-7144(1)	21(1)
C(8)	-5212(1)	-3778(2)	-6672(1)	29(1)
C(9)	-4693(2)	-3714(2)	-6345(1)	36(1)
C(10)	-4209(2)	-3351(3)	-6493(1)	38(1)
C(11)	-4238(1)	-3046(3)	-6959(1)	36(1)
C(12)	-4748(1)	-3118(2)	-7287(1)	28(1)
C(13)	-6194(1)	-4700(2)	-7435(1)	21(1)
C(14)	-6484(1)	-5747(2)	-8329(1)	24(1)
C(15)	-6217(1)	-6607(2)	-8251(1)	34(1)
C(16)	-5979(2)	-7025(3)	-8620(2)	47(1)
C(17)	-6012(2)	-6596(3)	-9062(2)	47(1)
C(18)	-6279(2)	-5742(3)	-9145(1)	41(1)
C(19)	-6517(1)	-5322(2)	-8778(1)	29(1)
C(20)	-7020(1)	-6166(2)	-7522(1)	23(1)
C(21)	-6772(2)	-6393(2)	-7050(1)	32(1)
C(22)	-6989(2)	-7127(2)	-6813(1)	38(1)
C(23)	-7442(2)	-7644(2)	-7043(1)	38(1)
C(24)	-7683(2)	-7436(3)	-7509(2)	43(1)
C(25)	-7479(2)	-6705(2)	-7747(1)	35(1)
C(26)	-6967(1)	-224(2)	-8162(1)	25(1)
C(27)	-6938(2)	-809(2)	-8552(1)	34(1)

C(28)	-6969(2)	-450(3)	-9015(1)	46(1)
C(29)	-7016(2)	489(3)	-9090(1)	45(1)
C(30)	-7049(2)	1078(3)	-8704(1)	38(1)
C(31)	-7030(1)	727(2)	-8242(1)	30(1)
C(32)	-6520(1)	114(2)	-7149(1)	23(1)
C(33)	-6092(1)	670(2)	-7293(1)	31(1)
C(34)	-5769(2)	1267(3)	-6964(2)	40(1)
C(35)	-5862(2)	1314(3)	-6498(2)	42(1)
C(36)	-6279(2)	761(3)	-6347(1)	38(1)
C(37)	-6613(1)	165(2)	-6672(1)	31(1)
C(38)	-7657(1)	-591(2)	-7402(1)	25(1)
C(39)	-8442(1)	-87(2)	-8260(1)	30(1)
C(40)	-8353(1)	-161(2)	-8737(1)	33(1)
C(41)	-8477(2)	586(3)	-9054(2)	46(1)
C(42)	-8688(2)	1401(3)	-8887(2)	59(1)
C(43)	-8770(2)	1475(3)	-8423(2)	52(1)
C(44)	-8653(2)	745(2)	-8106(2)	41(1)
C(45)	-8858(1)	-1034(2)	-7497(1)	27(1)
C(46)	-9378(1)	-1414(2)	-7721(1)	32(1)
C(47)	-9838(2)	-1495(3)	-7475(2)	43(1)
C(48)	-9787(2)	-1184(3)	-7002(2)	41(1)
C(49)	-9282(2)	-794(3)	-6784(2)	41(1)
C(50)	-8816(2)	-717(3)	-7023(1)	39(1)
C(51)	-9034(1)	-2043(2)	-9261(1)	21(1)
C(52)	-9547(1)	-1565(2)	-9254(1)	24(1)
C(53)	-9734(2)	-896(2)	-9595(1)	32(1)
C(54)	-9404(2)	-682(2)	-9946(1)	35(1)
C(55)	-8891(2)	-1124(3)	-9954(1)	36(1)
C(56)	-8699(1)	-1804(2)	-9611(1)	28(1)
C(57)	-9444(1)	-3435(2)	-8683(1)	21(1)
C(58)	-9874(1)	-3716(2)	-9061(1)	28(1)
C(59)	-10359(1)	-4183(2)	-8965(1)	34(1)

C(60)	-10421(2)	-4366(2)	-8495(2)	37(1)
C(61)	-10004(2)	-4080(3)	-8116(1)	39(1)
C(62)	-9514(1)	-3617(2)	-8211(1)	30(1)
C(63)	-8489(1)	-3788(2)	-9174(1)	21(1)
C(64)	-8743(1)	-5449(2)	-8660(1)	24(1)
C(65)	-9162(2)	-5799(2)	-9029(2)	39(1)
C(66)	-9612(2)	-6334(3)	-8914(2)	55(1)
C(67)	-9648(2)	-6522(3)	-8441(2)	54(1)
C(68)	-9238(2)	-6186(3)	-8079(2)	51(1)
C(69)	-8787(2)	-5655(2)	-8184(1)	37(1)
C(70)	-7894(1)	-5472(2)	-9256(1)	22(1)
C(71)	-7890(1)	-6431(2)	-9211(1)	29(1)
C(72)	-7697(2)	-6982(2)	-9558(1)	36(1)
C(73)	-7500(2)	-6574(3)	-9946(1)	37(1)
C(74)	-7494(2)	-5631(3)	-9990(1)	36(1)
C(75)	-7686(1)	-5074(2)	-9644(1)	29(1)
C(76)	-7318(1)	-3102(2)	-6942(1)	26(1)
C(77)	-7819(1)	-3635(2)	-6772(1)	28(1)
C(78)	-7825(2)	-4637(3)	-6931(2)	51(1)
C(79)	-8393(2)	-3165(3)	-6952(2)	46(1)
C(80)	-7702(2)	-3606(3)	-6217(1)	48(1)
C(81)	-5377(2)	-1207(2)	-6989(1)	32(1)
C(82)	-5589(2)	-1510(3)	-6548(1)	42(1)
C(83)	-4817(2)	-673(3)	-6916(2)	52(1)
C(84)	-7239(2)	2536(3)	-5101(2)	47(1)
C(85)	-7688(2)	2836(4)	-5512(2)	70(1)
C(86)	-6712(2)	2065(3)	-5215(2)	60(1)
C(87)	-5644(2)	-1676(3)	-5318(2)	58(1)
C(88)	-5624(2)	-705(3)	-5288(2)	54(1)
C(89)	-5125(2)	-238(4)	-5309(2)	60(1)
C(90)	-4624(2)	-722(5)	-5368(2)	81(2)
C(91)	-4636(3)	-1666(5)	-5393(2)	81(2)

C(92)	-5135(3)	-2132(4)	-5370(2)	68(2)
C(93)	-6185(2)	-2186(3)	-5317(3)	93(2)
C(94)	-4313(2)	2281(3)	-5383(2)	32(2)
C(95)	-4336(2)	3290(3)	-5260(2)	66(3)
C(96)	-4152(6)	2040(9)	-5818(5)	87(4)

Table 7.20 Bond lengths [Å] and angles [°] for **40**.

Pd(1)-O(1)	2.236(2)	Pd(1)-P(9)	2.2748(7)
Pd(1)-P(1)	2.3625(7)	Pd(1)-P(3)	2.3666(7)
Pd(2)-P(9)	2.2435(7)	Pd(2)-P(2)	2.2922(7)
Pd(2)-P(5)	2.3554(7)	Pd(2)-Pd(3)	2.6977(3)
Pd(3)-P(9)	2.2541(7)	Pd(3)-P(4)	2.3063(8)
Pd(3)-P(6)	2.3413(8)	P(1)-C(1)	1.809(3)
P(1)-C(7)	1.838(3)	P(1)-C(13)	1.839(3)
P(2)-C(14)	1.821(3)	P(2)-C(20)	1.831(3)
P(2)-C(13)	1.844(3)	P(3)-C(26)	1.826(3)
P(3)-C(32)	1.831(3)	P(3)-C(38)	1.835(3)
P(4)-C(39)	1.823(3)	P(4)-C(45)	1.832(3)
P(4)-C(38)	1.848(3)	P(5)-C(64)	1.823(3)
P(5)-C(70)	1.838(3)	P(5)-C(63)	1.842(3)
P(6)-C(51)	1.823(3)	P(6)-C(57)	1.828(3)
P(6)-C(63)	1.837(3)	P(7)-F(4')	1.430(16)
P(7)-F(3')	1.428(11)	P(7)-F(4)	1.521(4)
P(7)-F(3)	1.553(7)	P(7)-F(6)	1.572(4)
P(7)-F(2)	1.599(6)	P(7)-F(5')	1.56(3)
P(7)-F(1)	1.615(3)	P(7)-F(5)	1.677(6)
P(7)-F(2')	1.683(13)	P(8)-F(10)	1.568(3)
P(8)-F(9)	1.589(3)	P(8)-F(12)	1.592(3)
P(8)-F(7)	1.593(3)	P(8)-F(11)	1.597(3)
P(8)-F(8)	1.607(3)	P(9)-C(76)	1.865(3)
F(2)-F(4')	0.82(2)	F(2)-F(5')	1.59(5)

F(3)-F(5')	0.76(5)	F(3)-F(2')	1.56(3)
F(4)-F(2')	1.17(2)	F(4)-F(3')	1.324(17)
F(5)-F(3')	1.022(17)	F(5)-F(4')	1.60(3)
O(1)-C(81)	1.248(4)	O(2)-C(84)	1.230(5)
O(3)-C(94)	1.165(8)	C(1)-C(6)	1.394(4)
C(1)-C(2)	1.399(4)	C(2)-C(3)	1.378(5)
C(3)-C(4)	1.395(6)	C(4)-C(5)	1.371(6)
C(5)-C(6)	1.389(5)	C(7)-C(8)	1.377(4)
C(7)-C(12)	1.394(4)	C(8)-C(9)	1.401(4)
C(9)-C(10)	1.377(5)	C(10)-C(11)	1.371(5)
C(11)-C(12)	1.386(5)	C(14)-C(19)	1.393(5)
C(14)-C(15)	1.392(4)	C(15)-C(16)	1.396(5)
C(16)-C(17)	1.377(6)	C(17)-C(18)	1.386(6)
C(18)-C(19)	1.391(5)	C(20)-C(21)	1.392(4)
C(20)-C(25)	1.393(5)	C(21)-C(22)	1.394(5)
C(22)-C(23)	1.370(5)	C(23)-C(24)	1.368(6)
C(24)-C(25)	1.378(5)	C(26)-C(27)	1.393(5)
C(26)-C(31)	1.395(5)	C(27)-C(28)	1.391(5)
C(28)-C(29)	1.374(6)	C(29)-C(30)	1.390(6)
C(30)-C(31)	1.388(5)	C(32)-C(37)	1.392(4)
C(32)-C(33)	1.401(4)	C(33)-C(34)	1.391(5)
C(34)-C(35)	1.364(6)	C(35)-C(36)	1.386(6)
C(36)-C(37)	1.396(5)	C(39)-C(40)	1.393(5)
C(39)-C(44)	1.398(5)	C(40)-C(41)	1.398(5)
C(41)-C(42)	1.389(7)	C(42)-C(43)	1.352(7)
C(43)-C(44)	1.379(6)	C(45)-C(46)	1.391(5)
C(45)-C(50)	1.394(5)	C(46)-C(47)	1.382(5)
C(47)-C(48)	1.387(6)	C(48)-C(49)	1.362(6)
C(49)-C(50)	1.382(5)	C(51)-C(52)	1.393(4)
C(51)-C(56)	1.401(4)	C(52)-C(53)	1.379(4)
C(53)-C(54)	1.387(5)	C(54)-C(55)	1.369(5)
C(55)-C(56)	1.396(5)	C(57)-C(62)	1.386(4)
C(57)-C(58)	1.394(4)	C(58)-C(59)	1.390(4)

C(59)-C(60)	1.378(5)	C(60)-C(61)	1.382(6)
C(61)-C(62)	1.395(5)	C(64)-C(69)	1.392(5)
C(64)-C(65)	1.396(5)	C(65)-C(66)	1.389(5)
C(66)-C(67)	1.371(7)	C(67)-C(68)	1.367(7)
C(68)-C(69)	1.378(5)	C(70)-C(71)	1.392(4)
C(70)-C(75)	1.392(4)	C(71)-C(72)	1.394(5)
C(72)-C(73)	1.384(5)	C(73)-C(74)	1.368(5)
C(74)-C(75)	1.393(4)	C(76)-C(77)	1.550(4)
C(77)-C(78)	1.514(5)	C(77)-C(79)	1.517(5)
C(77)-C(80)	1.533(5)	C(81)-C(82)	1.476(5)
C(81)-C(83)	1.508(5)	C(84)-C(85)	1.489(7)
C(84)-C(86)	1.493(6)	C(87)-C(92)	1.395(7)
C(87)-C(88)	1.406(7)	C(87)-C(93)	1.469(6)
C(88)-C(89)	1.362(7)	C(89)-C(90)	1.403(8)
C(90)-C(91)	1.366(9)	C(91)-C(92)	1.361(9)
C(94)-C(96)	1.382(12)	C(94)-C(95)	1.5024
O(1)-Pd(1)-P(9)	176.17(7)	O(1)-Pd(1)-P(1)	88.45(6)
P(9)-Pd(1)-P(1)	92.17(3)	O(1)-Pd(1)-P(3)	87.44(6)
P(9)-Pd(1)-P(3)	92.28(3)	P(1)-Pd(1)-P(3)	173.38(3)
P(9)-Pd(2)-P(2)	102.34(3)	P(9)-Pd(2)-P(5)	148.26(3)
P(2)-Pd(2)-P(5)	109.39(3)	P(9)-Pd(2)-Pd(3)	53.326(19)
P(2)-Pd(2)-Pd(3)	155.59(2)	P(5)-Pd(2)-Pd(3)	94.933(18)
P(9)-Pd(3)-P(4)	102.01(3)	P(9)-Pd(3)-P(6)	146.20(3)
P(4)-Pd(3)-P(6)	111.79(3)	P(9)-Pd(3)-Pd(2)	52.963(19)
P(4)-Pd(3)-Pd(2)	154.97(2)	P(6)-Pd(3)-Pd(2)	93.238(19)
C(1)-P(1)-C(7)	104.36(14)	C(1)-P(1)-C(13)	105.44(14)
C(7)-P(1)-C(13)	101.58(14)	C(1)-P(1)-Pd(1)	109.66(10)
C(7)-P(1)-Pd(1)	110.54(9)	C(13)-P(1)-Pd(1)	123.50(10)
C(14)-P(2)-C(20)	101.86(14)	C(14)-P(2)-C(13)	105.08(13)
C(20)-P(2)-C(13)	101.96(14)	C(14)-P(2)-Pd(2)	116.40(11)
C(20)-P(2)-Pd(2)	115.15(10)	C(13)-P(2)-Pd(2)	114.55(9)
C(26)-P(3)-C(32)	105.07(14)	C(26)-P(3)-C(38)	106.72(15)

C(32)-P(3)-C(38)	101.24(14)	C(26)-P(3)-Pd(1)	109.06(10)
C(32)-P(3)-Pd(1)	111.30(10)	C(38)-P(3)-Pd(1)	122.05(11)
C(39)-P(4)-C(45)	102.49(15)	C(39)-P(4)-C(38)	102.80(15)
C(45)-P(4)-C(38)	102.11(14)	C(39)-P(4)-Pd(3)	120.88(12)
C(45)-P(4)-Pd(3)	112.65(10)	C(38)-P(4)-Pd(3)	113.67(10)
C(64)-P(5)-C(70)	100.39(14)	C(64)-P(5)-C(63)	105.20(14)
C(70)-P(5)-C(63)	100.78(13)	C(64)-P(5)-Pd(2)	115.39(11)
C(70)-P(5)-Pd(2)	123.47(10)	C(63)-P(5)-Pd(2)	109.40(10)
C(51)-P(6)-C(57)	102.72(13)	C(51)-P(6)-C(63)	100.71(13)
C(57)-P(6)-C(63)	103.12(14)	C(51)-P(6)-Pd(3)	120.22(10)
C(57)-P(6)-Pd(3)	116.20(10)	C(63)-P(6)-Pd(3)	111.50(10)
F(4')-P(7)-F(3')	95.3(13)	F(4')-P(7)-F(4)	146.8(11)
F(3')-P(7)-F(4)	53.3(7)	F(4')-P(7)-F(3)	110.7(11)
F(3')-P(7)-F(3)	152.3(9)	F(4)-P(7)-F(3)	99.2(6)
F(4')-P(7)-F(6)	77.1(11)	F(3')-P(7)-F(6)	86.3(7)
F(4)-P(7)-F(6)	89.1(3)	F(3)-P(7)-F(6)	90.2(4)
F(4')-P(7)-F(2)	30.7(10)	F(3')-P(7)-F(2)	120.8(9)
F(4)-P(7)-F(2)	172.0(5)	F(3)-P(7)-F(2)	87.0(5)
F(6)-P(7)-F(2)	96.1(3)	F(4')-P(7)-F(5')	83(2)
F(3')-P(7)-F(5')	170.0(13)	F(4)-P(7)-F(5')	126(2)
F(3)-P(7)-F(5')	28(2)	F(6)-P(7)-F(5')	83.7(12)
F(2)-P(7)-F(5')	60.6(19)	F(4')-P(7)-F(1)	103.1(11)
F(3')-P(7)-F(1)	92.3(7)	F(4)-P(7)-F(1)	90.1(2)
F(3)-P(7)-F(1)	91.0(3)	F(6)-P(7)-F(1)	178.6(2)
F(2)-P(7)-F(1)	84.6(3)	F(5')-P(7)-F(1)	97.7(12)
F(4')-P(7)-F(5)	61.2(11)	F(3')-P(7)-F(5)	37.3(7)
F(4)-P(7)-F(5)	90.1(5)	F(3)-P(7)-F(5)	170.2(4)
F(6)-P(7)-F(5)	93.0(3)	F(2)-P(7)-F(5)	83.5(4)
F(5')-P(7)-F(5)	143(2)	F(1)-P(7)-F(5)	85.9(3)
F(4')-P(7)-F(2')	166.2(13)	F(3')-P(7)-F(2')	95.6(12)
F(4)-P(7)-F(2')	42.4(9)	F(3)-P(7)-F(2')	57.3(9)
F(6)-P(7)-F(2')	95.2(7)	F(2)-P(7)-F(2')	142.5(11)
F(5')-P(7)-F(2')	85.3(19)	F(1)-P(7)-F(2')	85.0(7)

F(5)-P(7)-F(2')	131.4(10)	F(10)-P(8)-F(9)	90.93(18)
F(10)-P(8)-F(12)	90.04(18)	F(9)-P(8)-F(12)	89.39(15)
F(10)-P(8)-F(7)	92.11(18)	F(9)-P(8)-F(7)	176.83(18)
F(12)-P(8)-F(7)	89.72(15)	F(10)-P(8)-F(11)	91.24(17)
F(9)-P(8)-F(11)	89.73(15)	F(12)-P(8)-F(11)	178.45(17)
F(7)-P(8)-F(11)	91.10(16)	F(10)-P(8)-F(8)	179.72(19)
F(9)-P(8)-F(8)	88.81(16)	F(12)-P(8)-F(8)	90.07(17)
F(7)-P(8)-F(8)	88.15(17)	F(11)-P(8)-F(8)	88.64(16)
C(76)-P(9)-Pd(2)	121.28(11)	C(76)-P(9)-Pd(3)	122.16(10)
Pd(2)-P(9)-Pd(3)	73.71(2)	C(76)-P(9)-Pd(1)	97.24(10)
Pd(2)-P(9)-Pd(1)	122.71(3)	Pd(3)-P(9)-Pd(1)	121.59(3)
F(4')-F(2)-F(5')	105(2)	F(4')-F(2)-P(7)	63.2(14)
F(5')-F(2)-P(7)	58.3(12)	F(5')-F(3)-F(2')	141(3)
F(5')-F(3)-P(7)	76(3)	F(2')-F(3)-P(7)	65.6(6)
F(2')-F(4)-F(3')	135.8(13)	F(2')-F(4)-P(7)	76.2(11)
F(3')-F(4)-P(7)	59.8(6)	F(3')-F(5)-F(4')	105.5(12)
F(3')-F(5)-P(7)	57.9(7)	F(4')-F(5)-P(7)	51.7(6)
F(4)-F(2')-F(3)	117.7(10)	F(4)-F(2')-P(7)	61.3(6)
F(3)-F(2')-P(7)	57.1(7)	F(5)-F(3')-F(4)	149.6(12)
F(5)-F(3')-P(7)	84.7(11)	F(4)-F(3')-P(7)	67.0(6)
F(2)-F(4')-P(7)	86.2(17)	F(2)-F(4')-F(5)	126(3)
P(7)-F(4')-F(5)	67.1(10)	F(3)-F(5')-F(2)	131(4)
F(3)-F(5')-P(7)	76(2)	F(2)-F(5')-P(7)	61.1(14)
C(81)-O(1)-Pd(1)	120.8(2)	C(6)-C(1)-C(2)	119.1(3)
C(6)-C(1)-P(1)	119.8(2)	C(2)-C(1)-P(1)	121.1(2)
C(3)-C(2)-C(1)	120.0(3)	C(2)-C(3)-C(4)	120.3(3)
C(5)-C(4)-C(3)	120.0(3)	C(4)-C(5)-C(6)	120.2(4)
C(5)-C(6)-C(1)	120.3(3)	C(8)-C(7)-C(12)	119.2(3)
C(8)-C(7)-P(1)	120.1(2)	C(12)-C(7)-P(1)	120.6(2)
C(7)-C(8)-C(9)	120.3(3)	C(10)-C(9)-C(8)	119.9(3)
C(11)-C(10)-C(9)	120.0(3)	C(10)-C(11)-C(12)	120.5(3)
C(11)-C(12)-C(7)	120.1(3)	P(1)-C(13)-P(2)	117.71(16)
C(19)-C(14)-C(15)	119.3(3)	C(19)-C(14)-P(2)	119.2(2)

C(15)-C(14)-P(2)	121.4(3)	C(14)-C(15)-C(16)	119.7(4)
C(17)-C(16)-C(15)	120.4(4)	C(16)-C(17)-C(18)	120.5(3)
C(17)-C(18)-C(19)	119.4(4)	C(18)-C(19)-C(14)	120.7(3)
C(21)-C(20)-C(25)	117.9(3)	C(21)-C(20)-P(2)	124.8(2)
C(25)-C(20)-P(2)	117.3(2)	C(20)-C(21)-C(22)	120.4(3)
C(23)-C(22)-C(21)	120.6(3)	C(24)-C(23)-C(22)	119.5(3)
C(23)-C(24)-C(25)	120.8(3)	C(24)-C(25)-C(20)	120.9(3)
C(27)-C(26)-C(31)	119.4(3)	C(27)-C(26)-P(3)	119.2(2)
C(31)-C(26)-P(3)	121.4(2)	C(28)-C(27)-C(26)	120.3(3)
C(29)-C(28)-C(27)	120.2(4)	C(28)-C(29)-C(30)	119.8(3)
C(31)-C(30)-C(29)	120.6(4)	C(30)-C(31)-C(26)	119.6(3)
C(37)-C(32)-C(33)	119.0(3)	C(37)-C(32)-P(3)	119.2(2)
C(33)-C(32)-P(3)	121.7(2)	C(34)-C(33)-C(32)	120.1(3)
C(35)-C(34)-C(33)	120.7(3)	C(34)-C(35)-C(36)	120.0(3)
C(35)-C(36)-C(37)	120.2(3)	C(32)-C(37)-C(36)	120.0(3)
P(3)-C(38)-P(4)	116.24(16)	C(40)-C(39)-C(44)	118.9(3)
C(40)-C(39)-P(4)	120.2(2)	C(44)-C(39)-P(4)	120.9(3)
C(39)-C(40)-C(41)	120.2(4)	C(42)-C(41)-C(40)	119.2(4)
C(43)-C(42)-C(41)	120.6(4)	C(42)-C(43)-C(44)	121.1(4)
C(43)-C(44)-C(39)	120.0(4)	C(46)-C(45)-C(50)	118.5(3)
C(46)-C(45)-P(4)	116.4(3)	C(50)-C(45)-P(4)	125.0(2)
C(47)-C(46)-C(45)	120.6(3)	C(46)-C(47)-C(48)	120.2(3)
C(49)-C(48)-C(47)	119.5(3)	C(48)-C(49)-C(50)	121.1(4)
C(49)-C(50)-C(45)	120.2(3)	C(52)-C(51)-C(56)	118.5(3)
C(52)-C(51)-P(6)	121.2(2)	C(56)-C(51)-P(6)	120.2(2)
C(53)-C(52)-C(51)	120.8(3)	C(52)-C(53)-C(54)	119.9(3)
C(55)-C(54)-C(53)	120.6(3)	C(54)-C(55)-C(56)	119.9(3)
C(55)-C(56)-C(51)	120.3(3)	C(62)-C(57)-C(58)	118.9(3)
C(62)-C(57)-P(6)	119.9(2)	C(58)-C(57)-P(6)	121.0(2)
C(59)-C(58)-C(57)	120.4(3)	C(60)-C(59)-C(58)	120.1(3)
C(59)-C(60)-C(61)	120.2(3)	C(60)-C(61)-C(62)	119.8(3)
C(57)-C(62)-C(61)	120.5(3)	P(6)-C(63)-P(5)	111.03(15)
C(69)-C(64)-C(65)	118.4(3)	C(69)-C(64)-P(5)	120.4(3)

C(65)-C(64)-P(5)	121.2(3)	C(66)-C(65)-C(64)	119.9(4)
C(67)-C(66)-C(65)	120.6(4)	C(68)-C(67)-C(66)	119.8(4)
C(67)-C(68)-C(69)	120.7(4)	C(68)-C(69)-C(64)	120.6(4)
C(71)-C(70)-C(75)	119.0(3)	C(71)-C(70)-P(5)	120.1(2)
C(75)-C(70)-P(5)	120.8(2)	C(70)-C(71)-C(72)	120.2(3)
C(73)-C(72)-C(71)	119.9(3)	C(74)-C(73)-C(72)	120.3(3)
C(73)-C(74)-C(75)	120.2(3)	C(74)-C(75)-C(70)	120.3(3)
C(77)-C(76)-P(9)	119.9(2)	C(78)-C(77)-C(79)	111.5(3)
C(78)-C(77)-C(80)	108.5(3)	C(79)-C(77)-C(80)	108.9(3)
C(78)-C(77)-C(76)	110.7(3)	C(79)-C(77)-C(76)	110.7(3)
C(80)-C(77)-C(76)	106.5(3)	O(1)-C(81)-C(82)	123.6(3)
O(1)-C(81)-C(83)	119.7(4)	C(82)-C(81)-C(83)	116.6(3)
O(2)-C(84)-C(85)	121.2(4)	O(2)-C(84)-C(86)	120.7(5)
C(85)-C(84)-C(86)	118.1(4)	C(92)-C(87)-C(88)	117.1(5)
C(92)-C(87)-C(93)	121.4(5)	C(88)-C(87)-C(93)	121.4(4)
C(89)-C(88)-C(87)	120.8(5)	C(88)-C(89)-C(90)	120.3(5)
C(91)-C(90)-C(89)	119.4(6)	C(92)-C(91)-C(90)	120.2(6)
C(91)-C(92)-C(87)	122.1(5)	O(3)-C(94)-C(96)	125.6(8)
O(3)-C(94)-C(95)	116.1(5)	C(96)-C(94)-C(95)	118.3(6)

7.9 References

1 G.M. Sheldrick, *Acta Crystallogr. Sect. A*, 1990, **46**, 467.

2 G.M. Sheldrick, SHELXL-(&, Computer Program for Crystal Structure Refinement, University of Gõttingen, 1997.

3 P. McArdle, *J. Appl. Crystallogr.*, 1995, **28**, 65.